PERIODICAL ROOM
GENERAL LIBRARY
UNIV. OF MICH.
DEC 14 1925

VOLUME 26 SECOND SERIES NUMBER 6

# THE PHYSICAL REVIEW

## A JOURNAL OF EXPERIMENTAL AND THEORETICAL PHYSICS

CONDUCTED BY

## THE AMERICAN PHYSICAL SOCIETY

BOARD OF EDITORS

*Managing Editor:* GORDON A. FULCHER, Corning, New York;
A. H. COMPTON, E. H. KENNARD, LEIGH PAGE; H. D. BABCOCK, W. G. CADY,
JOHN T. TATE; K. K. DARROW, E. C. KEMBLE, F. L. MOSHER

## DECEMBER, 1925

Change of Wave-length of Scattered X-rays; Ionization Measurement — H. M. SHARP 691
Photo-electrons Produced by X-rays; Direction of Ejection — — — D. H. LOUGHRIDGE 697
Molybdenum K Series: Wave-lengths and Relative Intensities — — — — — — — — — SAMUEL K. ALLISON AND ALICE H. ARMSTRONG 701
Lines in the L Spectrum of Tungsten and the K Spectrum of Copper; Relative Intensities — — — SAMUEL K. ALLISON AND ALICE H. ARMSTRONG 714
X-ray Lines and Absorption Limits; Apparent Shape — — — — — F. K. RICHTMYER 724
Lattice Parameter and Density of Pure Tungsten — — — — — WHEELER P. DAVEY 736
Soft X-rays from Iron, Cobalt, Nickel and Copper — — — — CHARLES H. THOMAS 739
Relative Intensities in Series Spectra; Application of the Correspondence Principle to — — — — — — — — — — — — — FRANK C. HOTT 749
Fluorescence of Cadmium Vapor — — — — — — — — — — A. D. POWER 761
Absorption Spectrum of Manganese Vapor in the Visible and Ultraviolet — R. V. ZUMSTEIN 765
Infrared Absorption Spectrum of Water; Variation with Temperature — — J. R. COLLINS 771
Critical Potential of the Negative Band Spectrum of Nitrogen — — ENOS E. WITMER 780
Ionization of Nitrogen by Electron Impact — — — — T. R. HOGNESS AND E. G. LUNN 785
Striated Discharge in Hydrogen — — — — — — — — — ARTHUR BRAMLEY 794
Secondary Emission from Nickel Due to Slow Positive Ion Bombardment — — A. L. KLEIN 800
Mobility of Negative Ions in Various Fluids — — — — — — PAUL E. BOUCHER 807
Measurement of the Four Magnetic Transverse Effects — — — — — EDWIN H. HALL 809
Small Resistance Thermometer — — — — — — — — — — GEO. F. TAYLOR 841
Vapor Pressure of Metals; New Experimental Method — W. H. ROSSELSON AND A. L. DIXON 851
Mercury Vapor Pressure at Low Temperatures — — — — FRANKLIN E. POINDEXTER 859
Book Reviews — — — — — — — — — — — — — — — — — — 869
INDEX to Volume 26 — — — — — — — — — — — — — — — 877

PUBLISHED BY THE AMERICAN PHYSICAL SOCIETY
Ithaca, N. Y.

# THE AMERICAN PHYSICAL SOCIETY


**OFFICERS OF THE SOCIETY**

| | | |
|---|---|---|
| **President:** | D. C. MILLER | Case School of Applied Science, Cleveland, Ohio |
| **Vice-President:** | K. T. COMPTON | Princeton University, Princeton, N. J. |
| **Secretary:** | H. W. WEBB | Columbia University, New York City |
| **Treasurer:** | G. B. PEGRAM | Columbia University, New York City |
| **Editor:** | G. S. FULCHER | Corning, N. Y. |
| **Local Secretary for the Pacific Coast:** | D. L. WEBSTER | Stanford University, Calif. |


# THE PHYSICAL REVIEW


Published monthly — Two volumes annually


**First series.** From July 1, 1893 to January 1, 1913, the REVIEW was conducted by Edward L. Nichols, Ernest Merritt and Frederick Bedell, with the financial support of Cornell University. The first four volumes were issued annually; subsequent volumes, semi-annually; thirty-five volumes in all.

**Second series.** On January 1, 1913, the REVIEW was transferred to the American Physical Society as announced on the first page of the new series which was then begun. Since then it has been conducted by a Board of Editors elected by the Society. Semi-annual volumes begin in January and July.

**Contributors** are referred to page 2 of the advertisements for further information.

**Annual Subscription**, throughout the Postal Union, $7.00 in advance.

**Single Copies**, $.75.

**General Index**, 1893-1920, $4.00, in advance.

**Back Volumes**, $4.50 per volume; **Back Numbers**, $.75 per copy. Postage is free if remittance accompanies order; otherwise postage is extra. No bound volumes can be supplied. The REVIEW offers to purchase a limited number of First Series, Vol. 1, No. 1 (at $1.50 each); Second Series, Vol. 7, No. 1, January 1916; Vol. 7, March 1916 and Vol. 9, No. 2, February 1917 (at $1.50 each); Vol. 19, No. 1, January 1922 (at $.75 each).

**Advertisements.** Rates will be supplied by the Editor on request. Copy for each number must be received at Corning before the 1st of the preceding month; old copy is used until new copy is received. Send electrotypes direct to the printers, George Banta Publishing Co., Menasha, Wisconsin.

**Discount** of ten percent is allowed subscription agencies and members of the American Physical Society.

**Complaints** of failure to receive the REVIEW, in the case of members of the Physical Society, should be addressed to the Treasurer; otherwise, to the REVIEW, Corning, N.Y. *New copies will be sent free only if complaint is received within three months of date of issue.*

**Correspondence** should be addressed to the PHYSICAL REVIEW, Corning, N. Y.


Entered at the postoffice at Menasha, Wis., as second class matter.
Acceptance for mailing at special rate of postage provided for in section 1103, Act of October 3, 1917, authorized September 4, 1918.

*Second Series* *December, 1925* *Vol. 26, No. 6*

THE

# PHYSICAL REVIEW

## A PRECISION MEASUREMENT OF THE CHANGE OF WAVE-LENGTH OF SCATTERED X-RAYS

By H. M. Sharp

Abstract

According to the quantum theory, the change of wave-length due to scattering is $\delta\lambda = (h/mc)\ (1-\cos\phi)$ where $h$ is the radiation constant, $m$ the mass of an electron, $c$ the velocity of light and $\phi$ the angle of scattering. In the present experiments $\phi$ was made as large as possible (169°) by placing the slits and calcite crystal in a lead box fastened to the Coolidge tube. Mo $K\alpha$ and $K\beta$ radiation was scattered *from paraffin* back to the crystal and then to a photographic plate; Zr $K\alpha$ rays for comparison were obtained from a Zr radiator. The best plate required an exposure of 48 hr. The change of wave-length was measured 16 times by means of a special microphotometer. After certain corrections were made, the shift came out $(.04825 \pm .0002)$A; the theoretical value is $.04798 \pm .0001$. This agreement is an excellent confirmation of the theory. This effect may also be used to obtain a measurement of $m$ which is independent of $e/m$. The *value of the mass of the electron* thus computed from these measurements is $(8.99 \pm .034) \times 10^{-28}$ gm in agreement with the mean result from deflection experiments, whereas the spectroscopic value of $e/m$ gives 9.04.

ACCORDING to the quantum theory, the change of wave-length of x-rays when scattered is given by the expression[1]

$$\delta\lambda = (h/mc)\ (1-\cos\phi) \qquad (1)$$

where $h$ is Planck's radiation constant, $m$ is the mass of the electron, $c$ the velocity of light and $\phi$ the angle which the scattered beam makes with the primary beam. Of the many published tests of this equation, the ones for which the greatest precision is claimed are perhaps those of A. H. Compton,[2] Becker and others[3] and Kallman and Mark.[4] Compton used an ionization spectrometer and a carbon radiator, and made tests at different angles of scattering. His probable error was about 2 percent. The others obtained photographic spectra of rays scattered at about

[1] A. H. Compton, Phys. Rev. **21**, 207 and 483 (1923).

[2] A. H. Compton, Phys. Rev. **22**, 409 (1923).

[3] J. A. Becker, E. C. Watson, W. R. Smythe, R. B. Brode and L. M. Mott-Smith, Phys. Rev. **23**, 763 (1924).

[4] H. Kallman and H. Mark, Naturwissenschaften **13**, 297 (1925).

90°, Becker using aluminum as radiator, and Kallman and Mark using graphite. In both of the latter investigations the estimated probable error was about 1 percent. Greater precision in testing the equation should be obtained if the angle of scattering is increased to nearly 180°, for then $\delta\lambda$ is greater, and, since it is the cosine of the angle which enters into the equation, the error in the calculated value of $\delta\lambda$ resulting from an error in measuring $\phi$ is greatly reduced.

*Experimental procedure.* A test in which a large angle of scattering is used has been made with the apparatus shown diagrammatically in Fig. 1. X-rays from the molybdenum target $T$ of an x-ray tube fall on a paraffin radiator $R$, and some of the rays are scattered almost directly back to the calcite crystal $C$. The slit which determines the width of the spectrum lines is at $S$, and the photographic film is placed beyond the lead

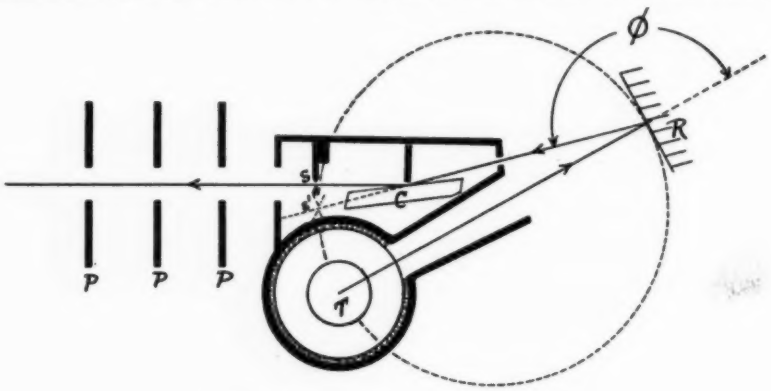


Fig. 1. Arrangement of apparatus.

screens $P$. The image $S'$ of the slit $S$ as reflected in the face of the crystal lies as close to the target $T$ as is conveniently possible. It will be seen also from the figure that the angle of scattering $TRS'$ varies but slightly as one alters the part of the radiator $R$ from which the rays are scattered. This arrangement therefore affords a means of securing a spectrum of rays scattered at a nearly definite as well as a large angle.

The x-ray tube employed was of the narrow cylindrical, water-cooled type described by Compton.[1] It was allowed to rectify its own current of 18 to 20 m-amp., which was supplied by a transformer operating at about 40 peak kv. Surrounding the tube to eliminate stray x-rays was a cylindrical lead sleeve, insulated from the glass walls of the tube by about 1.2 mm of mica. In this sleeve there was an aperture to permit x-rays to proceed in the direction of the radiator. The crystal was set in plaster of Paris and the crystal and slit were supported in a frame rigidly attached to the lead sleeve and were enclosed by lead except as indicated in Fig. 1.

The distance from the target to the radiator was 10 cm. The slit was .4 mm wide and 2.2 cm long and the distance from the slit to the film was about 30 cm.

An enlargement of the best of several photographs thus obtained is reproduced in Fig. 2. The negative shows plainly the molybdenum K$\alpha$ and $\beta$ lines. This represents an exposure, using an intensifying screen, of 32 hours with a paraffin radiator and 16 hours with a zirconium

Fig. 2. Enlargement of the spectrogram of which the density distribution is given in Fig. 3.

radiator. Attempts to secure photographs in which the molybdenum K$\beta$ modified and unmodified lines were strong enough to measure precisely were unsuccessful, due partly to the difficulty of making a tube operate under the conditions of the experiment with sufficient life to permit an exposure of the required length.

*Determination of* $\phi$. The angle $\phi$ between a line joining the center of the focal spot and the radiator and a line from the radiator to the crystal,

was determined by a geometrical method to be 169.7°. As we have seen, the variation in $\phi$ due to the fact that different portions of the scattered x-rays come from different portions of the radiator, is practically negligible; but there is a certain range of values of $\phi$ which results from the length of the slit and the size of the target. Rays which pass through the end of the slit are scattered at a larger angle than those which pass through the center. The range of $\phi$ due to the length of the slit was from 167.7 to 169.7°.

The target was photographed by allowing rays to pass through a pin-hole in a sheet of lead. From the size of the photograph and the distance of the film and target from the pin-hole, the size of the portion of the target from which x-rays proceeded was calculated. This was found to

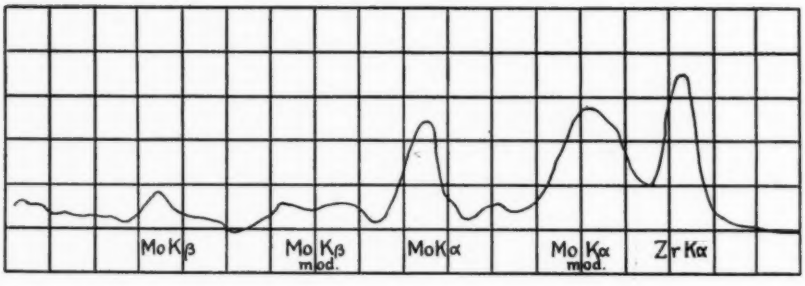


Fig. 3. Microphotometric measurement of the spectrogram reproduced in Fig.2.

be .5 cm in the vertical direction. The center of the target was 1.6 cm below the image of the slit. The smallest distance from the target to the image of the slit was thus 1.35 cm, and the largest distance 1.85 cm. Taking this into account the range of $\phi$ was from 166.3 to 171.5°.

*Measurement of* $\delta\lambda$. Measurements of $\delta\lambda$ were made on the film shown in Fig. 2. For this purpose 16 curves for different portions of the film were made with a microphotometer which consisted of a Coblentz thermopile of about 20 elements connected with a Leeds and Northrup high sensitivity galvanometer. One of these curves is shown in Fig. 3. The position of each peak was determined by making several measurements of the middle of the upper tenth of the curve representing the spectrum line. If $b$ is the measured distance in centimeters between the Mo K$\alpha$ peak and the Mo K$\alpha$ modified peak, $a$ the distance between the Mo K$\alpha$ peak and the Zr K$\alpha$ peak, and $\Delta$ the wave-length difference between the Mo K$\alpha_1$ and the Zr K$\alpha_1$ lines, the value of $\delta\lambda$ is approximately

$$\delta\lambda = (b/a)\Delta \qquad (2)$$

The value of $\Delta$ according to the recent wave-length determinations of Leide,[5] is $0.78429-0.70780=0.07649$A.

In order to obtain a precise result the following small corrections were applied:

(a) On the Mo K$\alpha$ peak: (1) For the effect of the $\alpha_2$ line in shifting the peak, due mainly to the $\alpha_1$ line. (2) For the effect of the Zr K$\beta$ line in shifting the peak of the combined Mo K$\alpha_1$ and Mo K$\alpha_2$ line.

(b) On the Mo K$\alpha$ modified peak: For the effect of the modified $\alpha_2$ line.

(c) On the Zr K$\alpha$ peak: (1) For the effect of the $\alpha_2$ line in shifting the $\alpha_1$ peak. (2) For the effect of the modified Mo K$\alpha$ line in shifting the Zr K$\alpha_1$ and K$\alpha_2$ peak.

(d) A correction to change from the measurement of the angle to the measurement of the sine, since $\lambda$ is proportional to $\sin\theta$.

The calculation of these corrections was facilitated by the observation that the photometer curve representing a simple spectrum line can be represented very approximately by an expression of the form $y=y_0e^{-x^2}$. When these corrections are taken into account, the change of wave-length can be expressed as

$$\delta\lambda=(b/a)\ (.07658\text{A})-.00040\text{A}. \qquad (3)$$

This differs from the approximate relation (2) by only 0.7 percent. The average value of $\delta\lambda$ thus obtained from 16 photometric curves is

$$\delta\lambda=(.04825\pm.00017)\text{A}. \quad \text{(expt.)}$$

In calculating $\delta\lambda$ from Eq. (1), we may take $1-\cos\phi=1.984\pm.001$. The value of $h$ as determined by Duane, Palmer and Chi-Sun-Yeh[6] is $(6.556\pm.0009)\times10^{-27}$ erg sec. $m$ is given by the expression $m=e/(e/m)$, where for $e$ we may use Millikan's[7] value of $(4.774\pm.005)\times10^{-10}$ e.s.u., and for $e/m$ Babcock's[8] value $(1.761\pm.001)\times10^{7}$ e.m.u. These values give

$$\delta\lambda=(.04798\pm.00009)\text{A}. \quad \text{(theory)}$$

This differs from the experimental value by an amount which is just within the combined probable error.

*Discussion.* This result is an excellent confirmation of the quantum formula for the change of wave-length of scattered x-rays.

[5] A. Leide, Comptes Rendus **180,** 1203 (1925).
[6] Duane, Palmer and Chi-Sun-Yeh, Jour. Opt. Soc. Am. **5,** 396 (1921).
[7] R. A. Millikan, Phil. Mag. (July, 1917).
[8] H. D. Babcock, Astrophysical Jour. **58,** 149 (1923).

If we write Eq. (1) in the form

$$m = h(1-\cos\phi)/c\delta\lambda\ ,$$

we see that a measurement of $\delta\lambda$ affords a method of measuring the mass of the electron, which is independent of $e/m$. This is of especial interest in view of the fact that the spectroscopic values of $e/m$ are consistently lower than those obtained by the deflection of streams of electrons.[9] Using for $c$ the value $2.9986\times10^{10}$ cm/sec and for $h$, $\delta\lambda$ and $\phi$ the values given above, $m$ is thus found to be $(8.99\pm.034)\times10^{-28}$ gm. This value is probably not as accurate as the value $(9.04\pm.01)\times10^{-28}$ gm based on Babcock's spectroscopic determinations of $e/m$; but it is interesting to note that it lies closer to the value $8.98\times10^{-28}$ gm calculated from Birge's average $e/m = 1.773\times10^{7}$ e.m.u. based chiefly on deflection experiments.[10]

In conclusion the writer desires to express his appreciation of the continued encouragement given by Professor A. H. Compton, who suggested the problem and has directed the work on it, and to acknowledge his indebtedness to his friend Mr. Y. H. Woo for assistance in evacuating the x-ray tubes.

RYERSON LABORATORY,
UNIVERSITY OF CHICAGO,
Sept. 22, 1925.

[9] Cf. Babcock, loc. cit.[8]
[10] R. T. Birge, Phys. Rev. **14**, 363 (1919).

# THE DIRECTION OF EJECTION OF PHOTO-ELECTRONS PRODUCED BY X-RAYS

By D. H. Loughridge

Abstract

Stereoscopic photographs of photo-electrons produced by 40 kv Mo Kα x-rays, were examined by a stereoscopic comparator which gave a quantitative measure of the initial direction of ejection in space. The measurement of twenty-four distinct tracks in a series of twenty-nine pairs of photographs showed that the most probable angle of ejection was about 70° with the primary beam. This supports the view that the electric vector of the radiation plays a very important part in the production of photo-electrons. The small forward or backward component, noticed in many tracks, must come from the random momentum of the electron in its orbit before ejection.

IT has been shown by Bothe[1] that the most probable direction of ejection of photo-electrons produced in various gases by x-rays of varying hardness, makes an angle between 80 and 85° with the primary beam. This varies slightly with the gas and with the hardness of the rays. P. Auger[2] has also reported similar results. However, C. T. R. Wilson observed three characteristic angles of ejection of photo-electrons in air, namely 45, 90, and 135° with the primary beam. The present experiment was performed in order to measure accurately the initial angles of ejection of photo-electrons in air produced by radiation of a definite frequency.

## Experimental Procedure

Stereoscopic photographs were taken of the photo-electron tracks produced in moist air at atmospheric pressure by the Kα radiation from molybdenum. The beam of x-rays (Fig. 1) from the molybdenum target of a water-cooled Coolidge tube, operated at about 40 kv and 35 m-amp., was sent horizontally through lead collimating slits and a zirconium oxide filter which gave practically homogeneous radiation. This beam passed through a Wilson cloud expansion chamber about 11 cm in diameter. An electric field of about 100 volts per cm was maintained, except when the picture was taken, between the top of the piston and the lower surface of the chamber top. The construction and assembly of the expansion chamber was similar to that described by C. T. R. Wilson.[3] An arc with

[1] Bothe, Zeits. f. Phys. **26**, 59-73 (1924).
[2] P. Auger, Comptes Rendus **178**, 929 (1924).
[3] C. T. R. Wilson, Proc. Roy. Soc. **104**, p. 1 (1923).

Sperry searchlight carbons, was used as a source of illumination. During adjustment of the apparatus it was operated at about 15 amp. but just before a picture was taken the current was increased to 100 amp. by short circuiting a series resistance. A shutter kept the light out of the chamber except when needed. This precaution was found necessary as even very slight heating effects within the chamber produced vortex motion of the gas which distorted the tracks. The illumination was sent in horizontally, by suitable condensing lenses, at right angles to the x-ray beam. The matched lenses were Tessar $f/4.5$, 5.5 cm focus and were mounted in a box camera with their centers 6.5 cm apart. A Graflex focal plane shutter which exposed the two plates simultaneously and was released by a plunger type solenoid, regulated the exposure. Eastman Speedway $3\frac{1}{4}\times4\frac{1}{4}''$ plates were used.

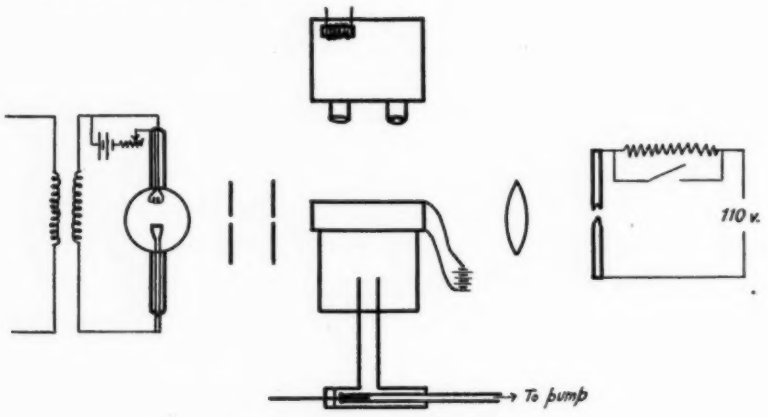


Fig. 1. Diagram of apparatus.

The timing was performed by two falling balls, released simultaneously by two solenoids in series; the first ball caused the expansion by opening the valve underneath the piston and the second ball, immediately afterward, closed the primary switch of the transformer operating the x-ray tube and then closed the circuit which operated the camera shutter. The adjustments on all these devices were regulated until sharp photographs were obtained. The switch, which controlled the solenoids holding the falling balls, also cut off the electrostatic field in the chamber.

## Results

A series of 26 pairs of photographs were obtained using expansion ratios between 1.29 and 1.34. Some of these contained too many tracks for accurate measurement but, by cutting down the size of the x-ray beam, photographs were obtained where distinct photo-electron tracks

could be found which did not overlie any others and were sharply in focus. The depth in the photograph was obtained by using a stereocomparator and the height and breadth were measured directly on the plate by dividers. By thus obtaining the difference between the coordinates of the initial point of the track and point where the first bend occurred, the initial direction of ejection in space could be calculated. For the calculation of the depth in the picture the angle between the optic axes of the two lenses was needed, which was 13°.

Twenty-five distinct tracks were found in the series of photographs. In all of these there was no ambiguity as to which was the head of the track. Arranged in order of increasing angle between the primary beam and the initial part of the track, the values found are 21, 45, 48, 49, 52, 53, 59, 59, 67, 69, 70, 73, 74, 80, 84, 88, 90, 96, 99, 100, 104, 107, 119 and 123°. These values are plotted in Fig. 2, with angles as abscissas, and the number

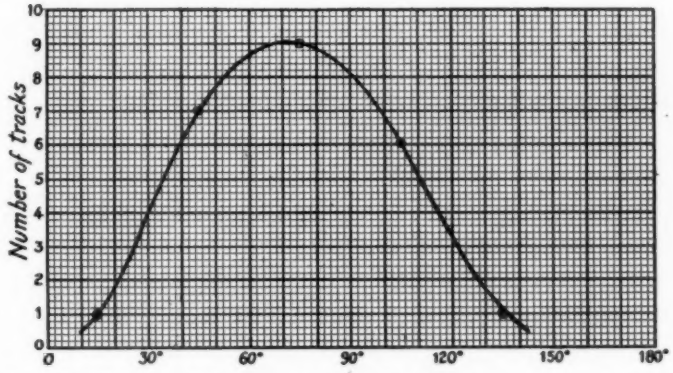


Fig. 2. Distribution of the directions of the 24 photo-electron tracks with respect to the x-ray beam.

of tracks starting within each 30° interval as ordinates. The curve clearly shows a marked angle of most probable emission around 70°. Practically the same maximum is obtained if the angular intervals chosen for plotting are 10°, 15°, 45°, or 60°; but the number of data hardly justifies the smaller intervals while the larger intervals give too few points to insure a clear curve. It is felt that the 30° interval chosen shows the effect fairly and clearly. It should also be pointed out that tracks lying close to 0° or 180° with the primary beam, would be the easiest to measure as they would all lie more nearly in the plane of the plate, while the ones bunched around 90° would contain some lying perpendicular to the plane of the plates and would therefore be more difficult to see. Thus it is obvious that if there existed a random distribution of the directions of

ejection one would probably find more around 0° and 180° than around 90°.

This tendency for the emission at nearly right angles to the primary beam is in agreement with the view that the electric vector of the rays plays a very important part in the process. In fact, Bubb has shown[4] that when polarized x-rays are used the most probable direction of emission lies in the plane containing the electric vector.

The small forward component noticed in most of the tracks supports the view that the energy of the primary quanta is imparted to the photo-electron by a forward impulse along with the sidewise impulse of the electric vector.[5] Because of these two effects alone, on the basis of conservation of momentum, no tracks with backward components would be expected, but by combining with them the random momentum of the electron in its orbit, a backward momentum becomes possible.

I am grateful to Professor R. A. Millikan for his advice and inspiration during the progress of this work.

NORMAN BRIDGE LABORATORY,
CALIFORNIA INSTITUTE OF TECHNOLOGY,
PASADENA, CALIFORNIA.
September 18, 1925.

[4] Bubb, Phys. Rev. **23,** p. 137 (1924).
[5] Bubb, Phil. Mag. **49,** p. 824 (1925).

# A REINVESTIGATION OF THE WAVE-LENGTHS AND RELATIVE INTENSITIES IN THE MOLYBDENUM K SERIES X-RAY SPECTRUM

By Samuel K. Allison[1] and Alice H. Armstrong

Abstract

The x-ray beam from a water-cooled target of a tube carrying 25 m-amp. from a 50 kv storage battery, was limited to 2 minutes and reflected from a calcite crystal of a spectrometer with a Genevoise scale reading to 2 seconds, into an ionisation chamber. The 3rd to 5th orders were used. The angle of reflection for each wave-length was determined by readings on both sides of the direct beam. Corrections were applied for the temperature of the crystal above 18°, for the eccentricity of the scale and for refraction. *The wave-lengths* are found to be (taking $d=3.028$A): $\alpha_2=.711835$, $\alpha_1=.707525$, $\beta_3=.631354$, $\beta_1=.630791$, $\gamma=.619526$. From 3 to 5 determinations were made for each line, the average deviation from the mean being .000025. The mean deviation from the last results of A. Leide is .00003 except for $\beta_1$ for which his value seems too high. The separation $\beta_3-\beta_1$ is .000563 in good agreement with the separation $L\beta_3-L\beta_4$ determined by Coster. The wave-lengths taking $d=3.02904$A and the $\nu/R$ and $\sqrt{\nu/R}$ values for the K lines and for the corresponding energy levels in the Mo spectrum are also given. The K absorption limit was found at .61830A. *Relative intensities.* Assuming each component of the $\beta$ doublet to be a single line of the same width, the relative intensities come out $K\beta_1/\beta_3=2.0$, in agreement with the theoretical predictions of Sommerfeld and of Coster and Goudsmit. In the case of the $\beta$ and $\gamma$ doublets the total intensity of each doublet was taken proportional to the area under it, correcting for the K absorption in the case of the $\gamma$ peak. The relative intensities then come out $K\beta/\gamma=7.7$, which is greater than the corresponding ratio for tungsten, indicating a decrease with increasing atomic number.

## Apparatus and Method of Measuring Wave-lengths

THIS paper is a report of experiments carried out in the laboratory of Professor William Duane at Harvard University. We have remeasured the wave-lengths of the lines in the molybdenum K series spectrum, and have redetermined the relative intensities of some of the lines which are not widely separated in wave-length.

The apparatus available for this investigation had several advantages over that with which the previous work on the molybdenum spectrum in this laboratory was performed. (1) We had at our disposal an ionisation spectrometer with a Genevoise scale, on which settings could be made to 2 seconds of arc. (2) Tubes with water-cooled targets were employed which permitted the use of much more power than that used

[1] National Research Fellow.

in the previous work. (3) A new 50,000 volt high capacity storage battery made it possible to operate at higher voltages and currents for longer intervals than before.

The new storage battery and general arrangement of the apparatus have been described.[2] The spectrometer measurements were made by the ionisation method, as used previously in this laboratory. The position of the crystal was read on the accurate silver scale with a traveling microscope, and the ionisation chamber was set approximately by reading its position on a brass scale concentric with the silver scale. Approximate settings of the ionisation chamber were sufficient to follow the reflected beam since the slit in front of the chamber was quite wide (6-8 mm). All angular readings used in the calculation of wave-lengths were settings of the crystal table. The x-ray beam incident upon the crystal was limited by two slits 37 cm apart. The slits were of approximately the same width, and limited the angular breadth of the beam to about 2 minutes of arc. The vertical height of the beam was limited by a stop 1 cm high placed between the x-ray tube and the crystal 5 cm from the crystal.

In the experiments on the wave-lengths of lines, the x-ray tube was run at 25 milliamperes and a constant battery voltage of about 50 kilovolts. The ionisation currents were read on an electrometer and scale system whose sensitivity was about 3 meters per volt.

The wave-length measurements reported here were all obtained in higher orders of reflection from calcite. In the crystal used there was no good evidence of broadening of the lines in higher orders. In a determination of wave-length, the crystal was rotated in steps of 15 seconds each through the angular range in which the center of a line had been found to lie by previous trials. Two settings could thus be located at which the ionisation current was higher than for any other two in the vicinity, and from the relative intensities at these two settings the position of the line could be estimated within 2 or 3 seconds of arc.[3] The crystal table and ionisation chamber were then at once shifted so that the same wave-length was reflected from the crystal on the opposite side of the direct beam, and again the setting of the crystal for the center of the line was determined. The temperature was taken during each observation. The two determinations of angle were made as nearly simultaneously as possible because it was found that from day to day, from unknown causes, the position of the crystal at which maximum reflection in a line was obtained varied through an angular range which

[2] Armstrong and Stifler, J. Opt. Soc. Amer. and Rev. Sci. Inst. **11**, 509 (1925).
[3] Cf J. C. Hudson, J. Opt. Soc. Amer. and Rev. Sci. Inst. **9**, 259 (1924).

in some cases was as large as a minute of arc. We have made determinations of angles of reflection in which the setting of the crystal was varied in steps of less than 15 seconds, but we believe that no additional accuracy is thereby gained.

In the measurement of the molybdenum K critical absorption wave-length, we used general radiation from a tube with a water-cooled copper target containing a button of tungsten. The absorbing substance was a screen of ammonium molybdate. The width of the beam in the absorption measurements was slightly over 4 minutes of arc. The angular measurements were made in the same way as those for line wave-lengths, except that the angular reading corresponding to an absorption wave-length is that of a point on the discontinuity half way between the base-lines of the radiation of shorter and longer wave-lengths.

## Corrections and Sources of Error

It is well known that in this method of measurement, in which the wave-lengths are calculated from angular settings of the crystal, the penetration of the rays into the crystal before reflection introduces no error. Since, also, the face of the crystal may be considered plane, no appreciable error is introduced if the point of effective reflection of the beam does not lie exactly in the axis of rotation of the spectrometer. In our experiments the method of making the point of effective reflection coincide approximately with the axis of rotation of the spectrometer was to limit by a narrow slit the beam entering the ionisation chamber, and then to vary the position of the crystal and other slits until the angle through which the ionisation chamber was turned to obtain maximum intensity for the beam reflected from the crystal was just twice the angle traversed by the crystal over a large range.

If the sleeve which carries the microscopes and crystal does not rotate about the same vertical axis as that which carries the scale, the angle as read on the scale by one microscope will not be the true angle between the two settings of the crystal. The true angle may be ascertained by reading two microscopes, $A$ and $B$, at each setting. $A$ and $B$ on our instrument are very nearly 180° apart. The true angle through which the crystal is turned is the average of the apparent angles as read on $A$ and $B$. Before measuring the wave-lengths of the molybdenum lines, we determined the correction to be applied to the scale in the region in which angular settings would be taken. We found that a correction of 6 seconds should be added to the apparent angle (35° to 70°) as read on microscope $A$. The eccentricity, of course, varied somewhat with the settings, but the variations were well within the limit of error of locating the

peaks, and we have corrected all readings on microscope $A$ in this range by 6 seconds. In the measurement of the wave-lengths of lines, all settings were made with vernier $A$ alone. This technique is probably not the best, as it is known that the eccentricity varies somewhat with temperature and other factors; therefore it would be advisable to read both microscopes for every wave-length determination. After the wave-lengths had been measured, we redetermined the eccentricity in the same part of the scale as before and found that it was not the same, but that the variations were well below the error in locating the positions of the lines themselves.

In the measurement of the critical absorption wave-length, the apparatus was slightly modified so as to permit the reading of both microscopes at once. The readings were taken in a different part of the scale, in which the eccentricity correction to be applied to $A$ was only two seconds.

The observed wave-lengths were corrected for the temperature of the crystal from the table in Siegbahn's "Spektroskopie der Röntgenstrahlen," p. 87. All corrections were made to a temperature of 18°C.

It is now known that a correction must be applied to the wave-length calculated by the simple Bragg law on account of the fact that the index of refraction of the crystal for the x-rays becomes appreciable when precision measurements are made. The true wave-length in air may be obtained by the formula[4]

$$n\lambda = 2d \sin\theta(1-\delta/\sin^2\theta) \qquad (1)$$

where $\lambda$ is the true wave-length in air, $d$ is the grating space, $\theta$ is the observed glancing angle, and $\delta = 1-\mu$, where $\mu$ is the index of refraction of the crystal for the x-rays. Hatley[5] has adopted a suggestion of Bergen Davis and by an ingenious method obtained a measurement of the index of refraction of calcite for Mo K$\alpha_1$ x-rays. The value given by Hatley for $\delta$ is $2.03\times10^{-6}$, which agrees well with that calculated by the Lorentz dispersion formula. In the higher orders of reflection, where $\theta$ is large, it may be seen from Eq. (1) that the deviation from the Bragg law is very slight. In the first order it is about $-.0001$A for Mo K$\alpha_1$ from calcite. We have neglected the change of index of refraction with wave-length throughout the molybdenum spectrum. We have instead based our calculations on the value given by Hatley, and have used for $\theta$ an angle lying between the critical angles for Mo K$\beta$ and Mo K$\alpha$. The extent of the correction applied is shown in the tables.

[4] A. H. Compton, Phil. Mag. **45**, 1121 (1923)
[5] C. C. Hatley, Phys. Rev. **24**, 486 (1924).

A possible source of error of unknown magnitude lies in the ruling of the scale of the instrument itself. It is quite possible that certain regular variations may recur in the rulings of these scales; through intervals of a degree or so five minute marks may be one or two seconds displaced. It seems unlikely that in the large angles measured such a periodic variation would introduce appreciable error. No calibration of the scale of our instrument has been attempted; accordingly our measurements are subject to such errors as may occur in the scale itself.

### Method of Calculation of Wave-length

Different investigators are not yet agreed on the proper value of $d$ for calcite. Recently A. H. Compton, O. K. DeFoe, and H. N. Beets[6] have redetermined the density and rhombohedral angle of calcite, and have recommended for $d$ the value used by Siegbahn in the calculation of his results, namely $3.02904 \times 10^{-8}$ cm at 18°C. The wave-lengths previously measured in this laboratory and some determined by Bergen Davis and his collaborators have been calculated on the basis $d = 3.028 \times 10^{-8}$ cm at 18°C. There seems to be some ground for the opinion that higher values of density should be given more weight than lower values in the averaging of a series of determinations. If this is true, then lower values of $d$ are more likely to be correct. The wave-lengths reported here are given both on the basis $d = 3.028$A and on $d = 3.02904$A at 18°C.

Compton and his collaborators report that in their measurements of the densities of representative samples of calcite differences in density greater than the experimental error occur. This at once raises the question of the generality of wave-length determinations based on crystalline diffraction. It seems highly probable that the precision measurements of wave-length now possible should be found to depend on the particular calcite crystal used, on account of the varying composition of calcite. The varying amounts of impurity in calcite may be a source of the discrepancies found in the wave-length determinations by different investigators. We know nothing of the previous history of the sample of calcite which we used. It is a small, clear, museum specimen which was found by trial to give sharp lines in higher orders of reflection.

The method employed in the calculation of the wave-length in air at 18°C from the observed angle was as follows. From the observed glancing angle a preliminary wave-length was calculated on the basis $d = 3.028$A. This preliminary wave-length was then corrected to 18°C; this correction was in general a small positive one, since the temperatures were usually above 18°C. After a number of these corrected preliminary

[6] Compton, DeFoe and Beets, Phys. Rev. **25**, 618-629 (1925).

wave-lengths had been obtained in the same order of reflection, they were weighted as to reliability and averaged. The true wave-length in air was obtained by correcting the order average for refraction. The temperature corrections were very small, as were also, on account of high order, those for refraction.

TABLE I

*Wave-lengths of Mo K series lines.*

Wave-lengths in this table are in angstroms and have been calculated on the basis $d(18°) = 3.028$A.

| | Order | Date | λ at 18°C | Wt. | av. λ for order | Corr. for refraction | λ in air at 18°C | Wt. | Final λ |
|---|---|---|---|---|---|---|---|---|---|
| $K\alpha_2$ | Third | Mar. 23 | .711789 | (1) | .711789 | −.000012 | .711777 | (1) | |
| | Fourth | Mar. 26 | .711834 | (1) | | | | | |
| | | Mar. 26 | .711670 | (0) | | | | | |
| | | Mar. 27 | .711897 | (1) | | | | | |
| | | Mar. 27 | .711834 | (1) | | | | | |
| | | Mar. 27 | .711862 | (1) | .711857 | −.000007 | .711850 | (4) | .711835 |
| $K\alpha_1$ | Third | Feb. 26 | .707558 | (1) | | | | | |
| | | Mar. 21 | .707590 | (1) | | | | | |
| | | Mar. 23 | .707577 | (1) | .707575 | −.000012 | .707563 | (3) | |
| | Fourth | Mar. 21 | .707535 | (1) | | | | | |
| | | Mar. 23 | .707534 | (1) | | | | | |
| | | Mar. 24 | .707484 | (1) | .707518 | −.000007 | .707511 | (3) | |
| | Fifth | Mar. 24 | .707453 | (1) | | | | | |
| | | Mar. 24 | .707532 | (1) | | | | | |
| | | Mar. 24 | .707532 | (1) | .707506 | −.000004 | .707502 | (3) | .707525 |
| $K\beta_1$ | Fourth | Mar. 5 | .630778 | (1) | | | | | |
| | | Mar. 7 | .630801 | (1) | .630790 | −.000007 | .630783 | (2) | |
| | Fifth | Mar. 12 | .630852 | (1) | | | | | |
| | | Mar. 17 | .630772 | (1) | | | | | |
| | | Mar. 17 | .630776 | (1) | .630800 | −.000004 | .630796 | (3) | .630791 |
| $K\gamma$ | Fourth | Mar. 13 | .619543 | (1) | | | | | |
| | | Mar. 14 | .619513 | (1) | | | | | |
| | | Mar. 17 | .619543 | (1) | .619533 | −.000007 | .619526 | | .619526 |
| $K_{abs}$ | Third | May 2 | .61848 | (1) | | | | | |
| | | June 8 | .61802 | (½) | | | | | |
| | | June 8 | .61832 | (1) | | | | | |
| | | June 8 | .61828 | (1) | .61831 | −.00001 | .61830 | | .61830 |

The later steps of the calculation are shown in Table I. Each of these determinations is an absolute measurement in the sense that $2\theta$ was measured directly. All the wave-length determinations which were made are included in the table. One measurement of $K\alpha_2$ gave a value so far from the mean of the others that we have not included it in the average and have weighted it zero.

In the fourth and, especially, the fifth orders, we obtained a good separation of the Mo Kβ doublet. This was announced in a preliminary

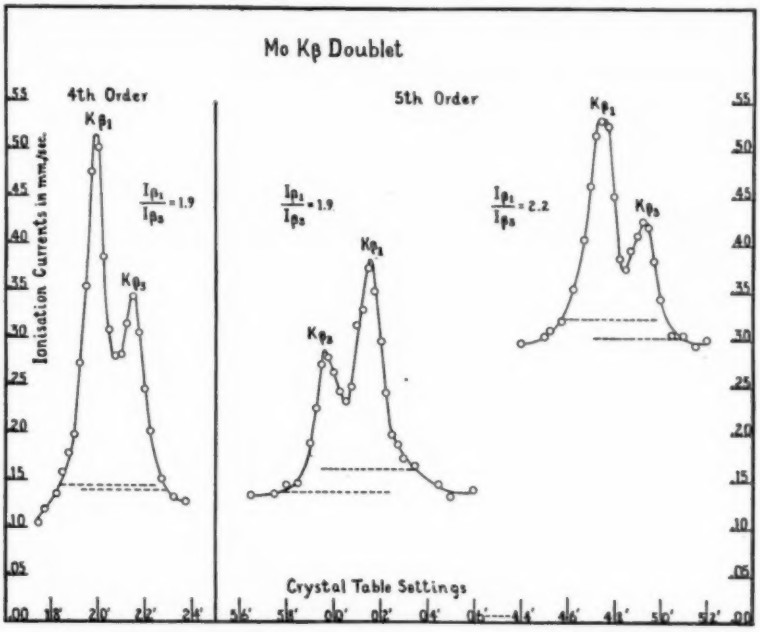


Fig. 1. Separation of Mo Kβ doublet.

report.[7] Some of the curves obtained are shown in Fig. 1 and the results in Table II. The doublet nature of this line has been experimentally

TABLE II

*Separation of Mo Kβ doublet and wave-length of Mo Kβ₁.*
Wave-lengths in this table are in angstroms and have been calculated on the basis $d(18°) = 3.028$ A.

| Order | Date | Separation | Wt. | Δλ | Average | Final Δλ | Mo Kβ₁ |
|---|---|---|---|---|---|---|---|
| Fourth | Mar. 10 | 1′22″ (L) | (1) | .000545 | | | |
| | Mar. 7 | 1′31″ (R) | (1) | .000606 | .000576 | | |
| Fifth | Mar. 10 | 1′56″ (L) | (1) | .000580 | | | |
| | Mar. 12 | 1′44″ (R) | (1) | .000520 | .000550 | .000563 | .631354 |

observed in Mo and other elements by various authors.[8] According to the accepted energy level diagram the same frequency difference should

[7] Allison and Armstrong, Phys. Rev. **25,** 882 (1925).

[8] M. de Broglie, Compt. Rend. **170,** 1053 and 1245 (1920).
Duane and Patterson, Bull. Nat. Res. Counc. Vol. 1, Part 6, p. 393 (1920).
C. B. Crofutt, Phys. Rev. **24,** 9 (1924).
A. Leide, Compt. Rend. **180,** 1203 (1925).

appear between the lines $L\beta_3$ and $L\beta_4$. Coster[9] has measured the wave-lengths of Mo $L\beta_3$ and Mo $L\beta_4$ and has found for the wave-lengths 5.0002 and 5.0358A respectively. From these values it may be calculated that the wave-length difference in the $K\beta$ doublet should be .000564A. Our observed value of .000563A agrees closely with this. The separation of .00039A reported by Leide[8] agrees less well with the measurements of Coster in the L series.

TABLE III

*Wave-length, $\nu/R$, and $\sqrt{\nu/R}$ values for Mo K spectrum.*

| Line | $\lambda$ | | $\nu/R$ | | $\sqrt{\nu/R}$ | |
|---|---|---|---|---|---|---|
| | $d=3.028$A | $d=3.02904$ | $d=3.028$ | $d=3.02904$ | $d=3.028$ | $d=3.02904$ |
| $K\alpha_2$ | .711835A | .712078 | 1280.17 | 1279.73 | 35.7795 | 35.7734 |
| $K\alpha_1$ | .707525 | .707768 | 1287.97 | 1287.53 | 35.8882 | 35.8821 |
| $K\beta_3$ | .631354 | .631571 | 1443.36 | 1442.86 | 37.9915 | 35.9850 |
| $K\beta_1$ | .630791 | .631009 | 1444.65 | 1444.15 | 38.0085 | 38.0020 |
| $K\gamma$ | .619526 | .619737 | 1470.91 | 1470.41 | 38.3525 | 38.3460 |
| $K_{abs}$ | .61830 | .61851 | 1473.83 | 1473.33 | 38.391 | 38.384 |

Table III contains a summary of the wave-length values and the $\nu/R$ ($R=109737$) and $\sqrt{\nu/R}$ values calculated from them. Table IV contains some of the energy levels which can be computed from the observed values in the K series by means of the combination principle.

TABLE IV

*Energy levels in the Mo spectrum.*

| Level | $\nu/R$ | | $\sqrt{\nu/R}$ | |
|---|---|---|---|---|
| | $d=3.028$A | $d=3.02904$ | $d=3.028$ | $d=3.02904$ |
| $K_{11}=K_{abs}$ | 1473.83 | 1473.33 | 38.395 | 38.384 |
| $L_{21}=K_{11}-K\alpha_2$ | 193.66 | 193.60 | 13.916 | 13.914 |
| $L_{22}=K_{11}-K\alpha_1$ | 185.86 | 185.80 | 13.633 | 13.631 |
| $M_{21}=K_{11}-K\beta_3$ | 30.47 | 30.47 | 5.520 | 5.520 |
| $M_{22}=K_{11}-K\beta_1$ | 29.19 | 29.18 | 5.403 | 5.402 |
| $N_{21}N_{22}=K_{11}-K\gamma$ | 2.92 | 2.92 | 1.71 | 1.71 |

In Table V we have given the results of other investigators who have measured the wave-lengths of the Mo K series. The values given by C. C. Hatley and by R. von Nardroff are corrected for index of refraction but apparently not for temperature of the crystal. As far as we know, these corrections have not been applied to the other previous measurements which we have listed. The later measurements of Leide agree well with the ones reported here, except for the line $K\beta_1$. In addi-

[9] D. Coster, Phil. Mag. **43**, 1070 (1922).

tion to the lines listed in Table V, Leide has reported a new line $\beta_4$ which he attributes to the transitions $\overline{O_{21}O_{22}} \rightarrow K_{11}$. One of us[10] has commented on this reported line, which should lie between K$\gamma$ and the absorption limit. According to the prevalent electron distribution schemes, such a line would probably be semi-optical. The corresponding transition

TABLE V

*Comparison of results of different investigations of the wave-lengths of the Mo K series lines.*

| | | K$\alpha_2$ | K$\alpha_1$ | K$\beta_3$ | K$\beta_1$ | K$\gamma$ | K$_{abs}$ |
|---|---|---|---|---|---|---|---|
| Duane and Patterson[9] (1920) | ($d$=3.028) | .71212A | .70783 | .63110 | | .6197 | .61842 |
| Overn[11] (1921) | ($d_{NaCl}$=2.814) | .7131 | .7087 | .6324 | | .6268 | .6214 |
| Leide(1)[12] | ($d$=3.02904) | .71187 | .70759 | .63075 | | .61927 | .... |
| Hatley[5] (1924) | ($d$=3.028) | .... | .707717 | .... | | .... | .... |
| von Nardroff[13] (1924) | ($d$=3.028) | .... | .... | .63102 | | .... | .... |
| Leide(2)[14] (1925) | ($d$=3.02904) | .71208 | .70780 | .63163 | .63124 | .61969 | .... |
| Present results | ($d$=3.028) | .711835 | .707525 | .631354 | .630791 | .619526 | .61830 |
| | ($d$=3.02904) | .712078 | .707768 | .631571 | .631009 | .619737 | .61851 |

in the L series (L$\gamma_4$) has not been observed in molybdenum.[9] In a photograph it might well be difficult to distinguish this line from the Mo K critical absorption which occurs on account of the absorption of the target for its own radiation. We have not observed this line, though we have taken readings in the fourth order through the region in which it should occur.*

## RELATIVE INTENSITIES OF THE LINES

It is now well known from the researches of Duane and Stenström, Duane and Patterson, and Siegbahn and Žáček,[15] that the relative intensity of the components of the K$\alpha$ doublet is 2/1 for a wide range of

[10] S. K. Allison, Nature **115**, 978 (1925).

[11] O. B. Overn, Phys. Rev. **18**, 350 (1921).

[12] A. Leide (1), Siegbahn, "Spektroskopie der Röntgenstrahlen," p. 102.

[13] R. von Nardroff, Phys. Rev. **24**, 143 (1924).

[14] A. Leide (2), loc. cit.[8]

* *Note added to proof.* In a later publication (Thesis, Lund 1925) Leide no longer assigns this line (.61825A) to the transition $\overline{O_{21}O_{22}} \rightarrow K_{11}$, stating that it probably results from a forbidden jump from the levels $N_{IV}N_V$. From photometer curves of the photographs taken by him it appears improbable that the presence of this line can be ascribed to a misinterpretation of the K critical absorption from the target.

[15] These results are summarized in Siegbahn, Spektroskopie der Röntgenstrahlen, p. 97.

elements. We have not attempted any experiments expressly designed to confirm this fact for molybdenum.

In our investigation of the Mo K$\beta$ doublet we have been able to measure the relative intensities of K$\beta_1$ and K$\beta_3$, and we find, within the limit of experimental error, the ratio 2/1 for $\beta_1/\beta_3$. M. de Broglie noted in his first measurement of the doublet that the component of longer wave-length was the one of lesser intensity, and our work confirms this observation. The very small difference in wave-length between the components makes corrections for differential absorption by the walls of the tube, etc., unnecessary. Since, however, the doublet is not completely separated even in the fifth order, it is essential to make some assumptions concerning the base-line under each peak. In the first place, we have assumed that each component of the doublet is itself a single line, and that both components have the same intrinsic wave-length breadth. In this case, then, it is permissible to take the ordinate from the tip of the peak to the radiation under the tip (from other sources) as proportional to the intensity of the component. In addition we have asssmed that the peaks representing the components are symmetrical about the ordinates determined by their tips. Then, if the separation of the doublet is $\Delta\lambda$, we may take the radiation at a point corresponding to $\lambda\beta_1-\Delta\lambda$ as the base-line for K$\beta_3$. This will include the general radiation under K$\beta_3$ and, by the symmetry assumption, also the amount of K$\beta_1$ which, because of incomplete resolution, is under the tip of K$\beta_3$. In the same way the radiation at $\lambda\beta_3+\Delta\lambda$ may be used as the base-line for K$\beta_1$. The base-lines given by this method are shown as dotted lines in Fig. 1. The method can be applied only when the resolution is great enough so that there is no appreciable radiation from $\beta_1$ at $\lambda\beta_3+\Delta\lambda$ and vice versa. The results of three of the most trustworthy measurements are given in Fig. 1 and Table VI.

TABLE VI

*Relative intensity of the lines Mo K$\beta_1$ and K$\beta_3$.*

| Date | Order | Ratio $\beta_1/\beta_3$ | Wt. | Average |
|---|---|---|---|---|
| Mar. 7 | 4 | 1.9 | (1) | |
| Mar. 10 | 5 | 1.9 | (1) | |
| Mar. 12 | 5 | 2.2 | (1) | 2.0 |

Duane and Patterson[16] have measured the relative intensity of Mo K$\beta$ to Mo K$\gamma$ in the first and second orders and have found 6.3 and 5.5 respectively. They obtained this ratio from the highest points on the two peaks. Although this method is sufficient for a first approximation,

[16] Duane and Patterson, Phys. Rev. **19**, 542 (1922); also, Proc. Nat. Acad. Sci. **8**, 85 (1922).

a better procedure is probably to consider the *area* under each peak, since $\beta$ and $\gamma$ are both undoubtedly doublets of unequal wave-length separation. We have therefore taken the area under each peak above the general radiation as proportional to its intensity. The area was measured by means of an integraph. A typical curve showing $\beta$ and $\gamma$ is given in Fig. 2. The slits limiting the beam incident upon the crystal were somewhat wider than those used for wave-length measurements. In these experiments on the $\beta$ and $\gamma$ relative intensities, the x-ray tube had a

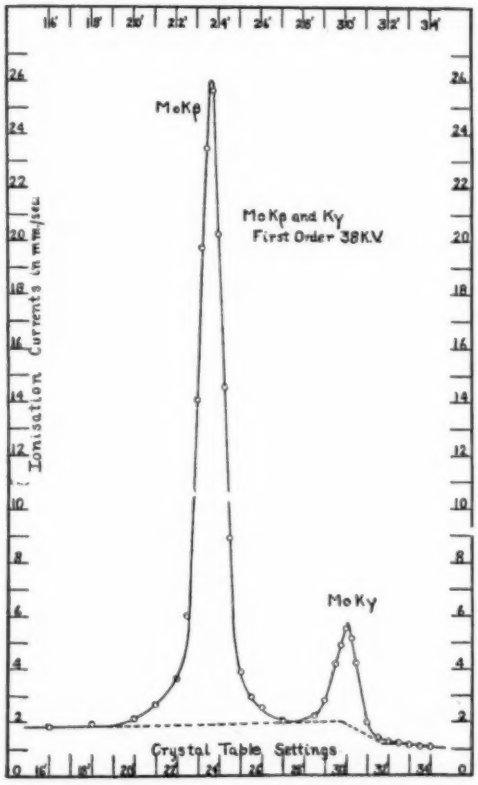


Fig. 2. Relative intensity of Mo K$\beta$ and K$\gamma$.

thin blown-glass window to reduce absorption, and the x-rays entered the ionisation chamber through a mica window .002 cm thick. The presence of absorption by the target itself is shown by the lower base-line on the short wave-length side of $\gamma$. On the assumptions that the center of the critical absorption rise lies 45 seconds to the short wave length side of $\gamma$, and that the breadth of the beam is equal to the breadth of the peak, we have drawn in the discontinuity as it must exist in the general radiation and have thus corrected the area of K$\gamma$. The critical

absorption and base-line are shown in dotted lines in Fig. 2. The results of several measurements of the relative intensity of K$\beta$ to K$\gamma$ are given in Table VII. In these determinations the voltage on the tube and the current through the tube were varied through rather wide limits, but no effect on the relative intensities of the lines could be detected. The relative intensities given are uncorrected for ordinary absorption effects.

TABLE VII

*Relative intensity of the lines Mo K$\beta$ and K$\gamma$.*

| Date | Order | Ratio $\beta/\gamma$ | Wt | Average |
|---|---|---|---|---|
| Mar. 30 | 1 | 7.3 | (1) | |
| Mar. 30 | 1 | 8.5 | (1) | |
| Mar. 31 | 1 | 8.3 | (1) | |
| Apr. 2 | 1 | 8.4 | (1) | |
| Apr. 4 | 1 | 6.6 | (1) | |
| Apr. 4 | 1 | 7.3 | (1) | 7.7 |

The relative intensity of K$\alpha$ to K$\beta$ has been measured for some elements in this region by Unnewehr[17] and by Siegbahn and Žáček.[18] We have not succeeded in obtaining a satisfactory value of this ratio for Mo because of the large correction for absorption which must enter.

## DISCUSSION OF THE INTENSITY RESULTS

Recently Sommerfeld[19] and Coster and Goudsmit[20] have made theoretical predictions of the relative intensities of some doublets and "compound doublets" in x-ray spectra. They have based their predictions on the results of Burger and Dorgelo,[21] who have measured relative intensities in the optical region.

These investigators have found that the relative intensity of the components of the doublets in the principal series ($1s-mp$) of the alkalis is 2/1. The well-known analogy of the x-ray levels to the optical levels of the alkalis would thus lead us to expect that the doublets of the K series would have the same relative intensity, 2/1. By this analogy the K$\beta$ doublet should correspond to the second member of the principal series ($1s-3p_2$, $3p_1$). The experimental intensity ratio reported here confirms the theoretical predictions of Sommerfeld and Coster and Goudsmit. It is also interesting to see that this simple ratio holds even though in falling from the M group to the K group the electrons pre-

[17] E. C. Unnewehr, Phys. Rev. **22**, 529 (1923).
[18] Siegbahn and Žáček, Ann. der Physik **71**, 187 (1923).
[19] A. Sommerfeld, Ann. der Physik **76**, 284 (1925).
[20] D. Coster and S. Goudsmit, Naturwissenschaften **1**, 11 (1925).
[21] Burger and Dorgelo, Zeits. f. Physik **23**, 258 (1924), etc.

sumably pass through the L group. Evidently in this case, at least, the relative intensity is not affected by the intervening group.

No quantitative theory has yet been devised to deal with the relative intensities of such lines as Mo K$\beta$ and K$\gamma$.[22] Duane and Stenström[23] have measured the relative intensity of $\beta$ to $\gamma$ in the K series spectrum of tungsten and find 35/15 or 2.3/1. The observed ratio 7.7/1 in molybdenum shows that the $\gamma$ line grows weaker as the atomic number of the radiating element decreases.

Our thanks are due Professor William Duane for his constant interest in this research.

CRUFT HIGH TENSION ELECTRICAL LABORATORY,
HARVARD UNIVERSITY,
August 11, 1925.

[22] *Note added to proof.* Our attention has been called to the paper of F. C. Hoyt (Phil. Mag. **46,** 135, 1923) (see also article in this issue) in which an attempt was made to calculate the relative intensity of lines of this type by application of Bohr's correspondence principle. A dependence of the relative intensity on the atomic number may be inferred from considerations advanced in this paper.

[23] Duane and Stenström, Proc. Nat. Acad. Sci. 6, 477 (1920).

# EXPERIMENTS ON THE RELATIVE INTENSITIES OF SOME X-RAY LINES IN THE L SPECTRUM OF TUNGSTEN AND THE K SPECTRUM OF COPPER

By Samuel K. Allison[1] and Alice H. Armstrong

Abstract

**Tungsten L series lines.**—The experiments of Duane and Patterson on the strong lines in the L series of tungsten were repeated with improved apparatus, and also some of the weaker lines were studied. The value 10 obtained by Duane and Patterson for the relative intensity of $L\alpha_1$ to $L\alpha_2$ was confirmed. The theoretical ratio is 9. For the $\beta$ group the *relative intensities* were found to be, $\beta_1 : \beta_2 : \beta_3 : \beta_4 : \beta_5 : \beta_6 : \beta_7 : \beta_9 : \beta_{10} = 100 : 49.3 : 15.0 : 7.7 : .47 : 2.0 : .4 : .68 : .60$. The relative intensities of the weak lines among themselves are not very reliable on account of the faintness of the lines and the critical absorption of the target, yet it is clear that the forbidden lines $\beta_9$, $\beta_{10}$ are of the same order of intensity as $\beta_5$, $\beta_7$. For the $\gamma$ group the relative intensities were found to be, $\gamma_1 : \gamma_2 : \gamma_3 : \gamma_4 : \gamma_5 : \gamma_6 : \gamma_8 = 100 : 14.0 : 22.3 : 7.0 : 3.0 : 2.3 : 1(?)$. $\gamma_8$ could not always be obtained. The determination of the intensity ratios for $\alpha_1$, $\beta_1$ and $\beta_2$, $\gamma_1$ was complicated by absorption in the target. The agreement of the observed value of the intensity ratio for $\beta_2/\beta_4$ with the theoretical value 2, tends to confirm Stoner's suggestion that there are twice as many electrons in the $M_{22}$ orbit as in the $M_{21}$. The deviation of the observed intensity ratio for $\gamma_3/\gamma_2$ from 2 may be due to the influence of intervening levels.

**Copper K series lines.**—The average of two determinations of the *relative intensity* of $\beta$ to $\gamma$ gave 100/2.4. No reliable evidence of the non-diagram lines $K\alpha_3\alpha_4$ was obtained at 30,700 volts.

THE experiments of Duane and Stenström[2] on the K series of tungsten and of Duane and Patterson[3] on the L series of tungsten and the K series of molybdenum furnish the first precision measurements of relative intensities of x-ray lines by the ionisation method, although the relative intensities of the K series lines of rhodium are shown in curves published still earlier by Duane and Hu[4] in their study of absorption and emission frequencies.

This problem of the relative intensities of x-ray lines has received a fresh impetus from the work of Ornstein, Burger, and Dorgelo on the relative intensities in the optical region.[5] These investigators have

[1] National Research Fellow.

[2] Duane and Stenström, Proc. Nat. Acad. Sci. **6**, 477 (1920).

[3] Duane and Patterson, Proc. Nat. Acad. Sci. **6**, 518 (1920); ibid **8**, 85 (1922).

[4] Duane and Hu, Phys. Rev. **14**, 369 (1919).

[5] Burger and Dorgelo, Zeits. f. Physik **23**, 258 (1924); etc.;
Ornstein and Burger, Zeits. f. Physik **24**, 41 (1924); etc.

found that the relative intensities of lines in multiplets are expressible in terms of whole numbers and are related to the inner quantum numbers of the states involved by the so-called "sum rules."

A. Sommerfeld[6] and also Coster and Goudsmit,[7] using the well-known optical analogy of the x-ray levels as a guide, have extended the results of Burger and Dorgelo to the region of x-ray spectra. Some of the theoretical relative intensities in the K and L series obtained by this method are shown in Table I.

TABLE I

*Theoretical relative intensities resulting from the extension of the rules of Burger and Dorgelo to x-ray spectra.*†

| | Lines | Optical analogy | Relative intensity |
|---|---|---|---|
| K series | $\alpha_1 : \alpha_2$ | $1s-2p_2,\ 2p_1$ | 2 : 1 |
| | $\beta_1 : \beta_2$ | $1s-3p_2,\ 3p_1$ | 2 : 1 |
| | $\gamma$-doublet | $1s-4p_2,\ 4p_1$ | 2 : 1 |
| L series | $\beta_3 : \beta_4$ | $2s-3p_2,\ 3p_1$ | 2 : 1 |
| | $\gamma_3 : \gamma_2$ | $2s-4p_2,\ 4p_1$ | 2 : 1 |
| | $\gamma_4$-doublet | $2s-5p_2,\ 5p_1$ | 2 : 1 |
| | $l : \eta$ | $2p_2,\ 2p_1-3s$ | 2 : 1 |
| | $\beta_6 : \gamma_5$ | $2p_2,\ 2p_1-4s$ | 2 : 1 |
| | $\beta_7 : \gamma_8$ | $2p_2,\ 2p_1-5s$ | 2 : 1 |
| | $\alpha_1 : \alpha_2 : \beta_1$ | $2p_2,\ 2p_1-3d_2,\ 3d_2$ | 9 : 1 : 5 |
| | $\beta_2 : \beta_{15} : \gamma_1$* | $2p_2,\ 2p_1-4d_2,\ 4d_2$ | 9 : 1 : 5 |
| | $\beta_5 : \beta_{16} : \gamma_6$* | $2p_2,\ 2p_1-5d_2,\ 5d_2$ | 9 : 1 : 5 |

† The notation is that recommended by Sommerfeld in the 4th edition of "Atombau und Spektrallinien."

* The wave-lengths of $\beta_{15}$ ($N_{22}\rightarrow L_{22}$) and $\beta_{16}$ ($O_{22}\rightarrow L_{23}$) were measured and the lines named by Crofutt (Phys. Rev. **24**, 9, 1924).

In the K series it is well known that the relative intensity of $K\alpha_1/K\alpha_2$ is 2/1, as predicted in Table I. This ratio has been verified for a wide range of elements by the researches of Siegbahn and Žáček[8] and those of Duane and Stenström and Duane and Patterson referred to above. We have recently found[9] that the relative intensity of the components of the $K\beta$ doublet is also 2/1, as predicted. Since the $K\gamma$ doublet has not yet been separated, we cannot experimentally test the theoretical predictions in this case.

Unfortunately, only a few of the relative intensities predicted in the L series are suitable for experimental verification. With the exception of the combinations $\beta_3\beta_4$, $\gamma_3\gamma_2$, $\alpha_1\alpha_2$, and possibly $\beta_2\beta_{15}$, the lines in

[6] A. Sommerfeld, Ann. der Physik **76**, 284 (1925).

[7] Coster and Goudsmit, Naturwissenschaften **1**, 11 (1925).

[8] Siegbahn and Žáček, Ann. der Physik **71**, 187 (1923).

[9] Allison and Armstrong, Phys. Rev. **25**, 882 (1925); also preceding paper in this issue.

question are too far separated in wave-length or too weak to be measured at present.

The only previous measurements of relative intensities of lines in the L series, other than the qualitative visual estimation of photographic negatives, are those of Duane and Patterson[3] on the L series of tungsten. The results obtained by them are given in Table II. Sommerfeld[6] and Coster and Goudsmit[7] have pointed out that the intensity results of Duane and Patterson are in fair agreement with the predicted values of Table I, except perhaps in the case of $L\gamma_2$ $L\gamma_3$.

TABLE II

*Results of Duane and Patterson on the relative intensities of L-series lines of tungsten.*

| Lines | Relative intensities |
|---|---|
| $\alpha_1 : \alpha_2$ | 10 : 1 |
| $\beta_1 : \beta_2 : \beta_3 : \beta_4$ | 100 : 55 : 16 : 9 |
| $\gamma_1 : \gamma_2 : \gamma_3 : \gamma_4$ | 100 : 14 : 18 : 6 |

We have recently repeated the experiments of Duane and Patterson with improved apparatus. The x-ray tube with which we worked had a water-cooled copper anode containing a button of tungsten on which the cathode rays from a Coolidge cathode fell. The radiation used in the spectrometer left the tube through a mica window .002 cm thick. This tube was constructed of glass and was pumped continuously while in operation on account of unavoidable leakage around the mica window. The tube was run at 20 m-amp. and a constant voltage of about 30.7 kv obtained from a high capacity 50 kv storage battery. This battery and the general arrangement of the apparatus have been described elsewhere.[10] The beam incident upon the calcite crystal was limited by two slits 37 cm apart. After reflection from the crystal the beam entered the ionisation chamber through a mica window .002 cm thick. The ionisation chamber was filled with the vapor of methyl iodide. It was constructed of Pyrex glass after the design developed in this laboratory[11] except that, as in the experiments of Duane and Patterson, an open end with a ground flange was substituted for the usual blown glass window. On this flange a steel plate in which a slit had been cut was fastened with DeKhotinsky cement and the mica was then cemented on to the plate over the slit. The resulting ionisation chamber was air tight and gave satisfactory results.

[10] Armstrong and Stifler, J. Opt. Soc. Amer. and Rev. Sci. Inst. **11**, 509 (1925).

[11] Blake and Duane, Phys. Rev. **10**, 624 (1917); cf also for description, J. C. Hudson, J. Opt. Soc. Amer. and Rev. Sci. Inst. **9**, 259 (1924).

The table which carried the crystal could be turned with precision through an angle of a few seconds and its position read by means of a traveling microscope sighted upon a Genevoise scale. The reflected beam was followed by turning the ionisation chamber through twice the angle traversed by the crystal after the well-known method of the Braggs.

The previous experiments of Duane and Patterson were made with the tube voltage slightly under 25 kv and with a tube which did not have a water-cooled target. By running our tube at 30,700 volts and 20 m-amp. we have been able to measure the relative intensities of the lines previously reported by Duane and Patterson with greater accuracy, and we have also been able to study some faint lines which they were not able to detect with certainty. The results which we have obtained agree well with the previous measurements.

## THE $L\alpha$ LINES

Duane and Patterson give for the relative intensity of $L\alpha_1/L\alpha_2$ the value 10. The predicted value (Table I) is 9.

We have made three measurements of the relative intensity of these lines. The resolution which we obtained was about the same as that shown in Fig. 3 of the previous report.[3] In this figure it is evident that the lines are not *completely* resolved, though doubtless they would appear so on a photographic negative. The base-line between $\alpha_1$ and $\alpha_2$ is not down to the level of the base-line on either side of the two lines. Elsewhere[12] we have described a method of estimating the relative intensities of such incompletely resolved lines based on the assumptions (1) that each line is single and of the same intrinsic wave-length breadth; (2) that the curve representing each line is symmetrical about the center of the line; (3) that the resolution is great enough so that the radiation due to a line is negligible at a wave-length $\lambda \pm 2\Delta\lambda$ (where $\Delta\lambda$ is the separation of the two lines). On the basis of these assumptions it is logical to take as a base-line for $\alpha_1$ the total radiation intensity at an angle corresponding to the wave-length $\lambda(\alpha_2) - \Delta\lambda$ and for $\alpha_2$ the total radiation intensity at $\lambda(\alpha_1) - \Delta\lambda$. By assumption (1) the ordinate from the highest point on the line to the appropriate base-line for the line is proportional to its intensity. In this way we have been able to correct for incomplete resolution, though the correction is almost negligible in the case of $L\alpha_2$ $L\alpha_1$.

Our three measurements of the ratio of the intensities of $L\alpha_1$ and $L\alpha_2$ gave the results: 10.3, 10.7 and 9.1. The average is 10.0, the same value as that obtained by Duane and Patterson.

[12] Allison and Armstrong, preceding paper in this issue.

## The Lβ Group

Besides the strong lines $\beta_1, \beta_2, \beta_3, \beta_4$ it is known from many researches[13] that a number of very faint lines lie in this region of the spectrum. In our present experiments we have been able to find evidence of $\beta_5$, $\beta_6$, $\beta_7$, $\beta_9$, $\beta_{10}$, though not of the line $\beta_8$ nor of the lines $\beta_{15}$ and $\beta_{16}$ of Crofutt.[13] This result should not be interpreted as questioning the reality of the

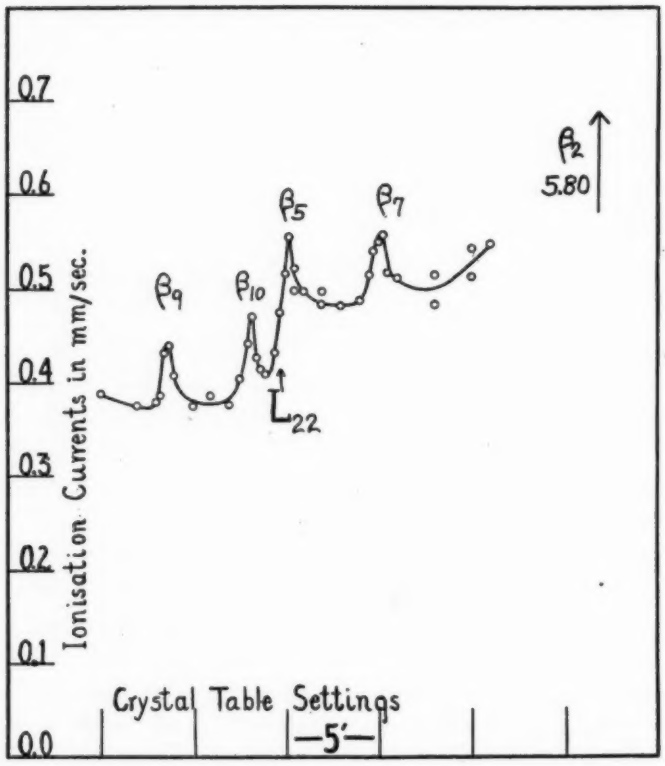


**Fig. 1. Weak lines in the Lβ group.**

lines, since they would undoubtedly appear with narrower slits than those we used. An attempt is now being made to separate $\beta_2$ and $\beta_{15}$ in the third order.

Some of the $\beta$ lines are shown in Fig. 1. On account of the wide range in intensity of these lines it is not practical to plot all of them on the

[13] E. Dershem, Phys. Rev. **11**, 461 (1918):
O. B. Overn, Phys. Rev. **14**, 137 (1919);
M. Siegbahn, Phil. Mag. **38**, 639 (1919);
D. Coster, Phil. Mag. **44**, 546 (1922), etc;
C. B. Crofutt, Phys. Rev. **24**, 9 (1924).

same scale. The results of the measurements are given in Table III. The critical absorption of the target ($L_{22}$) shows on the curve, and since $\beta_9$ and $\beta_{10}$ are on the short wave-length side, the values for these two lines given in Table III can be considered only as minimum ones. The

TABLE III

*Relative intensities of tungsten Lβ Lines.*

| Date | $\beta_1$ | $\beta_2$ | $\beta_3$ | $\beta_4$ | $\beta_5$ | $\beta_6$ | $\beta_7$ | $\beta_9$ | $\beta_{10}$ |
|---|---|---|---|---|---|---|---|---|---|
| May 19 | (100) | 51 | 16 | 8 | .... | 2 | | | |
| May 26 | (100) | 49 | 15 | 8 | .... | 2 | | | |
| June 13 | (100) | 48 | 14 | 7 | .... | 2 | | | |
| May 28 | .... | (49.3) | .... | .... | .5 | .... | .... | .6 | .3 |
| May 29 | .... | (49.3) | .... | .... | .6 | .... | .6 | .6 | .6 |
| June 11 | .... | (49.3) | .... | .... | .3 | .... | .2 | .9 | .9 |
| June 11 | .... | (49.3) | .... | .... | .... | .... | .... | .6 | .... |
| Averages | 100 | 49.3* | 15.0 | 7.7 | 0.47 | 2.0 | 0.4 | 0.68 | 0.60 |

* This value includes the small satellite $\beta_{15}$ found by Crofutt.

values for the very faint lines $\beta_5$, $\beta_7$, $\beta_9$, $\beta_{10}$ were difficult to reproduce in experiments carried out at different times. The slightest variation in the base-line due to general radiation and natural leak of the instrument was sufficient to change their apparent intensities greatly. The selection of a proper base-line for $\beta_5$ is complicated by the presence of the $L_{22}$ absorption on its short wave-length side. Consequently the relative intensities of these small lines among themselves are not highly reliable, though their order of magnitude with respect to the more intense lines is of interest. The lines $\beta_9$ and $\beta_{10}$ appear to be of about equal intensity.

The line $\beta_6$, which is not shown in the figure, appeared as a slight shelf on the long wave-length side of $\beta_1$.

Unfortunately, theoretical interpretations of most of the relative intensities which we have measured have not been advanced. The lines $\beta_3$, $\beta_4$, however, have according to our measurements an intensity ratio which is not appreciably different from the value 2 predicted in Table I. The lines $\beta_9$, $\beta_{10}$ are generally supposed to represent transitions in violation of the selection principle, but at 30,700 volts, at least, they are of the same order of intensity as some of the permitted lines.

## THE Lγ GROUP

In the γ group we have been able to obtain evidence of the lines $\gamma_1$, $\gamma_2$, $\gamma_3$, $\gamma_4$, $\gamma_5$, $\gamma_6$. In some of the curves we obtained slight evidence of $\gamma_8$, but the height of the peak above the general radiation was very variable. At times there seemed to be indications of the lines $\gamma_{11}$ and $\gamma_{12}$ of Cro-

futt,[13] but these were very uncertain. These lines must be very feeble. Fig. 2 is a composite of some of the curves obtained in this region. We have included readings which showed the presence of $\gamma_8$, although this

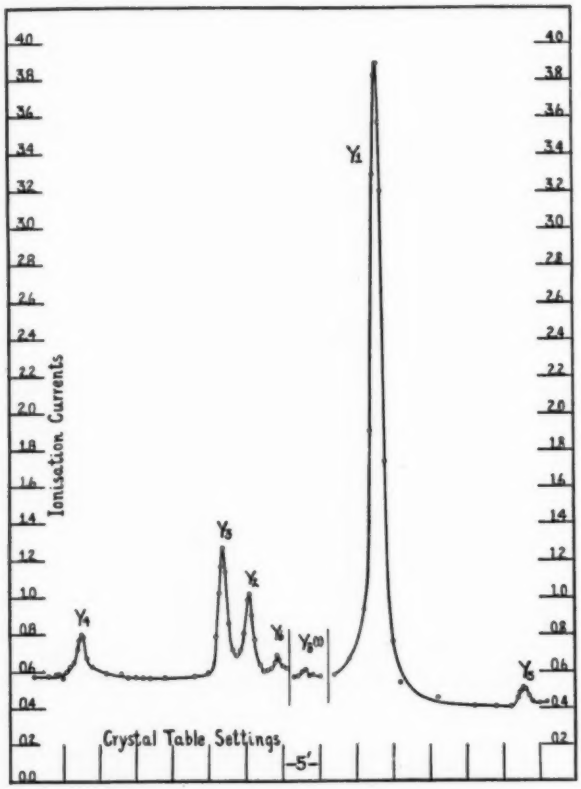


Fig. 2. The L$\gamma$ group of the tungsten spectrum.

peak could not always be reproduced with the same intensity. The intensity results are shown in Table IV. The estimation of the intensity of $\gamma_6$ is complicated by the absorption $L_{21}$ which lies very near this line.

TABLE IV

*Relative intensities of tungsten L$\gamma$ lines.*

| Date | $\gamma_1$ | $\gamma_2$ | $\gamma_3$ | $\gamma_4$ | $\gamma_5$ | $\gamma_6$ | $\gamma_8$ |
|---|---|---|---|---|---|---|---|
| May 21 | (100) | 14 | 24 | .... | .... | 3 | 1 |
| May 22 | (100) | 14 | 22 | .... | 3 | 1 | 1 |
| May 25 | (100) | 14 | 21 | 7 | .... | 3 | |
| June 10 | (100) | .... | .... | 7 | 3 | .... | |
| Averages | (100) | 14.0 | 22.3 | 7.0 | 3.0 | 2.3 | 1(?) |

In the case of the lines $\gamma_3$, $\gamma_2$, for which the intensity ratio predicted by Table I is 2, we find 1.59. Duane and Patterson found 1.29. If their curves are corrected for incomplete resolution by the method in use in this work, a value may be obtained more nearly like that given here. In this case, then, we may state with some confidence that there is at least an apparent exception to the extension of the rules of Burger and Dorgelo. The lines in question are close together, so that corrections due to absorption by materials in the path of the beam do not enter. The deviation from the rule is not in the direction to be corrected for by absorption effects outside of the ionisation chamber. The electron transfers which produce these lines pass through the M groups between their initial and final states in the N and L levels, and it is possible that this passage through intervening electron orbits may change the intensity ratio from the simple predicted value.

*Relative intensities of lines more widely separated in wave-length.*

It is of course of great interest to measure the relative intensity ratios for such pairs of lines as $\alpha_1$, $\beta_1$ and $\beta_2$, $\gamma_1$, for which the predicted values are 9/5. The difficulties accompanying such determinations, however, have not as yet been surmounted. From the results of Unnewehr[14] it is possible to correct for the absorption in the mica windows of the x-ray tube and ionisation chamber. The experiments of Davis and Stempel[15] indicate that the percentage of the monochromatic incident beam reflected by the crystal does not vary rapidly enough with wave-length to introduce large corrections. The point of uncertainty occurs in the absorption of the x-rays by the target itself. This is indicated in our curves by the presence of the L critical absorptions, notably $L_{22}$. A very small effective absorbing layer of the target substance would be sufficient to alter greatly the relative intensity of two such lines as $\alpha_1$ and $\beta_1$. In our experiments $\beta_1$ was slightly more intense than $\alpha_1$, while $\gamma_1$ was somewhat more than half as intense as $\beta_2$. It seems inadvisable to attempt to give values for use in testing theoretical predictions. Yet since the correction for absorption would change both ratios in the same direction, it could not bring them both to the value 9/5.

An interesting interpretation of the relative intensities in the K$\alpha$ doublet has been given by Stoner,[16] who points out that the observed ratio 2 may be taken as an indication that there are twice as many electrons in the $L_{22}$ orbit as in the $L_{21}$ orbit. He has extended this idea

[14] E. C. Unnewehr, Phys. Rev. **22**, 529 (1923).
[15] Davis and Stempel, Phys. Rev. **17**, 608 (1921).
[16] E. C. Stoner, Phil. Mag. **48**, 719 (1924).

to such lines as $L\beta_3$, $L\beta_4$, in which the influence of intervening electron levels is presumably small. Thus the observed intensity ratio 2 for $L\beta_3$, $L\beta_4$ is taken to be evidence that there are twice as may electrons in the $M_{22}$ orbit as in the $M_{21}$. If the perturbing effect of the L levels on the $K\beta$ transitions from M to K is small, our result of 2 for $K\beta_1/K\beta_3$ could be used as additional evidence of the relative numbers of electrons in $M_{22}$ and $M_{21}$. In the case of $L\gamma_3/L\gamma_2$, as Stoner has anticipated, there is a deviation which may well be due to the influence of intervening levels. Sommerfeld[6] has pointed out that the relative intensities of the

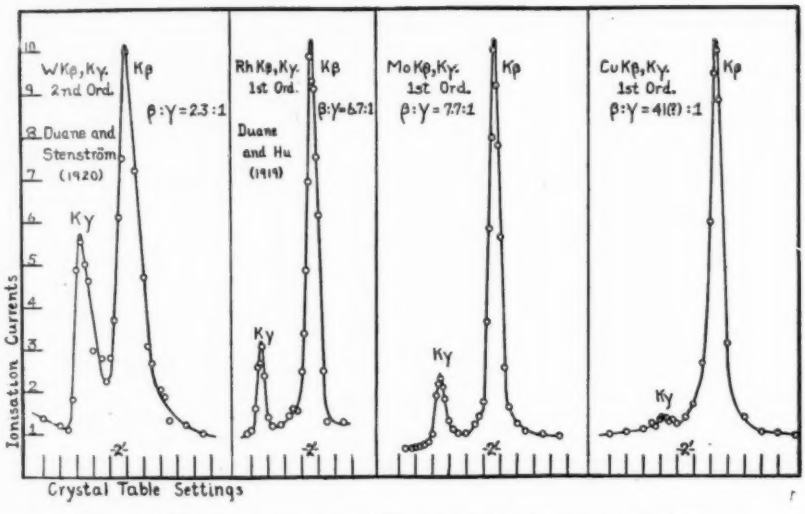


Fig. 3. Relative intensity of $K\beta$ to $K\gamma$ for W, Rh, Mo and Cu.

components of compound doublets are probably not related to the numbers of electrons in the orbits in the simple manner considered by Stoner.

## Intensities in the Copper K Spectrum

The copper K spectrum was emitted strongly from the copper part of the anode. Siegbahn and Žáček[8] have measured the relative intensities of $\alpha_1 : \alpha_2 : \beta_1$ in the copper K spectrum and find 100 : 51.2 : 25.

We have made two measurements of the intensity ratio of $\beta/\gamma$. The $\gamma$ line is extremely weak, and on account of the presence of the critical absorption in its immediate vicinity, estimates of its intensity are quite uncertain. For these two lines we have taken the difference between the highest point on the curve and the base-line as proportional to the intensity, since the uncertainty with regard to the $\gamma$ line makes the more

accurate method of area comparison superfluous. We obtained the values 100/2.7 and 100/2.2 for the intensity of $\beta$ relative to $\gamma$.

It is known that the $\gamma$ line becomes relatively weaker with decreasing atomic number, and we have drawn Fig. 3 to illustrate this fact. The values for tungsten are taken from the results of Duane and Stenström.[2] The curve for rhodium is obtained from one shown by Duane and Hu.[4] The numerical value of the intensity of Rh K$\beta$ relative to K$\gamma$ was determined by us by the method of areas. The curve for molybdenum is from the preceding paper.[12]

We have also examined the spectrum in the region of the non-diagram copper lines $K\alpha_3$, $K\alpha_4$, reported by Dolejsek and by Dolejsek and Siegbahn.[17] These lines have been interpreted as spark lines by Wentzel.[18] At 30,700 volts we could find no good evidence of this doublet, although the Cu $K\alpha_2$, $K\alpha_1$ lines were very strong. The relative intensity of $K\alpha_3$, $\alpha_4$ to $K\alpha_1$ at this voltage must be less than 1/100. It is well known that in elements lighter than copper the intensity of these "spark" lines is greater relative to the lines due to the singly ionised atom.

We are greatly indebted to Professor William Duane for his valuable suggestions and kindly criticisms.

CRUFT HIGH TENSION ELECTRICAL LABORATORY,
HARVARD UNIVERSITY,
August 11, 1925

[17] Siegbahn, Spektroskopie der Röntgenstrahlen, p. 102.
[18] G. Wentzel, Ann. der Physik **66**, 437 (1921).

# THE APPARENT SHAPE OF X-RAY LINES AND ABSORPTION LIMITS[1]

By F. K. Richtmyer[2]

Abstract

**Effect of instrumental factors on the observed intensity distribution of x-ray lines and at absorption limits.**—(1) *Slit width.* In the case of two slits of equal width, sharp lines reflected from a perfect crystal should give an isosceles triangle distribution. If the two slit widths are unequal, the triangle is truncated; this may shift the relative position of the lines of a partly resolved doublet. (2) *Slit height* widens the isosceles triangles slightly, making the long-wave-length side less steep. (3) *Non-uniform energy distribution over the focal spot* produces corresponding lack of symmetry. An actual distribution curve obtained with very narrow slits showed two unequal maxima near the edges of the spot. The same three factors affect the apparent sharpness of the absorption limit. In particular, the finite slit width results in the rounding off of a sharp discontinuity into a skew-symmetrical S curve consisting of parts of two parabolas whose axes are vertical and separated a distance equal to the angular slit width.

**Intensity distribution in the Kα doublet of Mo.**—The curves correspond to monochromatic lines of width .0003A or less. The relative intensity is very close to 2 (2.01). There is no line between them with intensity greater than 1 percent that of $K\alpha_1$.

**Sharpness of the K absorption limit of Ag.**—The curve obtained agrees with that for a limit which is sharp within experimental error, .0002A.

THE x-ray spectrometer used by the writer in studying absorption coefficients needs frequent calibration. For this purpose the several orders of the K series of the target-element (usually tungsten or molybdenum) have been used. In this connection certain peculiarities and characteristics of the x-ray spectrometer have been observed, which seem not without interest and which should be given consideration in studying the actual shape of x-ray lines and absorption edges and in making precision wave-length measurements.

The spectrometer is of the usual Bragg type. The x-ray beam is limited by two slits 38 cm apart placed between crystal and target. Each slit is about 2 cm high and is formed by two lead jaws 1 cm wide, ground plane, and very carefully adjusted to parallelism. The jaws may be moved

[1] This paper is based in part on papers read in February and April, 1924, before meetings of the American Physical Society. (See Richtmyer and Spencer, Phys. Rev. **23,** pp. 550 and 760.) The author takes pleasure in expressing his appreciation of the assistance rendered by Mr. Spencer.

[2] This work has been made possible by a grant to the author from the Heckscher Research Council of Cornell University.

bi-laterally by micrometer screws reading to .0001 inch (.0025 mm). The tube is adjusted so that the plane of the target makes an angle of about 8° with the line of the slits, the focal spot thus being equivalent to an ellipse approximately 15 mm high and 2 mm wide. The crystal is of calcite, a very perfect one kindly loaned to the writer by Professor Bergen Davis. Ionization currents are read in the usual way, by means of an electrometer of the Compton type.

## Factors Affecting the Apparent Shape and Width of Lines

Fig. 1 represents a typical calibration curve showing the first-order lines of Mo and taken with slits .075 mm wide.[3] The abscissas represent

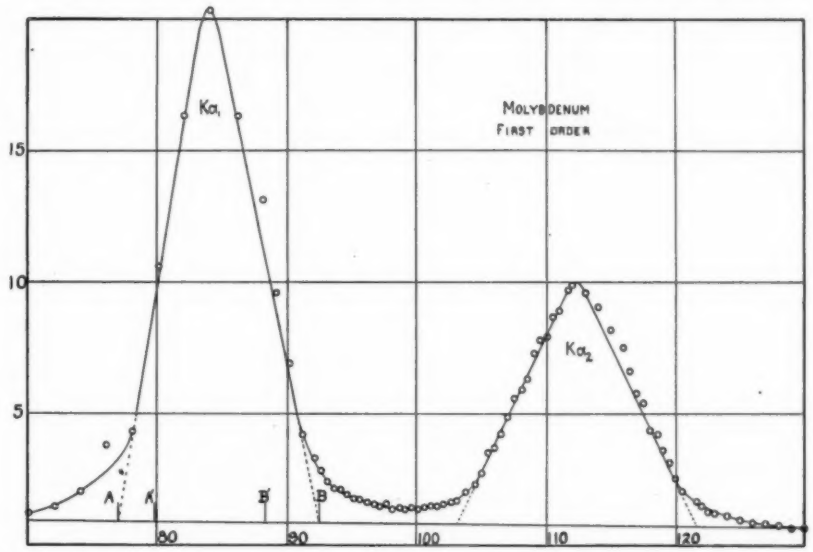


Fig 1. The first order Kα lines of Mo as used in calibrating the spectrometer. The lines are approximately triangles, but are slightly convex outward on the right (long wave-length) side.

arbitrary divisions on the scale of the spectrometer, each division corresponding approximately to .00015A. It will be noted that each line is approximately a triangle *but with the long wave-length side slightly convex outward*. It was this observation which started this investigation of the *instrumental factors* affecting the apparent shape of x-ray lines. Omitting the effect of the crystal[4] these factors are:

[3] This curve was taken with some care in order to investigate the region between $K\alpha_1$ and $K\alpha_2$ where it had been suggested to the author that a faint line might be found. It is quite obvious that no such line of appreciable intensity exists.

[4] See Bergen Davis and W. M. Stempel, Phys. Rev. **19**, p. 504 (1922).

(1) The width (actual and relative) of the slits limiting the beam.
(2) The "brightness" of different parts of the focal spot.
(3) The height of the slit.

*The effect of slit width.* In what follows we shall assume that we are dealing with a strictly monochromatic line of wave-length $\lambda$, and with a *perfect* crystal which reflects $\lambda$ at the angle $\theta_\lambda$ given by the usual equation

$$n\lambda = 2d \sin \theta_\lambda$$

In Fig. 2A let the two limiting slits be a distance $D$ apart and have the same width $s_1$. (In any actual case $D$ is very large compared to $s_1$.) Let $TT$ be the focal spot, the major axis of the ellipse being at right angles to the paper. The crystal, not shown, is at the right of the figure and is capable of rotation about an axis perpendicular to the plane of the

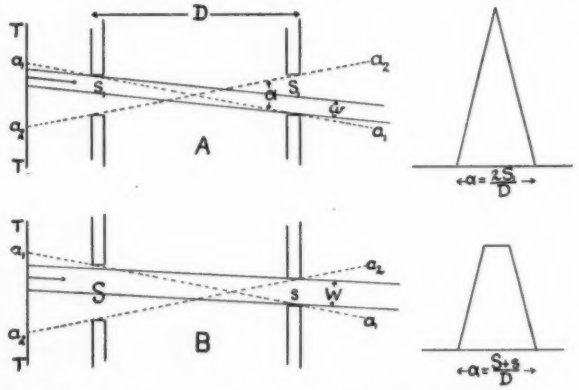


Fig. 2. Showing diagrammatically the effect of finite slit widths on the apparent shape of a line.

figure. Let the angular position of the crystal be measured, in the usual way, by the angle $\theta$ which the crystal planes make with the line passing through the centers of the two slits.

Starting from $\theta = 0$ and turning the crystal counter-clockwise, no reflection of the line $\lambda$ will be observed until the crystal planes make an angle $\theta_\lambda$ with the line $a_1a_1$ which is defined by the far edge of the left-hand slit and the near edge of the right-hand slit. As the crystal is rotated beyond this position the planes make the angle $\theta_\lambda$ with a beam of *parallel* rays of width $w$, as shown in the figure. This width $w$ will increase and the *apparent* intensity of the reflected line will accordingly increase until the crystal position is such that $w$ is equal to the slit width $s_1$. Beyond this point $w$ will decrease to zero when the crystal makes the angle $\theta_\lambda$ with the line $a_2a_2$. Since $s_1$ is always very small compared to $D$ this change of $w$ (increase or decrease) is a linear function of the angular position of the crystal. Hence the *observed* shape of the line

should be a triangle with a base of which the *angular* width is given by $2s_1/D$.

If the slits be of *unequal* width, say $S$ and $s$ as in Fig. 2B, similar considerations show that the apparent shape of the line will be an isosceles trapezoid of which the base has the angular width $(S+s)/D$.

Parenthetically, it is interesting to point out that the apparent shape of a close doublet will be materially influenced accordingly as the measurements are made with equal or unequal slits. Fig. 3A shows, diagramatically, the apparent shape of a doublet, such as $K\alpha_1$, $\alpha_2$, when observed by slits of unequal width. The inevitable rounding off of the corners would make this appear as a single line with the maximum at $h$ instead of $h_1$. Fig. 3B shows the appearance of the doublet when slits of equal width are used. The maximum of the more intense line appears in its correct position, and the presence of the weaker component is indicated by irregularity on the side of the curve.

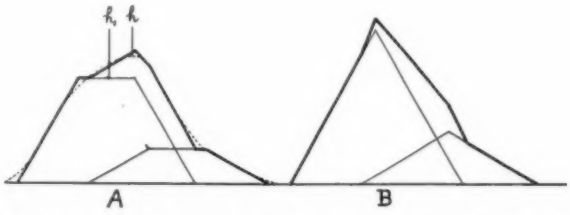


Fig. 3. A. The apparent shape of a doublet when observed by slits of unequal width. B. Same for slits of equal width. Curve A would evidently lead to an incorrect location of the more intense line.

*The effect of variation of "brightness" in the focal spot.* Referring to Fig. 2A it is readily observed that the apparent shape of the line can be a perfect isosceles triangle only if there is a constant x-ray brightness over that part of the focal spot falling within the solid angle defined by the slits (the angle between the lines $a_1a_1$ and $a_2a_2$). There is reason to expect such variation of brightness, partly because of space charge effects within the electron stream from filament to target, partly because of the dissymmetry in field introduced in tubes where the target makes an angle of 45° with the axis of the tube.

To test this point, the slits $s$ were made very narrow (less than .025 mm), thereby isolating a very narrow vertical strip ($aa$ Fig. 4) of the focal spot, parallel to its major axis. Using the direct beam, the intensity of the radiation was measured as the tube was moved by micrometer adjustment, so as to cause the focal spot to move past the axis of the slits. The resulting curve is shown in Fig. 4. The distance $R$ on the graph corresponds to the minor axis of the focal spot as seen from the slit

system. Two maxima, $A$ and $B$, are observed indicating that there is a ring of greater intensity just inside the focal spot, but that the one edge of the ring, $B$, is more intense than the other.

From Fig. 2A it is obvious that dissymmetry will be introduced into the triangle if for example the adjustment of the focal spot should be such that the hump $B$ corresponds to point $a_1$ and some point midway between the two humps corresponds to $a_2$. Something like this was apparently the case when the data for Fig. 1 were taken.

To test these two points the slits $s$ were carefully adjusted to .038 mm each, and the tube was so placed that the flat part of the curve, between $A$ and $B$ of Fig. 4, coincided with the region $a_1a_2$ of the focal spot in Fig.

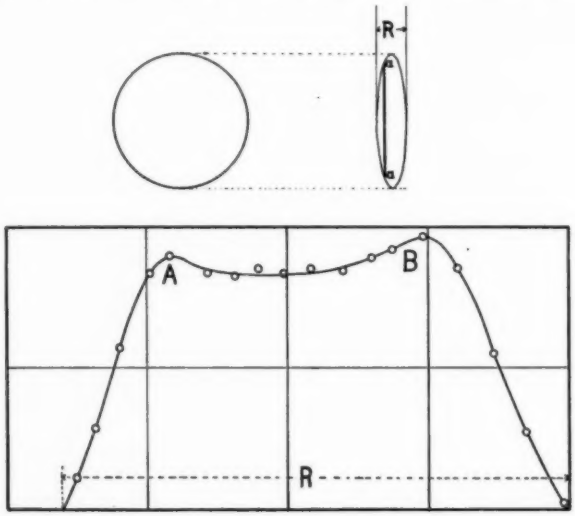


Fig. 4. The unequal distribution of energy across the focal spot of a tube. The focal spot is seen from the spectrometer as an ellipse with minor axis $R$.

2A. A run was then taken on the line $K\alpha_1$. The result is shown in Fig. 5. It is observed that the sides of this line correspond to the sides of a triangle, and that there is lateral symmetry, instead of the convexity observed in Fig. 1. The width of the base of the triangle is somewhat greater than predicted from the known slit width. But it is rather difficult to measure with high precision slit widths as narrow as .038 mm.

In the case of Fig. 1, the graph shows data taken with slits .076 mm wide. The full line just above the abscissa scale, represents, as nearly as could be estimated, the white radiation in the same region. Therefore one may find the width of the base of the triangle, for $\alpha_1$ for example, by projecting the sides down to this base line. In this way it is found that with these slits, the width of the base $AB$ corresponds to an equivalent

wave-length range of .00232A. The slits were then narrowed to .038 mm and another run taken. The data are not plotted but the base line was observed to be $A'B'$, corresponding to an equivalent wave-length range of .00136A. Extrapolating from these two results, zero slit width would correspond to a wave-length range of .0003A. That is to say, so far as these observations go the line $K\alpha_1$, is monochromatic to this extent. However, because of the difficulty of making precise measures of slit widths as small as these, not too much dependence should be put on this result.

Another point of some little importance when one is concerned with measuring wave-lengths to the highest precision, is brought out by the

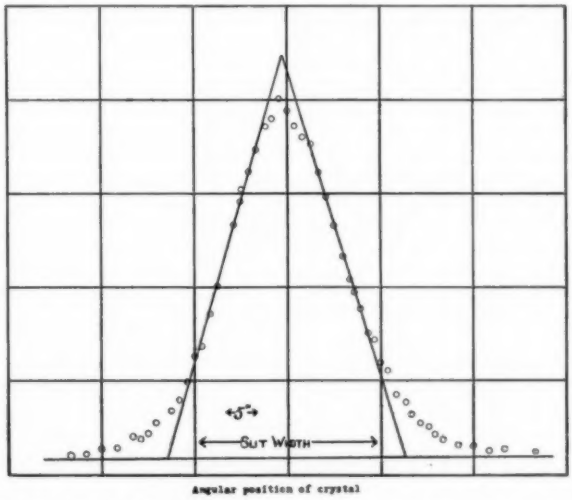


Fig. 5. The $K\alpha_1$ line of Mo (first order), taken with slits of equal width and with the tube so adjusted as to give nearly equal energy distribution over the part of the focal spot used.

$K\alpha_2$ line of Fig. 1. As has been pointed out above, the long wave-length side of the graph is convex outward because of the irregular distribution of energy over the focal spot. Had a smooth graph been drawn through these points and the *maximum* taken as the exact location of the line this maximum would differ from the one shown in the graph by approximately .00015A. While this difference is not large, it shows that the position of a line may be misjudged by an appreciable amount unless care be taken to work with equal energy distribution on the target.

*The effect of slit height.*[5] For most purposes this effect can be neglected but in work aiming at high precision it is of sufficient importance to be

[5] See also article by H. S. Uhler, Phys. Rev. **11**, p. 11 (1918).

worthy of mention. To simplify discussion, assume that the axis of rotation of the crystal is vertical and that the crystal planes are parallel to this axis; also that the slits limiting the x-ray beam are, as above, between crystal and tube (and are, of course, vertical). It is then usually assumed that the angle $\theta$ in the equation

$$n\lambda = 2d \sin \theta$$

is measured by the angle between the *plane* of the crystal face and a second plane passing through the axis of rotation and the two slits. This is obviously the case only for those rays which are *horizontal*. On account of the finite height of the slits there will be other rays, not horizontal, passing through the slit system. For a ray which makes an angle $\varphi$ with the horizontal, the glancing angle $\theta$ at which it meets the crystal planes, is given by the equation

$$\sin \theta' = \sin \theta \cos \varphi.$$

If the wave-length of this ray be $\lambda$, then the angle $\theta_\lambda$ at which it will be reflected will be given by

$$\sin \theta_\lambda = \sin \theta' = \sin \theta \cos \varphi,$$

or

$$\sin \theta = \sin \theta_\lambda / \cos \varphi;$$

that is, the greater the divergence of the ray from the horizontal the greater must be the angle $\theta$ for reflection to take place. In any actual case $\varphi$ is small, and its maximum value is given very nearly by the angle which the slit nearest the ionization chamber (or photographic plate) subtends at the slit farthest away from the chamber. The net result of this effect, with very narrow slits and a crystal thin enough to eliminate the penetration error, is to produce a reflected beam, as the crystal is turned, of which the cross section is similar to the cross section of a plano-concave lens, the plane side being sharp and turned toward shorter wave-lengths, while the curved side is slightly diffuse. For this reason the long wave-length side of the triangles, such as in Fig. 1, should be not quite so steep as the short wave-length side. *This effect is observed in practically every case.* To illustrate the magnitude of the effect, it may be pointed out that for a value of $\varphi$ of 1°, the observed position of the Ka lines of Mo will be shifted about 4″ from the true position, in the first order.

*Monochromaticity.* A question closely allied to the above is the extent to which the degree of monochromaticity of a reflected beam of white radiation is influenced by the finite width and height of slits. From the law of the crystal grating it follows by differentiation that

$$d\lambda = (2d/n) \cos \theta \, d\theta$$

from which, by knowing the angular divergence $d\theta$ of the reflected beam the value of $d\lambda$ can be obtained. From what has been said above it is obvious that $d\theta$ is made up of two parts, a part $\alpha$ due to the finite width of the slits and a part $\delta$ due to finite height of the slits. By reference to Fig. 2 it is readily seen that $\alpha$ is equal to twice the angle subtended by the width of one of the limiting slits at the other, if the slits be of equal width. We can compute $\delta$ as follows. From the preceding section

$$\sin \theta' = \sin \theta \cos \varphi_m$$

where $\varphi_m$ now represents the *maximum* value of $\varphi$ and is approximately the vertical angle subtended by the slit nearest the chamber at the slit

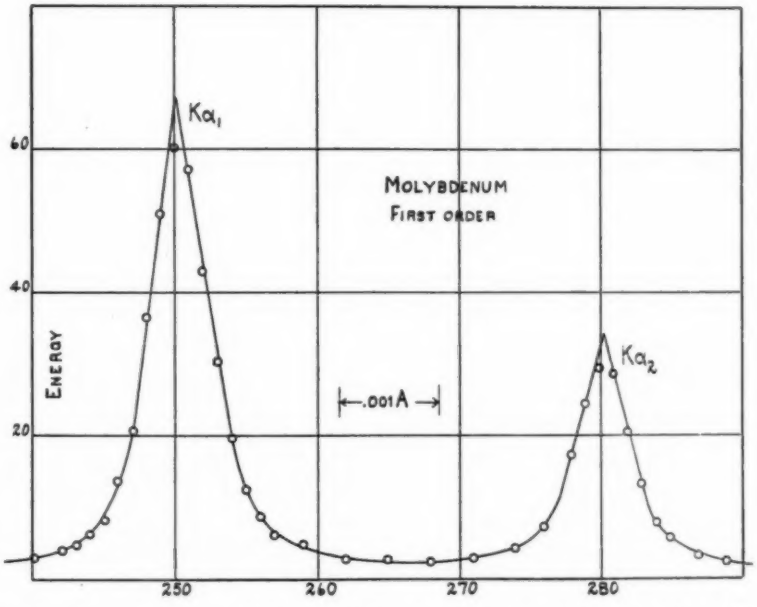


Fig. 6. The Kα lines of Mo (first order), taken with slits .0025 cm wide and .38 cm apart, showing that the curve for each line is an almost symmetrical triangle. Measured from the white radiation in the neighborhood, the height of $\alpha_1$ is almost exactly twice that of $\alpha_2$ (65.0/32.3). Note also the high resolving power.

farthest away, assuming the slits to be of equal height. Then

$$\delta = \theta - \theta' .$$

Fig. 6 gives observations of the Kα lines of Mo in the first order taken with the spectrometer described above using a calcite prism. The slits were all approximately 2.5 cm high. The slits limiting the beam were .025 mm wide and 38 cm apart. This gives a value of $\alpha$ of .00013 radian. The distance between the slits nearest and farthest from the ionization

chamber was about 100 cm, from which it is computed that $\delta$ is .000025 radian. Hence

$$d\theta = \alpha + \delta = .000155 \text{ radian}$$

and

$$d\lambda = .00094\text{A}$$

or about one fifth of the distance between the K$\alpha$ lines. This agrees with the excellent resolution shown in Fig. 6. In spite of this high resolution the radiation between the two lines is slightly greater than is to be expected from the magnitude of the white radiation on either side of the doublet. This may possibly be due to slight crystal imperfections. The effect is much more apparent in Fig. 1.

## The Apparent Width of the Absorption Limit

The methods used in determining the effect of the slit system on the apparent shape of x-ray lines may be applied equally well to absorption limits. Assume, as before, that we are dealing with a perfect crystal and further that the absorption limit of the absorber used is infinitely sharp and occurs at wave-length $\lambda_K$. We will also assume that the target has no characteristic lines in this neighborhood, so that we are dealing only with the white radiation. Let $I$ be the intensity of this white radiation, practically constant over the very narrow spectral region concerned. Let $\beta_1$ and $\beta_2$ be the fractional transmission coefficients on the short wave-length side and long wave-length side, respectively, of this absorption limit, and let the corresponding intensities be $\beta_1 I$ and $\beta_2 I$. Then on account of the finite slit widths the apparent absorption break will not be sharp, if high resolving power be used, but the rise from $\beta_1 I$ to $\beta_2 I$ will be gradual.

We can regard the continuous spectrum coming through the absorber as made up of a large number of adjacent lines, the intensity of which (see Fig. 7C) suddenly rises from $\beta_1 I$ to $\beta_2 I$ as the absorption limit is passed. These in turn can be regarded as a series of lines of intensity $(\beta_2 - \beta_1)I$ superimposed on the spectrum $\beta_1 I$. When the crystal is set at such an angle that none of the "lines" $(\beta_2 - \beta_1)I$ are reflected, the observed intensity will be constant and equal to $\beta_1 I$; but when the slit approaches the absorption limit[6] some of the "lines," will be reflected, each line giving rise to a triangle, as previously discussed, the base of the triangle being determined by the slit widths. The actual observed intensity, at any crystal angle, will be the sum of the intensities due to each of the separate triangles (Fig. 7B), i.e. the sum of the intercepts which the sides of the several triangles make on an ordinate erected at the abscissa corresponding to the crystal setting. Thus Fig. 7C repre-

[6] The "lines" are assumed narrow compared to the slit system.

sents the "lines" forming the transmitted spectrum, the absorption break occurring at $\theta_k$. To each line 1, 2, 3, . . . . there corresponds a triangle 1, 2, 3, . . . . (Fig. 7B) the base of which is defined by the slit width. If the crystal be set at the angle $\theta_k$, the energy observed at that setting will be proportional to the sum of the intercepts made on that ordinate by the first four triangles. This corresponds to point *p* of Fig. 7A. The locus of point *p*, from *b* to *o* is a parabola, tangent at *b* to the line *ab* and meeting, tangentially at *o* another similar parabola which is the locus of *p* from *o* to *c*, the latter parabola being tangent to the line

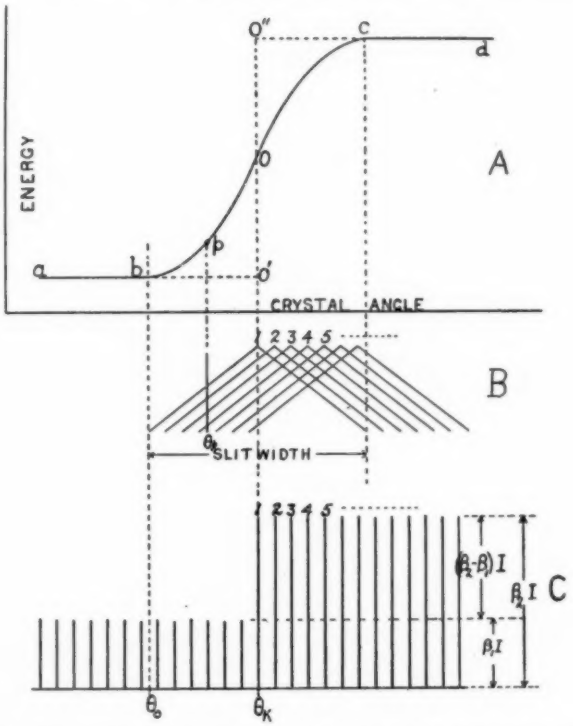


**Fig. 7.** Showing diagrammatically how the finite slit width determines the apparent shape of an absorption break.

*cd* at *c*. The line *ab* represents the constant intensity $\beta_1 I$, and the line *cd* the constant intensity $\beta_2 I$. For infinitely narrow slits the absorption break would be given by the line *o'o''*. For slits of finite width the absorption break is given by the line *boc*, the angular distance *bc* being exactly equal to the angle of the slits.

Fig. 8 shows such an energy distribution curve taken through the K limit of silver. The points *abocd* correspond to similar points in Fig. 7A. The full line *boc* is a *theoretical* curve, made up of two parabolas

tangent at *a* and *c* to the lines *ab* and *cd* respectively, and meeting each other tangentially at point *o*. The circles are actual observations. The observed points are seen to agree exceptionally well with the theoretical curve between *b* and *c*.

Furthermore it is to be noted that the actual observed width of the discontinuity agrees *within the limit of error* with the slit width, the difference being certainly not more than 4 percent. That is to say, the

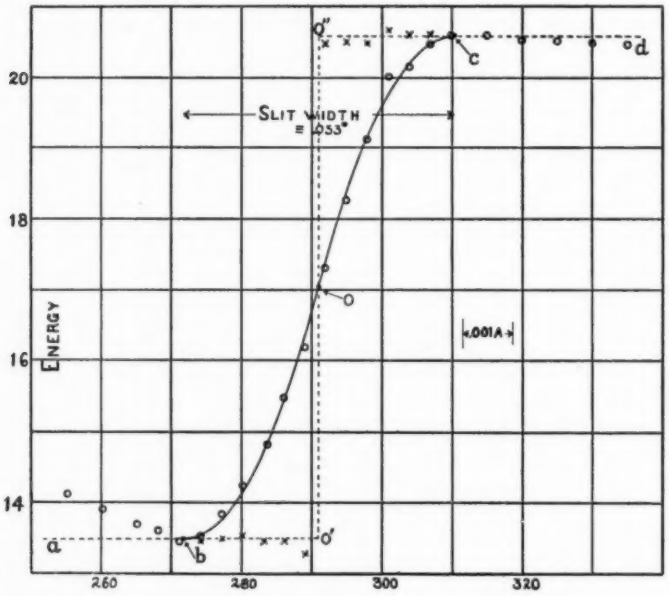


Fig. 8. The K absorption limit of silver, determined by taking an energy distribution curve of the white radiation from a Mo target with a silver absorber in the path of the beam. The curve *abocd* is a theoretical curve based on the known slit widths used. The circles are observed points. The crosses are the result of correcting the readings for slit width error. Note the sharpness of the absorption break.

K discontinuity of silver is sharp to this extent, the real width of the discontinuity, if it is different from zero, being probably less than .0002A.

It is now a very simple matter to plot a corrected discontinuity curve, eliminating the effect due to slit width. It is only necessary to move each observed point between *b* and *o* *downward* by the distance between the theoretical curve and the straight line *ab*, extended at that point. Similarly, each point between *o* and *c* should be moved upward. This has been done; the resulting points are represented by crosses. As noted in the preceding paragraph, the discontinuity is sharp within the limits of error of this experiment.

By this method it is possible to get values of the mass absorption coefficient very close to the absorption limit.

The author takes pleasure in expressing his very great obligations to the Research Laboratory of the General Electric Company for making available certain very essential parts of the equipment used in this investigation.

CORNELL UNIVERSITY,
July 2, 1925.

# THE LATTICE PARAMETER AND DENSITY OF PURE TUNGSTEN

By Wheeler P. Davey

Abstract

Because of the importance of knowing the values of these constants as accurately as possible, x-ray diffraction patterns were made for several samples differently treated as follows, (1) W plus 10 parts flour in comparison with NaCl in the other end of specimen tube; (2) the same in comparison with Au plus 10 parts flour, and (3) W plus 10 parts NaCl. The results agree within the reproducibility of the results, .001 to .003A, with the values previously obtained for *lattice parameter* ($a=3.155\pm.001$) and *density* ($D=19.32\pm.02$).

THE most accurate determinations of the diameters of fine wires are made in terms of their length and weight. All calculations of efficiency of light emission and of thermionic emission of W wires depend therefore upon a knowledge of their density. Experiment shows[1] that, within the experimental error, these W wires have the same lattice parameter as pure annealed W powder, so that the density of both must be identical. It therefore seemed desirable to attempt to check the value of the lattice parameter of pure W (99.999 percent) which was published recently.[1] That value was obtained in terms of the lattice parameter of NaCl. The W powder, diluted with ten times its volume of wheat flour so as to reduce its opacity to the x-rays, was inserted in one end of a specimen tube. NaCl diluted with its own volume of flour was in the other end. In this way the two diffraction patterns were obtained side by side on the same photographic film.

There was a possibility that the W had not been sufficiently diluted, so that the equivalent centers of the W and NaCl might not have been in the same straight line. This would have made the lattice parameter of W come out too small, thus giving too high a value for the density. A portion of the same lot of W was therefore mixed directly with ten times its volume of NaCl, so that the two diffraction patterns were superimposed.[2] In this way the equivalent centers of the W and of the NaCl were necessarily identical. Measurements of the lattice parameter of W made in this way were therefore free from any possible objection which might have been raised against the previous measurement. Pure Au furnishes a second check. The parameter of 99.999 percent Au previously

[1] Davey, Phys. Rev. **25**, 753 (1925).

[2] Havighurst, Mack and Blake, J. Amer. Chem. Soc. **46**, 2368 (1924).

published[1] gives a density which agrees within the error of experiment with the highest density found for Au by the ordinary methods.[3] Since the admixture of any impurities in gold must necessarily lower the density, this was taken to mean that the published parameter for pure Au was correct. A portion of the same sample of Au was mixed with ten times its volume of flour and inserted in one end of a specimen tube as a calibration standard. A portion of the original lot of W was mixed with ten times its volume of flour and inserted in the other end. The two diffraction patterns were thus obtained side by side. The two metals were both of such high atomic number that any error caused by differences in the equivalent centers of the two must have been negligible.

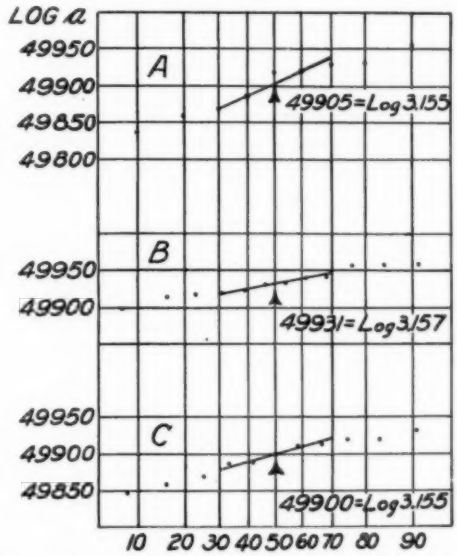


FIG. 1. Probability curves for the lattice parameter of tungsten.
A. W plus 10 parts flour; NaCl plus 1 flour at other end of specimen tube.
B. W plus 10 NaCl; calibration in terms of NaCl.
C. W plus 10 flour; Au plus 10 flour at other end of specimen tube.

Every line in the W diffraction pattern corresponding to an interplanar distance of less than 2.00A was corrected in terms of the calibration pattern on the same film, and each of these corrected readings was made to give a value of the lattice parameter. These results were then plotted on probability paper as previously described[4] to find the most probable values of the parameter. The reproducibility of such a result is $\pm 0.1$ percent for ordinary diffraction patterns. For the data originally pub-

[3] Averkieff, Zeits. anorg. Chem. **35**, 329 (1903).
[4] Davey, Phys. Rev. **19**, 538 (1922).

lished the lines were so fine that the reproducibility was considered to be $\pm 0.03$ percent. The probability curves for films from all three methods are given in Fig. I. It is interesting to note that, in every case, if the curve is lifted or lowered to the level of the point which lies furthest off the curve, the value of the lattice parameter $a$ is not changed by more than 0.001A.

The three methods give for the value of the lattice parameter of W, $3.155 \pm .001$A, $3.157 \pm .003$A, and $3.155 \pm .003$A, where $\pm$ refers to the degree of reproducibility of the data. It therefore seems justifiable to retain the original value 3.155A. The close agreement between the results given by the two methods of using the NaCl for calibration is at first sight surprising. It must mean that when W is mixed with as much as ten times its volume of flour, the dilution is sufficient to provide direct paths through the specimen through which the x-ray beams may travel to and from each particle of W with little or no absorption. Such a result was hardly to have been expected.

This parameter gives a density of $19.32 \pm .02$. As was pointed out in the original paper this is much higher than the values published in Van Nostrand's Chemical Annual and in Groth's Chemische Krystallographie. It is, however, consistent with the value 19.3 published by Fink[5] for rods 3.75 mm in diameter.

RESEARCH LABORATORY,
GENERAL ELECTRIC COMPANY,
SCHENECTADY, N. Y.
AUGUST 17, 1925.

[5] Fink, Trans. Amer. Electrochem. Soc. **17**, 229 (1910).

# SOFT X-RAYS FROM IRON, COBALT, NICKEL AND COPPER

By Charles H. Thomas

Abstract

**Critical potentials of Fe, Co, Ni and Co, to 1500 v.**—Using the photo-electric method previously described,[1] the study of iron has been extended, and critical potentials of Co and Ni have been determined throughout the range 0-1500 volts. The arrangement is more sensitive than that used by previous observers and readings were taken at intervals of 1/2 volt accelerating potential up to 100 volts and at corresponding small intervals for the higher ranges; hence the curves are more accurate and reproducible than those obtained by other investigators. Forty-six critical potentials were found for Ni, 48 for Co, and the number for Fe was increased to 46. More than 100 independent curves were obtained for each of these metals and the breaks reported were entirely reproducible. Copper was investigated only in the range 0-90 and 700-1200 volts; 25 critical potentials were found. The breaks are of two types with shapes which suggest that they correspond to ionizing and radiating potentials. There is a general correspondence, both in nature and value, between the critical potentials of iron, cobalt and nickel, with an upward shift of voltage with increasing atomic number. This correspondence is especially striking in the case of the nine breaks which have been designated as "ionizing" potentials. In the region of the L series, the critical potentials of copper also correspond accurately with those of the other metals, but in the region 0-90 volts there appears to be no similarity. The critical potentials which could be connected with *x-ray spectroscopic terms* with some certainty are: Fe, $L_I$ at 818.5 and $L_{III}$ at 704.3; Co, $L_I$ at 873.2 and $L_{III}$ at 764.8; Ni, $L_I$ at 948.0 and $L_{III}$ at 833.4; Cu, $L_I$ at 1017.0 and $L_{III}$ at 929.0 volts.

IN a previous paper[1] the writer has described a method and apparatus for the accurate determination of critical radiating potentials. This apparatus, based on a photo-electric detection of x-radiation, differs from previous apparatus of the same sort in that the detecting electrode completely surrounds the target, so as to intercept all the radiation emitted from it. The method is distinguished by extraordinary precautions to secure steadiness, especially in the thermionic emission from the Coolidge cathode, and in the use of small voltage intervals in covering the desired range of voltages. Details of the apparatus and operation are given in the preceding paper.

In the present paper a further study of iron is described, since spring weather conditions interfered with some of the earlier work on this metal, and the study is extended to cobalt and nickel from 0 to 1500 volts and to copper from 0 to 90 and 700 to 1200 volts.

[1] Thomas, Phys. Rev. **25**, p. 319 (1925).

## Results and Discussion

Critical potentials were determined from the positions of breaks which were found in the curves obtained when the ratio of the photo-electric to the thermionic current was plotted as a function of the voltage applied between the hot filament cathode and the target anode. This voltage was corrected for initial velocity, and contact difference of potential, and to it was added the "work function" $\phi$ of the metal, according to the relation $h\nu = e(V+\phi)$, from which the radiation frequencies may be computed. Two types of breaks have been observed and are designated as radiation ($R$) and ionization ($I$) potentials, following the analogy in the case of similar breaks observed when gases instead of metals are studied. The $R$ breaks are followed by a portion of the curve which is concave downward

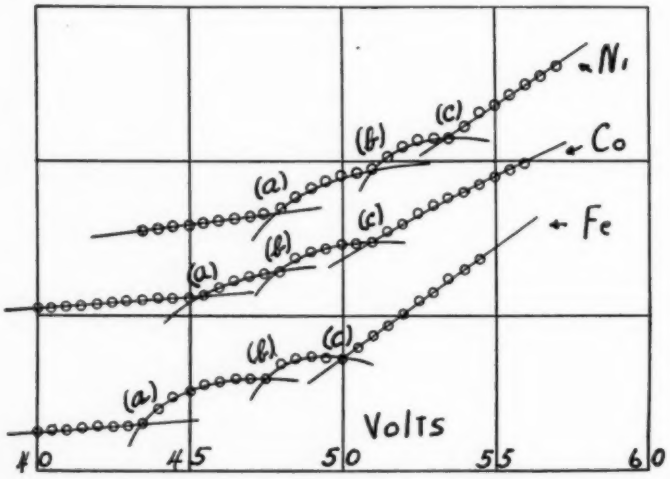


Fig. 1. Curves showing the progression with atomic number in the corresponding critical potentials of Fe, Co and Ni. Breaks $a$ and $b$ are of type $R$, while $c$ is of type $I$. These breaks, and those in Fig. 2, have been exaggerated by plotting as ordinates the differences between the experimental points and points on a straight line of convenient slope.

and the $I$ breaks are followed by portions of the curve which are straight or slightly concave upward. The designation may not correspond to the true physical facts, but is convenient as a basis of classification.

In the previous paper the reproduction of the curves was somewhat disappointing as regards the definiteness with which the breaks were shown. This was due to the fact that the change of slope was never large and often required careful examination to locate it. In order to bring out breaks more convincingly, the differences between the actual curves and straight lines of convenient slope have been plotted in Figs. 1 and 2. In

this manner no spurious breaks are introduced, but the actual breaks can be magnified so as to be as evident as desired. It should be said, however, that all actual locations of breaks were made from the original observations, plotted on large scale.

Fig. 1 shows typical curves, thus replotted. The curve for iron shows three breaks of which *a* and *b* are of the *R* type and *c* is of the *I* type. The curves for cobalt and nickel are very similar but with each break displaced toward higher voltages with increasing atomic number. This similarity, with the regular displacement, is apparent for the entire range 0 to 1500 volts.

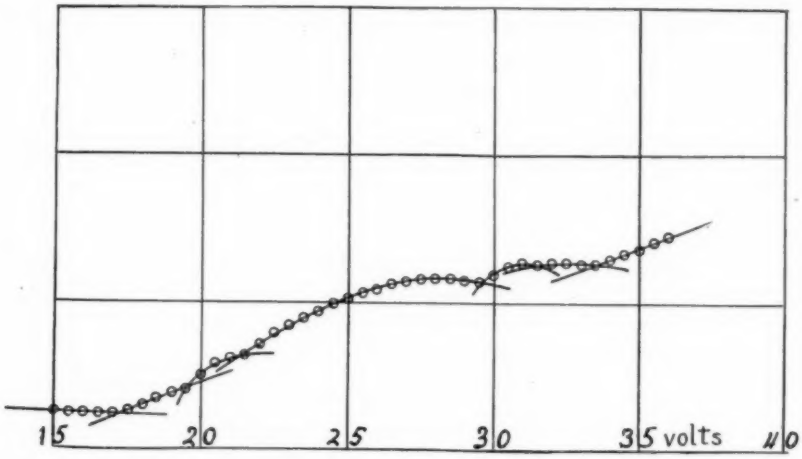


Fig. 2. Critical potentials of copper in the range 15 to 35 volts (uncorrected), as shown by a single run. Such curves were accurately reproduced in numerous check runs.

Fig. 2 is a replotted curve for copper. All the breaks shown are reproducible, appearing on all curves taken over this range. The break at 31.5 volts might be considered as questionable from this curve alone, but its appearance on other curves, especially those taken at smaller voltage intervals, indicates that it is genuine. In this connection it may be mentioned that more than 100 independent curves were obtained for each of the metals Fe, Co and Ni, and that the breaks here reported were consistently shown.

In several previous papers[2,3,4,5] on the photo-electric determination of critical potentials by essentially the same method, but with less sensitive

[2] Kurth, Phys. Rev. **18**, p. 461 (1921).
[3] Horton, Andrewes and Davies, Phil. Mag. **46**, p. 721 (1923).
[4] Miss Levi, Trans. Roy. Soc. Canada **18**, p. 159 (1924).
[5] Holtsmark, Phys. Zeits. **23**, p. 252 (1922); **24**, p. 225 (1923).

apparatus in which a considerably less proportion of the radiation was intercepted by the detecting electrode, previous authors have reported from one to four critical potentials in the range wherein the present work has shown 46 or 48. In order to illustrate the cause of this difference, the results of the present investigation were plotted at larger voltage intervals and the best lines drawn through these points. Fig. 3 shows such a curve for nickel, at two volt intervals. The curve shows breaks at 82 and at 104 or 110 volts, or both. In this range Miss Levi[3] has reported breaks at 76.8 and 102.8 volts; Horton et al.[2] found 104 volts; Holtzmark[4]

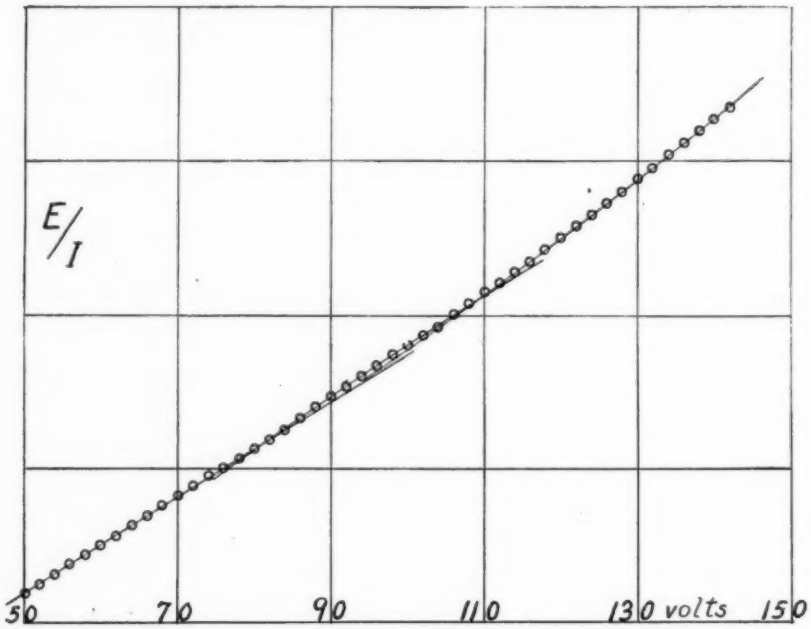


Fig. 3. Shows the result of plotting a larger range 50 to 150 volts at 2 volt intervals. The multiplicity of breaks is no longer visible, but there are points at which the slope of the curve changes, at 82 and at 104 or 110 volts. These points are identified with the critical potentials reported by previous observers.

reported 117.7 volts. These results, all uncorrected for work function, are in as good agreement as could be expected, since a break could not be located on a curve such as Fig. 3 without a possible error of two volts. It seems quite probable that the discrepancies between these values of the several investigators lie within the limits of accuracy of the several experiments. The same sort of agreement has been found in the other ranges and with both copper and iron also, insofar as these have been tested in this way. In the entire range 0 to 1500 volts for nickel, for instance, only four breaks stand out as permanent, considerable changes in

slope, and the curve is readily reconciled with Miss Levi's latest values of 53.6, 76.8, 102.8, 355.1 and 781.3 volts as the critical potentials. In the present work, however, 46 breaks appeared in curves which were reproducible when plotted to the full sensitivity of the apparatus and at small voltage intervals. We therefore conclude that the breaks shown by the present work are real and significant and that the failure of some previous investigators to discover them is due to lack of resolving power of their apparatus, resulting from lack of sensitivity or steadiness or the failure to take observations at sufficiently small voltage intervals. The present results are therefore not in conflict with previous work, but constitute an extension of it.

The potential drop across the filament, which consisted of several turns of helically wound tungsten wire, was from 2 to 2.6 volts, depending on its temperature. When the lead loss of about 1.25 volts is subtracted, there is left a potential range of from 0.75 to 1.35 volts over which the electrons are emitted. Taking the middle point of the filament as the source of electrons, making corrections for the contact difference of potential between the filament and the target, and allowing for the average initial energy of emission, it was estimated that the net correction amounted to 1.0 volt which should be subtracted from the applied voltage. To this was added the work function $\phi$, which has been taken as 5.0 volts for all the elements used, as explained in the preceding paper. These corrections are believed to be correct to $\pm 0.2$ volt, exclusive of the uncertainty in the value of $\phi$.

Table I gives the assembled results of the present investigations. At the head of the table are equations whereby the results may be converted into equivalent wave-lengths (in angstrom units) or into values of $\nu/R$. The $I$ or $R$ following the value for the intensity $J$ indicates the type of break. The voltages marked ? are doubtful breaks, since the breaks did not appear on every curve. $I$ or $R$ is followed by ? in each case in which it was difficult to classify the break, because it did not have the same shape on every curve. Except for the cases so marked, it is believed that the experiments are conclusive on the results as stated. In the case of iron the break at 159.8 volts replaces the one previously reported at 158.5, which was later found to be in error.

In order to show clearly the relation between these critical potentials of the several metals, they are plotted in Figs. 4 and 5. In Fig. 4 the position and relative intensity of the nine breaks of the $I$ type are plotted for iron, cobalt and nickel. The corresponding lines show a general agreement in intensity and an excellent agreement in position, for, in accordance with the Moseley law, each corresponding line is displaced

## TABLE I

*Critical potentials for Fe, Co, Ni and Cu.*
$V$ = critical potential, $J$ = intensity, $\lambda = 12354/V$,
$I$ = ionization break; $R$ = radiation break; $\nu/R = V/13.56$.

| Fe | | Co | | Ni | | Cu | |
|---|---|---|---|---|---|---|---|
| $V$ | $J$ | $V$ | $J$ | $V$ | $J$ | $V$ | $J$ |
| 7.3 | 2.5 $R$ | 8.8 | 1.2 $R$ | 8.6 | 2.4 $R$ | 10.3 | 2.3 $R$ |
| 11.1 | 2.7 $I$ | 11.6 | 3.5 $I$ | 11.7 | 4.0 $I$ | 12.3 | 3.4 $I$ |
| 14.1 | 2.2 $R$ | 14.4 | 2.5 $R$ | 14.6 | 2.0 $R$ | 14.2 | 2.4 $R$ |
| 16.5 | 2.9 $R$ | 17.0 | 3.1 $R$ | 18.0 | 2.4 $R$ | 15.7 | 2.0 $R$ |
| 19.4 | 1.8 $I$ | 20.9 | 2.3 $I$ | 22.2 | 2.3 $I$ | 19.0 | 2.3 $I$ |
| 24.3 | 1.3 $R$ | 25.7 | 1.8 $R$ | 27.3 | 1.6 $R$ | 20.7 | 1.4 $R$ |
| 28.8 | 2.5 $R$ | 29.3 | 1.2 $R$ | 31.0 | 1.4 $R$ | 23.8 | 1.8 $R$ |
| 34.3 | 2.0 $R$ | 32.2 | 2.2 $R$ | 34.6 | 2.2 $R$ | 25.5? | 1.4 $R$ |
| 37.5 | 1.1 $R$ | 38.5 | 1.9 $R$ | 39.8 | 1.4 $R$ | 33.7 | 1.8 $R$ |
| 41.2 | 2.5 $I$ | 43.2 | 1.6 $I$ | 44.7 | 1.5 $I$ | 35.5? | 0.8 $R$ |
| 48.0 | 2.4 $R$ | 49.3 | 1.8 $R$ | 51.3 | 2.0 $R$ | 37.5 | 2.8 $R$ |
| 51.3 | 1.6 $R$ | 52.8 | 1.2 $R$ | 54.8 | 0.9 $R$ | 40.0 | 1.2 $R$? |
| 54.6 | 3.1 $I$ | 55.8 | 2.9 $I$ | 57.4 | 3.1 $I$ | 42.0 | 1.8 $R$ |
| 62.0 | 2.7 $R$ | 62.8 | 1.7 $R$ | 65.6 | 2.0 $R$ | 45.9 | 1.2 $I$? |
| 67.6 | 1.6 $R$ | 70.7 | 1.1 $R$ | 71.9 | 1.5 $R$ | 49.0 | 0.9 $R$ |
| 75.3 | 2.2 $R$ | 76.7 | 1.8 $R$ | 79.8 | 1.7 $R$ | 51.0 | 1.9 $R$ |
| .... | ... | 81.0 | 1.2 $R$ | .... | ... | 53.8 | 2.2 $R$ |
| 82.7 | 2.3 $R$ | 84.3 | 1.9 $R$ | 87.2 | 1.6 $R$ | 62.0 | 1.8 $R$ |
| 87.0? | 1.1 $R$ | 89.4? | 1.3 $R$ | 91.2? | 0.9 $R$ | 64.5 | 1.6 $R$ |
| 91.2? | 1.3 $R$ | 92.5? | 1.5 $R$ | 94.9? | 1.2 $R$ | 74.0 | 1.6 $R$ |
| 94.8 | 1.3 $R$ | 97.7 | 1.7 $R$ | 98.3 | 1.7 $R$ | 84.0 | 1.8 $R$ |
| 103.5 | 2.0 $I$ | 104.4 | 2.0 $I$ | 106.5 | 2.0 $I$ | 88.0 | 1.4 $R$ |
| 112.2 | 1.7 $R$ | 114.3 | 1.9 $R$ | 116.6 | 1.2 $R$ | | |
| 125.7 | 1.5 $R$ | 125.5 | 1.3 $R$ | 127.0 | 1.0 $R$ | | |
| 131.8 | 1.9 $R$ | 131.4 | 1.5 $R$ | 133.7 | 1.4 $R$ | | |
| 136.0 | 1.3 $R$ | 138.3 | 1.5 $R$ | 139.6 | 1.4 $R$ | | |
| 140.7 | 1.6 $R$ | 143.8 | 1.5 $R$ | 145.0 | 1.3 $R$ | | |
| 150.2 | 1.6 $R$ | 154.0 | 1.3 $R$ | 156.8 | 1.4 $R$ | | |
| 159.8 | 1.3 $R$ | 163.5 | 1.3 $R$ | 167.3 | 1.0 $R$ | | |
| 169.4 | 2.3 $I$ | 173.3 | 1.3 $I$ | 178.2 | 1.2 $I$ | | |
| 181.6 | 1.2 $R$ | 185.5 | 1.2 $R$ | 186.2 | 1.2 $R$ | | |
| 192.0 | 1.8 $R$ | 195.6 | 1.6 $R$ | 197.7 | 1.8 $R$ | | |
| 212.0 | 1.5 $R$ | 214.0 | 1.3 $R$ | 217.7 | 1.3 $R$ | | |
| 221.3 | 1.1 $R$ | 223.0 | 1.4 $R$ | 228.2 | 1.1 $R$ | | |
| 228.1 | 2.8 $I$ | 230.8 | 1.9 $I$ | 232.7 | 1.8 $I$ | | |
| 241.0? | 1.0 $R$ | 244.8 | 1.1 $R$ | 247.7 | 1.3 $R$ | | |
| 250.8 | 1.4 $R$ | 255.5 | 1.5 $R$ | 257.0 | 1.6 $R$ | | |
| 261.5 | 1.1 $R$ | 264.6 | 1.3 $R$ | 265.9 | 1.4 $R$ | | |
| 271.5? | 1.2 $R$ | 277.4 | 1.8 $R$ | 280.0 | 2.0 $R$ | | |
| 277.4 | 1.4 $R$ | 285.1 | 1.5 $R$ | 286.5 | 1.4 $R$ | | |
| 288.6 | 1.1 $R$ | 293.7 | 1.2 $R$ | 294.9 | 0.9 $R$ | | |
| 303.7 | 1.8 $R$ | 306.5 | 2.1 $R$ | 311.5 | 1.8 $R$ | | |
| ..... | ... | 326.3 | 1.2 $R$ | ..... | ... | | |
| 331.0 | 1.6 $R$ | 335.8 | 2.3 $R$ | 341.3 | 2.0 $R$ | | |
| 639.0 | 0.9 $R$ | 705.2 | 1.1 $R$ | 774.0 | 0.9 $R$ | 820.4 | 1.4 $R$ |
| 704.3 | 1.5 $I$ | 764.8 | 1.8 $I$ | 833.4 | 2.1 $I$ | 929.0 | 2.2 $I$ |
| 818.5 | 2.0 $I$ | 873.2 | 2.0 $I$ | 948.0 | 2.0 $I$ | 1017.0 | 2.0 $I$ |
| ..... | ... | 950.1? | 1.3 $R$ | 1017.3 | 0.7 $R$ | | |

toward higher voltages with increasing atomic number, the amount of the displacement increasing with the voltage. This agreement in displacement is a strong support for the validity of these results, and their interpretation as indicating the excitation of soft x-rays. Fig. 5 similarly

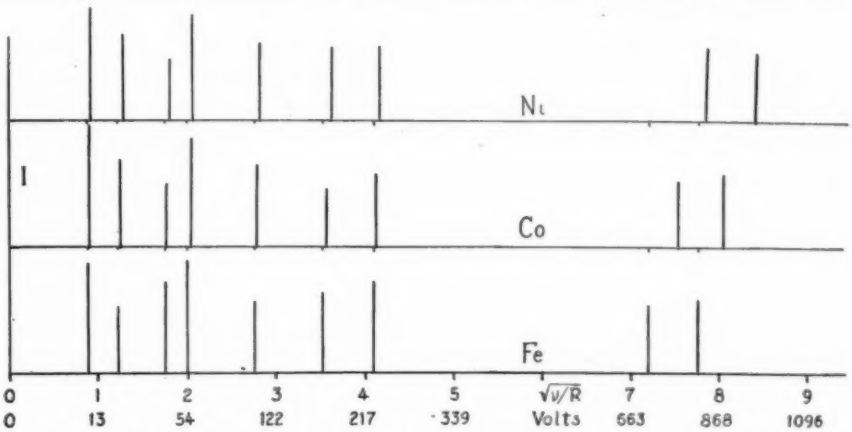


Fig. 4. Type $I$ breaks plotted to a scale of $\sqrt{\nu/R}$. Lengths are proportional to intensities of breaks. Dots on the axes for Co and Ni indicate the location of the Fe breaks, so as to bring out the displacement with atomic number.

represents the $R$ potentials up to 350 volts. Here, likewise, there is an evident correspondence and a regular displacement of the breaks in the case of iron, cobalt and nickel, but there is no obvious agreement in the case of copper. The lowest voltage break in each case could not be determined as accurately as the others. The next one, shown as a dotted line, is an $I$ potential, and shows good agreement for all four metals.

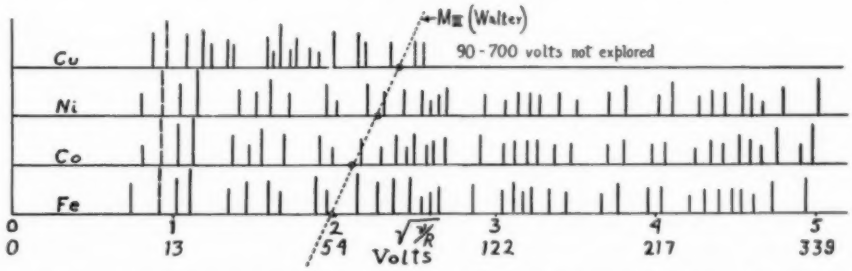


Fig. 5. Type $R$ breaks plotted to a scale of $\sqrt{\nu/R}$. The dotted line shows the positions of the $M_{III}$ critical potentials as calculated from the combination principle.

Cobalt shows two more breaks than does iron or nickel. The corresponding breaks were not certainly established for the latter metals, although there was a suggestion of these breaks on some of the curves. The fact that cobalt was used last, when the experimental technique had

been improved, possibly accounts for the location of these two extra breaks. The break at 34.3 volts in iron is not in good agreement with the corresponding breaks for cobalt and nickel. Careful check runs failed to detect any error in the determination of this voltage, so that the peculiarity seems to be real.

It is probable that the failure of the critical potentials of copper to correspond with those of the other metals in the lower voltage range is to be explained on the basis of the Bohr theory. Iron, nickel and cobalt form a transition group in which the outer electron configuration is probably similar in all three and the configuration is in a somewhat

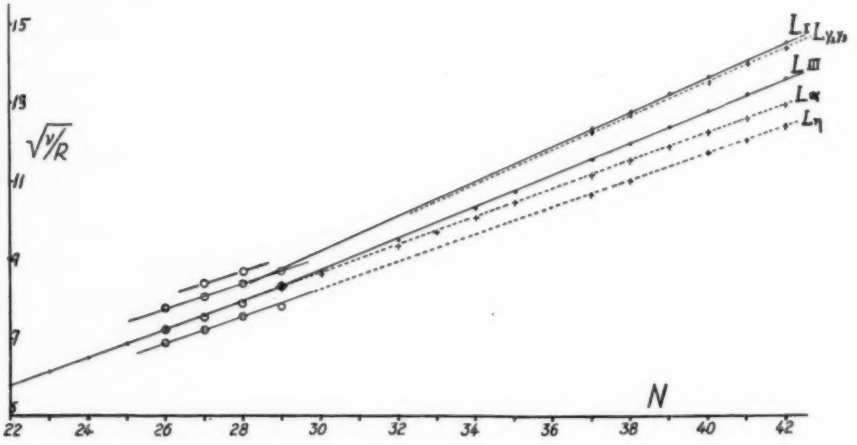


Fig. 6. Moseley diagram showing critical potentials of the L series. Circles represent results of the present investigation. Other points are taken from x-ray spectroscopic data.*

labile state. In copper these groups are believed to exist in definite stable configurations. In support of this belief is the fact that the Moseley curves show changes of slope between nickel and copper, as is illustrated by the curve $L_{III}$ in Fig. 6.

In attempting to correlate these critical potentials with spectroscopic data of x-rays, it must be born in mind that the only x-ray data which have been obtained for this spectral region are values of the $L_{III}$ absorption limits, which have been computed from K series data by Walter[6] and Bohr and Coster[7] and others. Emission data for the Lα line are given for elements down to (including) copper by Hudson[8] and by Siegbahn

[6] Walter, Zeits. f. Phys. **30**, 350 (1924).
[7] Bohr and Coster, Zeits. f. Phys. **9**, 286 (1924).
[8] Hudson, J. Opt. Soc. Am. and Rev. Sci. Inst. **9**, 286 (1924).
* Values of Siegbahn and Thoræus are not plotted.

and Thoræus[9] for the L$\alpha$ and L$\beta$ emission lines for the elements Cu, Ni Co and Fe. The Moseley curves can be drawn through this region for the L series only by extrapolation or by calculations based on the combination principle which are of limited accuracy. Fig. 6 shows the x-ray data[10] in this spectral region together with the data which have been obtained from the present investigation.

One of the critical potentials of type *I* for each metal is seen to agree almost exactly with the $L_{III}$ spectral term. The other *I* critical potential comes where we might expect the $L_I$ term to be, as shown by the extrapolated line. Both of these sets of potentials show the change of slope of the Moseley curves between nickel and copper. The lowest critical potential of type *R* for each metal is in about the right place to be identified with the L$\eta$ emission line. The highest *R* potentials, observed only in cobalt and nickel, cannot at present be identified with any term of the spectrum. The values of Siegbahn and Thoræus for the L$\alpha$ line agree within 1.5 percent with the author's values designated as $L_{III}$. The average of the L$\alpha$ and L$\beta$ lines by Siegbahn and Thoræus for each of these four elements shows equally good agreement with the corresponding values for $L_{III}$. This shows that the present method is not capable of differentiating between the lines L$\alpha$, L$\beta$ and the absorption limit $L_{III}$. Taken as a whole, there seems to be little room for doubt that these higher critical potentials are definitely associated with x-ray terms of the L series. Table II gives values of $\nu/R$ for $L_{III}$ as given by Walter,[8] by Bohr and Coster[7] and as calculated from the present work, together with the values of L$\alpha$ by Siegbahn and Thoræus.[9]

TABLE II

*Values of $\nu/R$ for $L_{III}$ and L$\alpha$*

| | Authority | Fe | Co | Ni | Cu |
|---|---|---|---|---|---|
| For $L_{III}$ | Walter | 52.19 | 57.5 | 63.1 | 69.09 |
| | Bohr and Coster | 52.2 | 58.5 | 61.3 | 69.8 |
| | Thomas | 52.01 | 56.46 | 61.52 | 68.58 |
| For L$\alpha$ | Siegbahn and Thoraeus | 51.63 | 56.73 | 62.23 | 68.09 |

Not much can be said with certainty regarding the M terms. The only one of these which is given with any assurance is the $M_{III}$ term, determined by the combination principle by Walter, and shown by the dotted line in Fig. 5. Probably the M terms would appear at voltages between

[9] Siegbahn and Thoræus, Arkiv f. Matematik, Astron. och Phys. **18**, No. 24 (1924).
[10] Values of Siegbahn and Thoræus are not plotted.

100 and 200, and the remaining M terms, together with the N, etc., terms, would be below 50 volts. This leaves a number of the critical potentials which seem to be too high to fit into the M scheme, but are quite definitely related to these rather than to the higher L terms.

It scarcely seems worth while to hazard an explanation of these numerous lower critical potentials, but three possibilities may be kept in mind. (1) Some of the critical potentials may be due to "multiple excitation"; that is, an electron may lose just enough energy to one atom to excite some type of radiation and retain just enough to excite another atom also. Such double excitation should give critical potentials which are the sum of others associated with single excitation. (2) Some of the critical potentials may be associated with the x-ray spark lines, which are unknown in this part of the spectrum but which must certainly be present. (3) It may be that the permanent changes in slope of the curves, such as are found when less resolving power is used, are the breaks which correspond to the x-ray terms. As mentioned earlier in the paper, such changes, in the case of nickel, occur at 82, 104 or 110 as well as 833 and 948 volts. It is possible to identify all these with $M_{III}$, $M_I$, $L_{III}$ and $L_I$ respectively.

In order to arrive at a satisfactory correlation and explanation of such critical potentials as are reported in this paper, it is desirable to make similar observations on metals of lower atomic number where the spectral relations should be simpler, and also on elements of higher atomic number whose x-ray relations have been more completely worked out. Such work is now in progress.

In conclusion, the writer wishes to express his thanks to Professor K. T. Compton for his encouragement and for his most helpful assistance during the course of this investigation.

PALMER PHYSICAL LABORATORY,
PRINCETON, N. J.
August 18, 1925.

# APPLICATION OF THE CORRESPONDENCE PRINCIPLE TO RELATIVE INTENSITIES IN SERIES SPECTRA

By Frank C. Hoyt

Abstract

A brief discussion is given of the representation of intensities in emission and absorption in terms of the probabilities of transition and of the estimation of the probability $A'_{n}$ of spontaneous transition in the usual way based on the correspondence principle. It is shown that on the basis of the Bohr theory approximate values of $A'_{n}$ may be obtained in many cases from the information as to the parameters of the stationary orbits which is given by the values of the spectral terms and their quantum numbers, together with the harmonic analysis of the penetrating orbits given in a previous paper.[1] In other cases a detailed knowledge of the intermediate orbits is shown to be necessary. Calculations are made of the *relative probabilities of the transitions involved in the principal series of sodium*. The values obtained by different methods of averaging are compared with the experimental results of Harrison (Phys. Rev. **25**, 768, 1925). A possible explanation is offered of the observed relative intensities in emission of certain lines with the same initial state. It is pointed out that the frequencies of the spectral lines may be approximately calculated from the orbital frequencies of the series electron when the orbits are similar as in the case of *sp* combinations.

## 1. Introduction

In a previous paper[1] a method was given for obtaining an approximate harmonic representation of the so-called orbits of the second kind or penetrating orbits of the electrons in the atom, based on the atomic theory of Bohr. In the present paper a brief discussion will be given of the application of the correspondence principle to the estimation of relative intensities in emission and absorption, followed by an outline of the way in which the analysis of the previous paper may be applied to line spectra. No data at present available on emission intensities appear to be sufficiently reliable for a comparison with the theoretical predictions, but in the case of some recent measurements on intensities in absorption in the principal series of sodium a quantitative comparison will be made with the calculations.

## 2. Theory of the Estimation of the Intensities of Spectral Lines on the Basis of the Correspondence Principle

We shall assume that the intensity $I$ in emission of a spectral line of frequency $\nu$ is given by the expression

$$I = N' A'_{n} h\nu \tag{1}$$

[1] F. C. Hoyt, Phys. Rev. **25**, 174 (1925). In what follows the results and notation of this previous paper will be used.

where $N'$ is the number of atoms present in the initial state, $h$ is Planck's constant and $A'_{,,}$ the probability as introduced by Einstein[2] that a given atom undergo in unit time a spontaneous transition from one stationary state indicated by a single prime to one of lesser energy indicated by a double prime.[3] An estimate of the probability $A'_{,,}$ may now be made on the basis of the correspondence principle in the well-known way[4] if the rate of emission of energy given by (1) is equated to that of an equivalent harmonic oscillator radiating according to the classical laws. This gives

$$A'_{,,}=\frac{1}{h\nu}\,\frac{32\pi^4e^2}{3c^3}(Q^2\nu_0^4) \tag{2}$$

where $Q$ is the effective amplitude and $\nu_0$ the effective frequency of the equivalent or "virtual" oscillator. The fact that the frequency $\nu$ may be represented for multiply periodic systems as an average value of the "corresponding" harmonic $\omega_0=\tau_1\omega_1+\ldots.+\tau_s\omega_s$ by an expression of the form

$$\nu=\int_0^1\omega_0 d\lambda \tag{3}$$

where $\lambda$ is a parameter defining a set of states intermediate between the initial and final states, suggests that $(Q^2\nu_0^4)$ may also be obtained from an average value of the same type of the quantity $C^2\omega_0^4$ or of some function of this quantity, where $C$ is the resultant amplitude of the corresponding harmonic component of the electric moment of the atom.[5]

A great variety of possible types of average[6] have been suggested but their evaluation is possible only in the simplest cases. However, in certain instances a sufficiently accurate estimate of $A'_{,,}$ may be obtained by representing $Q$ as a simple average of its values in the initial and final stationary states, as for example by

$$Q^2=\tfrac{1}{2}(C'^2+C''^2) \tag{4}$$

with

$$\nu_0=\nu$$

in which case

$$A'_{,,}=\left(\frac{32\pi^4e^2}{3c^3h}\right)Q^2\nu^3$$

[2] A. Einstein, Phys. Zeits. **18**, 121 (1917).

[3] In what follows quantities referring to the state of greater energy will always be denoted by a prime, while those referring to the state of lesser energy will be denoted by a double prime.

[4] See, for example, Ladenburg and Reiche, Naturwissenschaften **11**, 584 (1923).

[5] N. Bohr, Zeits. f. Physik **13**, 142 (1923).

[6] For a brief discussion of the possible types of average see F. C. Hoyt, Phil. Mag. **46**, 135 (1923).

and from Eq. (1)

$$I = \text{const.} \times Q^2\nu^4. \tag{5}$$

We must remember, however, that in many cases it will be necessary to take into account the amplitudes $C$ in the intermediate states. Such will in general be the case when these amplitudes differ greatly from those in the stationary states, and a certain criterion for the applicability of so simple an average as Eq. (4) may be found in the possibility of representing the frequency $\nu$ with sufficient accuracy by an average of the type

$$\nu = \tfrac{1}{2}(\omega_0' + \omega_0'') \tag{6}$$

involving only the orbital frequencies in the stationary states.

### 3. The Estimation of the Corresponding Amplitudes

In the previous paper a brief discussion was given of the character of the electron orbits involved in the emission of line spectra and the method of estimating the corresponding amplitudes was outlined. Here we shall consider in more detail the determination of these amplitudes in simple cases, using the results and notation of that paper. It is assumed that to a high degree of approximation the motion of the series electron may be regarded as a central motion, and hence the stationary states may be designated by the quantum symbol $n_k$, where $n$ is the principal quantum number and $k$ the subordinate quantum number. The value of the given spectral term is then a function of $n$ and $k$ and the terms may be arranged in series, each series corresponding to a certain value of $k$ and the terms within a given series being approximately representable by a Rydberg formula with successive integral values of $n$. In the case of the simple systems of series occurring in a large number of elements the values of the terms are given by series expressions

$$mt = p^2R/(n-q_t)^2 \tag{7}$$

where the $q$'s, which are ordinarily called the quantum defects, are to a first approximation independent of $n$. Here $p$ is the degree of ionization of the atom (i.e. $p$, which is the same as the $N-N_i$ of the previous paper, is 1 for the arc spectra, 2 for first spark spectra, etc.). The integer $m$ is merely the serial number of the term and is not to be confused with the quantum integer $n$, while $t$ stands for any one of the characteristic term series $s, p, d, f, \ldots$ for which $k = 1, 2, 3, 4, \ldots$ respectively.

The values of the $k$'s for the various series are readily assigned from simple considerations, but the fixation of the principal quantum numbers $n$ is a matter of greater difficulty. Obviously the quantum defects will be dependent on the values of $n$, as the denominator $(n-q)^2$ only is

fixed by the value of the term. Assuming any assignment of the $n$'s, however, we have the following approximate method of finding the corresponding amplitudes.

According to the formula derived in the previous paper the amplitudes $C_\tau$ of the circular vibrations

$$x+iy=\sum_{-\infty}^{+\infty} C_\tau e^{2\pi i(\tau\omega+\sigma)t}$$

into which the motion of the series electron referred to axes in the plane of the orbit may be resolved, are represented for a given value of $\tau$ as

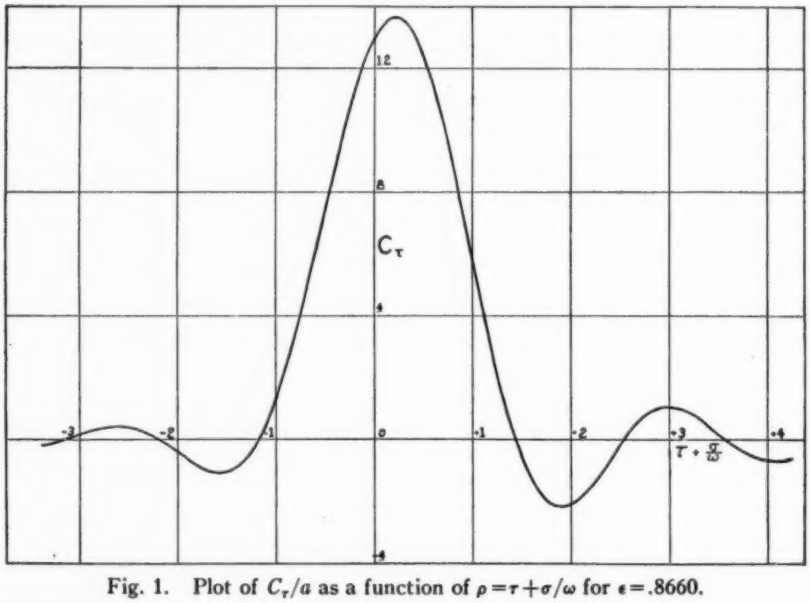


Fig. 1. Plot of $C_\tau/a$ as a function of $\rho=\tau+\sigma/\omega$ for $\epsilon=.8660$.

functions of the major axis $a$, the eccentricity $\epsilon$ of the outer loop, and the quantity $\sigma/\omega$ which for the penetrating type of orbit assumed is equal to the ratio of the frequency of precession to the radial frequency of the motion. The coefficients are of course directly proportional to the major axis. It will be seen from Eq. (22) of that paper, however, that in reality the amplitudes for given values of $a$ and $\epsilon$ are continuous functions of the quantity $\rho=\tau+\sigma/\omega$ in the case of penetrating orbits.[7] Fig. 1 shows the computed values of $C_\tau/a$ plotted as a function of $\rho$ for $\epsilon=.8660$, the eccentricity of a $2_1$ orbit in hydrogen. This plot may then be interpreted in two ways. If we consider only values of $\sigma/\omega$ between 0 and 1 the portion

[7] For orbits of the non-penetrating type the coefficients $C_\tau$ are given to a first approximation by Eq. (22) with $\sigma/\omega=0$.

of the curve from $\rho=0$ to $\rho=1$ represents $C_0$ as a function of $\sigma/\omega$ while that from $\rho=1$ to $\rho=2$ represents $C_1$ as a function of $\sigma/\omega$, and so on. If, however, we consider values of $\sigma/\omega$ greater than 1 as seems to be necessary in certain cases, we may think of the whole curve for positive $\rho$ as representing $C_0$ as a function of $\sigma/\omega$, or by proper shift of the origin as giving any $C_\tau$ as a function of $\sigma/\omega$. For the actual estimation of the amplitudes by graphical interpolation a plot of $C_\tau$ as a function of $\epsilon$ for discrete values of $\sigma/\omega$ is more convenient, but the diagram given here shows more clearly the effect of increasing rotation on the coefficients. The character of the curve does not depend greatly on the value of $\epsilon$ if $\epsilon$ is near 1. For $\epsilon=1$ the curve is symmetrical with respect to the vertical axis.

From a consideration of spectral data alone it is possible to estimate the value of $C_\tau$ corresponding to an assignment of the $n$'s and $k$'s to the various terms, as these data give approximate values of $\epsilon$, $a$, and $\sigma/\omega$. As already pointed out $\tau$ is given by the changes in the quantum numbers. Thus $\tau=\pm\Delta n$, the positive sign being taken if it changes in the same sense as $k$ and the negative sign being taken if it changes in the opposite sense.[8] The quantities $a$ and $\epsilon$ may be found in the well-known way from the effective quantum numbers by means of Eqs. (7), (8), and (9) of the previous paper. The values of $\sigma/\omega$ can be estimated as follows[9]: From the general theory of multiply periodic systems the values of $\omega$ and $\sigma$ satisfy the relations $\omega=\partial E/\partial J$, $\sigma=\partial E/\partial P$ where $J$ and $P$ are the "uniformization variables" conjugate to $\omega$ and $\sigma$ respectively. Since in the stationary states $J=nh$ and $P=kh$ we have,

$$\omega=\frac{1}{h}\frac{\partial E}{\partial n}, \quad \sigma=\frac{1}{h}\frac{\partial E}{\partial k} \tag{8}$$

where $E$ is the total energy of the motion. If we suppose this energy to be given by the formula

$$E=Rh/(n-q)^2$$

we get by carrying out the differentiation, remembering that $q$ depends only on $k$,

$$\sigma/\omega=-dq/dk. \tag{9}$$

Thus $\sigma/\omega$ is given approximately by the negative of the slope of the curve obtained by plotting $q$ as a function of $k$ for a constant value of $n$. It must be remembered that the values of $q$ depend on the $n$'s, and consequently the values of the corresponding amplitudes depend on the

[8] See p. 184 of the previous paper.

[9] See Thomas, Zeits. f. Phys. **24**, 169 (1924).

assignment of the principal quantum numbers not only through the order of the harmonic but also through the values of $\sigma/\omega$.

## 4. Calculation of Transition Probabilities for the Alkali Metals

In this section we shall discuss the application of the general considerations outlined above to some special types of transition in the arc spectra of the alkalis and give the quantitative results for the principal series transitions of sodium.

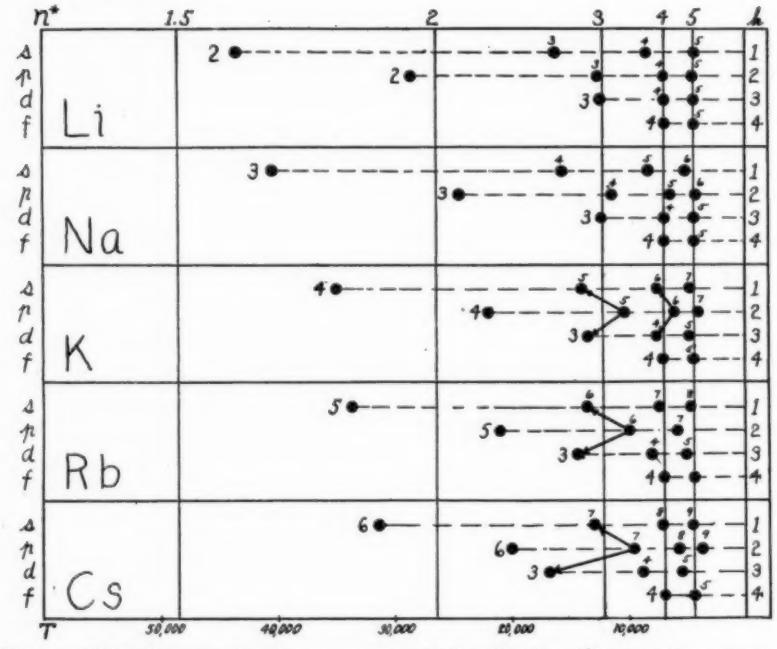


Fig. 2. Bohr diagrams for the arc spectra of the alkalies. The numbers attached to the terms are the principal quantum numbers $n$.

In Fig. 2 are shown Bohr diagrams for these alkali spectra. The numbers attached to the terms give the principal quantum numbers $n$ according to the assignment of Bohr, which is based on special considerations of quantum dynamics in relation to the periodic properties of the elements. The values of $n$ and $k$ give at once the order of the harmonic corresponding to any given transition.

In the diagrams the fine structure of the terms has been omitted. In disregarding this fine structure in the calculations we are proceeding as though we had to do with a plane doubly-periodic motion and assuming that this gives the total transition probability for the sum of the com-

ponents. Such a procedure cannot be strictly justified and in fact as pointed out by Kemble[10] and others the transition probability in such a case of degeneracy may be expected to depend in some way on the statistical weights of both initial and final states. It should be noted, however, that in comparing relative probabilities of transition of lines of the same series within which the statistical weights of initial and final states are the same, the existence of such a factor would not influence the results. In comparing lines of different series, however, it would probably have to be taken into account.

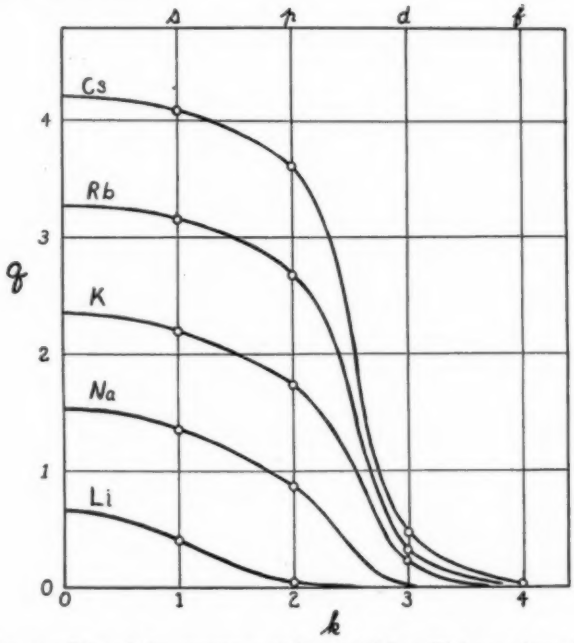


Fig. 3. Plot of the quantum defect $q$ (cf Eq. (7) ) as a function of $k$ for the arc spectra of the alkalies.

The values of $\sigma/\omega$ for the $s$ and $p$ states necessary for the estimation of the corresponding amplitudes as determined from Eq. (9) by means of a plot of the quantum defect $q$ against $k$ for constant $n$ (Fig. 3) are given in Table I. The variations of $q$ with $n$ have been neglected, as they are small compared to the uncertainties in drawing the curves and finding the slopes. For the $d, f, \ldots$ . terms we may suppose that the values of $\sigma/\omega$ are zero or at any rate very small, as according to Bohr[11] they are due to orbits of the non-penetrating type, while the $s$ and $p$ terms are due to orbits of the penetrating type.

[10] E. C. Kemble, Phys. Rev. **25**, 1 (1925).
[11] N. Bohr, Ann. der Phys. **71**, 228 (1923).

Values of the corresponding amplitudes in the stationary states may now be found for any desired transition, as described in Section 3. For this purpose plots of $C_\tau$ as a function of $\epsilon$ for different values of $\sigma/\omega$ were found most convenient. In estimating the transition probabilities, how-

TABLE I

*Values of $\sigma/\omega$ in the s and p states.*

| Element | *s* states | *p* states |
|---|---|---|
| Na | .35 | .70 |
| K | .31 | .67 |
| Rb | .29 | .86 |
| Cs | .28 | 1.00 |

ever, some consideration must be given to the probable values of the amplitudes in the "intermediate" states. In fact, as pointed out in Section 2, it is only in certain cases that we can hope to represent these probabilities in terms of the amplitudes in the stationary states alone, and a reasonable criterion for the possibility of representing the probabilities in this way may be found in the degree of approximation with which the frequency $\nu$ may be represented as an average of the type of Eq. (6), involving only the corresponding orbital frequencies in initial and final states.

TABLE II

*Comparison of computed and observed frequencies.*

| Element | Line | Calc. (1) | Calc. (2) | Obs. | $\overline{\sigma/\omega}$ |
|---|---|---|---|---|---|
| Na | $2s-3p$ | 4590 | | 4529 | |
| | $3d-3p$ | 5330 | 1170 | 1093 | .856 |
| K | $2s-3p$ | 3660 | | 3683 | |
| | $3d-3p$ | 13680 | 3900 | 3179 | 1.51 |
| K | $3s-4p$ | 1550 | | 1550 | |
| | $4d-4p$ | 4780 | 1730 | 1611 | 1.51 |
| Rb | $2s-3p$ | 3940 | | 3660 | |
| | $3d-3p$ | 21900 | 5270 | 4437 | 2.35 |
| Rb | $3s-4p$ | 1720 | | 1553 | |
| | $4d-4p$ | 9350 | 2260 | 2164 | 2.35 |
| Cs | $2s-3p$ | 4050 | | 3410 | |
| | $3d-3p$ | 25000 | 8040 | 7348 | 3.15 |

Calc. (1) : Frequencies computed from the equations $\nu=\frac{1}{2}(\omega_0'+\omega_0'')$; $\omega_0=(\tau+\sigma/\omega)(2R/n^{*2})$.

Calc. (2) : Frequencies computed from the equation $\nu=(\tau+\overline{\sigma/\omega})\bar{\omega}$ where $\overline{\sigma/\omega}$ is the slope of the straight line joining the stationary states in Fig. 3 and $\bar{\omega}=\frac{1}{2}(\omega'+\omega'')$. Values of $\overline{\sigma/\omega}$ used are given in the last column.

If we apply this criterion to the transitions involved in the alkali spectra we find that for transition between $s$ and $p$ terms the frequencies may be represented with a fair degree of accuracy by Eq. (6). For $pd$ combinations, on the other hand, Eq. (6) does not give even a first approximation. The results of computations of the frequencies for certain $sp$ and $pd$ combinations are shown in the first column of Table II. The frequencies $\omega_0=\tau\omega+\sigma=(\tau+\sigma/\omega)\omega$ of the corresponding harmonics have been found from the values of $\sigma/\omega$ in Table I and values of $\omega$ computed from the spectral terms by means of the relation $\omega=2R/n^{*3}$. In the second column are given values of $\nu$ computed from the harmonic of an intermediate orbit for which $\sigma/\omega$ is taken as the slope of a straight line joining the stationary states in Fig. 3. In this case the agreement is better, although not quantitative.

This difference between $sp$ and $pd$ combinations is probably due to the fact that the former are transitions between orbits both of which are of the same type (penetrating orbits) while the latter are transitions between penetrating and non-penetrating orbits, in which case one may expect very large values of the frequency of precession when the series electron penetrates almost tangentially into the inner region.

We may then conclude that for $sp$ combinations the transition probabilities may be approximately represented by an average of corresponding amplitudes in the stationary states. Computations have been made for various transitions, but it is only in the case of the principal series of sodium that a satisfactory comparison with experimental data seems possible at present, and hence only the results for these transitions are reproduced here. Table III gives the computed corresponding amplitudes necessary for a calculation of the transition probabilities for the first five lines.

TABLE III

*Computed values of corresponding harmonics for the principal series of sodium.*

| Term | $C_0$ | $C_1$ | $C_2$ | $C_3$ | $C_4$ |
|---|---|---|---|---|---|
| $1s$ | $3.38a_0$ | $.506a_0$ | $.356a_0$ | $.217a_0$ | $.143a_0$ |
| $2p$ | 4.55 | .... | .... | .... | .... |
| $3p$ | .... | 1.28 | .... | .... | .... |
| $4p$ | .... | .... | 1.14 | .... | .... |
| $5p$ | .... | .... | .... | 0.971 | .... |
| $6p$ | .... | .... | .... | .... | 0.830 |

The values are in terms of $a_0=.532\times10^{-8}$cm as unit.

The probability of spontaneous transition $A'_{,}$ may now be found from Eq. (2), but as mentioned in Section 2 the representation of $Q^2\nu_0^4$ as an average of $C^2\omega_0^4$ may be made in several different ways. Since the

results depend very considerably on the method of averaging the following six methods have been employed:

$$Q^2\nu_0^4=\tfrac{1}{2}(C'^2+C''^2)\nu^4 \qquad (A)$$

$$Q^2\nu_0^4=\tfrac{1}{4}(C'+C'')^2\nu^4 \qquad (B)$$

$$\log Q=\tfrac{1}{2}(\log C'+\log C'')\ ;\quad \nu_0=\nu \qquad (C)$$

$$Q^2\nu_0^4=\tfrac{1}{2}(C'^2\omega_0'^4+C''^2\omega_0''^4) \qquad (D)$$

$$Q^2\nu_0^4=\tfrac{1}{4}(C'\omega_0'^2+C''\omega_0''^2)^2 \qquad (E)$$

$$\log Q\nu_0^2=\tfrac{1}{2}(\log C'\omega_0'^2+\log C''\omega_0''^2) \qquad (F)$$

These averages correspond to the six methods of taking a continuous average which have been discussed previously in another connection.[6]

Table IV shows the computed values of $A'_{,,}$ as obtained by these six different methods.[12]

TABLE IV

*Relative values of $A'_{,,}$ for the principal series of sodium.*

| Lines | A | B | C | D | E | F |
|---|---|---|---|---|---|---|
| $1s-2p$ | 1 | 1 | 1 | 1 | 1 | 1 |
| $1s-3p$ | .33 | .29 | .24 | 1.2 | 2.9 | .20 |
| $1s-4p$ | .35 | .29 | .21 | 4.9 | 2.8 | .16 |
| $1s-5p$ | .33 | .24 | .15 | 7.1 | 3.6 | .013 |
| $1s-6p$ | .26 | .18 | .09 | 11.0 | 5.5 | .046 |

TABLE V

*Comparison of computed values of $A'_{,,}$ with Harrison's measurements.*
Ratios of $A'_{,,}$ for successive lines

| Lines | A | B | C | F | Experimental |
|---|---|---|---|---|---|
| $2p/3p$ | 3.0 | 3.4 | 4.2 | 5.0 | (4−12) |
| $3p/4p$ | .94 | 1.0 | 1.1 | 1.3 | 1.56 |
| $4p/5p$ | 1.1 | 1.2 | 1.4 | 2.2 | 1.38 |
| $5p/6p$ | 1.3 | 1.3 | 1.7 | 1.6 | 1.29 |

## 5. COMPARISON WITH EXPERIMENT

Relative values of the transition probabilities may be found directly from observed intensities in emission only in the case of two or more lines which have the same initial state. Such sets of lines are of rare occurrence in series spectra as ordinarily observed, and although in a few cases some estimates of intensities for such lines are available it would appear

[12] In a recent paper H. Bartels (Zeits. f. Phys. **32**, 415, 1925) has calculated transition probabilities for *sp* transitions in sodium, using a method of approximation for the amplitudes similar to that employed by the author. His calculations do not include the principal series transitions, but it is interesting to note that he also comes to the conclusion that averages involving only the stationary states are applicable to *sp* transitions, but not to *pd* transitions.

that they are too unreliable for a quantitative comparison where so many other uncertainties already enter in.

It may be mentioned here, however, that bolometric measurements of Paschen[13] and Randall[14] on infra-red combination lines of the alkalis give some information as to the relative intensities of certain *sp* and *pd* combinations with the same initial states. These transitions are marked with arrows in Fig. 2. Although probably not very accurate these measurements indicate that the *pd* combinations are in every case more intense than the corresponding *sp* combinations, even though the former correspond to harmonics of lower order than the later. For the reasons given in Section 4 it is not possible to make an estimate by the methods of approximation described here of the transition probabilities for *pd* combinations, but from Fig. 3 we can see that the intermediate states which will be of importance in determining the mean corresponding amplitudes will probably involve large values of the ratio $\sigma/\omega$. This fact offers a possible explanation of the abnormally large intensities of the *pd* combinations, as may be seen from Fig. 1 which shows how the amplitudes change with increasing values of $\sigma/\omega$. At the same time we must remember that since the statistical weights of initial and final states are not the same for these two types of transition, it may not be possible to compare directly the transition probabilities without taking into account this fact.

The most reliable estimates of transition probabilities at present available seem to be those of Harrison[15] and Slater[16] for the principal series of sodium. These are based on accurate measurements by Harrison of the relative absorption of these lines in sodium vapor, from which the probabilities were deduced by a method devised by Slater. These probabilities may be compared directly with the computed values of Table IV, and Table V shows the ratios of $A'_{,,}$ for successive lines calculated by different methods of averaging.[17] In the last column are the experimental results of Harrison. The averages D and E have been omitted from Table V as they give values widely at variance with the experimental results. Harrison's measurements give only a rough indication of the values for $1s-2p$ (the D-lines).

[13] F. Paschen, Ann. der Phys. **33**, 717 (1910).

[14] Randall, Ann. der Phys. **33**, 739 (1910).

[15] G. R. Harrison, Phys. Rev. **25**, 768 (1925).

[16] J. C. Slater, Phys. Rev. **25**, 783 (1925).

[17] That the agreement is not as good as indicated in Harrison's paper is due to the fact that the preliminary calculations sent to Dr. Harrison and published by him were found to be in error.

It must be admitted that the agreement by no one of the methods of averaging is very satisfactory. This may be attributed partly to the fact that the method of estimating the corresponding amplitudes is only an approximation, and partly to the fact that if any method of averaging is universally applicable it will certainly not be of a kind which involves only initial and final states.

NATIONAL RESEARCH FELLOWSHIP,
THE UNIVERSITY OF CHICAGO,
October, 1925

# FLUORESCENCE OF CADMIUM VAPOR

By A. D. Power

Abstract

**Fluorescence of cadmium vapor.**—Cadmium vapor, in an evacuated and carefully baked quartz tube, when illuminated by cadmium, iron and nickel sparks, was found to emit the lines 3262A ($1S-2p_2$), 4678A ($2p_3-1s$), 4800A ($2p_2-1s$) and 5086A ($2p_1-1s$) much more strongly from freshly formed vapor than from older vapor. The line 2289A ($1S-2P$) also appeared slightly stronger in the freshly formed vapor when illuminated by the cadmium spark; it was not excited by iron and nickel sparks. Experiments are described which indicate that it was the freshness of the vapor, not primarily the temperature or pressure, which determined the intensity of the radiation. The effective exciting light was absorbed by glass, hence shorter than 3300A. A Cu spark did not excite the lines, at least in the visible.

**Fluorescence of thallium and indium vapors.**—Impurities in the cadmium vapor gave strong fluorescent Th and In lines, ($2p_2-2s$) and ($2p_1-2s$), although spark spectra using the cadmium metal as electrodes did not reveal their presence. These lines were radiated only by the freshly formed vapor and appear to be the result of directly absorbed radiant energy rather than of collisions of the second kind. They were weaker with Cd spark excitation than when light from a Ni or Fe spark was used. Light from a Cu spark excited only the Th lines.

VAN DER LINGEN and Wood[1] have found that mercury vapor under aluminum spark excitation, radiates the line λ2537A much more strongly when the vapor is freshly formed from the liquid than when the vapor is older. It seemed of interest to investigate the behavior of cadmium vapor under comparable conditions.

In the first experiments, the cadmium was contained in a quartz vessel made from tubing having a diameter of about 3 mm and a length of 7 cm, with a bulb of about 1 cm diameter blown on each end. After introducing the cadmium this vessel was carefully evacuated and sealed off. The exciting spark was focused on one of the bulbs and any desired portion of this bulb was focused upon the slit of a quartz spectrograph, the arrangement being such that a minimum of reflected light entered the latter. The cadmium was maintained at various temperatures and driven from bulb to bulb by suitably arranged Bunsen burners.

It was found that when the cadmium vapor was illuminated by a cadmium spark, λ3262A with designation $1S-2p_2$ (accompanied by a bluish-green fluorescence to be discussed later) was emitted much more strongly when the cadmium was evaporating from the bulb than when

[1] Van der Lingen and Wood, Astrophys. J. **54**, 149 (1921).

condensing in it. This was expected from the work of van der Lingen and Wood. It was also found that under the same conditions there was a small increase in the intensity of 2289A ($1S-2P$). This increase in intensity of both lines under the same conditions is hardly in accord with the suggestion made by Scott[2] that perhaps at lower vapor pressures mercury entities may be more sensitive to radiation corresponding to 6.7 volts (1849A), while at higher pressures the preference may be for the 4.9 volt (2537A) type. No radiation of the wave-length 1849A ($1S-2P$) is mentioned by van der Lingen and Wood in the work indicated above.

When a nickel spark was used as a source of excitation, the cadmium line 2289A could not be found on any of the plates, but the line 3262A was present, with intensity varying with different conditions in the same manner as when a cadmium spark was used.

Due to the rather narrow bore of the connecting tube there was the possibility of large differences in vapor density, making it impossible to determine whether the variations in intensity of 3262A were due to the age of the vapor or to the variations in density. In order to test this point a new tube was constructed having about 1 cm inside diameter and a length of about 10 cm. The ends were merely rounded off and the tube supported by a quartz rod fused to one end.

In preparing the tube, considerable care was exercised to eliminate gases. It was joined by a constriction to a longer piece of quartz tubing, was heated thoroughly with a glass-blowing burner, and, after the cadmium had been introduced, it was sealed with wax to the vacuum system. The tubing between this seal and the constriction was surrounded by carbon dioxide snow, and a large trap nearer the pumps was cooled in the same manner. A fore-pump and two diffusion pumps in series gave a pressure too low to be measured with a MacLeod gage. Before the final sealing off, all parts of the tube were thoroughly heated several times with the glass-blowing burner, and during this process the cadmium was many times distilled from one part of the tube to another. The final seal was made slowly and at as low temperature as possible.

Experiment showed that the bluish green fluorescence mentioned above could be used as a test for the presence of 3262A and this made the investigation much easier than it otherwise would have been. When the vapor was dense, this fluorescence was confined to the side of the tube where the exciting light entered, but as the pressure was lowered, the fluorescence gradually extended through the whole width of the tube.

Three sets of glass blowing burners having five or six jets each were so arranged that they covered the whole tube except for about an inch at

[2] Scott, Phys. Rev. **22**, 447 (1923).

the bottom. The temperature of this lower part and thus the pressure, was controlled by three Bunsen burners. With the tube well heated, the liquid cadmium at a red heat and no appreciable condensation of cadmium at any point (a difficult condition to obtain), there was very little if any fluorescence visible even near the cadmium surface. Some fluorescence could exist without detection as there was considerable light due to the burners and spark. Then, without any other changes, one of the Bunsen flames which controlled the temperature of the cadmium was lowered, in order to reduce the vapor pressure. No fluorescence appeared. The temperature was again increased without producing fluorescence. Next some of the flames at the top of the tube were extinguished, and a very brilliant fluorescence appeared at the bottom as condensation occurred at the top. This fluorescence could be obtained for a distance of 4 or 5 cm up the tube, but the intensity fell off rapidly with distance from the cadmium surface.

If the appearance of the visible fluorescence was controlled by vapor density, it should have appeared while the temperature of the liquid cadmium was varied. The removal of the flames from the top of the tube with resulting condensation would cause a large increase in the amount of fresh vapor at the bottom and it was at this time that the brilliant fluorescence appeared. It is believed that this indicates quite definitely that the visible fluorescence and the appearance of 3262A really depend upon the freshness of the vapor, in agreement with the conclusion of van der Lingen and Wood in the case of mercury vapor.

For a general study of the radiations from the tube the glass blowing burners were not needed, one or two Bunsen burners being sufficient. When the vapor was illuminated with the nickel spark, 2289A did not appear, 3262A was very strongly radiated from the fresh vapor, and the visible fluorescence from the fresh vapor was found to contain the first terms of the second subordinate series of triplets 4678A ($2p_3-1s$), 4800A ($2p_2-1s$), and 5086A ($2p_1-1s$). This raises an interesting point. The lower levels occur in the order $1S$, $2p_{3,2,1}$, $2P$, and $1s$. The lines observed show transfers from $1s$ to $2p_{1,2,3}$ and from $2p_2$ to $1S$. Since the transfer from $1s$ to $2P$ with wave-length of about 12,800A, is not barred by the selection principle,[3] the transfer from $2P$ to $1S$ would be expected; however the corresponding line 2289A did not appear on the plates. It may be that the transfer from $1s$ to $2P$ is rare. No record of this line was found in the tables. Whatever the explanation, it appears that the electrons avoided the $2P$ level under the conditions of the experiment.

[3] Bohr, Ann. der Phys. **71**, 228 (1923).

In addition to the above cadmium lines, the fluorescing vapor gave the first pair of the second subordinate series of doublets for both thallium and indium. The lines are 3776A ($2p_2-2s$) and 5350A ($2p_1-2s$) for thallium, and 4102A and 4511A for indium. These metals might be expected as impurities since they occur in the minerals from which cadmium is obtained; the specimen used however, was supposedly quite pure, and spark spectra using the metallic cadmium as electrodes failed to show these impurities. The appearance of their fluorescent spectra under the conditions of the above experiment seems rather surprising since it appears that the concentration of impurities in the vapor state should be even less than in the solid or liquid state.

All the visible fluorescence disappeared when a sheet of glass was interposed between the spark and the quartz tube, showing that the radiations originated in the vapor and were produced by a wave-length shorter than 3300A.

No means were readily available for isolating the various ultraviolet lines of the exciting radiation, and so little can be said about the energy changes accompanying the radiations from the vapor. The thallium and indium vapors may have absorbed radiation directly from the spark, or may have received their energy through collisions of the second kind as studied by Franck and his students. The first explanation seems to be the more probable because while nickel and iron sparks brought out strongly all the lines mentioned above, the cadmium spark did not bring out the thallium and indium lines strongly, although the cadmium lines appeared with full intensity. The cadmium spark should have brought out the thallium and indium lines if they depended upon collisions of the second kind.

The results of nickel, iron and cadmium spark excitation have been indicated. Aluminum, tin, and lead sparks produced feeble fluorescence. Copper brought out the thallium line 5350A quite well but not the other visible lines.

Van der Lingen[4] while studying the absorption by cadmium vapor of the radiations from a cadmium spark, found no trace of visible fluorescence. It seems probable that he confined his work to lower temperatures than those used in the present work, and this may be the explanation.

The writer desires to express his obligation to Professor J. T. Tate for suggestions, criticism and interest during the progress of the work.

UNIVERSITY OF MINNESOTA,
MINNEAPOLIS, MINN.
August 3, 1925.

[4] Van der Lingen, Zeits. f. Physik **6**, 403 (1921).

# THE ABSORPTION SPECTRUM OF MANGANESE VAPOR IN THE VISIBLE AND ULTRAVIOLET

By R. V. Zumstein

Abstract

With an absorbing column of the vapor about 3 cm long heated to temperatures between 1200°C and 1600°C, absorption was observed at 31 lines. Grotrian had previously reported absorption at 6 of these lines. All of the absorptions are from manganese atoms in the normal state ($1^6s$ term) and occur in groups of 1, 2 and 3 lines. Five absorption lines represent $1^6s-{}^6d'$ combinations for which the rule of inner quantum numbers is obeyed but the azimuthal quantum number changes by 2. Four lines are $1^6s-{}^6p$ combinations and twelve are $1^6s-{}^6p$ combinations. Some of the remainder are perhaps $1^6s-{}^4p$ and $1^6s-{}^2p$ combinations.

THE spectrum of manganese is of particular interest as the article by M. A. Catalan[1] on the series spectrum of that element was the starting point of the theory of multiplets. The absorption spectrum of the vapor has been studied by Grotrian[2] who observed absorption at 6 lines. The present experiments were undertaken with the same method that has been employed for copper, silver, gold and lead[3] but with some important improvements. The spectrum from 6000 to 3800A is photographed with a 2 prism glass spectroscope, from 4000 to 2170A with a large Hilger quartz instrument size $E_1$, from 2170 to 1950A with a quartz spectroscope made in the Physics Shop of the University of Michigan and having slightly greater dispersion than the Hilger size $E_2$.

An ordinary 100 watt tungsten lamp was used as source of light for the visible spectrum. Below 4000A, a 75 ampere lead arc was employed. The upper terminal was a 1 cm carbon rod and the lower terminal a pool of molten lead 2 cm in diameter. The distance between the terminals was about 5 mm. This arc gives an intense continuous radiation from the visible to 1850A, with the more intense lead arc lines reversed. The intensity of the continuous radiation is so great that the manganese absorption lines at 2000A could be photographed in less than 1 minute. The vapor was obtained as before by heating the manganese in a small carbon tube with an oxy-acetylene torch to about 1600°C.

[1] M. A. Catalan, Trans. Roy. Soc. **223,** 127 (1922).
[2] W. Grotrian, Zeits. f. Phys. **18,** 169 (1923).
[3] Zumstein, Phys. Rev. **25,** 523 and **26,** 189 (1925).
[4] H. N. Russell, Astrophys. J. (May 1925).

Table I gives the wave-lengths at which absorption was observed. The intensities are those of the absorption lines on the basis of $I=10$ for the strongest lines, and are only rough estimates. The interpretation of the present experiments is based on Catalan's article, the energy diagram of manganese given in Sommerfeld's Atombau etc. 4th Ed., p. 702 and the scheme of the inner quantum numbers on page 591 of the same book.

Faint absorption was observed corresponding to the two emission lines 5394 and 5432. These were designated by Catalan as the inter combination lines $1S-1p_2$, $1S-1p_3$. Following H. N. Russell[4] we will call them

TABLE I

*Manganese absorption lines observed*

| λ(I.A.) | Int. | ν(I. vac.) | λ(I.A.) | Int. | ν(I. vac.) |
|---|---|---|---|---|---|
| 5394 .070 | 1 | 18531 .65 | 2208 .73 | 8 | 45260 .8 |
| 5432 .555 | 1 | 18402 .45 | 2184 .84 | 1 | 45755 .5 |
| 4034 .489* | 6 | 24779 .31 | 2174 .09 | 1 | 45981 .6 |
| 4033 .074* | 6 | 24788 .01 | 2173 .16 | 1 | 46001 .3 |
| 4030 .760* | 6 | 24802 .23 | 2109 .55 | 5 | 47388 .4 |
| 3224 .769 | 2 | 31001 .10 | 2106 .03 | 5 | 47467 .6 |
| 3216 .954 | 2 | 31076 .36 | 2097 .48 | 3 | 47661 .1 |
| 2801 .076* | 10 | 35690 .07 | 2093 .29 | 5 | 47756 .4 |
| 2798 .273* | 10 | 35725 .82 | 2092 .33 | 5 | 47778 .3 |
| 2794 .822* | 10 | 35769 .94 | 2091 .93 | 5 | 47787 .4 |
| 2384 .04 | 2 | 41932 .6 | 2072 .6 | 1 | 48232 |
| 2377 .12 | 2 | 42054 .7 | 2071 .1 | 1 | 48283 |
| 2372 .12 | 2 | 42143 .4 | | | |
| 2296 .86 | 3 | 43524 .2 | 2003 .4 | 9 | 49900 |
| 2221 .80 | 9 | 44994 .6 | 1998 .4 | 9 | 50022 |
| 2213 .80 | 9 | 45157 .1 | 1995 .1 | 9 | 50108 |

* Reported by W. Grotrian

$1^6s-1^8p$ combinations, thereby indicating that they are combinations between the $1s$ term of the sextet system and the $1p$ term of the octet system. The normal state of the manganese atom corresponds to a $1^6s$ term. This pair of lines can be excited with the least energy of all the lines of the manganese spectrum. The fact that their intensity in the arc and absorption spectrum is weak is in agreement with the rule that inter combinations between two systems (here sextet with octet) are weak while combinations in the same system (sextet with sextet) would give strong lines. The absorption observed at this pair is perhaps the best evidence afforded by the present experiments that the energy diagram as given by Sommerfeld is correct.

The narrow triplet 4030, 4033 and 4034 is easily reversed in the arc and also strongly absorbed by the vapor. They are $1^6s$—$1^6p$ combinations

[5] Catalan, Anal. Soc. Esp. Fis. y Chim. **21**, 321 (1923).

and were previously observed by Grotrian as absorption lines of the vapor. At higher temperatures these lines broaden and appear as one strong absorption line.

Two sharp absorption lines which showed no broadening with increase of temperature were observed at 3224.769 and 3216.954. Being a doublet, the scheme for the inner quantum numbers would suggest that they are $1^6s-{}^8p$ or $1^6s-{}^4p$ combinations. If we suppose at first that they are $1^6s-{}^8p$ combinations then they define two ${}^8p$ terms which would combine with the $2^8s$ term (9779.89) to give two emission lines 5239.32 and 5218.73. Similarly with the $2^8d$ term (13224 etc.) we would get 6395.37 and 6364.76. The fact that these four predicted lines are not given as manganese lines makes it probable that this doublet represents a $1^6s-{}^4p$ combination. Unfortunately one cannot test this point as no combinations between the quartet system and the other two are known. Several multiplets of the quartet system were given by Catalan[5] and by Back[6] but the observed frequency difference 75.26 is not given by them.

The triplet 2794, 2798, 2801 is a $1^6s-2^6p$ combination and was previously observed in absorption by Grotrian. At higher temperatures (about 1600°C) the triplet appears as one broad absorption line.

The triplet 2384.04, 2377.12, 2372.12 was always observed as sharp narrow lines in absorption, of the same appearance as reversals in the arc. It is a $1^6s$—$1^6d'$ combination involving the $d'$ level defined by multiplet 6 of Catalan. Lines 2384.04 and 2372.12 were given by Fuchs[7] as manganese arc lines; 2377.12 was not given by Fuchs and is my own measurement. For this group, the rule for inner quantum numbers is obeyed but the azimuthal quantum number changes by 2 units. Similar transitions have been reported by other experimenters.

The triplet 2221.80, 2213.80 and 2208.73 is a $1^6s-3^6p$ combination with the $p$ terms defined by multiplet 5. They showed considerable broadening when reversed in the arc and when absorbed by the vapor. In this region of the spectrum, the iron and manganese arcs were photographed for comparison. This triplet appeared as strong reversed lines in the manganese arc and as strong emission lines in the iron arc. The values here given for their wave-lengths are taken from Schuhmacher's[8] table of the iron lines. No connection with the series scheme could be found for the absorption lines 2296.86 and 2184.84. Their appearance as single isolated lines would indicate that they may be $1^6s-{}^2p$ combinations.

[6] E. Back, Zeits. f. Phys. **15**, 206 (1923).
[7] H. Fuchs, Zeits. f. Wiss. Phot. **14**, 279 (1915).
[8] Kayser and Konen, Spektroskopie **7**, p. 486.

The $2^8p$ term (13956.1) given by Catalan as doubtful should of course be a 3 fold term and should combine with the normal $1^6s$ term (59937.47) to give a doublet in absorption. The frequency of one of these absorption lines would be $59937.47-13956.1=45981.4$. A faint absorption line was observed on several plates of frequency 45981.6. This line was also reversed in the manganese arc. Nearby and apparently forming a doublet with this line is one of frequency 46001.3 which was of the same intensity and found to be reversed in the arc and absorbed by the vapor. If this doublet represents a $1^6s-2^8p$ combination, then we should expect a strong infrared line of frequency greater than that of λ15263.8 by 19.7. Randall and Barker[9] give a line of intensity 80 and differing in frequency from λ15263.8 by 17.9. This is therefore very good evidence that two members of the $2^8p$ term are 13956.1 and 13937, the third member being still unknown.

There is a group of 6 manganese absorption lines between 2109 and 2091A which are of especial interest. They are so strongly absorbed by the vapor that I expected no difficulty in fitting them in the series scheme. These expectations were far from fulfilled. 2097.48 was reversed in the arc spectrum and absorbed by the vapor as a sharp absorption line even at the highest temperatures (1600°). No combination lines between the term defined by this line and the other known manganese terms were observed. The other five lines of the group showed considerable broadening at high temperature, the two lines 2092.33 and 2091.93 appearing as one absorption line. From the magnitude of the absorption it was fairly certain that these lines represented combinations between the $1^6s$ term and $p$ terms of the same system ($^6p$ terms). These $^6p$ terms should combine with the $1^6d$ term to give a group of lines between 3400A and 3200A. The spectrum of a manganese arc of 125 amperes was therefore photographed with a quartz spectroscope having a dispersion of 7A per mm and examined for reversals, it having been previously noted that an arc of this magnitude gave as reversals all multiplets from the $1^6d$ term and from the $1^8p$ term. In this region of the spectrum 24 lines were observed reversed in addition to multiplet 9. These lines are all given in Fuchs' list with the exception of 3339.5. However the dispersion of the spectroscope was not great enough to be certain of the results in some cases.

λ2109.55 defines a $p$ term (12549.1) which combines with the $1^6d$ terms having inner quantum numbers 7/2 and 5/2. For the $p$ term $j$ (inner quantum number) is therefore 7/2 or 5/2. λ2106.03 defines a

[9] Randall and Barker, Astrophys. J. **49**, 59 (1919).

$p$ term (12469.9) which combines with the $1^6d$ terms for which $j$ is 1/2, 3/2 and 5/2. The value of $j$ for this term is 3/2. λ2093.29 defines a $p$ term (12181.1) which combines with the $1^6d$ terms of inner quantum numbers 3/2 and 7/2. For the $p$ term $j$ is 5/2 (?). The absence of the 5/2 combination makes this uncertain. λ2092.33 defines a $p$ term (12159.2) which combines with $1^6d$ terms ($j=9/2,\ 7/2,\ 5/2$). For the $p$ term $j$ is 7/2. λ2091.93 defines a $p$ term (12150.1) which combines with $1^6d$ terms ($j=1/2,\ 3/2,\ 5/2$). The $j$ value of the $p$ term is 3/2. For these last two $p$ terms the agreement between the observed and calculated frequencies is not very good. This is probably connected with the difficulty of getting accurate measurements of the wave-lengths of

TABLE II

*New combinations with the term* $1^6d$ (17052 .30)

| $p$ term | $j$ | $\nu$ calc | $\nu$ observed as reversal | λ observed |
|---|---|---|---|---|
| 12549 .1 | (7/2 or 5/2) | 29936 .9 | 29936 . | 3339 .5 A |
| | | 30106 .4 | 30105 .62 | 3320 .698 |
| 12469 .9 | 3/2 | 29830 .6 | 29829 .50 | 3351 .427 |
| | | 29899 .2 | 29898 .18 | 3343 .728 |
| | | 30016 .1 | 30015 .34 | 3330 .676 |
| 12181 .1 | 5/2? | 30188 .0 | 30185 .26 | 3311 .925 |
| | | 30474 .4 | 30472 .15 | 3280 .744 |
| 12159 .2 | 7/2 | 30326 .8 | 30322 .97 | 3296 .884 |
| | | 30496 .3 | 30492 .49 | 3278 .553 |
| | | 30726 .0 | 30722 .19 | 3254 .040 |
| 12150 .1 | 3/2 | 30150 .4 | 30145 .32 | 3316 .324 |
| | | 30219 .0 | 30213 .83 | 3308 .791 |
| | | 30335 .9 | 30330 .83 | 3296 .029 |

the two absorption lines. In Table II are collected these five $p$ terms, the values of $j$ as I have assigned them, the frequencies calculated for the combination of the $p$ term with certain members of the $1^6d$ term, also the frequency of a reversed line on my plates, and finally the wave-length of this reversed line. Three of the $p$ terms may be calculated directly from the arrangement given by Catalan (page 157) for a group of 10 lines which is obviously a mixture of several multiplets.

A second $^6d'$ term is fixed by multiplet 9 and we should expect the combination between this term and $1^6s$ to appear as a narrow triplet in absorption. Two of the predicted lines were readily observed as such on several plates λ2072.6 and λ2070.4. The third member if present was of much less intensity than the two observed.

Finally we have the triplet 2003.4, 1998.4, 1995.1A. All of these lines were strongly reversed in the arc and as absorption lines had considerable width. They are $1^6s-4^6p$ combinations with the $4^6p$ term defined by multiplet 7.

It is worth noting that no absorptions were observed that would indicate atoms in the $1^8p$ or $1^6d$ state. The frequency difference between the normal state and $1^6d$ is 17052.3. The temperature of the vapor was apparently not sufficient to put the atoms in these excited states. In conclusion we may say that the absorption spectrum of manganese contains a relatively small number of intense lines and that they occur in groups of 1, 2 or 3 lines. This is exactly what one would expect if the normal state of the atom corresponded to an $s$ term.

NATIONAL RESEARCH FELLOWSHIP,
PHYSICS DEPARTMENT,
UNIVERSITY OF MICHIGAN,
August 28, 1925.

# CHANGE IN THE INFRA-RED ABSORPTION SPECTRUM OF WATER WITH TEMPERATURE

J. R. COLLINS

ABSTRACT

By the use of two constant deviation spectrometers in series and a Coblentz linear thermopile, the absorption coefficient of water was measured for various temperatures from 0° to 95°C. The bands found showed maximum absorption at the following wave-lengths

| | | | | | | |
|---|---|---|---|---|---|---|
| at 0°C: | .775 | .... | .985 | 1.21 | 1.45 | 1.96$\mu$ |
| at 95°C: | .74 | .845 | .97 | 1.17 | 1.43 | 1.94$\mu$ |

There is a shift toward shorter wave-lengths as the temperature increases and also a marked increase in magnitude of the maximum absorption for the bands at .77, .98 and 1.21$\mu$. These changes are qualitatively explained by Roentgen's hypothesis that water is a mixture of at least two kinds of molecules, presumably $(H_2O)_2$ and $(H_2O)_3$, whose relative amounts change with a change of temperature.

## INTRODUCTION

BEGINNING with Roentgen[1] in 1892, the anomalous properties of liquid water have been explained by assuming that it is composed of two or more kinds of molecules. Roentgen assumed that there were two, which he termed water molecules and ice molecules. They are now generally called dihydrol and trihydrol on the supposition that they are the double and the triple molecule of water. Sutherland[2] has calculated the relative proportions of these constituents at various temperatures from the density-temperature curve by making certain assumptions about the densities of the constituents. Later writers[3] have made it seem likely that liquid water is composed of three components, namely, the simple, the double, and the triple molecule. The amount of hydrol, the simple molecule, at the freezing point is extremely small, and the amount of trihydrol at temperatures much above the normal boiling point is not great. The amount of hydrol and dihydrol increases at the expense of the trihydrol as the temperature increases from the freezing point, and at higher temperatures, presumably above the normal boiling point, the amount of dihydrol begins to decrease.

The relative amounts of the different constituents of liquid water may be changed by changing the physical conditions of the water, such as the

[1] Roentgen, Wied. Ann. **45**, p. 91 (1892).
[2] Sutherland, Phil. Mag. **50**, p. 460 (1900).
[3] Bousefield and Lowry; Guye, Proc. Faraday Soc. **6**, p. 85 (1910).

temperature, pressure, by the addition of dissolved substances, etc. Hudson[4] has shown, that, in the absence of hydration, the presence of dissolved substances results in a decrease in the amount of trihydrol. The change in the infra-red absorption spectrum of liquid water due to the presence of dissolved substances has been studied by several investigators.[5] It was suggested by the present author[6] that this change was due to the change in the relative proportions of two or more kinds of molecules present in the water. The formation of hydrates by the dissolved substance complicates the results, of course, and makes the interpretation of the absorption curves more difficult.

The absorption spectrum of liquid water should change with an increase in temperature in the same way as it changes as a result of the addition of a dissolved substance. The present paper gives the results of measurements of the absorption of liquid water at various temperatures between 0° and 100°C and throughout the spectral range from 0.7 to 2.1$\mu$.

## Apparatus and Experimental Procedure

The apparatus for determining the absorption of water is the same as that used by the author in a previous investigation.[6] Two constant deviation spectrometers were used in series to eliminate stray radiation, and a Coblentz linear thermopile was placed at the exit slit of the second spectrometer to measure the intensity of the radiation falling on it. The cell containing the water was held on a slider so that it could be placed in the beam of radiation passing through the spectrometers. The source of radiation was a 6000 lumen series street lighting incandescent lamp.

Inasmuch as the positions of some of the absorption bands of water determined by this apparatus did not agree with the results of other workers, the calibration of the spectrometer was carefully repeated. In addition to the emission lines of certain metals used previously, a film of air 0.000736 cm in thickness was placed in front of the slit of the spectrometer and the transmission of this film determined throughout the spectral range to be used for the study of water. The positions of the interference bands throughout the spectrum were calculated by use of observations made in the visible spectrum. Good agreement was obtained by the two methods, and good agreement with the previous calibration except in the region near 2.0$\mu$. In this region the emission lines were rather faint

[4] Hudson, Phys. Rev. **21**, p. 16 (1905).
[5] H. C. Jones et al., Phys. Zeits. **14**, p. 278 (1913); **15**, p. 447 (1914);
Angstrom, Phys. Rev. **3**, p. 47 (1914);
Grantham, Phys. Rev. **18**, p. 339 (1921).
[6] Collins, Phys. Rev. **20**, p. 486 (1922).

and difficult to locate accurately. The interference method was much more satisfactory in this region and the results from that method were used.

A double-walled brass cylinder was constructed to hold the absorption cell, and either ice or an electrical heating coil was placed around the inner cylinder to maintain the cell at constant temperature. Various thicknesses of water were used for the different portions of the spectral range covered by the experiments. The thicknesses used were: 10 cm from 0.70 to 0.90$\mu$; 2 cm from 0.90 to 1.10$\mu$; 1 cm from 1.10 to 1.30$\mu$; 0.04 cm from 1.30 to 1.70$\mu$; 0.0076 cm from 1.70 to 2.10$\mu$. The temperature of the water was determined by a thermocouple of copper and advance. In the case of the thicker layers the junction of the couple was in the water, while in the case of the two thinner layers the junction was in contact with the glass end of the cell containing the water. The distilled water used was boiled before using and no trouble was encountered due to bubbles in the cell.

In the case of the three thicker cells, a thinner cell was used for comparison to eliminate the effect of reflection at the surfaces. Except for room temperature, no comparison cell was used in the case of the two thinner cells. For other temperatures the reflection was calculated by means of Fresnel's formula. The lack of accurate correction for reflection does not lead to serious error, as the important thing here is the comparison of the absorption at different temperatures, which is unaffected by the reflection correction.

The experimental procedure was to hold the water at a constant temperature and to determine the transmission of the water throughout the spectral range for which the particular thickness of water was suitable. The thermopile was connected to a Leeds and Northrup high voltage sensitivity galvanometer for which a telescope and scale were provided. The scale was about five meters distant, and for the deflections used (up to 150 divisions) the readings were proportional to the voltage; hence they were taken as proportional to the intensity of radiation falling on the thermopile. After such a series of readings, the temperatures of the cell was changed to another constant value and transmission data taken for that temperature. For some positions in the spectrum, data were taken with the spectrometer setting constant and the temperature of the water changed to various values. This procedure is of particular value on the steep slope of an absorption band.

## Experimental Results

Figs. 1 to 6 show the results obtained for the six absorption bands of water studied. The mass coefficient of absorption is plotted as a function of the wave-length. The mass coefficient

$$k = (1/t\rho) \log (d_0/d)$$

is used because it is a quantity comparable at various temperatures. In this expression $t$ is the thickness of the water layer, $\rho$ is the density of the water at the temperature for which $d$ is the galvanometer deflection when the cell is in the path of the radiation, and $d_0$ is the galvanometer deflection when nothing is in the path of the radiation. The slit width

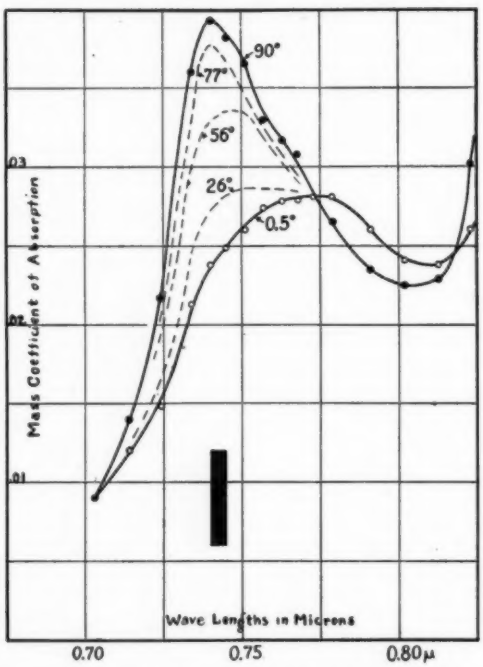


Fig. 1. Absorption band (.70−.80$\mu$) of liquid water at 0.5° to 90°C.

is indicated by a black strip below the curves. Complete curves are given for the highest and lowest temperatures, while for the intermediate temperatures a portion only of each curve is plotted to avoid confusion. In all portions of the spectrum the values of the coefficient for the intermediate temperatures fall in the order of the temperatures.

In all of the absorption bands, an increase in the temperature resulted in a shift of the position of the maximum absorption toward shorter wave-lengths. Probably the most striking change in a band is shown in

Fig. 2 (0.85$\mu$). At low temperatures there is just a faint indication that a band is in this region, but with increasing temperatures the band becomes very pronounced. Except in Fig. 5 an increase in temperature produces an increase in the value of the maximum coefficient. The results in Fig. 4 are probably not very accurate on account of the fact that the width of the slit is comparable to that of the band.

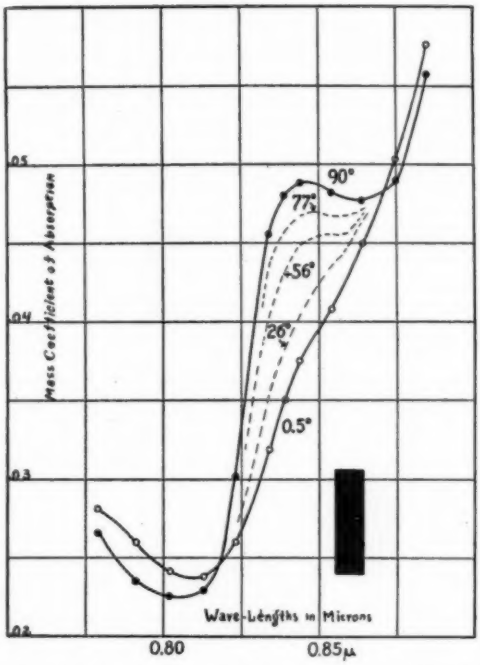


Fig. 2. Absorption band (0.8−0.9$\mu$) of liquid water at 0.5° to 90°C.

The positions of the maximum coefficient for the various absorption bands and the values of the maximum coefficients are given in Table I.

TABLE I

*Effect of change of temperature on the absorption bands of water*

| Wave-length of max. absorption | | Shift | Max. mass coeff. of absorption | |
|---|---|---|---|---|
| 0°C | 95°C | | 0°C | 95°C |
| 0.775$\mu$ | 0.740$\mu$ | .035$\mu$ | 0.0280 | 0.0395 |
| .. | 0.845 | .. | .. | 0.0490 |
| 0.985 | 0.970 | .015 | 0.430 | 0.630 |
| 1.21 | 1.17 | .04 | 1.28 | 1.43 |
| 1.45 | 1.43 | .02 | 29.8 | 29.8 |
| 1.96 | 1.94 | .02 | 108 | 112 |

The values of the maximum absorption coefficients are in good agreement with those of Jones[5] and with those of Dreish.[7] The values given

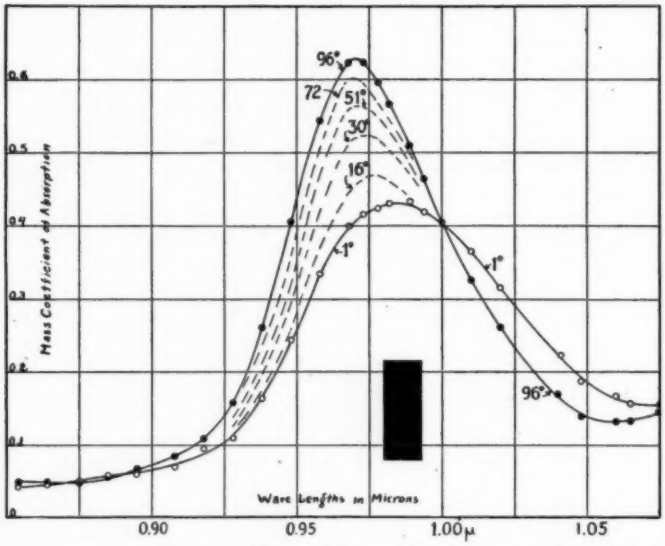


Fig. 3. Absorption band ($0.9-1.05\mu$) of liquid water at 0.5° to 90°C.

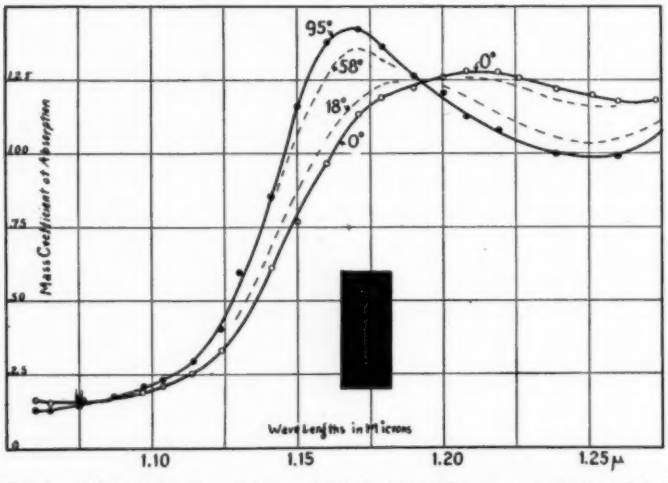


Fig. 4. Absorption band ($1.1-1.25\mu$) of liquid water at 0.5° to 90°C.

by Aschkinass[8] for the bands at 1.46 and $1.96\mu$ are much higher than those of Dreisch and in the present paper. The difference is probably due to an error in his thickness measurements.

[7] Dreish, Zeits. f. Physik **30**, p. 200 (1924).
[8] Aschkinass, Ann. d. Physik **55**, p. 401 (1895).

## Discussion of Results

The explanation offered to account for the change in the absorption of liquid water is that indicated in the first part of the paper. We may assume that there are two kinds of molecules present in the water,

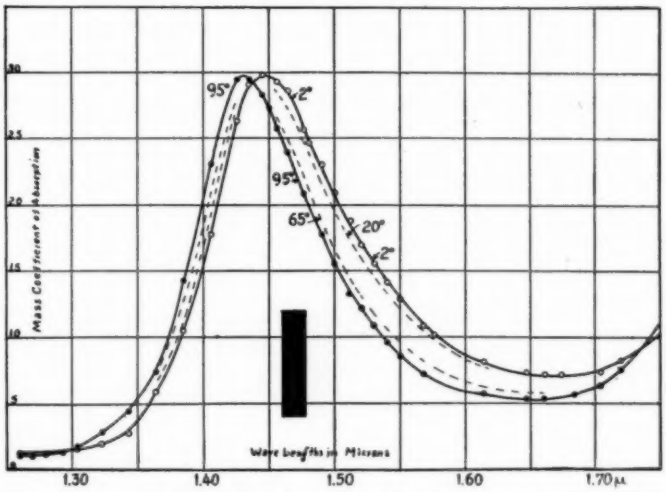


Fig. 5. Absorption band (1.3−1.7$\mu$) of liquid water at 0.5° to 90°C.

neglecting the effect of change in the amount of hydrol. The absorption spectrum of dihydrol is assumed to have its bands at slightly shorter wave-lengths than does that of trihydrol. The comparison of the ab-

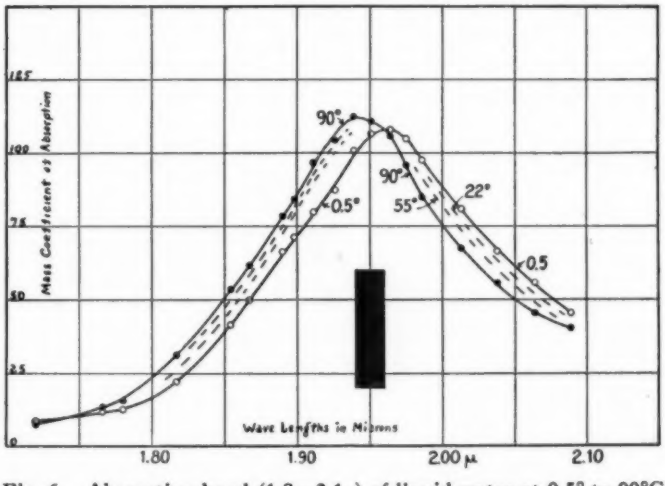


Fig. 6. Absorption band (1.8−2.1$\mu$) of liquid water at 0.5° to 90°C.

sorption spectra of water vapor, liquid water, and ice indicates that the bands of dihydrol near 1.45 and 1.96$\mu$ are not so intense as the cor-

responding bands of trihydrol. The other bands at shorter wave-lengths are more intense for dihydrol. In Fig. 7, the mass coefficient of absorption of water vapor, as given by Hettner[9] and by Dreisch,[7] and of liquid water, as given by Dreisch and in the present paper are plotted; the position of the ice absorption bands, as given by Plyler,[10] are also indicated. It is seen that there are corresponding bands in all the modifications of water. As the molecular structure gets more complex, the positions of maximum absorption shift towards longer wave-lengths. In the absorption bands near 1.45 and 1.96$\mu$ the intensity of the bands increases with increasing complexity of the molecule, while in the bands at shorter wave-lengths the reverse is true.

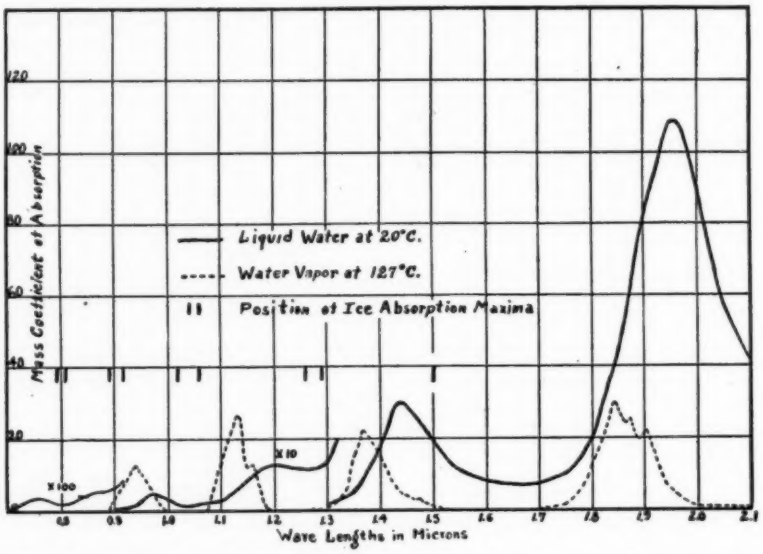


Fig. 7. Comparison of the absorption bands of liquid water with those of water-vapor and of ice.

If the observed absorption spectrum of liquid water is the result of superposing the absorption spectra of dihydrol and trihydrol, the result would be, if the corresponding bands are very close together, a broader band than either component would have alone. As the temperature increases, the intensity of the dihydrol bands increases, while that of the trihydrol decreases. This would produce an apparent shift in the position of the maximum absorption in the observed band toward the shorter wave-lengths. For the absorption bands in which the intensity is greater for the dihydrol than for the trihydrol, the result of increasing tempera-

[9] Hettner, Ann. d. Physik, **55**, p. 476 (1919).
[10] Plyler, J. Opt. Soc. Amer. and R.S.I. **9**, p. 545 (1924).

ture would be an increase in the intensity of the observed band. Both of these changes are observed to occur. In the cases where the intensity of the absorption is greater for the trihydrol, it is less certain what should happen to the intensity of the observed band. The number of dihydrol molecules resulting from the splitting up of the trihydrol is one and a half times the number of the trihydrol molecules, so that in spite of the decrease in the coefficient of absorption, the actual absorption of the dihydrol might be as great or greater than that of the dihydrol. This is apparently what has happened in the bands at 1.45 and 1.96$\mu$.

In all the bands, except that at 1.96$\mu$, it will be observed that there is a decided narrowing, as would be expected if the amount of trihydrol present at the higher temperatures is small compared to the amount of dihydrol. According to Guye[3] this is the case, although there seems no method at present to determine the relative proportions of the constituents accurately enough for any quantitative check.

CORNELL UNIVERSITY,
August 25, 1925.

# THE CRITICAL POTENTIAL OF THE NEGATIVE BAND SPECTRUM OF NITROGEN

ENOS E. WITMER*

ABSTRACT

The method used was to photograph the spectrum of the light excited inside an equipotential anode by electrons from a filament distant less than an electron mean free path. The straight filament of tungsten was placed 2 mm in front of the anode, a nickel pill box which was perforated with numerous holes on the side facing the filament. A rectangular opening in the convex side of the box permitted spectroscopic observation of the glow developed within. Chemically prepared nitrogen at about 0.1 mm pressure was used and precautions taken to ensure its purity. Using a Hilger constant deviation glass spectrograph, a series of spectrograms was obtained in the region above λ3900A at intervals of a volt from 17.75 to 22.75 volts (corrected) inclusive. The negative bands which are fairly intense at 22.75 volts gradually decrease in intensity as the voltage decreases, but on the 17.75 volt spectrogram 4278 is distinctly visible and there are traces of 4708 and 4236. These results seem to indicate that the negative bands appear as a whole at the ionization potential of nitrogen or between the ionization potential and 17.75 volts.

SINCE the method of electron impact has played such an important role in the study of line spectra and atomic structure, it is natural to suppose that it will prove of great importance in the study of band spectra and molecular structure. Up to the present, however, very little work has been done in this field. It is true that critical potentials have been determined for a number of substances in the molecular state, but the relation between these critical potentials and the spectrum emitted by the molecule has been investigated in only a few instances.

Nitrogen has a number of band groups. Kayser in his "Handbuch der Spektroskopie" mentions seven which have been ascribed to it. The identity of the molecule emitting several of these groups is in doubt, however. Three of the most important groups are the first and second positive groups, which lie in the visible and infrared, and the negative group, which lies in the visible and ultraviolet.

Bloch and Bloch[1] photographed the spectrum of nitrogen in the presence of mercury vapor at various voltages and came to the conclusion that the second positive spectrum appears at about 10 or 12 volts and the negative band λ3914 at 21.5 volts. These critical potentials do not seem to coincide with any of the resonance and ionization

* Harrison Research Fellow, University of Pennsylvania.

[1] Bloch and Bloch, Comptes Rendus **170,** 1380 (1920); **173,** 225 (1921).

potentials reported by various investigators. Using the photo-electric method of detecting radiation, Brandt[2] found a series of critical potentials between 7.5 and 8.2 volts. The spectral frequencies corresponding to these critical potentials (as determined by the relation $h\nu = W_1 - W_2$) suggested by their distribution a series of band heads. Foote, Mohler, and Meggers[3] investigated the spectrum of nitrogen in the presence of sodium vapor and found that the positive bands appear at 7 volts and that the negative band group is intense at 25 volts. Duffendack and Duncan[4] found that the first and second positive bands appear below the ionization potential and the negative bands above the ionization potential. The former they ascribed to the neutral molecule and the latter to the ionized molecule. More recently Duffendack[5] has come to the conclusion that the critical potential for the negative bands is 18.5 volts. The apparent discrepancies in these results show that further investigation of nitrogen is necessary.

In the present investigation the spectrum of the nitrogen glow in a two element electron tube was photographed at various plate voltages by the use of a Hilger constant deviation spectrograph with glass prisms and lenses. The investigation was limited to the region above λ3900.

## Description of Apparatus

The experimental tube shown diagrammatically in Fig. 1 was of Pyrex glass, 3.8 cm in diameter. The cathode $F$ was a straight filament of tungsten, 15 mils (.38 mm) in diameter. A thick filament was used in order to keep the potential drop in it as small as possible. The filament could be replaced by removing the stopper $S$, which was made of 702P glass. The stopper was accurately fitted to the main part of the tube by a ground joint. Because of the large amount of heat developed in the filament it was necessary to use water-cooling. This was provided by a water chamber $w$ in the stopper, with inlet and outlet tubes $EE$, through which water circulated. The portion of the filament leads at $A$ and $B$ where they pass through the glass were of tungsten. The filament was held in place by bushings provided with screws as shown in the figure. The anode consisted of a nickel pill box $N$ which was perforated with numerous holes in the side facing the filament, so as to form a grid. A rectangular opening in the side of the box permitted spectroscopic observation of the interior. The filament was placed 2 mm from the

[2] Brandt, Zeits. f. Phys. **8**, 32 (1921).
[3] Foote and Mohler, Origin of Spectra, p. 190.
[4] Duffendack and Duncan, Phys. Rev. **23**, 295 (1924).
[5] Duffendack, Astrophys. Jour. **61**, 209 (1925).

perforated face of the anode. The anode lead was sealed in at *G* with sealing wax, as were the filament leads at *C* and *D*. The nickel box used as anode was covered both inside and outside with a film of lampblack to prevent the scattering of the light of the filament.

This two element tube was connected through a liquid air trap, a stopcock, and another liquid air trap to the pumps, a McLeod gauge, a bulb of phosphoric anhydride, and a nitrogen reservoir. The pumping system consisted of two mercury diffusion pumps connected in series, and an oil backing pump.

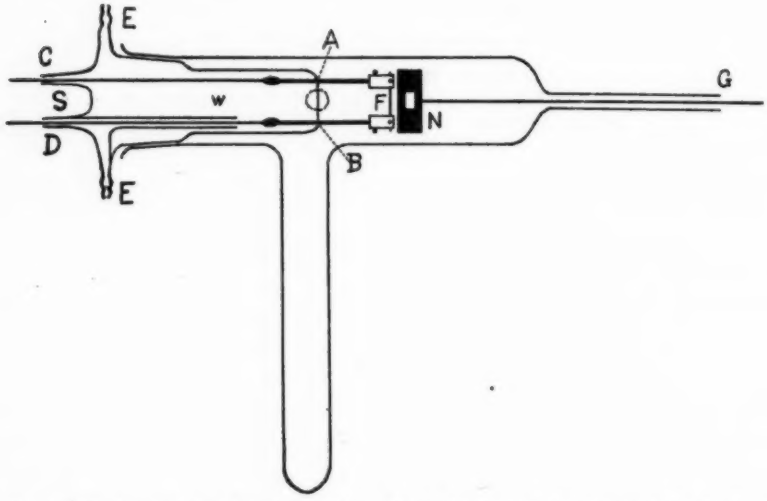


Fig. 1. Discharge tube showing pill box *N* in which glow is produced by electrons from filament *F*.

The filament required from 14 to 18 amp. The current for heating it was obtained from a 110 volt d.c. generator. The plate potential was obtained from a potential divider connected to a storage battery. The negative side of the plate potential was connected to the negative side of the filament.

Wratten and Wainwright Panchromatic Plates were used for photographing the spectrum.

## Experimental Procedure

In the final experiments chemically prepared nitrogen was used. This was made by the reaction of ammonium sulfate, sodium nitrite, and potassium dichlorate. The gas evolved was passed through water, a solution of sodium hydroxide, and finally liquid air traps for purification. The color of the glow obtained seemed to afford an index of the purity

of the nitrogen. The nitrogen glow is pink at low voltages, but certain impurities change this color to blue. Mercury vapor was one of the chief contaminants to guard against. This was effectually kept out of the experimental tube by the two liquid air traps which connected through a stopcock. Every precaution was taken to ensure the purity of the nitrogen since the effect of impurities is uncertain.

The experimental tube was thoroughly baked out after evacuation by wrapping it with resistance wire and heating it electrically to 300°C for several hours with the pumps running. The metal box within the tube was then heated by an induction furnace until free of occluded gases, and finally the filament was glowed. Nitrogen was then introduced from the nitrogen reservoir until the desired pressure of nitrogen was obtained. A glow could then be developed by suitable adjustment of the filament current and box potential. The spectrum of the glow in the equipotential space within the box was then photographed at various potentials.

## Results

Due to the fact that an arc could not be maintained in pure nitrogen below about 17 volts, this investigation was limited to the critical potential for the negative bands. A series of spectrograms was taken at an interval of a volt from 18 to 23 volts. The nitrogen pressure varied from .085 to .140 mm; it could not be kept constant because of the continual absorption in the experimental tube. The following table gives the plate current and the photographic exposure for the six spectrograms.

| Voltage | Plate current | Exposure |
|---|---|---|
| 18.0 | 70 m-amp. | 4 hr |
| 19.0 | 120 | 2 |
| 20.0 | 160 | 2 |
| 21.0 | 200 | 2 |
| 22.0 | 200 | 1⅓ |
| 23.0 | 200 | 1⅓ |

The wave-lengths of the negative bands identified are given in the following table, arranged according to groups.

| Group 1 | Group 2 | Group 3 | Group 4 |
|---|---|---|---|
| 5228A | 4708A | 4278A | 3914A |
| 5151 | 4651 | 4326 | |
| | 4599 | 4199 | |
| | | 4167 | |

In each group the bands decrease in intensity from the top of the column down. The band λ4278 is photographically the brightest of the negative bands on our plates.

As we go to lower voltages the fainter bands of the negative group fade out, but on the 19 volt spectrogram one can easily identify 4708;

4278, 4236; and 3914, while there is a faint trace of 4599. On the 18 volt spectrogram the negative band 4278 is distinctly visible and there are traces of 4708 and 4236.

The first positive group and all the bands of the second positive group listed by Kayser in his Handbuch der Spektroskopie between λ3900 and 4950 have been found on these plates. Two bands of the second positive spectrum, 4649 and 4200, overlap or at least lie so close to two of the negative bands listed above as to be indistinguishable from them on these plates. The positive band 4649 is not very intense, however. Both of the corresponding negative bands, namely 4651 and 4199, give evidence of their presence by the increase in intensity of the superposed bands as we go from 18 volts to 23 volts.

The fact that nothing but the nitrogen bands appeared with sufficient intensity on these plates to be measured and identified is evidence of the purity of the nitrogen used.

## Discussion and Remarks

These results seem to indicate that the negative band spectrum appears as a whole at the ionization potential of nitrogen or somewhere between that and 18 volts. The fact that some of the weaker bands are not present on the spectrograms at the lower voltages seems to be due to the fact that they have become too weak to be recorded on the photographic plate or in other words that they have faded out.

Attempts to obtain a spectrogram at 17.0 or 17.5 volts in pure nitrogen were not successfull because that is too near the minimum potential at which an arc can be maintained. It was found that at 0.1 and 0.2 mm the lowest voltage at which an arc could be maintained in pure nitrogen was 17.0 volts, while at 0.63 mm the lowest voltage was 16.5.

All the voltages mentioned thus far have been uncorrected voltages. The voltage correction was obtained by filling the experimental tube with mercury vapor, running ionization curves, and taking the ionization potential of mercury vapor as 10.4 volts. The ionization potential of mercury vapor according to these curves was 10.65 volts, which makes the voltage correction $-.25$ volt.

In work of this kind the mean free path of the electrons should not be less than the distance from filament to box. According to Wahlin[6] the mean free path of the electrons in nitrogen is .000131 cm at a pressure of 760 mm. This is about 2.7 times the kinetic theory value. Since the pressure of the nitrogen in these experiments was about .1 mm, it follows, using Wahlin's value, that the mean free path of the electrons in our

[6] Wahlin, Phys. Rev. **23**, 169 (1924).

case was about 10 mm, which was five times the distance from filament to box.

Tests were made several times to detect the presence of oscillations in the arc by the use of a peak voltmeter, but no evidence of oscillations was ever detected in this way in spite of the fact that noises could sometimes be heard in telephone receivers connected across the gap between anode and filament.

Our results are in accord with those of Duffendack and Duncan,[4] who found that the "negative bands appear above the ionizing potential" of nitrogen. They are also in accord with the observations of Foote, Mohler, and Meggers.[3] They are not in accord, however, with the results of Bloch and Bloch,[1] who found that the negative band 3914 appeared at 21 or 22 volts. On our plates the band 3914, though never very intense because it is in a region where the glass of the spectrograph absorbs a considerable part of the light, can still be identified at 19 volts.

In conclusion the writer wishes to acknowledge his indebtedness to Dr. C. B. Bazzoni, who suggested this investigation and under whose direction it was carried out.

RESEARCH SECTION,
RANDAL MORGAN LABORATORY,
UNIVERSITY OF PENNSYLVANIA.
August 24, 1925.

# THE IONIZATION OF NITROGEN BY ELECTRON IMPACT AS INTERPRETED BY POSITIVE RAY ANALYSIS

By T. R. Hogness and E. G. Lunn

Abstract

Using an apparatus previously described in which ions formed by impact of electrons of energy $(V_1+V_2)$, or by secondary processes, are pulled from the ionization chamber by the field $V_3$ and then analyzed magnetically by Dempster's method, the relative numbers of ions of type $N_1^+$ and $N_2^+$ are measured for various pressures and voltages. At low pressures (less than $10^{-5}$ mm) only $N_2^+$ was observed; as the pressure was increased the percentage of $N_1^+$ increased regularly and reached 60 at .006 mm. The percentage of $N_1^+$ was markedly greater when helium at a relatively high partial pressure was present. Below 24 volts, no $N_1^+$ ions were produced, although $N_2^+$ ions appeared with $(V_1+V_2)$ greater than 17 volts. These $N_2^+$ ions must therefore be stable toward collisions, while above 24 volts $N_2^+$ ions are produced which may be disrupted on collision to form $N_1^+$ ions. The critical potentials for nitrogen of 16.95 and 24.6, then, correspond to the formation of $N_2^+$ (stable) and $N_2^+$ (unstable). $N_1^+$ ions are therefore produced only by dissociation of unstable $N_2^+$ ions. The percentage of $N_1^+$ was found to be independent of the field $V_3$ from 2.7 to 27 volts, hence the dissociation of an unstable $N_2^+$ ion is independent of its speed over this range. $N_1^{++}$ ions are not produced at all below 500 volts. The $N_2^-$ ions found by Smyth were present but too weak to be studied. A diagrammatic representation of the electrons distributed in the two types of $N_2^+$ ion is suggested in accordance with the ideas of G. N. Lewis. Correlation with spectroscopic evidence indicates that the negative bands are emitted by the stable ions.

THE method for the positive ray analysis of the products of electron-impact ionization of gases previously described[1,2] in its application to hydrogen is here used to study the ionization of nitrogen.

*Apparatus and method.* Electrons from the oxide-coated platinum filament $E$ (Fig. 1) are accelerated by the field $(V_1+V_2)$ into the ionization chamber $H$. The ions formed there by the primary process of electron impact and by secondary processes, are accelerated by the small field $V_3$, then by the large analyzing[3] field $V_4$. Those that pass through the slit $B$ enter the analyzing magnetic field where they are bent through the arc of a circle; the ion beam is focused on to the slit $M$ and the electrometer collecting plate by varying either $V_4$ or the magnetic field.

[1] Hogness and Lunn, Proc. Nat. Acad. Sci. **10,** 398 (1924).
[2] Hogness and Lunn, Phys. Rev. **26,** 44 (1925).
[3] Dempster, Phys. Rev. **11,** 316 (1918).

The nitrogen was prepared by the action of bromine-water on aqueous ammonia and was purified with solid potassium hydroxide, liquid air, and phosphorus pentoxide.

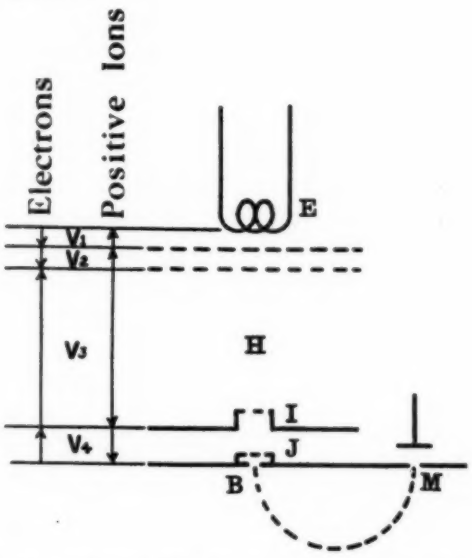


Fig. 1. Diagram showing method of analysis of ions.

*Positive ions.* $N_2^+$ and $N_1^+$ were the only positive ions found. It may be recalled that in the ionization of hydrogen by electron impact the

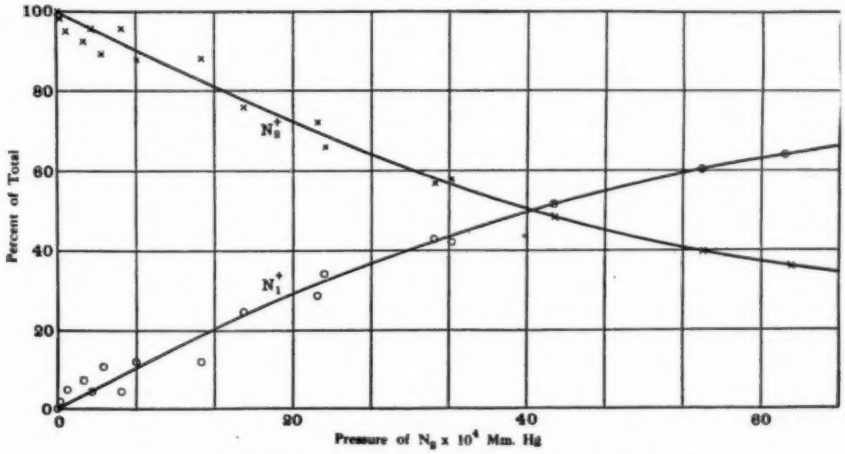


Fig. 2. Percentage of $N_1^+$ and of $N_2^+$ as a function of pressure.

formation of the singly-charged molecular ion is the primary process.[4,5,2] That, analogously, the formation of $N_2^+$ is the primary process and that

[4] Dempster, Phil. Mag. **31**, 438 (1916); Phys. Rev. **6**, 651 (1916).
[5] Smyth, Phys. Rev. **25**, 452 (1925), and references there cited.

$N_1^+$ is formed by collision of unstable $N_2^+$ with gas molecules, is shown by Figs. 2 and 3. In Fig. 2 the percentage of $N_1^+$ and $N_2^+$ as measured by the relative peak intensities is plotted against the pressure of nitrogen. It is evident that the percentage of $N_1^+$ extrapolates to zero at zero pressure; $N_1^+$ can therefore be formed only by secondary collision. Confirmatory experiments failed to show any trace of $N_1^+$ at pressures of less than $10^{-5}$ mm, although the intensity of $N_2^+$ was still large.

The conclusion that $N_1^+$ is formed by collision is further confirmed by the results of a study of the relative ionic intensities in mixtures of helium and nitrogen. The intensity peaks $N_1^+$ and $N_2^+$ were first obtained for a low pressure (Fig. 3A); helium was then mixed with the nitrogen in the reservoir, the partial pressure of the latter being therefore the same

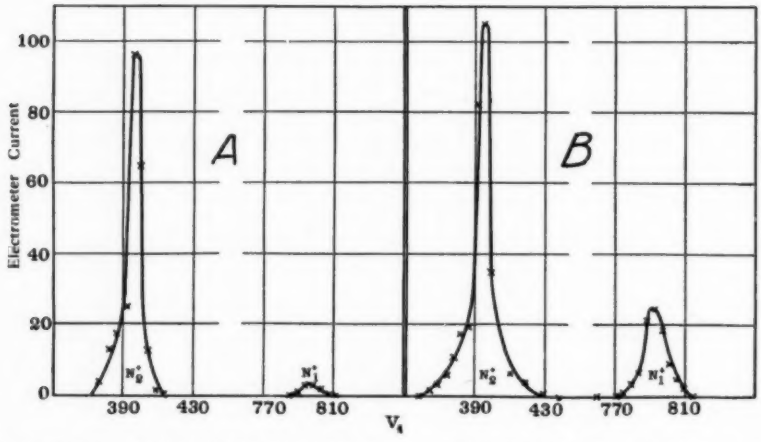


Fig. 3. Peaks obtained (A) with pure nitrogen, (B) with a mixture of nitrogen and helium.

as its previous total pressure, and the intensity peaks were again measured with other conditions the same. The percentage of $N_1^+$ was appreciably greater (Fig. 3B). The presence of the helium increased the chance of collision of the unstable $N_2^+$ and its consequent disruption:

$$N_2^+ = N_1^+ + N.$$

The experiments of Figs. 2 and 3 were made with 84-volt electrons.

Now consider, however, the experimental results presented in Fig. 4 in which the percentage of $N_1^+$ and $N_2^+$ is plotted against the corrected voltage of the impact electron ($V_1 + V_2$). (The smaller figure relates to another experiment extending to higher voltages.) From 17-24 volts no $N_1^+$ ions were formed. Similarly, Fig. 5A shows the results of an intensity-peak experiment made with 23-volt electrons at a high pressure, which

normally favors the formation of $N_1^+$, yet no evidence thereof is shown. Fig. 5B was obtained with 84-volt electrons under the same conditions, except that the filament current was reduced to make the $N_2^+$ intensity

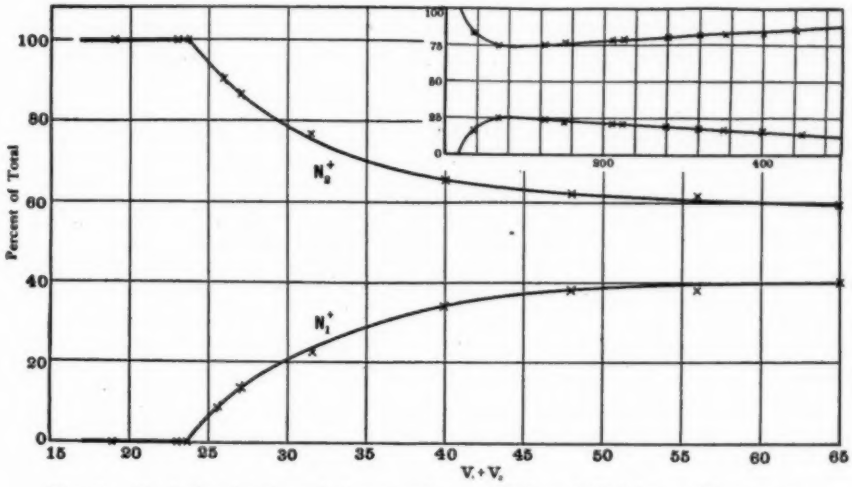


Fig. 4. Variation in the relative numbers of $N_1^+$ and $N_2^+$ ions with energy of impact electrons.

comparable with that in Fig. 5A. Now, Figs. 2 and 3 give evidence that $N_1^+$ is formed only by collision of $N_2^+$ with gas molecules; Figs. 4 and 5

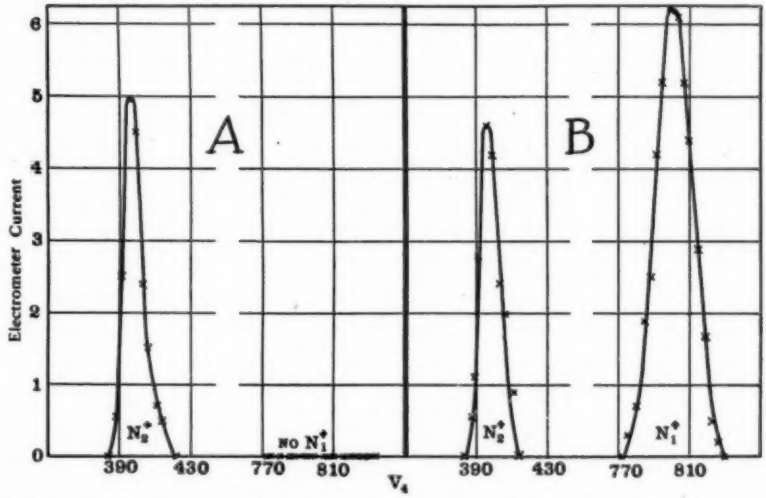


Fig. 5. Peaks obtained (A) with 23-volt and (B) with 84-volt impact electrons.

give evidence that $N_1^+$ is not formed below 24 volts. There are, therefore, two kinds of $N_2^+$ ions: the unstable form, which is produced by impact

electrons of energy greater than 24 volts and is disrupted on collision with gas molecules; the stable modification, which has energy equivalent to 17-volt electrons and is not disrupted by such collision. The critical potentials of 17 and 24 volts for the formation of the stable and unstable $N_2^+$ ions respectively are the means of six determinations made in essentially the manner previously described[2] for hydrogen with the use of helium as the calibrating gas. The disappearing-potential curves $N_1^+$, $N_2^+$ and $He^+$ (Fig. 6) when extended to higher voltages approach the same "saturation" intensity; this, as was previously shown, is a necessary condition for the more accurate determination of ionization potentials by this method.

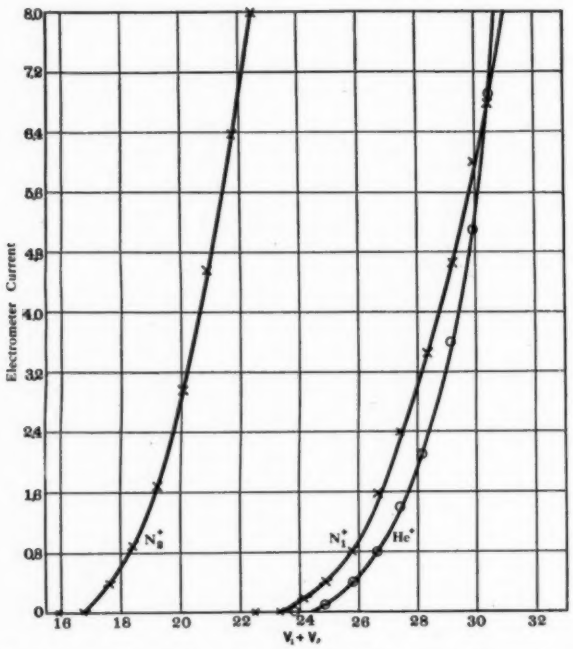


Fig. 6. Variation of intensity of peaks $N_2^+$, $N_1^+$ and $He^+$ with energy of impact electrons.

Study of the relative intensities of $N_1^+$ and $N_2^+$ as a function of $V_3$ showed that over a range of 2.7 to 27 volts the percentage of $N_1^+$ is independent of $V_3$. The dissociation of the unstable $N_2^+$ ion is therefore independent of its speed over this range.

*Negative ions.* $N_2^-$ was the only negative ion detected. Under all conditions of pressure, filament current, etc., studied, its intensity was very small—too small to make feasible a study of its origin.

## Discussion

The principal conclusions of Smyth[6] from his study of the ionization of nitrogen may be briefly summarized as follows: (1) The ions $N_2^+$, $N_1^+$ and $N^{++}$ are formed as the result of primary ionization by impact electrons at ionization potentials of (16.9), $27.7 \pm 0.8$ and $24.1 \pm 1.0$ volts, respectively; (2) the percentage of $N_1^+$ and $N^{++}$ ions increases sharply at 350-400 volts; and (3) negatively charged molecular ions are formed. Smyth's conclusion that $N_1^+$ is formed directly by electron impact is made untenable by the facts presented above. In the light of his subsequent work on hydrogen[5] it seems probable that the ion of apparent $m/e=7$ which Smyth ascribed to $N^{++}$ is one of the type $N_{2-1}^+$, namely, an ion $N_2^+$ which dissociated after it had fallen through the full analyzing field $V_4$. This view he has since hinted at.[7] The ionization potentials attributed by him to the formation of $N_1^+$ and $N^{++}$ should have been the same according to this view. Smyth's value of $27.7 \pm 0.8$ volts should then be considered as spurious, while the 24.1 value agrees with that found by us, within experimental error. Traces of an ion having an apparent $m/e=7$ were found also in the present work, but only at the highest pressures employed. They could be formed by disruption of $N_2^+$ ions in the region between the gauge $J$ and the slit $B$ (Fig. 1). The insert of Fig. 4 shows no evidence of the abrupt increase in the percentage of $N_1^+$ at 350-400 volts found by Smyth.

The several determinations of the critical potentials of nitrogen[8] all show a critical point near 17 volts. The accurate measurements of Brandt[9] gave 16.95 volts as its value, and in addition show two higher potentials of 24.6 and 29.9 volts. In the light of the present work the 16.95 and 24.6 volt potentials are those for the formation of the $N_2^+$ (stable) and $N_2^+$ (unstable) respectively.

In studying the synthesis of ammonia from nitrogen and hydrogen in the low-voltage arc, Storch and Olson[10] found an abrupt increase in the amount of ammonia with 23-volt impact electrons. The approximate coincidence of this critical potential with that found above suggests that the sharp increase is due to the formation and disruption of the unstable $N_2^+$ ion.

[6] Smyth, Proc. Roy. Soc. **104** A, 121 (1923).

[7] Smyth, J. Franklin Inst. **198**, 795 (1924).

[8] For a summary of these see Compton and Mohler, Bull. Nat. Res. Council, vol. 9, part 1, Critical Potentials.

[9] Brandt, Zeits. f. Physik **8**, 32 (1921). See also Franck, ibid. **11**, 155 (1922).

[10] Storch and Olson, J. Am. Chem. Soc. **45**, 1605 (1923).

Studies of the excitation of the spectra of nitrogen by impact electrons have shown that the negative bands appear at about 20 volts,[11] and that the line spectrum does not appear much below 30 volts.[12] Presumably, then, these negative bands are due to the stable configuration of the $N_2^+$ ion. The critical voltage of 30 for the appearance of the line-spectrum is in reasonable agreement with the ionization potential for the formation of the unstable $N_2^+$ ion when the question of spectroscopic intensity is considered.

The effect of helium in increasing the percentage of $N_1^+$ as noted above is in agreement with the observations of Merton and Pilley[13] on the effect of helium on the spectrum of nitrogen. The difference between the effects of argon and helium in exciting the line spectrum may be ascribed to the

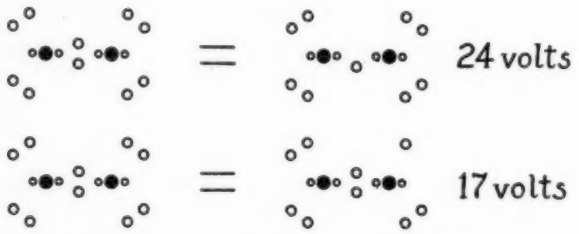


Fig. 7. Diagrammatic representation of the ionization of the two types of $N_2^+$ ions, in accordance with the ideas of G. N. Lewis.

relatively lower ionization potential of argon and to collisions of the second kind[14] in which argon is ionized by the $N_2^+$ (unstable) ion

$$N_2^+(\text{unstable}) + A = A^+ + N_2.$$

A probable explanation of the two kinds of $N_2^+$ ions is that two types of electrons are concerned in the ionization processes here studied. The electron removed at 17 volts is a non-bonding electron, and the $N_2^+$ ion formed by its removal is stable; the electron removed by impact electrons of greater than 24 volts is, by analogy with the $H_2^+$ ion, a bonding one, the removal of which forms the unstable $N_2^+$ ion. Adopting the general scheme of the two-electron bond and the pairing of electrons proposed by G. N. Lewis,[15] the formation of the two types of $N_2^+$ ions may be represented by the diagrammatic equations given in Fig. 7 where there are

[11] L. Bloch and F. Bloch, Compt. Rend. **170,** 1380 (1920); **173,** 225 (1921); Duffendack, Astro. J. **61,** 209 (1925).

[12] Duffendack, Phys. Rev. **20,** 665 (1922). Duffendack and Duncan, ibid. **23,** 295 (1924).

[13] Merton and Pilley, Proc. Roy. Soc. **107A,** 411 (1925).

[14] Klein and Rosseland, Zeits. f. Physik **4,** 46 (1921); Franck, ibid. **9,** 259 (1922).

[15] G. N. Lewis, "Valence and the Structure of Atoms and Molecules," Chemical Catalog Co., New York, 1923.

four non-bonding electrons for eachatom in the molecule, all of which are at the same energy level. Any difference of energy in the two pairs in each atom as proposed by Stoner[16] would be too slight to be detected by the present method.

Studies of the dissociation of nitrogen[17,12,18] confirm the chemical evidence as to its stability. Langmuir's experiments on the dissociation of nitrogen by incandescent tungsten led him to estimate the heat of dissociation as greater than 10 volts. This fact, together with the great chemical stability, precludes the possibility of the $N_2^+$ ion formed at 17 volts dissociating unless the ionization potential of the nitrogen atom is very low. Eucken[19] has recently calculated the heat of dissociation of nitrogen to be 19.1 volts, a value higher than that indicated by the present experiments.

The similarity in the ionization of nitrogen and oxygen found by Smyth[20] naturally suggests that the processes of ionization are similar. Experiments to investigate this are in progress.

DEPARTMENT OF CHEMISTRY,
UNIVERSITY OF CALIFORNIA.
September 5, 1925.

[16] Stoner, Phil. Mag. **48**, 719 (1924); also Smith, Chem. and Ind. **43**, 323 (1924).
[17] Langmuir, J. Am. Chem. Soc. **34**, 860 (1912); Langmuir and Mackay, ibid. **36**, 1708 (1914); Langmuir, ibid. **37**, 417 (1915).
[18] Duffendack and Compton, Phys. Rev. **23**, 583 (1924).
[19] Eucken, Ann. der Chem. **440**, 111 (1924).
[20] Smyth, Proc. Roy. Soc. **105A**, 116 (1924).

# STRIATED DISCHARGE IN HYDROGEN

By Arthur Bramley

Abstract

*Potential distribution, electron concentration and mean electron energy* at eleven points were determined for a discharge through a tube 15 cm long at pressures of .625, .20, .09 and .02 mm, using Langmuir's probe method. The total potential difference was 270-300 volts. The potential dropped to a minimum within 2 mm of the cathode, of 125, 60 and 20 volts for pressures .20, .09 and .02 respectively, giving a reverse gradient in a region 1 to 2 cm long through which the current must have been carried by diffusion of positive ions and electrons. The gradient was also reversed at the anode edge of a striation for pressures of .20 and .09 mm—the lower pressure .02 mm gave a uniform positive column. The electron concentration reached a maximum 1 to 2 cm in front of the cathode; the values, in general, are lower the higher the pressure. The mean electron energy decreases sharply at the cathode to a minimum of 1 to 2 volts, then rises gradually to about 10 volts at the beginning of the positive column; it also reaches 10 volts at a striation. Such electrons have sufficient energy to cause the ionization which is associated with the luminosity in the positive column. The anode drop within 2 mm was only 5 to 15 volts, the potential distribution depending on the position of the nearest striation.

ALTHOUGH a large amount of work has been done on the striated discharge in monatomic gases, very little has been done recently on the discharge in diatomic gases at low pressures, where the presence of various kinds of ions renders the interpretation of the results obtained more difficult.

The method employed in this investigation is the one suggested by Langmuir. If a wire is introduced into the discharge and maintained at a negative potential with regard to the surrounding space, a positive space charge arises which limits the positive ion current reaching the wire. As the potential of the wire is raised, electrons reach the wire against the potential of the field until the resultant current becomes zero. Finally, when the wire exceeds the potential of the space, positive ions are prevented from reaching the wire, so that it becomes surrounded with a negative space charge. Therefore when the potential of the wire becomes equal to that of the space surrounding it, a change in the law governing the current to the wire must take place.

If there is a Maxwellian distribution of velocity the current reaching the wire can be expressed in the following form

$$I = N_0 e \sqrt{(e\bar{v}/3\pi m)}\, \epsilon^{-3(v_0 - v)/2\bar{v}} \qquad (1)$$

where $I$ is the current to the exploring electrode, $N_0$ the concentration of the electrons, $m$ and $e$ the mass and charge of an electron, $\bar{v}$ the average velocity of the electron, expressed in equivalent volts, $v$ the potential of the wire and $v_0$ the potential of the space. From this equation it follows that

$$\log I = -(3/2)\,(v_0 - v)/\bar{v} + \text{const.}$$

so that if $\log I$ is plotted against $v$ a straight line ought to be obtained, whenever there is a Maxwellian distribution of velocities. The slope of this curve ($\tan \theta$) enables us to find the average velocity of the electrons at once, for $\tan \theta = 3/2\bar{v}$. The potential of the space will be the potential at which the graph of $\log I$ plotted against $v$ begins to deviate from a straight line.

When $v_0 - v = 0$ the equation simplifies to the form

$$I = N_0 e \sqrt{(e\bar{v}/2\pi m)}$$

so that, knowing $\bar{v}$ from the slope of the curve, we can compute the concentration of the electrons.

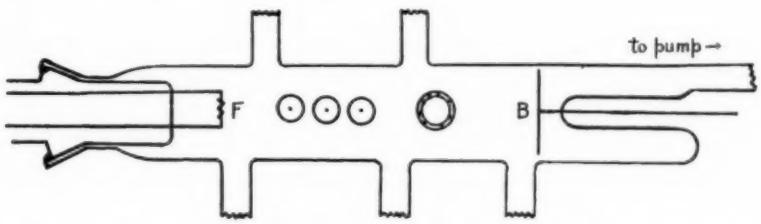


Fig. 1. Discharge tube with exploring electrodes inserted through side tubes.

A diagram of the apparatus used in this experiment is given in Fig. 1. The filament $F$, which serves as a hot cathode to maintain the discharge at low voltages, and the anode $B$ were fixed with respect to the main tube of 3.8 cm diameter. The exploring electrodes, of which there were eleven placed at different positions in the path of the discharge, were each of 4 mil (.1 mm) tungsten wire covered with glass to within a few millimeters of the end which was placed as near the axis of the discharge as possible. The object of using the eleven fixed electrodes in preference to a moving cathode-anode system and a single electrode was to enable a series of readings of the current to be taken without altering conditions in the discharge.

Fig. 2 gives a few typical $\log I$ vs potential curves for different conditions in the tube. Curves 1 and 2 represent the type obtained near the cathode where we have relatively high speed electrons together with slow ones. In this type of curve, we find first a linear part with small

slope which represents large energy since the energy varies inversely as the slope, curving upwards as the slow speed electrons reach the electrode against the space charge sheath; this second part which becomes also a straight line with much greater slope than the first changes into a parabolic curve when the potential of the space is reached. Curve 3 gives the form of curve obtained in the positive column; the breaks in this curve at 12 volts apart which are found above the potential of the field have received as yet no adequate explanation. The breaks in the

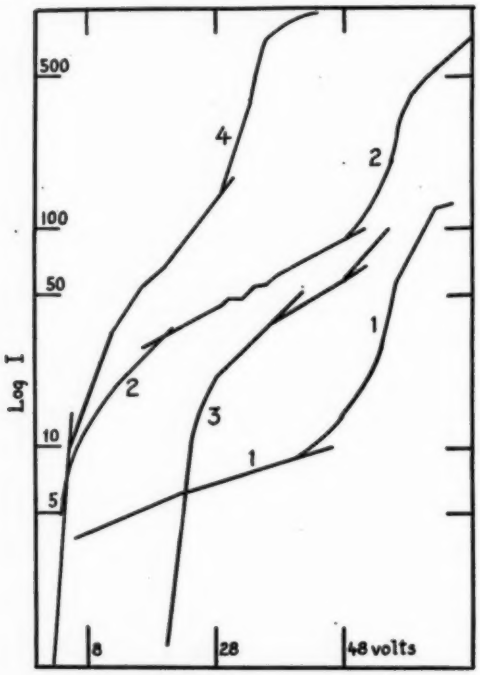


Fig. 2. Typical log $I$ vs potential curves for exploring electrodes.

curves fall about 16 and 12 volts apart on the average and may represent the ionization of the hydrogen molecule and atom respectively. Curve 4 is typical of the curves obtained at high pressure ($p = .625$ mm) where the mean free path is so small that different conditions from those obtained at the other pressures seem to be present.

In Fig. 3 the distribution of potential, the log of the concentration of the electrons and the mean energy of the electrons for the different points in the discharge from cathode to anode where the exploring electrodes are situated are given for pressures of .625, .20, .09 and .02 mm. Below .015 mm no discharge would pass through the gas although the potential across the tube was increased from 270 to 750 volts. At .02 mm it was

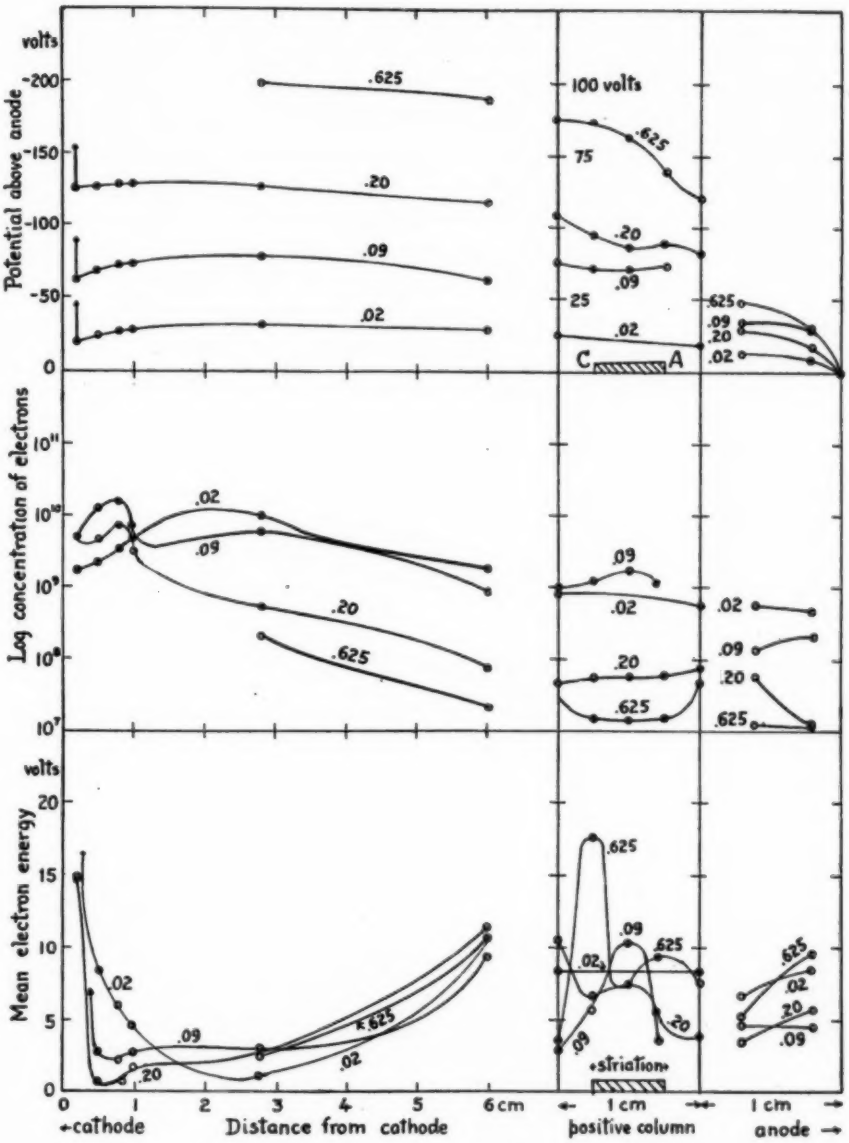


Fig. 3. Potential, logarithm of concentration of electrons, and mean electron energy at different parts of the discharge within 6 cm of the cathode (left), in a striation (middle) and within 1 cm of the anode (right) where the eleven fixed exploring electrodes were situated, for pressures of .02, .09, .20 and .625 mm. For the lowest pressure there were no striations, merely a uniform positive column. In the positive column the indicated position of the striation is only approximate; the maximum mean electron energy occurs near the cathode edge in each case.

found impossible to maintain a striated discharge in the gas through the same potential range. The explanation of this is probably connected, as we shall see, with the condition of the discharge in the neighborhood of the cathode.

We shall first consider the conditions near the cathode and in the region of the Faraday dark space. As the pressure of the gas in the tube is diminished the cathode fall becomes a greater fraction of the total potential applied to the tube until a pressure is finally reached such that the electric intensity is reversed in the Faraday dark space. In this case there is a group of higher speed electrons proceeding from the cathode together with the group of slow electrons which have a large concentration in this region. The higher speed electrons evidently cause continual ionization which results in the large concentration of low speed electrons, the current in the tube being carried by diffusion of positive ions toward the cathode. At high pressures the concentration of electrons is much smaller and the current is due to the electric field; in this case the first term of the equation

$$F = N_0 eE - kT\, dN_0/dx$$

predominates while at low pressures (since both $N$ and $E$ are very small as compared with $dN/dx$ and $kT$—see Fig. 3), the last term (which is due to diffusion) governs the conditions in the discharge. In this equation $F$ is the force on the ions, $E$ the electric field and $kT$ is two-thirds the kinetic energy of the ions.[1] If the pressure is lowered still further, the intensity of ionization must become smaller until a point is reached where the concentration of positive ions is not sufficient to maintain the discharge.

From the concentration and average velocity of high speed electrons for the pressure of .02 mm, a calculation of the total emission from the filament (using Eq. 1) gave results in approximate agreement with the total current in the tube. The total emission calculated was 50 milli-amp. while the total current in the tube as calculated from the measured concentrations was 35 milli-amp. In the calculation the higher speed electrons were assumed to move radially from the cathode without taking into account (1) the possibility of collisions before reaching the electrode, (2) ionization in the region of the space charge sheath surrounding the electrode, and (3) loss due to collisions with the walls of the tube, since the mean free path was nearly four times the radius of the tube.

[1] A thorough discussion of the effects of the electric field intensity and diffusion on the type of discharge has been given by K. T. Compton, Louis A. Turner and W. H. McCurdy, Phys. Rev. **24**, pp. 597-615 (Dec. 1924).

As we move down the tube, the average energy of the electron increases until, as we approach the head of the positive column, the energy becomes nearly equal the ionization potential of hydrogen. In the positive column, the fall in potential over a striation decreased from 30 volts to about 11 volts as the pressure decreased from .625 mm to .09 mm; at the same time, however, the average velocity of the electrons within the striation did not decrease appreciably. Throughout this range of pressure a group of electrons, with average velocity over 10 equivalent volts, was found in the striation toward the cathode side. These electrons must cause the ionization which results in the luminous striated discharge since accumulative ionization has not been found in hydrogen. When the pressure was still further lowered to .02 mm the positive column was uniform and the average energy of the electrons was constant at about 8.4 volts throughout this region.

At the anode the fall of potential within 2 mm never exceeded 15 volts and seemed to be determined by the position of the last striation relative to the anode. In the case of the uniform column (.02 mm) the fall of potential was only about 5 volts.

In the positive column, the character of the discharge at high pressures is determined by the conductivity due to the large electric gradient while at low pressures since the electric field is very small and even negative in some places, the diffusion of the electrons and ions plays a more fundamental rôle than the electric field.

In conclusion, I wish to express my gratitude to Professor K. T. Compton for suggesting the problem and for his helpful suggestions during the course of the investigation.

PALMER PHYSICAL LABORATORY,
PRINCETON, NEW JERSEY,
June 22, 1925.

# THE SECONDARY EMISSION FROM A NICKEL SURFACE DUE TO SLOW POSITIVE ION BOMBARDMENT

By A. L. Klein

Abstract

The apparatus was arranged so that positive ions from a heated Mo strip coated with aluminum phosphate, were accelerated radially through slots in shields $A$ and $B$, and a wider slot in an electrode $C$ to the target $T$, from which the secondary emission to the electrode $C$ was measured. The parts $A$,$B$,$C$ and $T$ were all concentric nickel cylinders, symmetrically placed about the emitter. If the potential of the emitter is made zero and the accelerating potential $V_1$, when the collector is at zero potential only reflected positives are collected. As the potential is increased, secondaries also reach it, the net negative charge increasing until a saturating potential $2V_1$ is reached, when all negatives and no positives are collected. The percentage saturated *secondary electron emission* was found to increase approximately as the square of the primary ion energy, reaching 22 percent of the primary ion current, for primary ions of energies corresponding to 380 volts. The curves show that large numbers of *reflected positive ions* have energies between zero and two volts, and there is also a group of reflected positive ions with energies approximately 0.9 of the primary energy.

THE problem of the secondary emission from metallic surfaces due to positive ion bombardment has been attacked by several workers. Among others Fuchtbauer,[1] Cheney,[2] Baerwald,[3] Hahn,[4] and Baderau[5] have made important contributions.

*The apparatus* used in this work consisted of a number of coaxial nickel cylinders arranged symmetrically around a central molybdenum positive ion emitter. The emitter consisted of a strip of molybdenum 0.13 mm thick, 2.5 mm wide, and 12 mm long; this strip was bent into an open circular band, and heated by passing an electric current through it. The emitter was activated by covering it with a thick layer of $AlPO_4$. The innermost cylinder designated in Fig. 1 as $A$, was 10 cm long and 3 cm in diameter, and has a slot 1.5 mm wide cut around its center, except in three places where legs were left to hold the two parts of the cylinder together. The ends of the tube were closed by means of nickel caps. The next cylinder $B$ is 5 cm long and 3.5 cm in diameter. It has a slot around its center aligned with the one in $A$, but three mm wide. The two collect-

[1] Fuchtbauer, Phys. Zeits. **7**, 153 and 748 (1906); Ann. der Phys. **23**, 308 (1907).
[2] Cheney, Phys. Rev. **10**, 335 (1917).
[3] Baerwald, Ann. der Phys. **41**, 643 (1913); **60**, 1 (1919); **65**, 167 (1921).
[4] Hahn, Zeits. f. Phys. **14**, 335 (1923).
[5] Baderau, Phys. Zeits. **25**, 137 (1924).

ing cylinders $C'$ and $C''$ are each 4 cm in diameter and 2.5 cm long. The distance between them is 13 mm. The fourth cylinder $T$ is the target and is 5 cm in diameter and 5 cm long. This cylinder is pierced with an observation hole approximately 8 mm in diameter. This cylinder has attached to it a constantan-tungsten thermocouple.

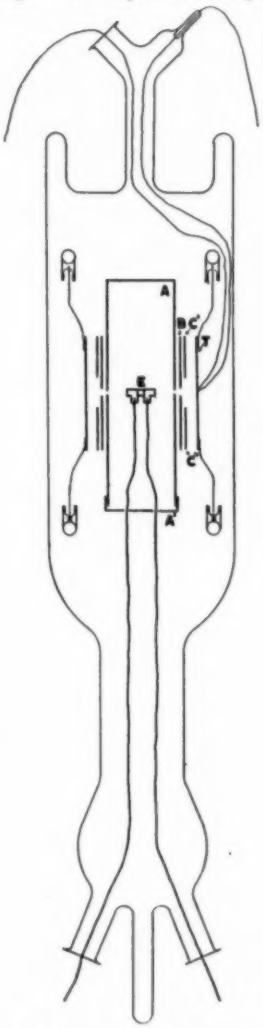


Fig. 1. Diagram of the apparatus.

The apparatus was inclosed in a Pyrex glass bulb and evacuated by means of a two stage mercury diffusion pump backed by a Cenco Hyvac pump. Liquid air was kept on the apparatus during observations and the pressure was measured by means of a McLeod gauge. Before taking any observations the target was always glowed out at 1000°C for three or four minutes by means of induced currents.

The electrical connections are shown in Fig. 2. The emitter $E$ was heated by means of a large six volt storage battery. The cylinder $B$ is grounded and the emitter is made positive; the cylinder $A$ is made less positive than $E$ so that part of the potential drop occurs between $E$ and $A$ and the remainder between $A$ and $B$. The target $T$ is connected to the cylinder $B$ through the galvanometer $G_1$. The two collecting cylinders $C'$ and $C''$ are connected together and then through the galvanometer $G_2$ and the variable potential $V_3$ to the target $T$. Thus a positive ion on evaporating from $E$ is accelerated through the slots in $A$ and $B$ and then impacts against $T$; then by means of the variable potential $V_3$ a saturation curve of the emission from $T$ due to the impact of the positive ions upon it can be obtained.

The galvanometer $G_1$ (Leeds and Northrup type R) has a sensitivity of the order of 1800 megohms; galvanometer $G_2$ (Leeds and Northrup

type HS) has a sensitivity of the order of 16,000 megohms. It will be noticed that $G_1$ reads all of the positive ion current that arrives at the target or collectors, while $G_2$ reads only the current between the collectors and the target. Consequently the reading of $G_2$ gives for any particular voltage $V_3$ the sum of the secondary electron emission and the secondary or reflected positive ion emission. By dividing the reading of $G_2$ by the reading of $G_1$ the ratio of the secondary current to the primary current is obtained.

*Method of procedure.* In taking a series of observations the target is first glowed out at 1000°C for a few minutes and the emitter heating current is turned on. The apparatus is then left for about 15 minutes

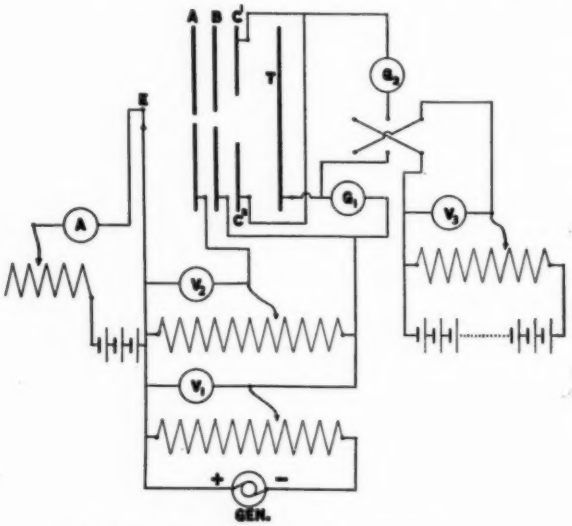


Fig. 2. Diagram of electrical connections.

until the temperature conditions become stable as shown by the thermojunction. Then the fields are applied so that the positive ions are accelerated from the emitter through the slots in $A$ and $B$ against the target $T$. Observations are started by making the collectors $C'$ and $C''$ negative with a potential equal to that of the positive ions incident on the target. A reading of $G_1$ and $G_2$ is then taken, after which the potential of the collectors is decreased somewhat towards zero, and another reading is taken. This is repeated until the potential reaches zero, and then the potential is increased in the positive direction by small increments until it reaches a positive voltage equal to twice the voltage of the incident positive ions. If the ratio of the readings of $G_2$ to $G_1$ is plotted against the potential of the collectors, a saturation curve is

obtained for the current between the collectors and the target. The curves obtained in this way for various voltages of positive ions are shown in Figs. 3, 4, and 5. During observations the vacuum was always

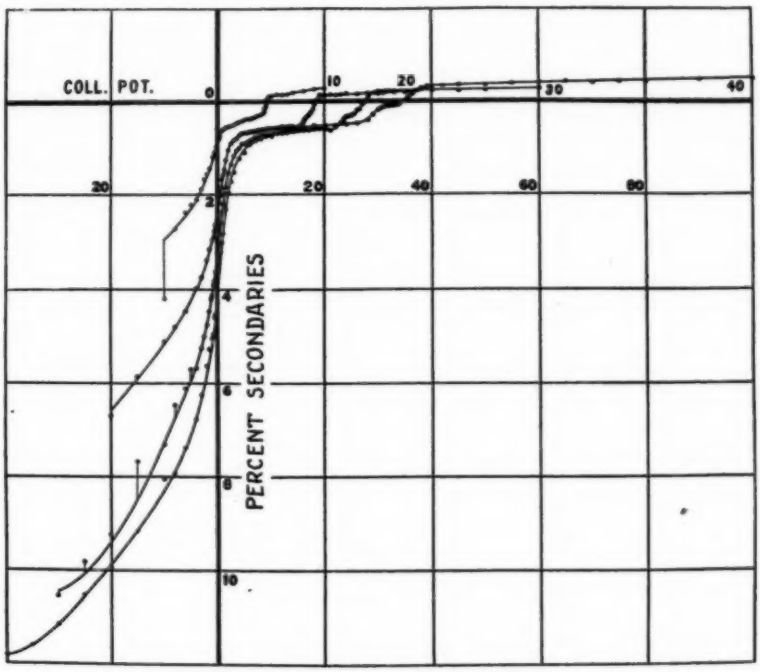


Fig. 3. Curves for accelerating potentials of 10, 20, 30 and 40 volts.

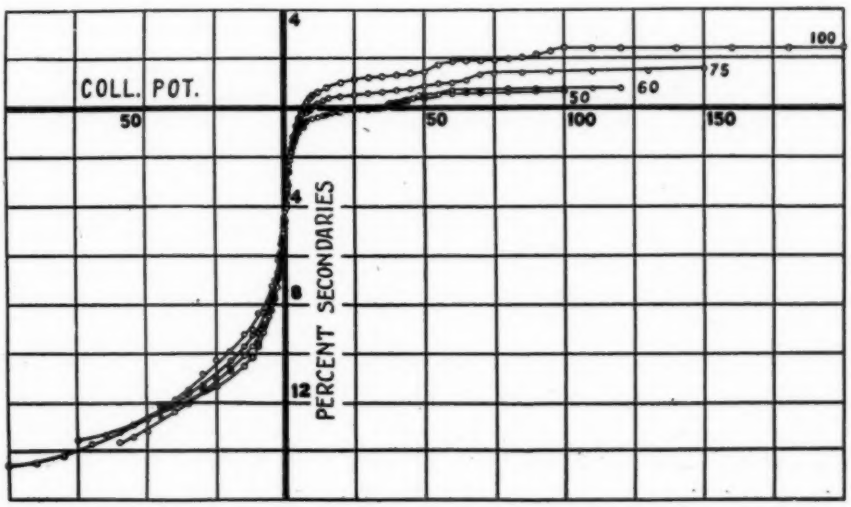


Fig. 4. Curves for accelerating potentials of 50, 60, 75 and 100 volts.

less than $10^{-5}$ mm of Hg. The temperature of the target was always between 160°C and 180°C.

The positive ions used were obtained from hot $AlPO_4$, and, according to Dempster,[6] are ions of sodium and potassium. The writer has had no opportunity to determine the constitution of the ions used, but he hopes to do so in the immediate future.

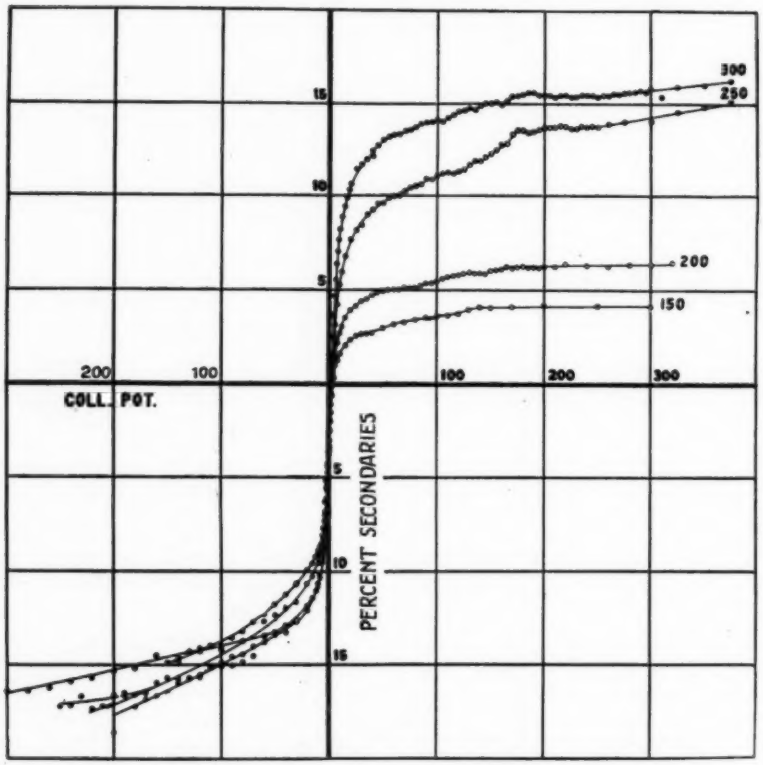


Fig. 5. Curves for accelerating potentials of 150, 200, 250 and 300 volts.

*Discussion of curves.* The saturation curves shown in Figs. 3, 4, and 5 are all plotted with the ordinates representing the percentage ratio of the secondary to the primary current. The abscissas represent the collecting potential, and the numbers at the end of the curves show the value of the primary ion energy for that particular curve. In the plots the ordinates above the axis represent secondary electron emission, those below represent reflected or secondary positive ions; the abscissas to the right represent positive collecting potentials, those to the left negative. It will be noticed that the points to the left of the $y$-axis are rather

[6] Dempster, Phys. Rev. **11**, 320 (1922).

scattered and do not lie on a smooth curve as do the points to the right of the $y$-axis. This condition is due to the pulling of the ions out of the primary beam by the potential of the collector. As the negative collecting potential comes nearer to that of the primary beam the points scatter more and more. It is evident that curves to the left of the axis are practically identical for all of the different voltages, being simply traced further and further to the left as the voltage of the primary ions increases. There could be no object in increasing the negative potential on the collector to more than the accelerating potential, as then the collector would simply gather in the ions from the primary beam. Also it will be seen that all of the curves have strong points of inflection in the vicinity of zero volts. This large change in the value of the ordinate must mean that there are large quantities of reflected positive ions with energies in the neighborhood of zero volts, as the change is far greater than the total electron saturation current could possibly cause. After this the curves flatten out, pass through one or more new breaks, and finally reach a satisfactory saturation value when the collecting potential has the correct value. The fact that for low accelerating voltages (Fig. 3) the curves do not cross the axis until they are practically at the saturation voltage means that there are large numbers of positive ions reflected with high velocities. There seems to be one group of these reflected positive ions whose energy is about 0.9 that of the incident beam. Other groups of ions are reflected with different energies. This phenomenon serves to mask the emission of the secondary electrons so that only the curves where the energy of the incident beam is high becomes negative when the collecting potential is small.

After it was discovered that the curves all reached a saturation value when the collecting potential was higher than the primary ion potential, a curve was taken by varying the accelerating potential and maintaining the collecting potential always twenty-five percent greater. This curve (Fig. 6) shows the variation of the total secondary current with the positive ion voltage. It will be noticed that the secondary electron current is less than one percent for values below 50 volts. It increases rapidly with the primary voltage reaching a value of 22 percent at 380 volts.

There are a great many other things to be done in the future on this problem. It is proposed to study other target surfaces, to use other kinds of positive ions, and also higher voltages. For the different kinds of positive ions, hydrogen together with the series of alkali metals would be most satisfactory. Ionized hydrogen would give as a bombarding particle a proton which is the smallest known particle. The series of the

alkali metals would give as ions a series with complete K, L, M, N, and O shells. This will be very desirable, as with them the second ionizing potential will be very high, and consequently the probability that an ion will be doubly ionized is very remote. In order to determine the kind of ions that are given off by the emitter it will be necessary to use a mass spectrograph.

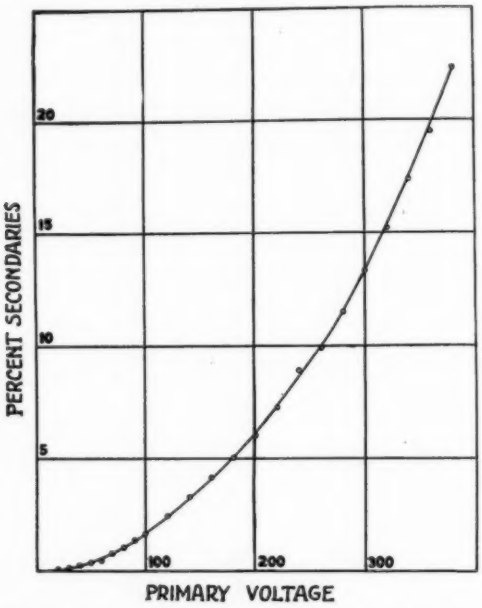


Fig. 6. Dependence of total secondary current on primary voltage.

The writer wishes to express his great indebtedness to Dr. Millikan for his help during the progress of this research. Also he wishes to thank Mr. G. A. Alles and Mr. A. L. Raymond for their help in preparing the aluminum phosphate used, and to express his deepest appreciation to Mr. W. Clancy and Mr. J. Pearson for their assistance in the design and construction of the apparatus used.

NORMAN BRIDGE LABORATORY OF PHYSICS,
PASADENA, CALIFORNIA.
June 24, 1925.

# THE MOBILITY OF NEGATIVE IONS IN GASOLINE, HYDROGEN, AND HYDROGEN-CHLORINE FLAMES

By Paul E. Boucher

Abstract

The Hall effect method of measuring the mobility of the negative ions was used, the horizontal or vertical flame being placed in a field of 4000 to 5000 gauss. The Pt cathode was coated with sealing wax. The temperature was varied by control of the air or oxygen intake and was measured, relatively, by a Pt-PtRh couple. In a hydrogen flame the mobility increases with temperature somewhat for potential gradients over 25 volts/cm, but in a gasoline vapor flame the mobility decreases markedly. The addition of Cl, Br, $CHCl_3$, $CCl_4$, $NH_4Cl$ or I (in alcohol) to the hydrogen and gasoline flame decreases the mobility, the effect being greatest for Cl and being progressively less for the other substances in the order given. In the hydrogen-chlorine flame values as low as 52 cm/sec. per volt/cm were obtained. Addition of NaCl, $Na_2CO_3$ or KCl increases the mobility somewhat. The highest value obtained is 5600 for hydrogen flame with NaCl sprayed in, about 30 percent higher than for a similarly sprayed gasoline flame. In explanation of these variations it is suggested that when certain substances, particularly the halogens, are added to the flame, the negative ion which is normally a free electron for the greater part of its life, tends to be attached to form a cluster so that the average period during which it is a free electron is decreased and hence the mobility also. Temperature changes and potential changes probably affect the mobility by influencing the formation of these clusters.

## Introduction

ALL measurements made on the ordinary bunsen flame agree in that the mobility of the negative ion is a thousand or more times greater than that of the positive ion. Some of the early measurements for the negative ion gave a mobility of 1000 cm per sec. per volt per cm. E. Gold[1] obtained two values of 8000 and 12900. H. A. Wilson[2] found an average value of 2450 using the Hall effect method. J. S. Watt,[3] using the Hall effect method, found the mobility to vary from 2700 to 1600 for potential gradients of 1 to 32 volts per cm. His results also indicate that the mobility is slightly less for salted flames than for free flames. H. A. Wilson and A. B. Bryan,[4] using an alternating current method of measurement at a constant frequency, found mobilities ranging from 6000 to 19300 for potential gradients from 64 to 9.4 volts per cm. By varying the frequency

[1] E. Gold, Proc. Roy. Soc. A, **79,** 43 (1906).
[2] H. A. Wilson, Phys. Rev. **3,** 375 (1914).
[3] J. S. Watt, Phys. Rev. **25,** 69 (1925).
[4] H. A. Wilson and A. B. Bryan, Phys. Rev. **23,** 195 (1924).

from $10\times10^5$ to $4\times10^5$, keeping the gradient and concentration approximately constant, they were able to vary the mobility from 24000 to 8800. They found by varying any one of three factors, potential gradient, frequency of applied potential, or concentration, that the mobility of the negative ions could be made to vary through a wide range.

The character of a flame has been found by others to be profoundly influenced by the addition of chlorine or some of its compounds. Tufts[5] found that the introduction of chloroform into a salted flame decreased the conductivity and also the intensity of the light emitted. Wilson[6] has suggested that when HCl is fed into a flame it may possibly condense on negative ions and diminish their velocity. J. Franck and P. Pringsheim[7] found in the hydrogen-chlorine flame that the anode fall of potential was greater than the cathode fall of potential, and from a comparison of the conductivities of the salted flame and the hydrogen-chlorine flame, concluded that free electrons could not exist in the latter flame and therefore that the negative carrier consists of an atom or a cluster of atoms. Their results seemed to indicate that the mobility of the positive ion was greater than that of the negative ion in the hydrogen-chlorine flame. S. Kalandyk[8] concludes from measurements of the conductivity of flames, that the mobility of the negative ion is greater in the oxy-salted flames and the mobility of the positive ion is greater in the hydrogen-chlorine flame.

The successful development of methods by which very steady hydrogen and gasoline vapor flames can be maintained made it seem desirable to investigate the various factors which appear to influence the mobility of the negative ion. In particular, the effect of temperature and the chemical nature of the flame has been studied. The following types of flame were used in this investigation: air-hydrogen, oxygen-hydrogen air-gasoline vapor, oxygen-gasoline vapor, hydrogen-chlorine. These flames were modified by varying the proportions of the constituent gases and by the introduction of the following chemicals: $CCl_4$, $CHCl_3$, I, Br, Cl, NaCl, $Na_2CO_3$, $NH_4Cl$, and KCl.

## Experimental Procedure

The Hall effect method as described in detail by Wilson[2] was used. The burner was placed between the pole-pieces of a Weiss electromagnet. The pole-pieces were 10 cm in diameter and 5 cm apart. Magnetic fields

[5] F. Tufts, Phys. Zeits. **5**, 76 (1904).
[6] H. A. Wilson, Phil. Trans. **A216**, 63 (1916).
[7] J. Franck and P. Pringsheim, Deutsch. Phys. Gesell. Verh. **13**, 328 (1911).
[8] S. Kalandyk, Journ. de Phys. **5**, 345 (1924).

of 4000 to 5000 gauss were used. A very steady gasoline or hydrogen flame was obtained by passing the gas into a gasometer then through an oxy-acetylene blow-pipe to the burner. The needle valves of the blow-pipe gave a very fine adjustment of both gas and air or chlorine.

Experiments were carried out on both vertical and horizontal flames. In the former the electrodes are placed one above the other; in the latter, which is a broad flat flame, the electrodes are arranged to conduct the current horizontally. For the vertical hydrogen flame a special copper tip was used on the blow-pipe. This gave a flame about 2 to 3 cm in diameter and from 1 to 20 cm in length as desired. The bore of the copper tip was about 3 mm in diameter at the outlet and 4 mm at the intake end. This conical bore prevented backfiring and steadied the flame. Two horizontal burners were made, one for gasoline vapor and one for hydrogen. These burners differ from previous types in that the number of quartz tubes used per unit length was increased by using tubing of a small diameter; thus the cones in the flame were small and close together. For the gasoline burner, 17 quartz tubes, each 2.5 cm long and having an inside diameter of 2.5 mm, were mounted on a brass tube of about 1.5 cm inside diameter. The centers of the tubes were placed about 0.5 cm apart, thus making the burner about 8.5 cm long.

This burner could not be used for hydrogen, for the addition of a small amount of air would cause the flame to blow back and burn inside. It was found however by taking small quartz tubing of about 3 mm inside diameter and heating one end in an oxy-hydrogen flame until it contracted to a diameter of about 2 mm, that considerable air could be added to the hydrogen flame before it blew back inside the burner. The horizontal burner was not so easy to control as the vertical blow-pipe, so that most of the work with hydrogen was done using the blow-pipe.

Gouy sprayers were used to mix various salts with the air. In the case of chloroform, carbon tetrachloride, and bromine, a double air path was used. By means of pinch-cocks the air could be made to pass over the liquid carrying the vapor with it, or by the other path air alone entered the burner.

The hydrogen and chlorine were obtained in the usual commercial tanks, and by suitable pressure regulators, any desired amount of each could be admitted to the flame. A motor driven blower, acting through a pipe line opening over the flame, was used to pump the HCl gas outdoors. Even then it was necessary to wear a gas mask while working with the hydrogen-chlorine flame.

The electrodes consisted of platinum wire, with small cross wires on the end. The negative electrode was kept coated with sealing wax and

the resulting oxides served to reduce the negative fall of potential and produce a uniform gradient in the flame. The potential difference was applied by means of a 300 volt battery connected in series with a galvanometer. The Hall effect angle was measured by means of two platinum probes mounted on the ends of two copper wires which were insulated from each other and supported by two coaxial quartz tubes. This probe assembly extended into the flame through a hole drilled in one of the pole-pieces of the magnet. The copper leads on the outside were connected to an electrometer having a sensitivity of about 5 cm per volt. The galvanometer and electrometer circuits were kept entirely insulated from the ground.

There is no simple method by which the absolute temperature of a flame can be quickly determined, and since relative values serve almost as well in the present case, a platinum platinum-rhodium thermocouple was adopted. This thermocouple was placed near one of the electrodes in such a position as not to affect the current. In a well oxidized blue gasoline flame the couple gave a temperature of 1200°C. The actual temperature[9] of such a flame is about 1870°C. In all cases the temperature as given by the couple has been used in this paper. The thermocouple was very useful in maintaining constant flame conditions. Flames of the same character at a given temperature could be consistently reproduced from day to day.

## Theory

The mobility of the positive and negative ions in a horizontal flame may be expressed by the following formula;[10] $k_1 - k_2 = (1 - dR/R) Y/XH$, where $k_1$ = mobility of positive ions, $k_2$ = mobility of negative ions, $X$ = horizontal electric field, $Y$ = vertical electric field due to the Hall effect, $H$ = magnetic field, and $dR/R$ = magneto-resistance effect, or fractional increase of resistance of the flame when the magnetic field is on.

Since $k_1$ is small compared with $k_2$, and $Y/X = \tan \theta$, where $\theta$ is the angle through which the probes must be rotated to bring the electrometer deflection back to zero when the magnetic field is on, the formula becomes, neglecting the resistance term, $k_2 = -10^8 \tan \theta/H$ cm/sec. per volt per cm. In all measurements of the angle $\theta$, the necessary data for computing the potential gradient and the temperature were recorded at the same time. The magneto-resistance term $dR/R$ was omitted in the formula, for the correction amounted to not more than 4 percent about the magnitude of the experimental error.

[9] Hodgman and Lange, Handbook of Chemistry and Physics, p. 526.
[10] C. W. Heaps, Phys. Rev. **24**, 652 (1924).

The simple type of theory indicates that the mobility of negative ions in a gas should vary with the square root of the absolute temperature if the mass remains constant. By varying the temperature it was thought that some confirmation of this conclusion might be found. The data, however, do not agree with this theory, hence there must be other factors entering which the simple type of theory does not contemplate. It seems probable that the mass of the ion is a function of the temperature. Above the flame where the temperature was 475°C, Saxer[11] found the mobility

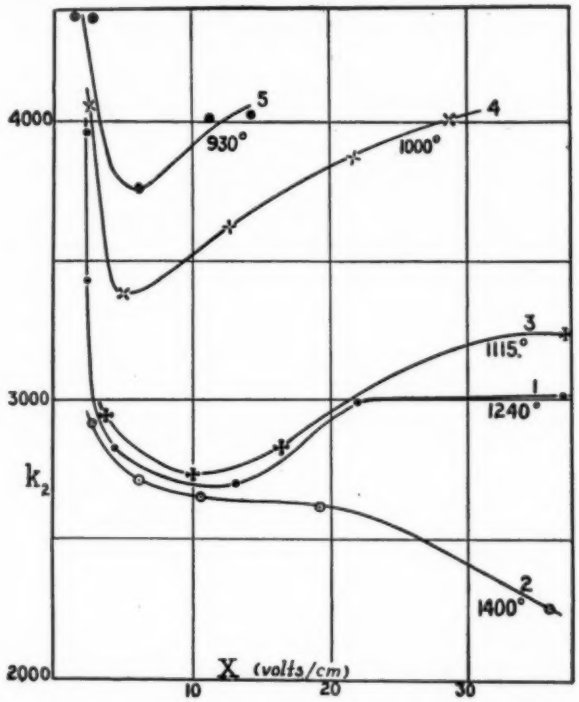


Fig. 1. Mobility of negative ions in the horizontal gasoline flame as a function of potential gradient for various flame temperatures.

of the negative ions to be only 4.39, a value comparable with that of the positive ions. In the hot part of the flame the mobility may be several thousand, so it appears that high temperatures may tend to break up cluster ions, decreasing their average mass and thus increasing $k_2$.

## Experimental Results

A. *Temperature variation.* By the addition of air and oxygen the temperature of the gasoline and hydrogen flames was varied and measurements of the mobility and potential gradient made. Fig. 1 shows graph-

[11] A. H. Saxer, Phys. Rev. **3**, 325 (1914).

ically the effect of varying the temperature of the horizontal gasoline flame. Each curve represents measurements taken at a constant temperature. Curve 1 was obtained with a well oxidized blue flame, the temperature of the thermocouple being 1240°C. Oxygen was added to raise the temperature to 1400°C and data for Curve 2 were taken. The mobility for large gradients decreased. The Curves 3, 4, and 5 at the lower temperatures, were obtained by reducing the air supply. The upper part of the flame for these curves was luminous, though the electrodes were kept in the blue part of the flame. If the electrodes are placed in the luminous part, carbon collects rapidly on the electrodes and measurements are not reliable. For large gradients it will be noted that the mobility was varied from 2300 to 4000 by adding various amounts of air and oxygen.

In the horizontal hydrogen flame the mobility varied from 3500 to 2600 for a variation of potential gradient from 3 to 20 volts per cm. The temperature could not be changed much, and $k_2$ was practically constant for the temperatures used. Two sets of data chosen at random from that taken with the vertical hydrogen flame are given in Table I.

TABLE I

*Typical results for vertical hydrogen flame*

| Temp. | Battery e.m.f. (volts) | Current ($10^{-8}$ amp.) | $X$ (volts/cm) | $k_2$ |
|---|---|---|---|---|
| 1215°C | 20 | 24 | 4.1 | 4170 |
| | 40 | 44 | 9.3 | 4310 |
| | 80 | 75 | 20.4 | 4600 |
| | 130 | 90 | 32.2 | 3420 |
| | 170 | 110 | 44.1 | 3900 |
| 1370 | 20 | 30 | 4.2 | 4170 |
| | 40 | 59 | 8.8 | 4120 |
| | 80 | 105 | 19.5 | 4520 |
| | 130 | 170 | 33.8 | 5340 |
| | 170 | 190 | 42.2 | 5100 |

For low values of $X$ the value of $k_2$ is about the same for both temperatures, but for large gradients the value of $k_2$ is larger at the higher temperature. All data taken show the same variation, so that the mobility for large gradients in the hydrogen flame undoubtedly increases with temperature.

B. *The effect of chloroform and carbon tetrachloride.* A two way air path was connected so that when desired the air furnished to the vertical hydrogen flame could be made to pass over liquid chloroform. A constant voltage of 80 was applied to the flame, the electrodes being one above the other, and the mobility was measured for various proportions of hydrogen,

air, and chloroform. At a thermocouple temperature of 1410°C (the electrodes were near the melting point and the hydrogen flame was probably around 2000°C), the value of $k_2$ for the free flame was 4800. Then as the chloroform path was opened, $k_2$ dropped to 4380, and finally with all the air passing over chloroform, $k_2$ was 3250. Then on lowering the temperature from 1410°C to 1190°C, by reducing the amount of hydrogen, leaving air and chloroform the same, $k_2$ dropped to 1625. The Hall effect angle for other potential gradients, with the air passing over liquid chloroform, varied from 3.2° to 4.8°, corresponding to values of $k_2$ ranging from 1230 to 1875.

The effect of the chloroform on the gasoline flame was even more striking, for here the Hall effect angle of 10.5° for the free blue flame dropped to 1.1° for a magnetic field of 5000 gauss. These angles correspond to a change of $k_2$ from 3690 to 384.

Another compound of chlorine, carbon tetrachloride, was mixed with the air-hydrogen flame. Table II shows the effect of varying the temperature of the flame while the amount of $CCl_4$ added remained constant.

TABLE II

*Results for air-hydrogen flame with $CCl_4$ added*

| Temp. | $X$ (volts/cm) | Angle | $H$ (gauss) | $k_2$ |
|---|---|---|---|---|
| 1180°C | 2.48 | 2.85° | 4500 | 1110 |
| | 9.85 | 2.85 | 4500 | 1110 |
| | 20.6 | 3.3 | 4480 | 1285 |
| | 39.0 | 3.75 | 4500 | 1450 |
| | 46.0 | 4.15 | 4500 | 1610 |
| 1350 | 2.35 | 5.35 | 4480 | 2090 |
| | 8.7 | 6.35 | 4480 | 2490 |
| | 17.3 | 7.2 | 4400 | 2870 |
| | 35.0 | 9.1 | 4400 | 3640 |
| 1180 | 45.0 | 4.55 | 4400 | 1800 |

The temperature was varied by adjusting the hydrogen needle valve, the amount of air and $CCl_4$ remaining approximately constant. By changing the temperature of the thermocouple from 1180°C to 1350°C the mobility of the negative ion was practically doubled. When the temperature was again reduced to 1180°C $k_2$ dropped to 1800, a somewhat higher value than in the first instance. The lack of agreement is probably due to the rate of introduction of $CCl_4$ decreasing with time.

Hydrochloric acid gas is formed in the flame by the breaking up of chloroform and carbon tetrachloride. Any salt or oxide coating placed on the electrodes is removed in the flame in a few minutes. The electrodes

are so well cleaned that when subsequently used in the free hydrogen flame, with considerable applied potential, the current is so small that measurements of the gradient and Hall effect angle cannot be made. Most of the potential drop occurs very near the cathode if the latter is free of lime or salts.

C. *The effect of iodine and bromine.* Since compounds of chlorine cause such marked decreases in $k_2$ in the flame, it was thought that iodine and bromine, being also electronegative and having other properties similar to chlorine, might decrease $k_2$. Iodine exists in a crystalline form at ordinary temperatures and is therefore more difficult to add to the flame, than chloroform. The data for Table III were obtained by first spraying alcohol into the flame, and then a solution of iodine crystals in alcohol.

TABLE III

*Results for hydrogen flame when alcohol and solution of iodine in alcohol is added*

| Spray | Temp. | Battery e.m.f. (volts) | Current ($10^{-7}$ amp.) | $X$ (volts/cm) | $k_2$ |
|---|---|---|---|---|---|
| Alcohol | 1330°C | 20 | 40 | 5.1 | 4580 |
| | | 40 | 101 | 9.7 | 4880 |
| | | 100 | 175 | 24.6 | 4550 |
| | | 190 | 200 | 46.0 | 5360 |
| | | 275 | 250 | 75.0 | 5690 |
| Alcohol and iodine | 1340 | 20 | 20 | 4.9 | 3810 |
| | | 40 | 57 | 9.1 | 4660 |
| | | 100 | 72 | 22.6 | 4380 |
| | | 190 | 83 | 69.7 | 4680 |
| | | 275 | 130 | 82.0 | 4000 |

With the addition of the iodine to the alcohol the current for the same applied voltage was decreased to one half and $k_2$ shows a definite decrease for all values of potential gradient. The quantity of iodine added to the flame in this experiment was probably small compared with the amount of chloroform added in the previous experiment. It is possible that larger proportions of iodine to air would cause a decrease in $k_2$ comparable with that produced by chloroform.

Liquid bromine was placed in one air path and added to the hydrogen flame. Bromine boils at 58.7°C and being quite volatile its vapor mixed readily with the passing air. The flame became bluish in color with a faint trace of yellow, and the oxide coat on the cathode disappeared as a deep red vapor. The Hall effect angle decreased from 10° to less than 1° for a field of 4800 gauss, which is the largest decrease in angle produced by any of the substances except chlorine gas. The corresponding decrease in $k_2$ is from 3700 to 360.

D. *The effect of NaCl, $Na_2CO_3$, $NH_4Cl$, and KCl.* The effect on $k_2$ produced by the addition of the chlorine compounds already described made it seem worth while to test other compounds of chlorine. For this purpose normal solutions of sodium chloride and sodium carbonate were sprayed into the hydrogen flame under the same conditions and compared. Table IV shows some of the data obtained at constant temperature.

TABLE IV

*Results for hydrogen flame into which normal solutions of NaCl and $Na_2CO_3$ are sprayed*

| Salt | Temp. | $X$ (volts/cm) | Angle | $k_2$ |
|---|---|---|---|---|
| NaCl | 1290°C | 2.1 | 14.9° | 5610 |
| | | 2.9 | 13.9 | 5180 |
| | | 5.1 | 13.9 | 5330 |
| | | 10.1 | 13.5 | 5210 |
| $Na_2CO_3$ | 1290° | 2.2 | 13.3 | 5190 |
| | | 3.4 | 13.6 | 5200 |
| | | 7.2 | 13.8 | 5400 |
| | | 10.1 | 13.6 | 5380 |

The values of $k_2$ for NaCl and $Na_2CO_3$ in the hydrogen flame are practically the same.[12] Thus Cl introduced in the form of NaCl has no more effect on the mobility than $CO_3$ introduced as $Na_2CO_3$. The above data show that the value of $k_2$ for the salted vertical hydrogen flame is about 20 percent higher than for the free hydrogen flame at the same temperature.

A normal solution of potassium chloride sprayed into the hydrogen flame gave a mobility practically the same as was obtained with sodium chloride.

A concentrated solution of ammonium chloride was sprayed into the flame. The oxide coated cathode gave off a red vapor just as when chloroform was added. No doubt considerable HCl was formed in the flame since $NH_4Cl$ dissociates into ammonia and hydrochloric acid at a temperature of 337.8°C. Values of $k_2$ were obtained varying from 3400 to 1770. The $NH_4Cl$ thus produces a diminution of mobility which is quite appreciable.

E. *Distilled water and NaCl solution in the gasoline flame.* Some measurements were made on the gasoline flame, first spraying distilled water and then a solution of NaCl into the flame. The results for the small quartz tube burner were similar to those obtained by Watt,[3] who

[12] H. A. Wilson has reached this same conclusion in the case of a gasoline vapor flame, loc. cit.[2]

used a large burner, large electrodes, and a larger current. The value of $k_2$ varied from about 3000 to 2000 and decreased with the increase in potential gradient, as he found to be the case. Contrary to his results, $k_2$ for small gradients at least was slightly higher for the salted flame than for the one containing distilled water. This behavior is similar to that in the case of the hydrogen flame, where $k_2$ is higher for the salted than for the free flame.

F. *The effect of chlorine gas using the hydrogen flame.* At ordinary pressures and temperatures chlorine may be fed directly to the hydrogen flame, using the blow-pipe, without air being added. The hydrogen-chlorine flame is characterized by a blue greenish color and a high temperature, equal to that of the air-hydrogen flame. Any salts on the electrodes are rapidly removed. The current through the flame was of the same order as that in an air-hydrogen flame with the cathode coated with oxides. The electrometer reading was much steadier than in the air-hydrogen flame.

Other writers working with the hydrogen-chlorine flame, have concluded that the positive ions have a greater mobility than the negative ions. The theory of the Hall effect indicates that if the mobility $k_1$ of of the positive ions equals $k_2$ for the negative ions, the Hall effect will be zero, and if the positive ions have a greater mobility than the negative ions, the Hall effect changes sign.

Chlorine was added until the temperature of the flame was almost sufficient to melt the electrodes, but in no case could a reversal in the Hall effect angle be detected. Samples of values obtained for the angle and for $k_2$ are shown in Table V.

TABLE V

*Results for hydrogen-chlorine flame*

| Angle | $H$ | $k_2$ |
|---|---|---|
| 1.65° | 5000 gauss | 576 |
| 0.15 | 4975 | 52 |
| 0.6 | 4975 | 210 |
| 0.25 | 4650 | 94 |
| 0.3 | 4650 | 113 |
| 0.25 | 4650 | 94 |
| 0.2 | 4650 | 70 |

The smallest angle measured was 0.15°. Although the experiments were repeated on several days, there was no doubt about the direction of rotation of the Hall effect angle; it always indicated a greater mobility of the negative than of the positive ion.

Next some measurements were made on the potential gradient at different parts of the flame. Kalendyk[8] found a larger potential gradient at the anode than at the cathode for the hydrogen-chlorine flame.

The flame and the current electrodes were arranged so that they could be moved vertically, the potential probes being fixed through the pole-pieces of the magnet. In all trials the potential gradient was found to be greater at the anode, which was the lower electrode. But a large drop of potential at the anode indicates that the positive ions have a greater velocity than the negative ions. By the Hall effect method, however, $k_2$ was always greater than $k_1$. Then it was thought that the velocity of the flame gases might have some influence on the potential drop, so the potential gradient was measured with the upper electrode as the anode. Again a much larger drop in potential was found near the lower electrode, now the cathode. These tests were repeated several times on different days and always agreed. The conclusion to be drawn is that $k_2$ is greater than $k_1$ in the hydrogen-chlorine flame but that the actual velocity of the positive ions may be greater than that of the negative ions. The velocity of the flame gases is an important factor to consider. For a quartz tube burner the velocity is about 200 cm per sec. The velocity for the blow-pipe burner used was certainly very much greater than this, so that when plenty of chlorine is used in the flame the velocity given to the negative ions by the flame motion is greater than the velocity given by the electric field, unless the latter is quite large.

The large potential drop at the lower electrode no matter whether it is made the anode or cathode is therefore explained as follows. If the lower electrode is the anode then the positive ions are carried up both by the flame and by the electric field while the negative ions must move down against the flame motion. Thus the positive ions have their velocity increased and the negative ions have theirs decreased, the resultant velocity of the positive ions is greater than that of the negative ions, and a negative space charge is set up around the anode. The anode fall of potential is in this case greater than the cathode fall. The Hall effect angle indicates that under these conditions the mobility of the negative ions is not much greater than that of the positive ions.

If the upper electrode is now made the anode, the positive ions must move down against the flame motion and the negative carriers will move up with the flame gases. Thus the negative ions have a greater velocity than the positive ions, which in this case are retarded by the gas motion. This condition results in a larger potential drop at the cathode than at the anode.

The effect of chlorine on the gasoline flame is similar to that of chloroform. If no air is mixed with the gasoline vapor the flame becomes luminous. On adding chlorine gas, the flame remains luminous, $k_2$ is small, and measurements are difficult since carbon collects rapidly on the electrodes.

## Conclusions

The effect of flame temperature on the mobility of the negative ion cannot be predicted by the simple formula of kinetic theory. As the temperature of a gasoline vapor flame is raised by the addition of oxygen the mobility of the ion decreases. If hydrogen is burned instead of gasoline vapor the mobility increases with temperature, at least in a strong electric field. It appears probable that the negative ion during its life is a free electron part of the time and a charged atom or cluster of atoms the rest of the time. The mobility will diminish as the fraction of the ion's life as a free electron diminishes. A high temperature should be unfavorable to the existence of ionic clusters, so one would expect the mobility to increase with temperature. However, to increase a flame temperature the character of the flame must be changed and possibly constituents appear which have a tendency to attach the free electrons. In this way the diminution of mobility of the negative ion in the gasoline flame may be explained.

The experiments show clearly that feeding Cl, Br, and I into a flame diminishes the mobility of the negative ion. Franck and Pringsheim maintain that in a hydrogen-chlorine flame the negative ion is practically never a free electron. The present experiments indicate that Br and I behave like Cl in the hydrogen flame, and that the electron is quickly attached to atoms of the introduced halogen, or possibly to combinations of the halogen with hydrogen. When the temperature of the $H_2$-air-$CCl_4$ flame was raised by varying only the $H_2$ constituent the mobility of the negative ion increased. In this case the higher temperature evidently tended to prevent the attachment of Cl or of HCl to the electron.

If Cl is fed into the flame as NaCl or KCl it does not appear to slow up the negative ion. However, when introduced as $NH_4Cl$, $CCl_4$, or $CHCl_3$ its effect is decidedly evident. The latter compounds are easily broken up so that a Cl or possibly HCl molecule is free to attach an electron. The breaking up of the salts of the metals does not appear to be extensive enough to produce constituents which can attach electrons, or possibly an electron is produced for each atom of metallic salt which is broken up. In the latter case the negative ions would be a mixture of free electrons and ionic clusters.

These experiments do not corroborate the conclusion of Franck and Pringsheim that the mobility of the negative ion in the hydrogen-chlorine flame is less than that of the positive ion. The presence of a potential drop at the anode larger than that at the cathode may be caused by the high velocity of the flame gases, even though the mobility of the negative ion is greater than that of the positive ion.

I wish to express my thanks to Dr. C. W. Heaps for his unfailing interest and helpful suggestions in carrying out this investigation. I am also indebted to Dr. H. A. Wilson for making the arrangements by which I could carry on the work.

PHYSICAL LABORATORY,
THE RICE INSTITUTE,
July 8, 1925.

# MEASUREMENT OF THE FOUR MAGNETIC TRANSVERSE EFFECTS

By Edwin H. Hall

Abstract

This paper presents in detail the experimental arrangements and technique used by the author in measuring the four magnetic transverse effects (the Hall, Ettingshausen, Nernst and Leduc effects) on the same strip of metal, in succession. The strip 5 cm long by 2 cm wide by .01 to .06 cm thick depending on the metal, is soldered to two brass end blocks which may be independently cooled or heated with water or steam. The pole pieces, 4.5 cm in diameter and 0.7 cm apart, are thermally insulated from the strip by flannel and mica. The temperature of these pole pieces is adjusted to approximately that of the middle of the strip, by water cooling or heating. Ten thermo-junctions are soldered at various points along one edge and along the median line of the strip and one at the middle of the other edge. These enable longitudinal and transverse potential and temperature gradients to be measured. Various corrections are discussed, including (a) effect of size of thermo-junctions, (b) the effect of the limited length of the strip with reference to the width, (c) masking influence of one transverse effect on another, (d) effects of non-uniformity of temperature gradients due to heat leakage to or from the strip. Also certain precautions in the measurement of the separate effects are given. Results for Au, Pd, Ni, Co, previously published in summary are here given with some details, including corrected values for the *Ettingshausen effect for palladium.*

I PROPOSE to exhibit in this paper the methods and devices which I have used in recent experimental work[1] upon the four "transverse" effects of the magnetic field, the definitions and sign conventions of which are illustrated by Figs. 1-4.

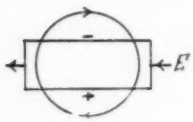


Fig. 1
Hall effect,
$R$ or ${}_cT_e$
positive.

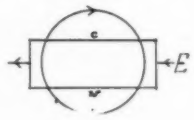


Fig. 2
Ettingshausen effect,
$P$ or ${}_cT_h$
positive.

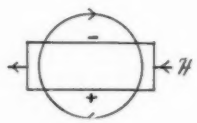


Fig. 3
Nernst effect
$Q$ or ${}_hT_e$,
positive.

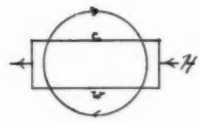


Fig. 4
Leduc effect,
$S$ or ${}_hT_h$,
positive.

## Apparatus

The pole pieces of my magnet are about 4.5 cm wide, and I usually have them 0.7 cm apart. The strip or plate of metal to be studied is commonly about 5 cm long and 2 cm wide, and it is mounted in such a

[1] E. H. Hall, Proc. Nat. Acad. Sci. **11**, p. 416 (July 1925).

way that, barring accidents, it need not be removed from its position between the poles, or even be disturbed there, during the measurement of all four effects at various temperatures. Thus, in Fig. 5, the scale of which is half full size, *WW* is a board (a small drawing-board, 9 inches wide, is suitable) in which a hole is bored just large enough to admit the magnet pole *P*; it is backed by a wooden boss of such thickness as to bring the outer surface of the board a little beyond the face of the pole; it carries two brass blocks *BB* bolted to it, and to the thinned opposed ends of these blocks the ends of the experimental metal strip *m* are soldered. The distance of *m* from the pole *P* is about 0.25 cm and from the pole *P'* somewhat greater, this greater distance allowing room for

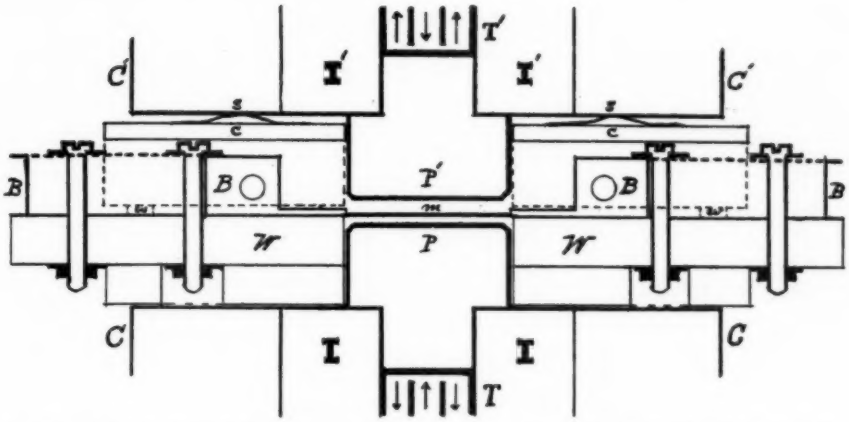


Fig. 5. The experimental plate *m*, and the method of mounting between the poles of the electromagnet, all as seen from above.

the somewhat elaborate wire connections indicated in Fig. 6. A wooden cover *cc*, channeled in such a way as to bridge over the blocks *BB*, is fastened by screws, not shown, to the board *WW*, *ww* being washers of such thickness as to prevent pressure on the tops of the bolts passing through *BB*. Springs, indicated or suggested by *ss*, pressing against the face of the coil *C'C'*, hold the rear surface of the wooden boss, behind *WW*, against the face of the coil *CC*, thus fixing the position of *m* between the poles. Everything shown between the face of *CC* and the face of *C'C'* can be handled as one coherent *ensemble*. Before measurements begin, crevices leading into this *ensemble* or existing between it and the faces of the coils are stuffed with cotton, to reduce currents of air, which otherwise are likely to make trouble when a considerable difference of temperature exists between the interior and the exterior.

Fig. 6, which is also half full size, shows one corner of the board $WW$ and the things it carries. The right-hand block $B$ is channeled, and its channel leads into a short horizontal brass tube connecting with a larger vertical one, to which is attached, by means of the coupling $K$, a stuffing-box $S$ carrying a thermometer $t$. Water, entering through a tube at $T$, circulates through the channel of $B$ and escapes at $T'$, just above the bulb of the thermometer. When steam instead of water is used, it enters at $T'$ and comes out at $T$. $G$ is a brass guide piece intended to maintain

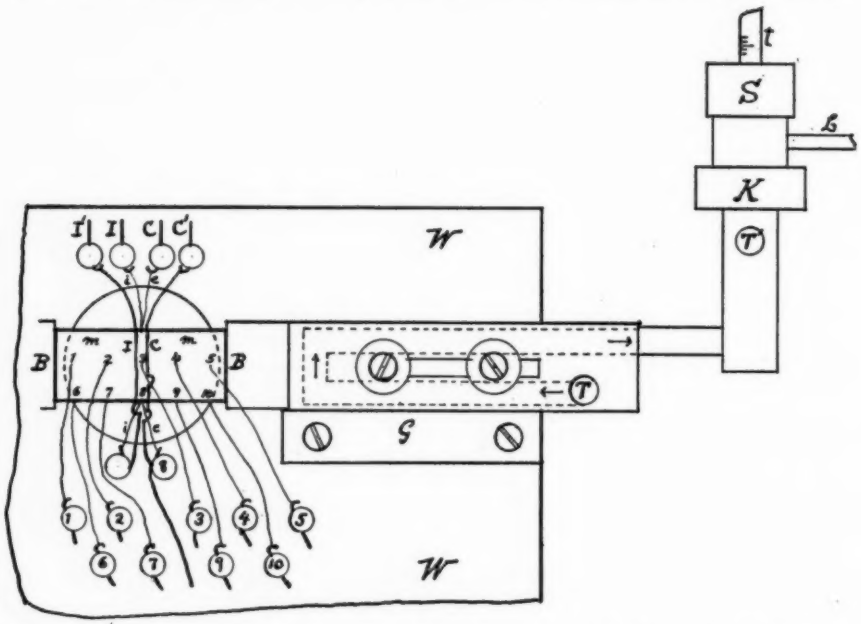


Fig. 6. $WW$ is one corner of the board carrying the experimental plate $mm$ and its attachments. The circle behind $mm$ represents one pole of the electromagnet.

the proper alignment of $B$ when the bolts fastening the latter to the board are loosened. The other block $B$, the end only of which is shown in Fig. 6, is, with its connections, a left-hand counterpart of the right-hand block.

When one of the electromagnetic effects, the Hall or the Ettingshausen, is to be measured, streams of the same temperature are sent through both channels so as to give both of the blocks $B$, and thus both ends of the metal strip $mm$ connecting them, the same temperature. Then an electric current is led in or led out by the wire $L$ and a corresponding wire at the other end of the apparatus. Of course, the mid-length part of $mm$ will not necessarily have the same temperature as the ends. The whole matter of the temperature control of the middle part will be discussed at length farther on.

When one of the thermo-magnetic effects, the Nernst or the Righi-Leduc, is to be measured, electric connection is broken at each *L* and streams of different temperature, one being sometimes a flow of steam, are sent through the two channels, thus producing a temperature gradient along the plate *mm*.

At point 8, mid-point of the lower edge of the plate *mm*, a thermo-electric junction, of No. 40 copper wire and No. 40 "ideal" wire twisted together, is soldered. A similar couple is attached in the same way at the mid-point of the upper edge of *mm*. Much care should be taken with these junctions. They should be small, compact, firm, and firmly attached to the plate, with no superfluity of solder. A method of making them is indicated in Fig. 7. *A* is a fixed bar carrying two screws 16 cm apart, beneath the heads of which the fine wires, one of copper, the other of "ideal," are fastened. *B* is a movable bar about 8 cm from *A*. As shown

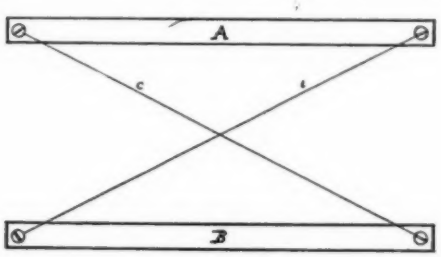


Fig. 7

Fig. 8

Fig. 7. Illustrating the method of making the thermo-electric junctions.

in the figure the two wires are merely crossing each other in contact. Bar *B* is now turned, in a vertical plane, through a complete revolution and thus reaches its original position, a gentle tension on the wires being all the time maintained. Each wire is thus twisted once completely around the other in a close spiral about 0.5 mm long. This junction is now soldered, the wires having been cleaned before twisting. Then with a sharp knife the wires on one side, say the side toward *B*, are cut off close to the junction, which is thus ready to be soldered to the plate. (See "8" in Fig. 8, corresponding to the point marked in the same way in Fig. 6.) The two opposite junctions, each extending about 0.5 mm on the plate 2 cm wide, reduce its effective width to an extent not easy to determine with precision, but the maximum must be less than 5 percent. I suggest that a correction, to be called *correction* (*a*), be added to each of the observed transverse differences of potential or of temperature, this correction being such a percentage of the observed value as the length of *one* junction is to the width of the plate.

If a junction does not have very good and close attachment to the plate, we can not be sure that its changes of temperature follow satisfactorily those of the plate at the point of attachment. In fact, under the best practicable conditions the temperature of a junction cannot be controlled solely by that of the plate, as the packing material, and the fine wires leading away from the junction, must have some influence. This condition tends to make the observed transverse temperature differences, from which the Ettingshausen and the Righi-Leduc coefficients are estimated, somewhat less than the real differences existing in the plate.

The wires indicated in Fig. 8 should be so arranged as to make the circuits into which they enter as nearly non-inductive as may be, for changes of intensity of the magnetic field. Otherwise, a slight change of strength of the magnetizing current, say 1 percent, occurring suddenly by reason of an imperfect connection, may produce a very disturbing deflection of the galvanometer needle.

The copper wires only of these two junctions are used when transverse potential differences, the Hall and the Nernst effects, are to be measured. More will be said farther on concerning the thermo-electric use of the junctions.

The other wires shown in Fig. 6 as attached to the plate *mm* are for the purpose of measuring the longitudinal temperature differences along two lines of the plate, the median line and the lower boundary line. These wires should not be larger than No. 40, about .08 mm in diam., and must be of such material as to give effective thermo-electric couples with the material of the plate. Thus, if the latter is of nickel, palladium, cobalt; etc., the wires should be of copper. If the plate is of copper, or of gold or silver, these wires may be of constantan ("ideal"). The points of attachment of the wires are intended to be 1 cm apart, but since accurate placing is difficult, measurements of distances are made after the soldering, and these actual distances are used in calculating temperature gradients. At no great distance from the plate *mm* each of the fine wires attached to it is soldered to a thicker wire of the same material to lessen electrical resistance and the danger of breaking.

*Calibration of thermo-electric couples.* On the advice of Mr. W. P. White of the Carnegie Geophysical Laboratory, I use the soft, "ideal," constantan wire that is produced by the Electrical Alloy Company of Morristown, N. J. My own calibration tests of couples made of No. 40 "ideal" and No. 40 copper wire show, all the way from 0°C to 85°C, sensitivity values about 6 percent greater than those given in the tables of Mr. L. H. Adams for copper-constantan couples. Couples made of copper

and the coarser "ideal" wire mentioned above were about 3 percent less sensitive than those having the fine wire. I did not attempt to allow for this difference in using, as described above, circuits in which coarse wires were joined to fine wires, but took the values given by the fine wire couples as holding in my measurements of the transverse effects.

I made a special test for any effect of the magnetic field, about 9000 gauss, on the sensitiveness of a copper-ideal couple, both junctions of which, besides the whole length of the constantan wire, were between the poles. The effect of the field, if there was any effect, was only a small fraction of one percent of the total power of the couple.

For couples in which constantan was not one of the metals, I made no calibration tests but calculated the thermo-electric powers from data given by Bridgman in his paper[2] on "Thermo-electric Qualities Under Pressure."

*The question of strip dimensions; correction* (*b*). The best length and width of the metal strip to be used will naturally depend on the width of the magnetic field that can be regarded as fairly uniform. With pole pieces 4.5 cm in diameter I use, as has been said above, a strip about 2 cm wide and 5 cm long, between lines of attachment to the blocks *B* and *B*. Considerable width is desirable, in order to reduce the importance of the encroachment of the junctions upon the plate, as in Fig. 8; but, on the other hand, great width tends to increase the short-circuiting influence of the ends which lie outside the intense magnetic field, and of the blocks *BB*, to which these ends are fastened. This short-circuiting, which doubtless occurs with all four of the transverse effects and is probably about equally great, relatively, for all of them, was observed in 1886 by Ettingshausen and Nernst[3] working with a plate of bismuth and by myself[3] in 1888 working with a plate of soft steel, in experiments showing that the Hall effect is, other things being equal, notably smaller in a short strip of metal than in a long strip. I have recently made more careful and extended observations for the purpose of determining, approximately, what percentage of correction should be made for the error due to the fact that the strip I use is of limited length. I studied the Hall effect in a thin gold strip of variable effective length.

Fig. 9 illustrates the apparatus used. *WW* is, as before, a flat board, with a hole to receive the pole piece *P*. A thin glass plate *gg* is sunk into a depression in this board and on this plate rests a gold strip *m*, 2 cm wide, 5.1 cm long and about 0.013 cm thick. Semi-cylindrical blocks of

[2] Bridgman, Proc. Amer. Acad. **53**, 269-386.

[3] See Campbell, "Galvanomagnetic and Thermomagnetic Effects" (Longmans), pp. 31 and 32.

brass, *cc*, somewhat longer than the width of the gold, rest on *m* and are pressed firmly against it by the stiff springs *ss*. The distance between these blocks, beginning with 0.5 cm as shown in Fig. 9, could be increased by convenient stages till it equalled almost the whole length of the strip. It is assumed that the Hall effect in the thick movable blocks is negligible

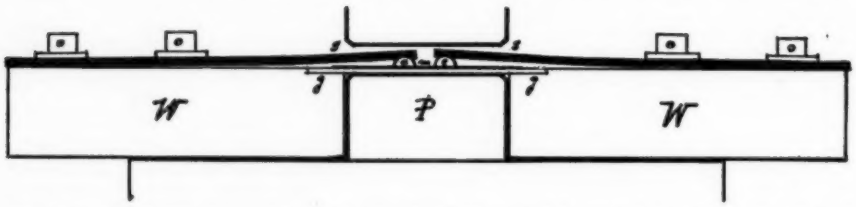


Fig. 9. This shows, as seen from above, the device used for varying the effective length of the experimental strop.

and that the gold immediately under and in contact with a block can be treated as a part of the block. The values of the Hall coefficient $R$ found are given in Table I.

TABLE I

*Variation of Hall coefficient with the effective length x of the strip*

| $x$ | $R$(obs.) | $R$ (calc.) | Contribution to $R$ of | |
|---|---|---|---|---|
| 0.5 cm | −0.000500 | −0.000531 | 1st 0.5 cm | −0.000531 |
| 1.0 | −0.000594 | −0.000593 | 2nd " | −0.000062 |
| 1.5 | −0.000622 | −0.000627 | 3d " | −0.000034 |
| 2.0 | −0.000646 | −0.000649 | 4th " | −0.000022 |
| 2.5 | −0.000669 | −0.000665 | 5th " | −0.000016 |
| 3.0 | −0.000683 | −0.000678 | 6th " | −0.000013 |
| 3.5 | −0.000688* | −0.000688 | 7th " | −0.000010 |
| 4.0 | −0.000695 | −0.000695 | 8th " | −0.000007 |
| 4.8 | −0.000705 | −0.000705 | 9th (0.8 cm) | −0.000010 |

* This is the mean of two values 691 and 685 obtained several days apart.

Representing by $x$ the variable block-distance in centimeters, I found by an empirical process the following formula, which corresponds fairly well with the observations.

$$R = -0.00077(1 - 0.23^{x^{1/5}}). \tag{1}$$

It must be noted that the distance $x$ was not very accurately measured and that any given error in the value of $x$ will have its greatest effect when this distance is small. The values calculated with this formula are also given in Table I.

Of course formula (1) indicates that with an infinite value of $x$, in a magnetic field of uniform strength, the maximum value of $R$ would be $-0.000770$. As the value of $x$ is about 5 cm in my ordinary experiments, Table I, which gives $R = -0.000705$ for $x = 4.8$ cm, indicates that I

should add about 8 percent to my ordinarily observed values of $R$ in order to make due correction for the limited length of the metal strip used. This is for a strip 2 cm wide. The correction to be applied increases with the width of the strip.

As this correction is due to the short-circuiting effect of transverse conduction around the ends, and as such conduction should have about the same proportional effect in the case of transverse thermal difference as in the case of transverse potential difference, I assume that to every transverse gradient *actually existing* at mid-length of a strip 5 cm long and 2 cm wide, an addition of 8 percent should be made, to take proper account of this short-circuiting influence. This correction, then, *which hereinafter will be called correction* (*b*), applies to all four of the transverse effects. In some cases, where other corrections to be applied are large, it is a matter for consideration whether this 8 percent shall be added before or after other corrections. The words "actually existing," which I have italicized, are decisive in this connection.

There is, however, another way of looking at this matter, a way which I find useful in another connection, as will presently appear. This is to think of the middle half-centimeter of the strip as contributing a certain amount to the transverse gradient, whether electrical or thermal, which is found there, and of each successive element of the length of the strip, toward either end, as contributing also its share, these contributions, for a given increment of length, decreasing as distance from the middle increases. The last column of Table I was made in accordance with this view from the values given under $R$ (calc.).

*Thermo-electric complication in measurement of transverse potential difference; correction* (*c*). If in the measurement of a transverse potential (Hall effect or Nernst effect), the side-connection wires used are not of the same metal as the strip $m$, these wires, together with the part of $m$ which connects them, constitute a thermo-electric couple which, because of the difference of temperature of its two junctions (Ettingshausen effect or Righi-Leduc effect), tends to make the Hall effect or the Nernst effect appear either greater or less than it should be. Correction of the observed transverse potential difference must be made accordingly, and so the Ettingshausen effect must be measured before the final value of the Hall effect can be known, and the Righi-Leduc effect before the final value of the Nernst effect can be known.

This correction, *which will be called correction* (*c*), may be very large. Thus in one case, with copper wires leading from a cobalt strip, the final value of the Nernst coefficient $Q$ was about 70 percent of the value found without this correction.

*Longitudinal temperature gradient; corrections (d) and (e).* The temperature conditions of the strip *m* are difficult to control satisfactorily. Through a packing of cotton flannel and mica disks there is a notable flow of heat between the strip and the neighboring pole-faces, unless the latter are in some way brought nearly to the same temperature as the strip itself. Unwin[4] interposed between *m* and the poles a thin metal channel through which water of any desired temperature flowed, and I have tried a similar device, but on the whole I do not like it. Unless one makes the distance between the pole pieces greater than the distance I have used, 0.7 cm, he must make the water channel so thin that it is likely to become obstructed by bubbles when hot water is used.

In my more recent experiments I have endeavored to keep the temperature of the pole pieces as nearly as possible the same as that of the middle of the strip *m*. For this purpose I have sent through the double brass tubes *T* and *T'* (Fig. 5), which fit into the bore of the magnet cores, water of suitable temperature. But this device, used alone, operates rather slowly, and I am planning to use magnet coils the windings of which will consist of copper tubing carrying a stream of water, cold or hot according to the pole temperature desired. A thermo-electric couple, one junction of which presses against the side of a pole piece, enables me to keep watch of its temperature changes.

It is evident from what has been said that a uniform temperature gradient cannot be maintained from one end to the other of the strip *m*. If the pole pieces have the same temperature as the mid-length of the strip, the warmer end of the strip will lose heat to the poles and the cooler end will gain heat from the poles, the result being that the longitudinal temperature gradient of the strip will be flattened in the middle but steeper at each end, the general shape being that shown by the curve in Fig. 10. This is a line of double curvature, the point of change from concave to convex being near the middle of the strip, in fact just at the middle, if this has exactly the same temperature as the pole faces. If the poles are cooler, the point in question is displaced toward the cooler end, if they are the warmer, toward the warmer end, of the strip.

For each temperature stage in the measurement of *Q* or *S* a careful study should be made of such a temperature-gradient curve. Data for plotting it are obtained by measuring the temperature differences of points (1) and (2), (2) and (3), (3) and (4), (4) and (5), (6) and (7), (7) and (8), (8) and (9), (9) and (10), of Fig. 6, in the order given and then in the reverse order, first with the gradient running from right to left,

[4] Unwin, Proc. Roy. Soc. of Edin. **34**, p. 210 (1913-14).

then with it running in the reverse direction. The gradient along the (1) to (5) line is not exactly the same as that along the (6) to (10) line, the edge of the strip being rather more affected by the inflow and outflow of heat than the median lengthwise line. Assuming that the gradient along the upper edge is the same as that along the lower edge, and so letting the lower-edge observations represent both edges, I have taken the mean of the (1) to (5) and the (6) to (10) observations, thus making the median line of equal importance with the two edges in estimating the general temperature-gradient. In palladium the temperature-gradient near the mid-length of the plate was usually about 10 percent less along the lower edge than along the median line, and, accordingly, taking the mean of these values was equivalent to reducing the first estimate of this gradient (made from the observed temperature differences between points (2) and (4) on the median line) about 5 percent. *This correction will be called correction (d).*

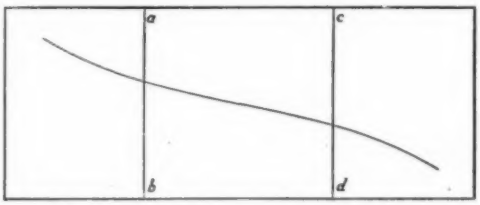


Fig. 10. The curve illustrates the variation of longitudinal temperature gradient along the experimental strip, in observations of the Ettingshausen and the Righi-Leduc effects.

Moreover, I have averaged the right-to-left gradient observations with the left-to-right gradient observations, making due allowance for inaccuracies of placing of the contact points. Thus I have obtained data for plotting a representative hot-to-cold curve corresponding to each mid-point temperature at which I undertook to measure $Q$ and $S$. For example, I have plotted three such curves in the case of palladium, for the three mid-point temperatures 25°, 44.5° and 65°, approximately. In fact, I plotted two such curves with a mid-point temperature near 45°, one with a mid-section temperature-gradient of about 10.5° per cm, the other with a gradient about half as great. For the first of these I used in one of the blocks $B$ (Fig. 5) a stream of water at about 11°C. and in the other a stream of steam. For the second I used two water streams, one near 30° and the other near 75°.

All these curves were carefully plotted and carefully studied. The temperature corresponding to the point of inflexion of any curve I took to be the temperature of the pole-faces. It was usually a little below that

of the mid-point of the plate. Taking any given section of the curve, I could from the difference of gradient at the ends of this section estimate the amount of heat that leaked out from or into the corresponding section of the plate *m*. Then, knowing the mean distance from the plate to the pole-faces and, approximately, the mean difference of temperature between these faces and the section of the plate, I could make a rough determination of *k*, the thermal conductivity of the packing between the poles and the plate. Of course, slight inaccuracies in drawing the temperature-gradient curve might affect seriously the value found for *k* at any one section, but the errors of different sections tended to neutralize each other. Values found for *k* in the case of palladium, with a packing consisting mainly of cotton flannel, with one thin layer of mica, are given below:

TABLE II

*Thermal conductivity of packing around the palladium strip*

| Middle temp. | Middle gradient | *k* below mid-point | *k* above mid-point | Means |
|---|---|---|---|---|
| 25°C | 4.3°/cm | 0.00021 | | |
| | | 0.00016 | | |
| | | 0.00019 | | |
| | | | | 0.00019 |
| 44.5 | 10.7 | 0.00028 | 0.00014 | |
| | | 0.00018 | 0.00026 | |
| | | 0.00014 | 0.00020 | |
| | | | | 0.00020 |
| 45.5 | 5.5 | 0.00035 | | |
| | | 0.00021 | | |
| | | 0.00012 | | |
| | | | | 0.00023 |
| 65.1 | 5.5 | 0.00019 | 0.00028 | |
| | | 0.00015 | 0.00017 | |
| | | 0.00008 | 0.00010 | |
| | | | | 0.00016 |
| | | | Final mean | 0.00020 |

Kaye and Laby give 0.00023 as the thermal conductivity of flannel. It appears probable, therefore, that the leakage of heat was maintained, for the most part, by simple conduction between plate and poles, and not by convection due to air-currents moving upward or downward past the plate. That is, one can make a helpful estimate, in advance, of what the leakage will be by assuming that it will be caused by conduction only through the packing.

It is to be observed that, in my experiments on the Nernst and on the Righi-Leduc effect, I measure the difference of temperature of the two points (2) and (4) of Fig. 6, which are 2 cm apart, and assume, provisionally, that a uniform temperature gradient extends from one to the other, thus finding a value for the gradient at the mid-point. Careful study of the temperature gradient curves shows, however, that the mid-point

gradient arrived at in this way—that is, by taking the mean gradient between points (2) and (4)—is somewhat too large, perhaps 5 or 10 percent greater than the true value. Should we, then, make correction to the full extent of this divergence? This raises the question whether the effective longitudinal temperature-gradient, the gradient value which appears as $\Delta$ in the formulas $Q=\delta_e/H\Delta$ and $S=\delta_h/H\Delta$, for the Nernst and the Righi-Leduc coefficients, respectively, should be the precise value which holds at the mid-line of the plate between the junction point (8) in Fig. 6 and the opposite point on the upper edge of the plate. The discussion already given of "short-circuiting" due to parts of the plate or its connections in which the potential or temperature gradient is not the same as at the middle, requires us to answer this question in the negative. The proper value of $\Delta$ to be used in the formulas above given is to be arrived at by a synthetic process in which the middle-half centimeter length of the plate will have a predominating but not an exclusive influence.

I shall assume that if we start at the middle cross-line of the plate and extend the length under consideration by 0.5 cm stages, the boundaries moving to right and left equally, each successive half cm length will affect the transverse gradient (of potential in the Nernst effect, of temperature in the Righi-Leduc effect) to an extent proportional to the product of the mean temperature-gradient (longitudinal) of this half cm by a *weight-factor* indicated by the significant figures set opposite this half cm length in the last column of Table I. I shall call the value of $\Delta$ found in this way the *synthetic* value, or $\Delta_s$, and this is the value to be used in the formulas for $Q$ and $S$.

The relations of $\Delta_s$ to various gradients taken from the four temperature curves for palladium, $\Delta_{0.5}$ for the middle 0.5 cm, $\Delta_1$ for the middle 1 cm, etc., are shown in Table III.

TABLE III

*Longitudinal temperature gradients at different distances from the median line*

| $\Delta_{0.5}$ | $\Delta_1$ | $\Delta_{1.5}$ | $\Delta_2$ | $\Delta_s$ |
|---|---|---|---|---|
| 4.04 | 4.14 | 4.17 | 4.31 | 4.26 |
| 9.24 | 9.74 | 10.16 | 10.76 | 10.07 |
| 4.88 | 5.00 | 5.21 | 5.52 | 5.25 |
| 4.76 | 4.94 | 5.18 | 5.48 | 5.17 |

It appears from this table that, on the average, $\Delta_s$ was about 8 percent greater than $\Delta_{0.5}$, 4 percent greater than $\Delta_1$, 0.5 percent greater than $\Delta_{1.5}$, and 4.5 percent less than $\Delta_2$. Accordingly, the values first found for $Q$ and $S$, in the case of palladium, were to be increased about 4.5 percent to make allowance for the too great vaue of $\Delta$ provisionally used. *This will be called correction* (*e*).

*Transverse temperature-gradient; correction* ($f$). The method of measuring the difference of temperature actually existing at any time between point (8), of Fig. 6, and the opposite point on the upper edge of the plate, will be explained later. My view of the matter is that the Ettingshausen effect or the Righi-Leduc effect is all the time tending to increase the transverse temperature difference and that the heat conductivity of the plate $m$, assisted by the conductivity of the packing lying between the plate and the pole-faces, tends to reduce it. What we measure is the compromise result of these tendencies. We are now concerned with the question how much greater this difference would be if, other things being equal, the packing were thoroughly non-conductive for heat.

Study of the longitudinal temperature curve helps us here. For simplicity let us assume, for the present, that the temperature of the mid-point of the plate $m$ is the same as that of the pole-faces, this bringing the point of symmetry of the temperature-curve to lie on the median transverse line of the plate, as in Fig. 10. Then the slope of the curve, at the line $ab$ of Fig. 10, 1 cm to the left of the middle line, will be the same as the slope at the line $cd$, 1 cm to the right of the middle. This implies, if we neglect the slight difference of thermal conductivity due to difference of temperature, that the amount of heat carried by the plate across line $ab$ is the same as the amount carried by it across the line $cd$. Moreover, this amount of heat is equal to that which would be carried from $ab$ to $cd$ *by the plate alone*, if the *temperature-gradient* existing at $ab$ and at $cd$ existed all the way from one line to the other, and it is considerably greater than the amount that would flow with a uniform gradient descending from the *temperature* of $ab$ to the *temperature* of $cd$. In fact, if $\Delta T$ represents the temperature of $ab$ minus the temperature of $cd$, and if $\gamma$ represents the *temperature-gradient* at $ab$ and $cd$, the ratio of the heat actually conveyed from $ab$ to $cd$, by plate, packing, etc., to that which would be conveyed by the plate alone, with the existing temperatures at $ab$ and $cd$, is $2\gamma/\Delta T$. In some instances I have found this ratio to be as great as 1.19.

Turning now to the *transverse* conveyance of heat, let us suppose the line $ac$ to be warmer than the line $bd$, and that we have measured their difference of temperature and found it to be $\delta T$. Assuming the plate to be of standard width, 2 cm, we find line $ac$ analogous to $ab$ and $bd$ to $cd$, and so we conclude that, if the packing were non-conductive, the transverse temperature difference, in order to carry as much heat transversely as is now carried by plate and packing together, would have to be approximately, $\delta T \times (2\gamma/\Delta T)$. Accordingly, we amend our observed transverse

temperature-difference by means of the correcting factor $(2\gamma/\Delta T)$. *This correction will be called correction* $(f)$.

I have provisionally made the assumption, in constructing Fig. (10), that the mid-point of the plate has the same temperature as the pole-faces, so that the line *ac* will be as much above the temperature of the poles as the line *bd* will be below that temperature. If this condition is not exactly maintained, and usually it will not be, a slight divergence from it will not seriously affect the accuracy of the correction just described. For example, if the pole-faces are a degree or two colder than the transverse mid-line of the plate, we shall have superposed on the equal out-and-in flows of heat which I have assumed, a flow outward from all parts of this transverse line. Such a flow will affect the transverse *gradient* in the plate but little, though it is better to keep it as small as practicable—that is, the poles should be kept as nearly as may be at the temperature of the middle of the plate.

*Thickness and method of support of plate.* It is evident that, other things being equal, the disturbing influence of heat leakage through the packing will be less the greater the thickness and the heat conductivity of the plate. The nickel plate I have used is about 0.058 cm thick, the cobalt plate about 0.053 cm, the gold plate about 0.0124 cm, the palladium plate about 0.0105 cm. Very thin plates are objectionable, even for the Hall effect, as it is difficult to measure their effective thickness with accuracy, and they are liable to serious mechanical injury unless very securely supported. Of course, where temperature gradients play no part, there is no objection to fastening the metal with cement to a glass plate; but such a backing is not desirable, in general, where temperature differences are concerned. Accordingly, my practice, when all four effects are to be measured, is to support the metal plate merely by its attachments to the blocks *BB*, Figs. (5) and (6). In the case of cobalt, however, since this metal, so far as my acquaintance with it goes, is very brittle, I felt obliged to use a backing of glass, which made the heat leakage greater than it would have been with a packing of flannel only.

In order to prevent buckling of the cobalt plate on heating, one of the leads *B* (see Fig. 6) was left slightly loose under its retaining screws, alignment being maintained by means of the guide *G*.

*Measurement of magnetic field strength.* Fundamentally, my method of measuring the field strength is to withdraw suddenly from between the pole-pieces a test-coil of known integral area, in circuit with a standard induction and a ballistic d'Arsonval galvanometer. But use of the test-coil is hardly practicable when a plate with all its small-wire attachments is in place between the poles. Accordingly I use the test-coil in

advance of the final installation of the plate, making observations of the galvanometer throw with various strengths of magnetizing current, and so getting data for plotting a curve showing the relation between the strength of this current and the intensity of the field. Two or three such curves should be made, each for a different temperature of the magnet pole-pieces, according to the range of temperature to be used in the main experiments.

When a magnetic metal plate is to be studied, it or an equally thick piece of like material should be in place between the poles when these observations with the test-coil are made.

Of course care should be taken to see that the distance between the pole-pieces is the same during the main experiments as during the preliminary test-coil work. I gauge this distance by means of a steel cylinder turned to the required thickness. Moreover, as the electro-magnet which I use suffers a perceptible decrease of pole-distance, unless care is taken to prevent it, when a strong magnetizing current is applied, I use a stop between the faces of the two magnetizing coils, near their upper edge.

## Measurement of the Hall Effect

This operation is simple and easy, after the plate is properly mounted and connected. I have used a non-astatic Dubois-Rubens "armored" galvanometer of about 11 ohms series resistance, which rests on a platform suspended by three stout wires from a bracket bolted to a brick partition wall of the laboratory. Suspended beneath the platform is a vertical cylinder about 8 cm in diameter, which is partly submerged in an oil bath, to dampen vibrations. On the upper surface of the platform is a sheet of hair-felt about 3.5 cm thick, on which is a board about 2 cm thick carrying four rubber "sponges" compressed to a thickness of about 1 cm by the load they carry, which is a sheet of slate about 1.3 cm thick on which rest three glass cups receiving the feet of the galvanometer. I mention all these details because this Julius suspension arrangement, for which I am indebted to my former colleague Dr. E. R. Schaeffer, has proved eminently satisfactory, in a building subject to much disturbance, and has saved me a vast amount of work and worry.

The galvanometer, as I have used it, is not very sensitive. With a scale distance of 1.8 meters, 1 cm deflection is given by about $1.8 \times 10^{-8}$ ampere. My ordinary method of determining its sensitivity is to find by trial how great a fraction of one volt is required to produce 1 cm deflection under the conditions of the actual Hall effect observations—that is, with

a greater or less amount of "introduced" resistance in the galvanometer circuit.

The galvanometer needle, provided with an air vane, has a vibration period of about 20 seconds, and is nearly "dead-heat." Readings with a reversal of the magnetic field at the plate *m*, are taken 45 seconds apart, a considerable interval being needed for all conditions to reach a final state after the reversal. As it is usually impracticable to arrange the side connecting wires at the plate in such a way as to make that part of the galvanometer circuit non-inductive, this circuit is opened just before the magnet reversal and closed a second or two after this reversal, a procedure which saves the needle from a too disturbing impulse.

It sometimes happens, especially at forced temperatures, that an appreciable longitudinal temperature-gradient exists at the middle of the plate during the Hall effect observations, thus superposing a Nernst effect. To eliminate error from this cause, two sets of observations should always be made, one with the longitudinal current running from left to right and one with its direction reversed. Another reason for this reversal is that it tends to exclude error that might otherwise come through a slight leakage of electric current from the magnet circuit into the galvanometer circuit. If reasonable precautions are taken, such leakage is not likely to be troublesome when the laboratory is artificially heated, but during the damp summer months it may become apparent and bothersome.

The temperature of the mid-part of the plate *m* during Hall effect observations can be found by means of a thermo-electric couple consisting of one of the junctions, let us say the top one, soldered to the plate (see Fig. 6) and another junction kept at a known temperature outside the magnetic field. The condition of this second junction is indicated in Fig. 11, which shows, one third full size, a double-walled glass tube, through the outer compartment of which runs water of the desired temperature while the inner contains oil of a sort that will not act injuriously on the wires that are immersed in it. An "ideal" wire *I*, leading from the junction on the plate, enters a narrow glass tube held in a cork stopper and extending nearly to the bottom of the oil. Near the bottom of this tube the ideal wire is soldered to a copper wire *C*, which, together with the copper wire coming directly from the junction on the plate, leads off to the galvanometer. A thermometer *T*, with the middle of its bulb on a level with the junction in the oil, gives the temperature of this junction.

The value of the Hall effect coefficient *R* as found directly from the observations made, is subject to the three corrections, (a), (b), and (c),

already described. Corrections (a) and (c) should be applied first and then (b), the latter being taken as a certain percentage of the value obtained by applying the (a) and (c) corrections. As correction (c) depends on the size of the Ettingshausen effect, the value of $P$, or rather the transverse temperature-difference actually existing because of the Ettingshausen effect, must be found before that of $R$ can be finally determined.

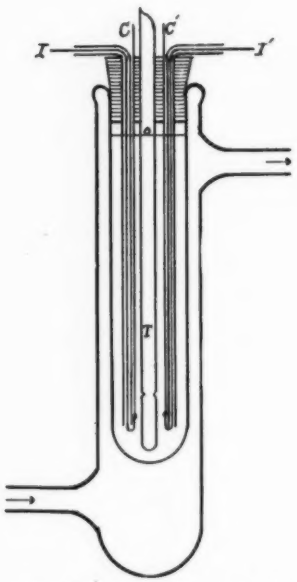


Fig. 11. Arrangement for controlling the temperature of thermo-electric couples.

The strength of the longitudinal current sent through the strip $m$ should be adapted to the case in hand, the weakest current that will give satisfactorily large transverse effects being the best. Through a gold strip about 2 cm wide and 0.0125 cm thick, I used at times a current of about 30 amp.; but a current of equal strength sent through a palladium strip of like dimensions heats the middle many degrees, and is therefore objectionable unless a high temperature is desired.

Within the limits of accuracy of my observations, the transverse effect, whether of potential or of temperature, is, other things being equal, proportional to the strength of the longitudinal current. I do not, however, take this proportionality for granted in dealing with any new metal, and it is my custom to test it by experiment.

## Measurement of the Ettingshausen Effect

This effect consists of a small difference of temperature, sometimes not more than 0.01 degree in my experiments, between the same two points at which the attachments are made for measurement of the Hall effect. In fact, unless unusual precautions are taken to prevent the combination, these two effects always coexist. To measure the Ettingshausen effect alone, Unwin,[5] who has done good work on all four of the transverse effects, did not establish metallic contact of thermo-electric junctions with the two points in question, but used an interposed thin sheet of mica, making correction for the failure of this device to establish

[5] Unwin, Proc. Roy. Soc. Edin. **34**, p. 208 (1913-14), and **41**, p. 44 (1920-21).

complete equality of temperature between the junctions and the points on the plate at which they were applied. Thus he had only a single thermo-electric circuit and could connect this with an ordinary sensitive galvanometer in the ordinary way.

My method, much less simple in some aspects, has been to employ two independent thermo-electric couples, one having a junction soldered to one of the two points on the plate (see Fig. 8), the other having a junction soldered to the other of these points, and to connect these two couples to the coils of a galvanometer used differentially. The second junction of each couple is maintained at a known temperature, by being placed beside the other in an oil bath like that shown in Fig. 11.

My galvanometer, the same that I have used for measuring the Hall effect, was not intended for differential use, having only a single needle-group. To use it differentially for purposes of careful measurement was a somewhat novel and venturesome experiment, involving a rather complicated and laborious operation for determining the sensitiveness of the instrument as thus used. This operation ran as follows: With the two thermo-electric circuits sending their currents in opposite directions, one through coil $A$, the other through coil $B$ of the galvanometer, the deflection produced by the introduction of a known e.m.f. into the circuit of coil $A$ was measured, and next, with both the opposed currents reversed in the galvanometer coils, the effect of the same e.m.f. was measured again. Then corresponding measurements were made by introducing a known e.m.f. into the circuit of coil $B$. The variation of sensitiveness indicated by comparison of any two of these four measurements was often many percent, but the steadiness of the mean value of the four measurements through months of observation gave me great confidence in the substantial correctness of this mean. Nevertheless, I hope to use a properly wound differential galvanometer for measurement of the Ettingshausen and the Righi-Leduc effects hereafter.

Assuming it possible to keep the two oil-bath junctions (in Fig.11) at the same temperature, one might suppose it to be a matter of indifference what this temperature was to be, but in practice it is found best to keep this temperature as nearly as may be the same as the mean temperature of the junctions on the plate $m$. If the difference between these two temperatures becomes large, there is so great an e.m.f. in each of the two opposing circuits that a slight change of resistance in one of them, such as may be due to local temperature influence, may upset their equilibrium enough to produce very troublesome galvanometer deflections. It is true that a compensating e.m.f. from a storage cell may be

introduced into each circuit in such a way as to make the net e.m.f. in each nearly zero, and of this device I make habitual use; but even so it is best to have the temperature difference in question as small as practicable; for storage cells are not always sufficiently constant in their e.m.f. to be depended on for much "compensating" action.

The two junction-points near the bottom of the oil-bath should be brought nearer together than they are shown to be in Fig. 11, due care being taken to prevent conductive contact of the two circuits, and these junctions should be symmetrically placed, so that, if possible, neither will be affected before the other by any change of temperature of the water stream surrounding the oil bath. Moreover, all thin wires in either circuit, and especially all junctions of thin wires, should be covered in such a way as to protect them from sudden temperature changes, such as a varying current of air or changing illumination might produce. Attention to such details may save a great deal of time and worry in the galvanometer measurements.

After the transverse temperature difference existing between the two side junctions on the plate $m$ has been found by experiment, correction (a) should be applied, and to the value thus found corrections (b) and (f) should be added.

## The Nernst Effect

This effect, a transverse potential-difference accompanying a longitudinal temperature-gradient across the magnetic field, is not usually difficult to discover or even to measure. The longitudinal temperature-gradient, however, is naturally less convenient to deal with than a longitudinal electric current. I have said about all that I need say in regard to this matter, in my discussion of corrections (d) and (e). I do not, as a rule, have much trouble with inconstancy of this temperature-gradient, though it should be measured frequently.

Within the limits of accuracy of my observations, the Nernst transverse potential-differences, other things being equal, are proportional to the steepness of this gradient.

To reach the final value of the coefficient $Q$, corrections (a), (d), (e), (c) and (b) should be applied. The application of correction (c) requires knowledge of the transverse temperature difference, due to the Righi-Leduc effect, which accompanies the Nernst effect.

## The Righi-Leduc Effect

This effect, a transverse temperature-difference accompanying a longitudinal temperature-gradient, across the magnetic field, is perhaps

even more troublesome to measure than the Ettingshausen effect, but I have already discussed most of the difficulties likely to be encountered here.

Within the limits of accuracy of my observations, the transverse temperature difference is, other things being equal, proportional to the longitudinal temperature gradient. The corrections to be applied are (a), (d), (e), (f), and (b).

## Quality of Metals; Numerical Results

The four metals that I have studied especially during the past two years are gold, palladium, nickel and cobalt.

The gold is the purest and softest obtainable from the S. S. White Dental Manufacturing Company of Boston.

The palladium is the purest that could be furnished me in February 1922, by Baker and Company of Newark. It was "of special high purity but not guaranteed chemically pure."

The nickel plate was given me by Leeds and Northrup and probably is of a high degree of purity, though its chemical analysis has not been made.

The cobalt was given me in 1913 by Dr. H. T. Kalmus of the Research Laboratory of the School of Mining, Kingston, Ont. He wrote "our cobalt runs very erratically from substantially pure metal to metal with nearly 1 percent of impurities." The plate probably contains some iron and nickel; as I have already indicated, it is decidedly brittle.

A summary table of the results obtained with these metals was given in the Proceedings of the National Academy of Science for July 1925, but as the values there given for $P$ in palladium are all about 7 percent too large, the whole table, with the necessary correction, is here repeated.

Table IV

*Values of R, P, Q and S in certain metals*

| Metal | Temp. | $R\times10^8$ | $P\times10^9$ | Temp. | $Q\times10^8$ | $S\times10^9$ |
|---|---|---|---|---|---|---|
| Gold | 17° | − 705 | − 1.2 | 25° | − 181 | −300 |
| | 72 | − 696 | − 0.4 | 57 | − 181 | −263 |
| Palladium | 26 | − 845 | + 16.2 | 25 | + 327 | − 48.7 |
| | 45 | − 855 | + 17.8 | 45 | + 326 | − 41.4 |
| | 64 | − 844 | + 20.6 | 67 | + 335 | − 37.8 |
| Nickel | 22 | −4520 | + 60.6 | 38 | +2590 | −528 |
| | 57 | −5910 | +105.7 | 57 | +3040 | −494 |
| | 86 | −7280 | +154.2 | 77 | +3660 | −447 |
| Cobalt | 19 | +3550 | + 81.0 | 25 | +1900 | +377 |
| | 48 | +4440 | +109.0 | 47 | +2190 | +429 |

A more detailed statement for one of the metals, palladium, may be of interest here, as it will give some idea of the precision of the measurements, their agreement or disagreement among themselves, and of the range of experimental conditions. In the following table, $T$ indicates the tempera-

TABLE V

*Sample results for palladium*

These were obtained on various dates in Nov. and Dec. 1924 and in Jan. 1915 as indicated in parentheses; (N4) = Nov. 4 etc.

| $T$ | $I$ | $R\times10^6$ | $P\times10^9$ | $T$ | $G$ | $Q\times10^6$ | $S\times10^9$ |
|---|---|---|---|---|---|---|---|
| 28.0°C | 414 | −852(N4) | | 21.5°C | 4.2 | +327(D9) | |
| 24.0 | 571 | −836(D1) | | 24.7 | 4.4 | +328(D23) | |
| 28.0 | 410 | | +16.1(N4) | 26.2 | 3.8 | +326(J31) | |
| 25.0 | 567 | | +16.5(D4) | 24.5 | 4.2 | | −46.5(D10) |
| 43.6 | 399 | −862(N6) | | 26.1 | 4.4 | | −50.8(D22) |
| 44.0 | 976 | −846(D1) | | 45.8 | 10.9 | +329(D30) | |
| 47.0 | 633 | | +17.6(N28) | 45.1 | 5.5 | +322(J9) | |
| 45.0 | 962 | | +18.2(N29) | 45.4 | 10.6 | | −412(J2) |
| 64.0 | 952 | −844(N26) | | 45.2 | 5.6 | | −414(J7) |
| 63.0 | 957 | | +20.3(N24) | 67.0 | 5.5 | +336(J13) | |
| 64.0 | 943 | | +21.1(N26) | 68.0 | 5.3 | +332(J28) | |
| | | | | 66.0 | 5.4 | | −38.3(J15) |
| | | | | 66.8 | 5.0 | | −37.5(J30) |

ture at mid-point of the plate under examination, $I$ is the current density in amperes per square centimeter of cross-section of the plate, $G$ is the longitudinal temperature-gradient. The intensity of the magnetic field varied from about 8700 to about 9200.

JEFFERSON PHYSICAL LABORATORY,
HARVARD UNIVERSITY.
August 12, 1925.

# A SMALL RESISTANCE THERMOMETER

By Geo. F. Taylor

Abstract

**Small resistance thermometer.**—This thermometer, which was developed for field observations in the Department of Agriculture, fits into a sheath only about 6.4 cm long and 0.24 cm in diameter (and may be made even smaller). It consists of a Pb filament 1.5 cm long and $2\times10^{-3}$ mm in diam. in a glass tube $4\times10^{-5}$ mm thick, embedded in a typemetal which makes contact with one end of the filament. The method of drawing such filaments has been previously described.[1] The resistance of the filament is 448 ohms so that with a portable galvanometer a sensitivity of .005° is readily obtained. The temperature lag is about 10 sec. The technique of manufacture is described. After being made, the resistance decreases about .06 percent in the first two hours, then gradually increases about .05 percent, reaching a constant value in about 3 weeks. This time effect is due chiefly to the typemetal. After seasoning, the reading at 0°C is constant to within .02°. Fifty of these thermometers have been in service for some time, in the range −20° to 40°C.

**Thermal expansion of typemetal** (Pb 85, Sb 12, Sn 3).—The coefficient was found to be .864 times that of Pb, 0° to 100°C, or $25.23\times10^{-6}$ per degree. After casting, rods were observed to decrease in length .06 percent, reaching a minimum, in 4 hr, .08 percent less than the initial length.

IN a recent number of the Physical Review mention was made[1] of a new type of small resistance thermometer. In the present article a detailed description is given of the construction of this instrument and of its performance.

The main object sought was to produce a resistance thermometer which would be comparable in size to the thermocouple and thus combine the advantages of both.

After considerable experimenting it was found necessary to make a radical departure from the ordinary coil-of-wire type, mainly for the reasons that for very small thermometers, the required sensitivity could not be obtained with the maximum current allowable and because no means could be found for supporting the wire in such a way that the resistance would remain constant. Thermometers were made by depositing films of metal on nonconductors but were not successful. Films of Pt, Au, Ag and Bi deposited on glass, quartz, mica, and calcite changed in resistance from ½ to 5 percent over a period of one month, and the heating was also too great.

The type of conducting unit which was finally found to be successful was a fine thread of metal drawn in glass and embedded in another metal.

[1] Geo. F. Taylor, Phys. Rev. **23**, 658 (May, 1924).

## Description of the Thermometer

The external appearance of one of the set of fifty direct reading thermometers now in use (two-thirds actual size) is shown in Fig. 1(f), and an enlarged section in Fig. 1(e). The stem or case $A$, Fig. 1(e), which consists of a manganan or brass tube of .005 inch (.127 mm) wall thickness, 3/32 inch (.238 cm) diameter and 2.5 inch (6.35 cm) length, fits into a hard rubber head $h$ of 3/8 inch diameter and ½ inch length. The head is provided with brass terminal posts, $P$ and $P'$ to which the connecting wires from the bridge (not shown) are attached with removable clips. The

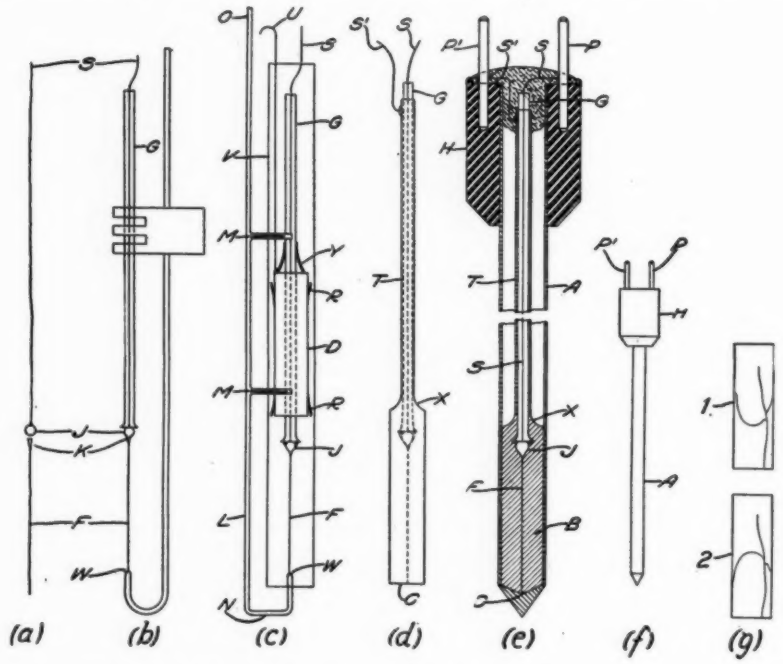


Fig. 1. (a)-(e). Details of construction of the thermometer.
(f) External appearance, two-thirds full size.
(g) Effect of meniscus on filament.

thermometers of this set were purposely made large and strong to stand rather rough usage though they may be—and in fact, some were—made only 1/32 inch in diameter and 2 inches long. This is as small as a 5 junction thermocouple of No. 40 wire can well be made and the depth of emersion necessary is no greater. The No. 33 copper or manganan lead wire $S$, which, when in the case, is soldered to the post $P$, fits in a glass tube $G$. On the lower end of the wire $S$, at the point $J$, a fine filament $F$ is soldered. This filament, which will be referred to as the resistance element or unit,

is a Pb wire of about $2\times10^{-3}$ mm diam., insulated with a covering of glass about $4\times10^{-5}$ mm thick and has a resistance of 447.5 ohms. This filament $F$, including the lower ends of the leads $S$ and $T$, is embedded in a mass of metal $B$, cylindrical in shape and 1 to 1.5 cm long, by flowing a fused alloy around these parts and allowing it to solidify. Type metal, having the composition 85 Pb, 12 Sb, and 3 Sn was the alloy used. The Pb filament $F$ makes electric contact with the metal body $B$ at the point $C$, and only at this point, since both the filament $F$ and the lead $S$ are insulated with glass throughout their length except at their soldered junction $J$ which is insulated by a thin coating of porcelain cement. The return lead $T$ is a copper or manganan tube of 1/32 in. diameter and .005 inch wall thickness which fits closely around the glass tube $G$ and has its lower end embedded in or soldered to the body of metal $B$ at the point $X$. When in the case, a short wire $S'$ connects the upper end of the tube $T$ to the terminal post $P'$. Manganan is preferable to copper because of its lower thermal conductivity, but both leads must, of course, be of the same material.

## Performance

The performance of the thermometer is well known only over the range $-20$°C to 40°C. After a seasoning process, to be described presently, the ice point is constant within about 0.02°. The curve of resistance as a function of temperature over this range is straighter than that of free Pb. The probable reasons will be mentioned later.

When the thermometers are first made they undergo rather large changes in resistance and should be seasoned or aged for a period of two months or more before they are cut off to the desired resistance and finished. Immediately after casting, the resistance drops sharply (Fig. 2A), reaches a minimum value in about three hours and remains there for several hours, after which it rises gradually over a period of several weeks (Fig. 2B), then remaining constant within the limits already stated. Fig. 2A and B are characteristic curves which represent, without exception, the behavior of all of the large number observed. The total change of resistance during the period of seasoning may amount to as much as 0.06 percent of the total resistance.

Merk's "Blue Label" Pb was used and the temperature coefficient in all cases was $.00401\pm.00001$.

Experiments were made to ascertain, if possible, whether the changes in resistance during seasoning were due to the alloy in which the filament was embedded, the glass surrounding the Pb filament, or to the Pb itself.

A rod *a*, Fig. 3, 48 cm long and 0.4 cm in diameter was cast from a specimen of the type metal used. This rod was seasoned by repeated boilings and allowed to rest at room temperature for four months. A similar rod *a'* was then cast and, as quickly as possible, the two were welded together at one end and placed in an upright position with the welded ends down. A yoke or rocker *b* bearing a small mirror *c* was placed across the upper ends. The two small rods of quartz *r* and *r'* rested separately on the two metal rods and carried, on their upper ends, two separate platforms *i* and *i'* for the points of support for the yoke bearing the mirror. The rods *r* and *r'* being of the same length and material and at the same

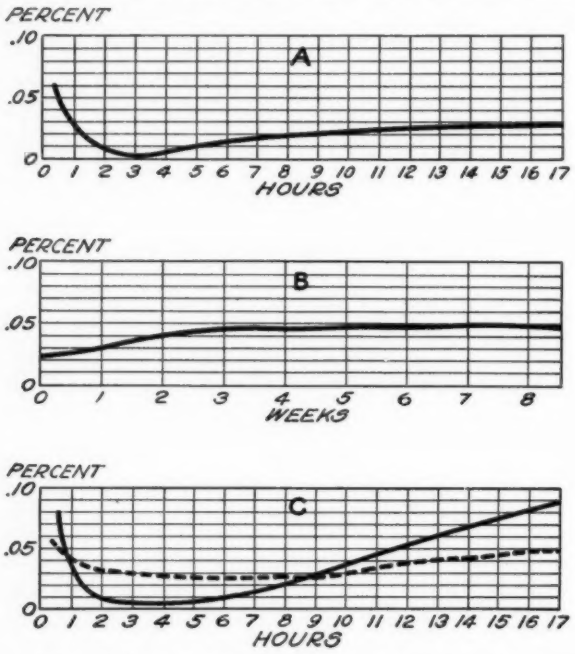


Fig. 2. A and B. Ageing effect on resistance of thermometer; percent change as a function of time.

C. Ageing effect on length of freshly cast rod of typemetal (full line curve) and of lead (dashed curve).

temperature, did not enter into the calculations. The points supporting the mirror were 0.502 cm apart and the mirror was observed through a telescope 4 meters away. This gave a multiplication of sixteen hundred times the motion between the two points of support and made it possible to detect a change in length as small as $10^{-7}$ cm per cm. A glass jacket *d* around the two rods provided a means for a steam or ice bath.

The full line curve in Fig. 2C gives the results. The similarity of the curves shown in Figs. 2A and 2C indicates that most of the change in

resistance is due to type metal, doubtless through the pressure exerted upon the filament on shrinking and the release of pressure on expanding.

To ascertain whether or not Pb also undergoes a change of volume after fusing and resolidifying, a Pb rod which had been seasoned for several months was compared with a freshly cast Pb rod in the manner just described. The changes during the first ten hours are indicated by the dashed curve in Fig. 2C.

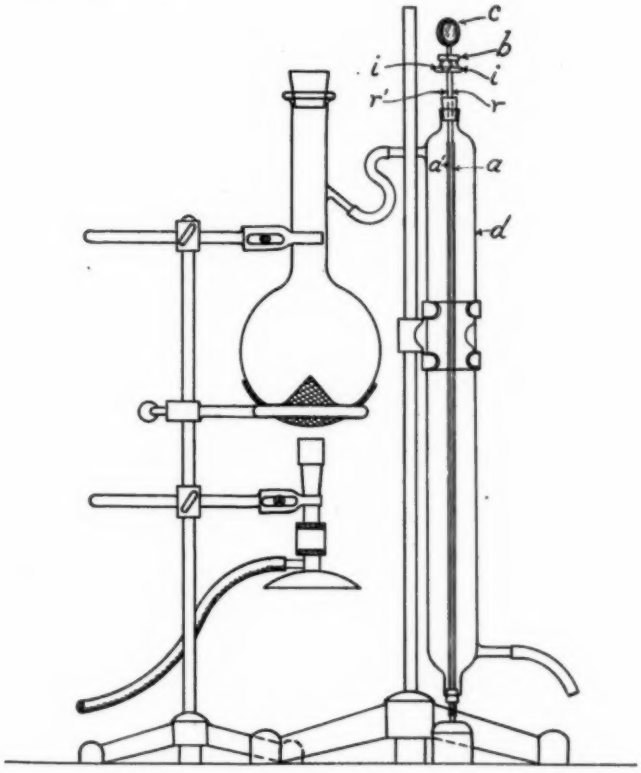


Fig. 3. Apparatus for studying the ageing effect on length of rods.

The coefficient of expansion of the type metal between 0 and 100°C was also determined by measuring the difference of expansion between two rods, one made of Pb and the other of type metal, in the same apparatus. Taking the coefficient of Pb as 29.30, that of the type metal was calculated and found to be $25.23 \times 10^{-6}$.

The Pb filament when embedded in the alloy, cannot expand more than the latter except within the narrow limits of the compressibility of the alloy and this only radially. The result is that, at the higher temperatures, the filament is under a greater pressure than at the lower temperatures

where it may even be under tension, and the temperature-resistance curve, which is normally steeper toward the higher temperatures, is straightened out by the resistance-pressure component which acts in the opposite direction.

The changes in resistance and probably also in volume, continue for indefinite periods after fusion, strong heating or distortion of shape, and it is not likely that they ever cease altogether in Pb or any other solid metal exposed to varying temperatures. It is not to be expected therefore that any newly made resistance thermometer will remain quite constant or that we can ever establish an absolute standard of temperature based on the resistance of a solid metal. The same may also be said of thermo-electric power.

It is well known that the electrical properties of metals cast in glass tubing are slightly different from those of the metals unconfined, but when the glass is made thin enough to behave as an elastic membrane and not as a rigid body ($5\times10^{-5}$ mm or thinner) its effect upon the enclosed metal is negligible. Fibers of this degree of tenuity may be stretched a measurable percentage of their length or drawn red hot into water without breaking.

Since the temperature-resistance curve can be straightened by pressure, it does not seem desirable, in the case of Pb, that the thermal coefficient of expansion of the two metals be the same. But Pb was selected partly for its property of being self annealing at ordinary temperatures and it has not been determined whether or not the hard metals, under long continued pressure, would undergo strain hardening accompanied by a progressive increase in resistance. This effect, which is observed in a bent wire or coil, is the result of unsymmetrical strain, one side of the wire being under pressure and the other under tension, and is not well enough understood to enable us to predict the effect of uniform pressure upon a microscopic wire upon the resistance.

Recently quartz insulated filaments of Pt, Ir, Rh and some other very refractory metals have been made and it is quite likely that one of these embedded in a pure metal will have a more constant resistance than Pb in type metal, besides permitting a much higher temperature range.

*Heating and lag.* The heating is .01°C for a current of 1.8 milliamp. By using a specially designed bridge with high resistance ratio arms[2] a sensibility of .01 ohm (or .01°F) was easily obtained with a portable galvanometer. The temperature lag is about 10 seconds.

[2] The writer is indebted to Dr. W. P. White of the Geophysical Lab., and to Dr. Frank Wenner of the Bureau of Standards, for this valuable suggestion.

## Technique of Manufacture

A sample of Pb of the highest purity obtainable is melted and sucked up into glass tubes about 1.5 mm diam., the glass removed with HF and the remaining Pb rods cut into pieces about 1 cm long. A number of glass tubes, all slightly larger than those used for casting the rods, are next drawn. The walls of these tubes should be of such thinness that they can just be conveniently handled without collapsing between the fingers, which will be from 1/25 to 1/50 of the diameter. The glass recommended for this purpose is Corning G80.

Using the material already prepared, glass insulated Pb wire 2 or $3\times10^{-3}$ mm in diameter is made by the process previously described[1] for use as the resistance element in the thermometer. Since one end of each resistance element must be soldered to a copper connecting wire, it is necessary that a short length of the larger wire from which it is drawn, be left attached (see *K*, Fig. 1(a)). The resistance of the filament may be measured at once by laying it across two Pb plates which are connected to a Wheatstone's bridge and cutting off the ends with a pen knife. The pressure of the knife edge welds the filament to the blocks at the points of cutting and completes the circuit through the filament.

The connecting wires just mentioned are made by cutting No. 33 bare or enameled wire into lengths of 3 or 4 inches, touching the end of each to an oxy-acetylene flame until it rolls up into a small globule, *J* in Fig. 1 (a), and tinning this end with soft solder. They are now ready to be soldered to the resistance elements, which is done as follows.

The resistance element, *F* in Fig. 1, already prepared is laid on a cork stopper with the enlarged end of the filament extending about 1 mm over the edge of the stopper and held in this position by a similar stopper placed upon it. The end of the filament is then moistened with soldering flux. The connecting wire *S* is clamped in a mechanical device by means of which it can be moved in any one of three directions. An adjustable microscope stage was used for this purpose. The wire should be clamped at a point about 4 cm from the soldered end. By this means the globular end *J* of the lead wire *S* is brought into a position such that the enlarged end *K* of the filament barely touches the center of the globule. One quick passage of a thin flame across the wire near the globule, but a safe distance from the filament, is all that is necessary to secure a good soldered connection. The wire *S* with attached filament *F* is then taken out of the clamp and a glass tube *G* 1/32 inch outside diameter is slipped over the wire until it is stopped by the globule *J*. The lead wire and attached filament then are placed in a temporary support (Fig. 1(b)) and the end of

the filament is attached at the point $W$ to prevent it from becoming tangled or broken off. The soldered junction $JK$, Fig. 1(b) between the wire and filament is then covered with porcelain cement.

The filament or resistance unit is embedded by supporting it in the center of a tube and immersing this tube in a fused metal so that the metal, entering the end of the tube, flows around and encloses the filament, leaving when cooled, a solid cast with the filament embedded in its center. The filament is about the size of a spider's web and has no sensible rigidity and very little tensile strength. Unless it is supported near the center of the convex meniscus formed by the liquid metal in a glass tube, it is likely to be thrust aside and broken by the unbalanced surface forces of the liquid metal (see 2, Fig. 1(g)). If a concave surface is formed, as with a metal tube, the filament is held in the center without support (see 1, Fig. 1(g)). Glass was used, however, on account of its transparency.

The device for supporting the filament in the center of the tube is shown in Fig. 1(c). The upper support $D$, which is inside the casting tube $V$, is a short brass rod, provided with friction springs $R$ to hold it in place and a hole through the axis for admitting the lead wire $S$ with its insulating tube $G$. The lower support $L$, which is outside the tube, is a steel wire with one end attached to the tube by spring clips $M$, and the other end $N$, bent into a U shape which terminates along the axis of the casting tube $V$. Both supports $D$ and $L$ can be moved, either separately or together, along the casting tube by means of stiff wire handles $O$ and $U$ attached to the supports and extending past the upper end of the tube $V$. With the supports near the lower end of the tube $V$, the small tube $G$, carrying the filament and lead wire, is passed through the support $D$, and the end of the filament is attached with porcelain cement to the lower support at the point $W$. Both supports are then moved together to the position shown in Fig. 1(c). The casting tube (with all attachments) is now placed in a vertical position in the apparatus shown in Fig. 4, by which it can be moved up and down over a melting pot. The melting pot $P$ is a solid copper cylinder with two holes $HH$, one for the metal from which the cast is to be made, and the other for a mercury thermometer.

Keeping the temperature of the melting pot always a few degrees above the melting point of the metal, the casting tube is slowly lowered into the fused metal until all the space below the upper support is filled. To prevent the metal from running back as the casting tube is raised, suction is applied with the mouth through the rubber tube $T$ which is

slipped over the upper end of the casting tube. Care must be taken not to allow bubbles of gas from the cement to be trapped in the cast.

The cast is now slipped out of the tube and the supports removed. The return lead tube $T$, Fig. 1(d) and (e), is slipped over the glass tube $G$, and soldered to the head, or bulb, at the point $X$, Fig. 1(e). After this, it is put in a lathe and turned down to fit the case and the end cut off (also in the lathe) until the resistance is somewhat above the final resistance. After a period of seasoning an ice reading is again made and the

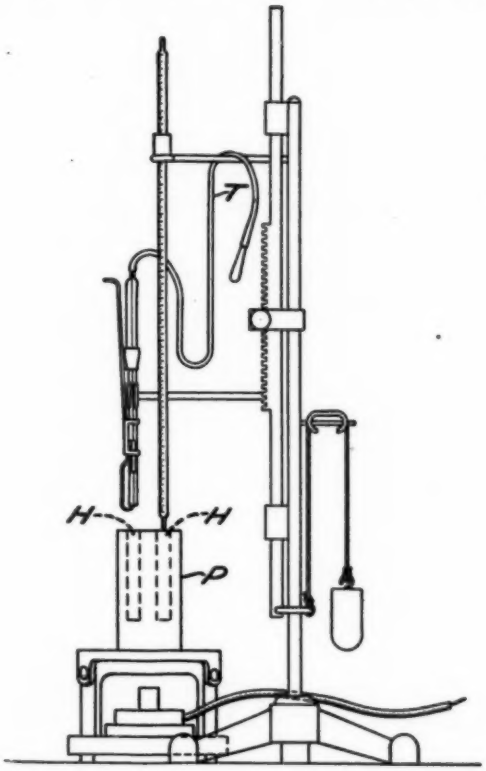


Fig. 4. Apparatus for casting typemetal around the filament.

thermometer is again put in the lathe and cut off just the amount necessary to bring it to the final resistance, after which it is plated with copper.

A precision jeweler's lathe with a slide rest and a special cutting tool were used. The thermometer, while turning in the lathe is connected to a bridge so that the resistance can be followed to a hundredth of an ohm at all times. The current is carried to and from the thermometer while in the lathe by rotating copper disks which dip in wells of mercury.

A lamp and scale were used with the galvanometer, and the scale, which was 2 m from the galvanometer, was placed just over the lathe so that the motion of the image could be followed without taking the eyes off the work. Although the filament is surrounded with glass, whenever the metal head in which the filament is embedded is cut through, a permanent contact is always made between the filament and the metal at the point of cutting.

After the upper ends of the lead wires $SS'$, Fig. 1(d) and (e), have been soldered to the terminal posts $PP'$, a mixture of equal parts of beeswax and rosin was melted and flowed over the top of the hard rubber head. This serves to support the lead wires $S$ and $S'$ and to prevent the formation of films of moisture between the terminal posts, should the thermometer be used in a damp place.

A feature to be noted about this type of thermometer is that large sets can be made equal to each other and of such resistance that 1 ohm is equivalent to 1°C or F so that they can be read directly on any bridge.

UNITED STATES DEPARTMENT OF AGRICULTURE,
BUREAU OF PLANT INDUSTRY,
WASHINGTON, D. C.
March 4, 1925.

# THE VAPOR PRESSURES OF METALS; A NEW EXPERIMENTAL METHOD

By Worth H. Rodebush and Alfred L. Dixon[1]

Abstract

**Quasi-static method of measuring vapor pressures.**—The vessel $A$ containing the liquid and surrounded by a furnace for maintaining a uniform temperature, is connected by one tube $C$ to a manometer $M$ and a reservoir containing a neutral gas such as nitrogen at a suitable pressure, and by another tube $B$ to an intermittent pump. Outside the furnace the two tubes are connected to opposite sides of a differential manometer $D$. Successive portions of the nitrogen are pumped off through $B$ until the manometer $D$ begins to show a permanent difference of pressure; then the reading of $M$ is the vapor pressure desired. The action depends on the fact that when the pressure in $M$ is less than the vapor pressure, nitrogen can get from $C$ to $B$ to equalize any difference of pressure caused by the pump, only by diffusion against the up-streaming vapor in $C$, and inter-diffusion in the case of a tube 3 to 4 mm in diameter is slow. A test of the method gave values for the *vapor pressure of mercury 170° to 203°C* only .04 mm greater on the average than those of Smith and Menzies.

**Vapor pressure of lead, 1118° to 1235°C** was found to vary from 5.70 mm to 19.70 mm in good agreement with the equation $\log_{10} p(\text{mm}) = -10372/T - \log_{10} T - 11.35$, which also fits the best results of Egerton at lower temperatures. The *heat of vaporization of lead at its melting point* is calculated to be 46,300 cal. The chemical constant comes out $-1.40$ which is close to the value $-1.59$ computed from the quantum theory of monatomic gases.

THE accurate determination of the vapor pressures of the less volatile metals is a matter of very considerable experimental difficulty. Because of the very high temperatures the exact measurement of the boiling point is out of the question, while the measurement of the boiling point under reduced pressure is subject to large errors because of radiation losses from the thermocouple and the tendency of vapors to superheat. The fact that these two effects cause errors in opposite directions does not reduce the uncertainty.[2] The dynamical method[3] has been applied at high temperatures but it seems to be very unsatisfactory. The best results are to be expected from some form of static method since we can attain a much more uniform and exact temperature in our apparatus if

[1] Research Fellow of the Chas. A. Coffin Foundation.

[2] The authors (Jour. Am. Chem. Soc. **47**, 1036, 1925) have measured the vapor pressure of lead by this method. The mean of that series of observations is confirmed by our new measurements but the discrepancies between individual observations are very great.

[3] Haber and Zisch, Zeits. f. Physik **9**, 325 (1922).

we minimize the rate at which heat is carried away from it. This is especially important since we have no liquids suitable for baths in a high temperature thermostat. In the ordinary application of the static method a portion of a vapor is trapped off over its own liquid in a U-tube, the liquid serving as a manometer. Such a method has been used successfully, for instance, in measuring the vapor pressure of mercury. At higher temperatures there are two serious difficulties: (1) The quartz glass or other material becomes opaque so that we cannot read the level of the liquid, (2) because of the evolution of absorbed gases we cannot keep a pure vapor in the enclosed space. To avoid these difficulties the authors have evolved a method which approaches static conditions as a limit in operation.

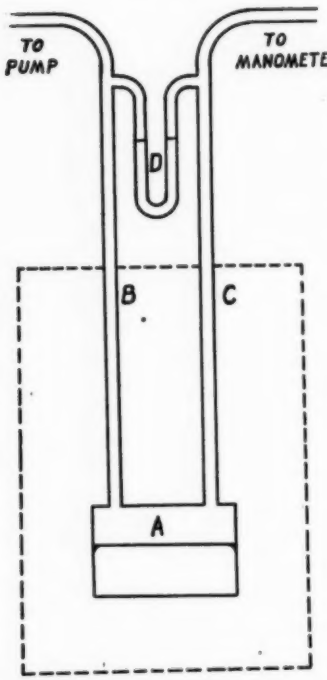

Fig. 1. Diagram of apparatus.

## Method

The apparatus, constructed of Pyrex, quartz glass or other material suited to the working conditions, is shown diagrammatically in Fig. 1. The metal or other substance whose vapor pressure is to be obtained is contained in a shallow reservoir *A* not less than 2 cm internal diameter. The tubes *B* and *C* of 3 to 4 mm internal diameter are of sufficient length so that the upper part of the apparatus remains cool when immersed in a furnace to the depth shown by the dotted line. A differential manometer *D* is provided, containing a suitable liquid, such as paraffin oil. The temperature is measured by a thermocouple attached to the outre wall of *A*.

In operation the apparatus is filled with nitrogen to a pressure greater than the expected vapor pressure and the furnace is brought to constant temperature. Successive portions of nitrogen are pumped off through the tube *B*, sufficient time being allowed after each withdrawal for the liquid levels in the manometer *D* to stop moving. While the theory is somewhat involved the actual behavior of the apparatus is simple. So long as the pressure of the nitrogen in *C* is greater than the vapor pressure of the substance in *A* no permanent difference in level on the two sides

of the differential manometer can be established. As soon as the pressure of the nitrogen drops below the vapor pressure, the vapor in $A$ acts as a valve to prevent the passage of nitrogen through from $C$ to $B$ and a permanent difference in level can be set up in the manometer $D$, which is approximately equal to the difference between the vapor pressure of the substance and the pressure of the nitrogen in $B$. For reasons which will be elaborated below it is necessary to obtain the reading when the difference is as small as can be observed in order to fix the vapor pressure with accuracy.

## Theory of the Method

While the apparatus works in a very simple manner it is not obvious why this is so, since diffusion effects might be expected to play an important part at higher temperatures. The theory which applies to the case has been elaborated by Gaede[4] and the reader is referred to his papers for the fundamental considerations. We have a vapor rising in a tube and being totally condensed against an external pressure of a gas. Let us call the partial pressure of the vapor $P$ and the partial pressure of the inert gas $p$, using the subscript 1 to denote pressures in the reservoir $A$ and the subscript 2 to denote pressures in the tubes $B$,$C$ above the condensation line of the vapor. In the hydrodynamic equation for the flow of gases in tubes of 3 to 4 mm bore at 10 mm pressure, the term containing the viscosity of the gas is large in comparison with the term containing the coefficient of friction against the walls of the tube. If there were no gas above the vapor in the apparatus then the equation for the upward flow of the vapor (in gram mols per second) would be

$$m=\frac{\pi r^4(P_1+P_2)}{16\,RTL\eta}(P_1-P_2)\,. \tag{1}$$

Here $r$ is the radius and $L$ the length of the tube, $R$ the gas constant, $\eta$ is the coefficient of viscosity and $P_1$ and $P_2$ are the vapor pressures at the two ends of the tube. If now there is a gas with pressure $p_1$ above the vapor, then we have the added resistance of diffusion which may be treated as a pressure drop $\Delta P=\Delta p$ equal in magnitude for gas and vapor but in opposite directions, Eq. (1) now becomes

$$m=\frac{\pi r^4(P_1+P_2)}{16\,RTL\eta}(P_1-P_2-\Delta P)\,. \tag{2}$$

A similar equation holds for the gas. The vapor is being continually condensed in the upper part of the tube so that $P_2=0$. The gas is diffusing

[4] Gaede, Ann. der Physik **41**, 289 (1913); **46**, 357 (1915).

into the closed chamber $A$ so that $p_1$ must reach some limiting value and the gas flow become zero when the gas pressures on the two sides of the apparatus are equal.

Now if the gas flow is zero,

$$\Delta P = \Delta p = p_2 - p_1 \tag{3}$$

and Gaede obtains for the general conditions of equilibrium:

$$p_1 + P_1 = p_2 + \frac{16\eta D}{P_1 r^2} \log_e\left(\frac{p_2}{p_1}\right). \tag{4}$$

There are three cases to distinguish. For the case $P_1 < p_2$ it is apparent that if any inequality in the pressure $p_2$ is produced between the two sides of the apparatus, the gas must sweep through the vapor from one side of the apparatus to the other and equalize the pressure. It only remains to calculate the rate of reflux of the vapor up the tube since a too rapid escape of heat by this way would disturb the static condition desired. The equation for the rate of reflux is obtained by combining (2), (3) and (4), obtaining

$$m = \frac{\pi r^2 D}{RTL} \cdot \log_e\left(\frac{p_2}{p_1}\right). \tag{5}$$

Here $R$, the gas constant, should be expressed in c.g.s. units. So long as $p_2 > P_1$ the term log $(p_2/p_1)$ must remain small and since the diffusion coefficient $D$ is of the order of magnitude $10^6$ at unit pressure, the rate of reflux will be very small indeed.

As the external pressure is lowered and we approach the condition $p_2 = P_1$ we find that $p_1$ at equilibrium is still appreciable and the term log $(p_2/p_1)$ may be calculated from Eq. (4). The coefficient of viscosity $\eta$ has been shown to be of the order of magnitude $10^{-3}$. If we substitute rough values in c.g.s. units for the constants in (4), remembering that $p_2 = P_1$, we have

$$p_1 = \left[\frac{2.3 \times 16 \times 10^{-3} \times 10^6}{1.3 \times 10^4 + (0.3)^2}\right] \log_{10}\left(\frac{p_2}{p_1}\right).$$

The numerical coefficient is approximately 30. Hence if $p_2 = 10$ mm, $p_1$ is less than 0.1 mm, and Eq. (5) shows that the rate of flow of the vapor up the tubes remains small.

If the external pressure is reduced considerably below the vapor pressure in $A$, then the rate of flow of vapor up the tubes will become so large that the vapor in $A$ will (because of rapid escape of heat, etc.) become unsaturated; i.e. $P$ will be less than the true vapor pressure

corresponding to the external temperature. This effect was always observed experimentally if the external pressure was lowered greatly. For this reason it is desirable that the reservoir $A$ be of as large cross-section as possible. We can keep the unsaturation as small as we please by keeping the permanent difference of pressure which we set up small.

It remains to show that permanent difference of pressure can be maintained when the external pressure on one side is equal to the vapor pressure and on the other side is slightly less. Here it is a question of rate of diffusion. The equation for the rate of diffusion of the gas against the ascending vapor is given by the expression similar to Eq. (2).

$$m' = \frac{\pi r^4 (p_1 + p_2)}{16\, RTL\eta} (p_2 - p_1 - \Delta P) \tag{6}$$

where $\Delta P$ is the drop in pressure in the ascending vapor, which is to be ascribed to the "diffusion resistance." When $p_2 - p_1 = \Delta P$ we have zero gas flow and the condition of equilibrium given by Eq. (2).

Now if $p_2 = P_1$ on one side of the apparatus while $p_2$ is decreased slightly on the other side, $p_1$ will decrease and tend to remain in equilibrium with the lower value of $p_2$. For a first approximation let us assume that $p_1$ is decreased by 1 dyne per cm$^2$ but that the upward flow of vapor is undisturbed and hence unchanged in value. The net value of the last parenthesis in (6) will then be 1, and

$$m' = \frac{\pi \times (0.3)^4 \times 1.3 \times 10^4}{16 \times 8.3 \times 10^7 \times 10^3 \times 10 \times 10^{-3}} = 10^{-8} \text{ (approx.)}.$$

As a matter of fact the downward movement of gas against the ascending vapor means that $\Delta P$, the pressure drop in the vapor due to diffusion, must be increased, since the vapor flow is retarded and less of its pressure drop is expended on external friction. We have therefore used too large a value for the parenthesis in (6), and the rate of flow calculated is too great. In actual operation of the apparatus it was demonstrated repeatedly that a considerable difference of pressure could be maintained indefinitely between the two sides of the apparatus when the gas pressure was equal to the vapor pressure.

## Experimental Procedure

The difference in levels in the paraffin oil in $D$ was read to 0.01 mm with a cathetometer. $C$ was connected to one limb of a U-tube manometer, the other limb being connected to a pump capable of producing a high vacuum. Sulfuric acid was used as a liquid in this manometer and the difference in levels was likewise read with the cathetometer.

Sulfuric acid was used instead of mercury because of its smaller density and smaller surface tension. Not only is the absolute difference of level for a given pressure much greater but the percentage error from the capillary effects of dissimilarities in the sides of the manometer is greatly reduced.

Considerable experimentation was required to determine the exact size of the tubes *B* and *C* to give the most satisfactory operation. When *B* and *C* were too large, disturbing effects were produced by too rapid flow of the vapor up the tubes, while if they were too small they were clogged by the returning condensed liquid. A bore slightly in excess of 3 mm was found to be the most satisfactory.

## Vapor Pressure of Mercury

As a test of the method a number of determinations were made on mercury with a Pyrex apparatus. The apparatus was placed in an electrically heated oil bath and the temperatures were read with a copper-constantan thermocouple which had been calibrated at the boiling points of water and benzophenone. The results are shown in Table I together

Table I

*Vapor pressure of mercury*

| *T* | *P*(obs) | *P* (Smith and Menzies) |
|---|---|---|
| 170.4°C | 6.29 mm Hg | 6.22 mm Hg |
| 178.1 | 8.30 | 8.22 |
| 180.1 | 8.80 | 8.82 |
| 183.9 | 10.13 | 10.08 |
| 189.6 | 12.33 | 12.24 |
| 197.2 | 15.78 | 15.77 |
| 202.8 | 18.90 | 18.90 |

with values interpolated from the reliable measurements of Smith and Menzies.[5] The agreement is excellent. Any deviations are to be attributed to differences between the temperature scales used by Smith and Menzies and that of the authors.

## Vapor Pressure of Lead

In order to measure the vapor pressure of lead, the part of the apparatus which was to be heated was constructed of quartz glass. This part of the apparatus was placed in a Vitreosil test tube and this in turn inserted in an electric tube furnace mounted in a vertical position. The bulb *A* was placed about 10 cm from the bottom of the furnace and the lower part of the furnace was plugged with insulating material. The top of the furnace extended about 20 cm above the reservoir *A* and the

[5] Smith and Menzies, Jour. Am. Chem. Soc. **32**, 1434 (1910).

vitreosil test tube was filled in around the tubes $B$ and $C$ with quartz beads. The furnace was wound with chromel wire. The temperature was measured by a Pt-PtRh thermocouple which was tied to the outside of $A$ with platinum wire. The temperature was regulated with a hand controlled rheostat and it was not difficult to avoid fluctuations of more than 0.2-0.3 degree at 1200°C. Since the apparatus was insulated above and below and separated from the heating coil by double insulating walls it is believed that the temperature was not only constant but nearly uniform for a considerable distance above the reservoir. The thermocouple was calibrated at the melting points of potassium chloride[6] and potassium sulfate and showed only small deviations from the standard table of Adams.[7] The lead was free from appreciable amounts of impurities.

The results are shown in Table II. These results agree with the other measurements by the authors previously referred to but are in marked disagreement with those of Ingold[8] who also used the boiling point method. The only other data of importance on the vapor pressure of lead are those of Egerton[9] who used the method of Knudsen at much lower temperatures.

TABLE II

*Vapor pressure of lead*

| $T$ | $P$ (obs) | $P$ (calc) |
|---|---|---|
| 1391°K | 5.70 mm Hg | 5.63 mm Hg |
| 1408 | 6.80 | 6.83 |
| 1424 | 8.25 | 8.18 |
| 1441 | 9.86 | 9.85 |
| 1458 | 11.82 | 11.81 |
| 1475 | 14.21 | 14.10 |
| 1491 | 16.70 | 16.58 |
| 1508 | 19.70 | 19.66 |

When our data for log $p$ are plotted as a function of $1/T$, they lie on a straight line within very narrow limits. This would imply that $C_p$ the atomic heat capacity at constant pressure was the same for molten lead as for lead vapor. The work of Iitaka[10] shows that $C_p$ for liquid lead is apparently independent of temperature and equal to 7 calories. Since $C_p$ for monatomic vapors is 5 calories, in setting up a vapor pressure equation we have assumed $C_p = 2$ and have obtained the equation

$$\log_{10} P(mm) = 10372/T - \log_{10} T + 11.3500. \tag{10}$$

[6] Roberts, Phys. Rev. **23**, 286 (1924).
[7] Adams, "Pyrometry," Am. Inst. Min. Metallurg. Engineers, N. Y. (1920).
[8] Ingold, J. Chem. Soc. **121**, 2419 (1922).
[9] Egerton, Proc. Roy. Soc. **103**, 496 (1923).
[10] Iitaka, Science Reports, Tokohu Imp. Univ. p. 899 (1919).

The values calculated from this equation are shown in the third column of Table II. This equation also fits very closely those data which Egerton has designated as his best at lower temperatures. The heat of vaporization of lead at its melting point may be calculated by the Clapeyron relation from this equation; the value found is 46,300 cal.

In an apparatus of the sort described above, thermal effusion effects may be expected to produce errors. Careful experiments showed that with tubes of 3 to 4 mm bore the effects due to thermal transpiration were of the order of magnitude of 0.01 mm.

Since pressures can be read with a precision of 0.001 mm the accuracy obtainable with this method depends upon the temperature control and the patience of the operator. The exact location of the highest pressure at which a readable pressure difference can be maintained is necessarily a time-consuming operation.

## The Chemical Constant

According to the quantum theory of monatomic gases[11] the constant $C_0$ in the following equation (in which $M$ is the atomic weight)

$$\log_{10} p(\text{atm}) = -\frac{\Delta H}{2.3RT} + \frac{5}{2}\log_{10} T - \frac{1}{2.3R}\int_0^T \frac{C_p dT}{T} + \frac{2.5}{2.3} + \frac{3}{2}\log_{10} M + C_0 \quad (11)$$

should be equal to $-1.588$. Using the best values obtainable for specific heats and heats of fusion[12] to evaluate the integral and the values for $\Delta H$ and $\log p$ obtained from Eq. (11) above, we find[13] $C_0 = -1.40$. While it is difficult to estimate the experimental error, there is little doubt that it is sufficient to account for the discrepancy. The greatest source of uncertainty is probably in the specific heat values used both above and below the melting point.

Laboratory of Physical Chemistry,
University of Illinois,
May 6, 1925.

[11] Tetrode, Ann. Physik (4) **38**, 434 (1912).
Einstein, Berl. Akad. p. 261 (1924).

[12] The data for specific heats were taken from the work of Eucken and Schwers (Verh. Deut. Physik. Ges. **15**, 582, 1913), Griffiths and Griffiths (Trans. Roy. Soc. London **214A**, 319, 1914) and Iitaka, loc. cit.[10] The heat of fusion was also determined by Iitaka.

[13] Cf Simon, Zeits. Physik. Chem. **110**, 572 (1924). Simon uses the data of Ingold in his calculation and gets a value $C_0 = -0.8$. His theory that $C_0$ is a function of the heat of vaporization appears to us to depend for experimental support upon Ingold's data.

# MERCURY VAPOR PRESSURE AT LOW TEMPERATURES

By Franklin E. Poindexter

Abstract

**Mercury vapor pressure, 20° to −80°C.**—A modified Buckley ionization gage is described with a range from $10^{-2}$ to $4\times10^{-3}$ mm. This was used to measure the vapor pressure of mercury. Correction for thermal effusion was made, ranging from 25 percent at −80°C to zero at 0°C. The gage was calibrated at 0°C from Knudsen's value. The results correspond to the equations $\log_{10}p$ (liquid) $=8.86-3.44(10^3/T)$; $\log_{10}p$ (solid) $=9.35-3.55(10^3/T)$.

**Heat of vaporization of mercury, 20° to −80°.**—From a large-scale plot of $\log p$ against $1/T$ the heats of vaporization were calculated from the relation $\lambda=-Rd(\log p)/d(1/T)$. Above the melting point the results correspond to the equation $\lambda=15{,}900-10t$ where $t$ is temperature centigrade. A slight discontinuity in slope of the $(\log p, 1/T)$ curve gives at the melting point a sudden increase in the heat of vaporization of some 600 calories, which is in good agreement with the heat of fusion by direct experiment.

Aside from the theoretical considerations of thermodynamics, the use of mercury diffusion pumps, etc., in high vacuum work lends practical importance to a knowledge of the vapor pressure of mercury at different temperatures. The range from 0°C up has been covered by a number of representative experimenters such as Knudsen,[1] Smith and Menzies,[2] A. C. Egerton,[3] Menzies,[4] and others. Volmer and Estermann,[5] however, seem to have been the only ones to have covered the range from 0°C to −65°C. The present paper covers the range from 20°C to −80°C.

## Experimental Method

*Ionization pressure gage.* In the eighteen months of continuous work with the Buckley ionization gage preceding this research, the writer has constructed and used four different types of ionization gages and it seems not out of place to discuss here the details and advantages of the one used in the present research.

Dushman[6] points out the importance of keeping the various lead-in wires separated as far as is possible to prevent electrical leakage from one to the other over the glass. The writer finds that leakages may occur

[1] Knudsen, Ann. der Phys. **29,** 179 (1909).

[2] Smith and Menzies, Jour. Amer. Chem. Soc. **32,** 1434 (1910).

[3] A. C. Egerton, Phil. Mag. **33,** 33 (1917).

[4] Menzies, Jour. Amer. Chem. Soc. **41,** 1783 (1919).

[5] Volmer and Estermann, Zeits. f. Physik. **7,** 1 (1921). The writer wishes to thank Professor John Johnston of Yale University for calling his attention to this paper.

[6] Dushman, Phys. Rev. **17,** 7 (1921).

both inside and outside over the glass from one lead to another, so a system of nickel wire collars $c_1$, $c_2$, $c_3$, and $c_4$ were incorporated in the structure. The protecting collars $c_1$ and $c_2$ are connected to ground. The collars $c_3$ and $c_4$ are maintained at $-25$ volts, which is the same potential as that of the grid, by means of a separate wire leading directly to the battery. The filament $F$ is a straight loop of 10 mil (.25 mm) tungsten wire braced by means of a tungsten wire thrust into the glass between the leads. The stem carrying the filament can be easily cut from the

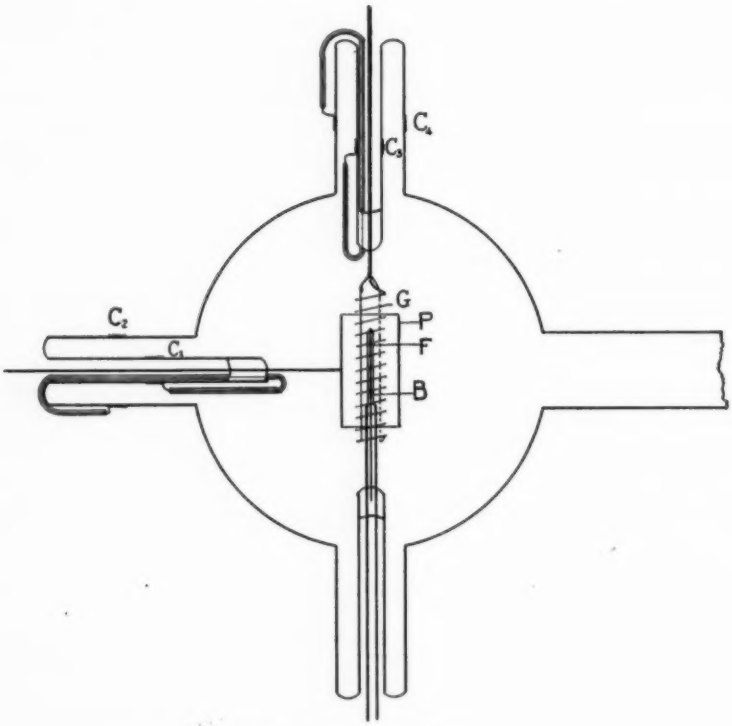


Fig. 1. Ionization gage.

gage and a new filament installed. The grid is a spiral of 7 mil tungsten wire carried by a 10 mil tungsten frame extending down each side, each end of the spiral being welded to the supporting frame. The plate $P$ is of nickel and somewhat longer than the filament while the grid $G$ is longer than the plate. This extra length in the plate and grid is a precaution against stray ions or electrons collecting upon the glass walls of the gage, which may give erratic results. The main part of the gage is a one liter Pyrex flask. It is made large so that its temperature while the gage is in use is considerably lower than the outgassing temperature.

The glass parts are of Pyrex glass and were outgassed by baking in the direct flame of a hand blow torch for an hour or so. The plate and grid were outgassed at a bright red heat by means of electron bombardment using a 10,000 volt transformer to supply the voltage between the filament and plate. When properly outgassed, the residual gas pressure is less than $4\times10^{-9}$ mm, which is the limiting pressure that could be measured in this experiment.

The ionization gage is particularly well adapted for pressures below $10^{-2}$ mm. Since it is an indirect method and the ionization for a given electron current is different for different gases, it is necessary to calibrate

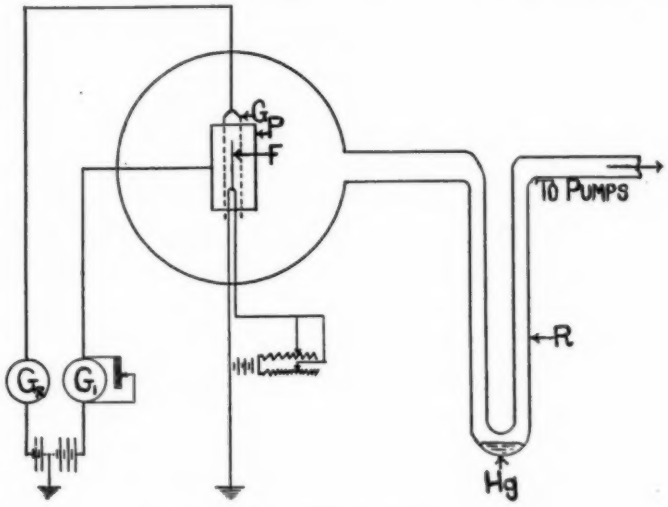


Fig. 2. Arrangement of apparatus.

the gage at some one temperature for mercury vapor. Then the ratio of the ionization in that gas at any other temperature to that at the calibrating temperature is equal to the ratio of the respective pressures.

The apparatus and the arrangement is practically the same as that used by the writer[7] in his work on the sodium trap for mercury vapor. The plate $P$ Fig. 2, was maintained at $+250$ volts relative to the filament $F$ by means of a storage battery. The galvanometer $G_1$ used to measure the electron current from filament to plate, was a Leeds and Northrup type P galvanometer having a sensitivity of $2.7\times10^{-8}$ amp. per scale division. A universal shunt was used with $G_1$ which multiplied the electron current readings in steps of 10. The deflection of $G_1$ was held at

[7] Poindexter, J.O.S.A. and R.S.I. **9**, 629 (1924).

100 mm throughout the experiment, the shunt being set at 10 to 1, 100 to 1, and 1000 to 1. This eliminated any possibility of error due to non-uniformity of the galvanometer scale. The grid $G$ was maintained at $-25$ volts with respect to the filament. The positive ions formed by the collisions of electrons with the molecules of gas between $F$ and $P$ were collected on the grid $G$. The ion current from $G$ was measured by the highly sensitive, critically damped, Leeds and Northrup type R galvanometer $G_2$, having a sensitivity of $8\times10^{-10}$ amp. per scale division. The sensitivity of this galvanometer was found to be constant over all parts of the scale.

The U shaped tube $R$ was used as a mercury reservoir. The mercury used was twice distilled in a current of air according to the method described by Hulett.[8] Liquid air was first placed about the lower portion of the reservoir and the apparatus thoroughly outgassed. Then the liquid air was replaced with cooled alcohol, care being taken that the alcohol extended several inches higher than the part cooled by the liquid air. The temperature of the bath was raised in steps of some 7°C by adding small quantities of alcohol with stirring. The time between readings varied from over an hour at low temperatures to approximately 25 minutes at the highest. It takes some time for mercury vapor to reach equilibrium after the temperature is changed. This appears to be due to a "soaking in" process into the surface of the glass. A few minutes heating of the glass with liquid air on the reservoir is sufficient to drive off this surface mercury, but 24 hours are not sufficient without heating. For increasing temperatures, equilibrium is obtained in the times allowed between readings. For this reason, all of the runs had to be taken with increasing temperatures.

A platinum resistance thermometer of approximately 25 ohms resistance and carrying a current of .01 ampere was used to determine the temperatures. The potentiometer balance method against a standard held at constant temperature was used, the balance being obtained through a Leeds and Northrup type R galvanometer. The platinum thermometer was calibrated three times at the ice, steam, and liquid oxygen points, the first two calibrations being made before starting the experiment and the last one near the end. These calibrations checked. The constants and potential differences found by Callander[9] and others are in close agreement with those of this thermometer, so it is thought that the temperatures are probably correct to 1/100°.

[8] G. A. Hulett, Phys. Rev. 1st series 21, 388 (1905).

[9] Callander, Phil. Mag. **47**, 191 (1899).

## Results

The vapor pressure $P'$ in the ionization gage $G$ is proportional to the ratio of the positive ion current $I$ to the electron current $E$. That is,

$$P' = K\, I/E$$

Knudsen's value of $P'$ (.0001846 mm) at 0°C was used to calibrate the gage. When $P'$ is in mm of mercury, $I$ in scale divisions and $E = 1000$ scale divisions, then,

$$K = 3.91 \times 10^{-6} \text{ mm/1 scale division ion current.}$$

The results are given in Table I. After much preliminary work to ascertain the best working conditions, the runs labeled A and B in the table were made Jan. 28th and 29th respectively. The values of $P'$ are given in column six of Table I as uncorrected pressures because the pressures above the mercury in the reservoir are not directly proportional to the positive ion current on account of the phenomenon of thermal effusion as pointed out by Knudsen,[10] West,[11] and others.

Table I

*Data for vapor pressure of mercury at low temperatures.*

| Run | Temp. | Electron current | Ion current | | Vapor pressure | |
|---|---|---|---|---|---|---|
| | | $E$ | $I$ | $kI/E$ | $P'$ (uncorr.) | $P$ (corr.) |
| A | −79.61°C | $2.66\times10^{-3}$ amp. | .1 | .001 | $4.00\times10^{-9}$ | $3.00\times10^{-9}$ |
| B | −69.94 | | .2 | .002 | $8.00\times10^{-9}$ | $6.00\times10^{-9}$ |
| A | −66.89 | | .6 | .006 | $2.00\times10^{-8}$ | $4.00\times10^{-8}$ |
| B | −63.72 | | .4 | .004 | $1.56\times10^{-8}$ | $1.27\times10^{-8}$ |
| A | −57.76 | | 1.5 | .015 | $5.87\times10^{-8}$ | $4.85\times10^{-8}$ |
| B | −56.88 | | 1.6 | .016 | $6.26\times10^{-8}$ | $5.18\times10^{-8}$ |
| A | −49.89 | | 7.2 | .072 | $2.80\times10^{-7}$ | $2.37\times10^{-7}$ |
| B | −43.43 | | 21.9 | .219 | $8.56\times10^{-7}$ | $7.31\times10^{-7}$ |
| A | −42.80 | | 22.8 | .228 | $8.92\times10^{-7}$ | $7.52\times10^{-7}$ |
| A | −41.79 | | 25.5 | .255 | $9.98\times10^{-7}$ | $8.54\times10^{-7}$ |
| B | −37.84 | | 40.7 | .407 | $1.59\times10^{-6}$ | $1.38\times10^{-6}$ |
| B | −32.74 | | 79.7 | .797 | $3.12\times10^{-6}$ | $2.72\times10^{-6}$ |
| A | −30.97 | | 108.3 | 1.083 | $4.24\times10^{-6}$ | $3.71\times10^{-6}$ |
| B | −28.14 | | 165.7 | 1.657 | $6.48\times10^{-6}$ | $5.70\times10^{-6}$ |
| B | −22.74 | | 335.7 | 3.357 | $1.31\times10^{-5}$ | $1.17\times10^{-5}$ |
| A | −20.57 | $2.66\times10^{-4}$ amp. | 47.2 | 4.72 | $1.84\times10^{-5}$ | $1.752\times10^{-5}$ |
| B | −17.22 | | 65.8 | 6.58 | $2.60\times10^{-5}$ | $2.460\times10^{-5}$ |
| A | −12.00 | | 138.0 | 13.8 | $5.40\times10^{-5}$ | $5.213\times10^{-5}$ |
| B | −10.81 | | 155.9 | 15.59 | $6.10\times10^{-5}$ | $5.895\times10^{-5}$ |
| A | − 5.71 | | 263.0 | 26.3 | $1.028\times10^{-4}$ | $1.005\times10^{-4}$ |
| B | − 3.98 | | 323.5 | 32.35 | $1.265\times10^{-4}$ | $1.240\times10^{-4}$ |
| A | + 0.21 | $2.66\times10^{-5}$ amp. | 48.2 | 48.2 | $1.885\times10^{-4}$ | $1.887\times10^{-4}$ |
| B | 1.76 | | 55.8 | 55.8 | $2.181\times10^{-4}$ | $2.190\times10^{-4}$ |
| A | 7.99 | | 108.8 | 108.8 | $4.260\times10^{-4}$ | $4.320\times10^{-4}$ |
| B | 10.86 | | 145.0 | 145.0 | $5.670\times10^{-4}$ | $5.786\times10^{-4}$ |
| A | 13.04 | | 179.9 | 179.9 | $7.038\times10^{-4}$ | $7.206\times10^{-4}$ |
| B | 19.73 | | 298.5 | 298.5 | $1.165\times10^{-3}$ | $1.210\times10^{-3}$ |

[10] M. Knudsen, Ann. d. Physik **31**, 205 and **33**, 1435 (1910).

[11] G. D. West, Proc. Phys. Soc. **31**, 278 (1919).

## Thermal Effusion Correction

A correction for thermal effusion between two regions of different temperature in a system is necessary when the mean free path is great compared to the dimensions of the parts connecting the two regions. In this research the tube connecting the Hg reservoir to the ionization gage was approximately 1 cm in diameter, and since the mean free path at the highest pressure measured ($1.2\times10^{-3}$ mm) was of the order of 2 cm, it is necessary to make this correction. Fortunately this correction for thermal effusion is a comparatively simple matter. If the two regions are at the temperatures $T_1$ and $T_2$ degrees absolute then their respective pressures are related by the equation

$$P_1/P_2 = \sqrt{T_1/T_2}\,. \tag{1}$$

In this particular case, let us designate the temperatures and pressures in the two regions—the Hg reservoir and the ionization gage—as follows. Let $P_{RT}$ and $P_{RO}$ = pressures above Hg in the reservoir $R$ at any temperature $T$ and at 0°C, respectively. From Knudsen's work $P_{RO}$ is assumed equal to .0001846 mm.

$P_{GT}$ and $P_{GO}$ = pressures in ionization gage $G$ when $R$ is at temperatures $T$ and 0°C, respectively.

$T$ = temperature absolute in the reservoir $R$.

$T_{GT}$ and $T_{GO}$ = temperatures of ionization gage when $R$ is at temperatures $T$ and 0°C, respectively.

Then as in equation (1) we have,

$$P_{RT}/P_{GT} = \sqrt{T/T_{GT}} \quad \text{and} \quad P_{RO}/P_{GO} = \sqrt{273/T_{GO}}\,.$$

Solving these equations for $P_{RT}$ we have,

$$P_{RT} = P_{RO}\frac{P_{GT}}{P_{GO}}\sqrt{\frac{T}{273}\times\frac{T_{GO}}{T_{GT}}}\,. \tag{2}$$

Now $P_{GO}/P_{GT} = S_O/S_T$ where $S_O$ and $S_T$ represent the scale deflections of ion current at temperatures 273° and $T$ respectively. The temperature of the gage remains constant as long as the electron current is constant so that in this particular case $T_{GO} = T_{GT}$ and equation (2) becomes simply

$$P_{RT} = .0001846\frac{S_T}{S_O}\sqrt{\frac{T}{273}}\,. \tag{3}$$

When, however, the electron current is changed from that at which the gage was calibrated—1000 scale divisions in this case—then the

temperature of the gage changes by a small amount. We can get at the temperature of the place where ionization occurs as follows.

First, assuming Stefan's Law, and taking the area of the anode as 81 times that of the filament, we may estimate the temperature of the anode if the temperatures of the filament and of the bulb surrounding the anode are known, and this can be taken as sensibly equal to that of the gage.

There were three electron currents used as indicated in column 3 of Table I, namely $2.66\times10^{-5}$, $2.66\times10^{-4}$ and $2.66\times10^{-3}$ amp. respectively. Since the area of the filament was 1/4 cm$^2$ these currents are equivalent to $1.064\times10^{-4}$, $1.064\times10^{-3}$ and $1.064\times10^{-2}$ amp. per cm$^2$. Substituting these values in Richardson's equation for thermionic emission we readily compute the corresponding temperatures of the filament $T_f$ to be 1825°, 1900° and 2076°K, respectively.

The temperature of the bulb was observed to be approximately 325°K when $T_f$ is 2076° and 300°K when $T_f$ is 1825°. These values of filament and bulb temperatures yield 708° and 615°K as the maximum and minimum temperatures of the gage. Therefore, the correction factor in the case of the largest current is $\sqrt{T_{GO}/T_{GT}}=\sqrt{615/708}=.93$; for the medium current it is .987. It will be seen that the correction for temperature changes in the gage is small and hence our rough method of calculation may be taken as sufficiently accurate.

It will be noticed from column 4 in the table that the ion current readings for the first four points are less than 1 mm, and are therefore only approximate. In fact even the fifth and sixth points are liable to an error of some 12 percent since the scale could not be read closer than .2 mm.

The results of runs A and B are also represented in Fig. 3, curve *a*, log $p$ being plotted as a function of $1/T$. It will be noticed that the graph is almost a straight line, but that there is indication of a slight discontinuity in slope near the melting point. This discontinuity together with the slopes of the two parts will be discussed later on in the paper.

## Comparison with Other Results

The work of Volmer and Estermann[5] was referred to in the introduction. The dotted curve *b*, Fig. 3, is plotted from their values. It will be noticed that their values are slightly higher and that there is no indication of a break at the melting point. They, as well as the writer, used Knudsen's value of .0001846 mm at 0°C to calibrate their apparatus, so the two curves agree at 0°C. The agreement from 0°C to −40°C is close con-

sidering that both methods are indirect and entirely different. The slight departure may perhaps be explained as follows. No mention is made in their paper of a temperature-gradient correction from bath to surface of mercury. Of course if this gradient were the same at the high and low temperatures, then it would cancel out in the calibration, but if this gradient is greater at 0°C than at −60°C as a study of their apparatus

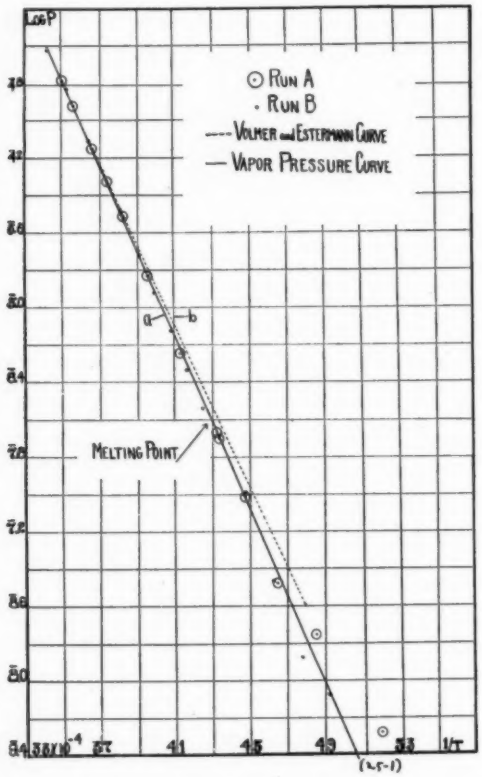


Fig. 3. Logarithm of pressure as a function of $1/T$. Curve a: Results of two runs indicated respectively by dots and by dots in circles. Curve b: Curve given by Volmer and Estermann.

indicates that it probably was, then the pressures at the lower temperatures would be progressively higher as the gradient diminishes. This would give a departure from the writers' curve in the same direction as that shown in Fig. 3.

## Theoretical Considerations

From the fact that the heat of vaporization $\lambda$ varies but little with the temperature, we may assume as a first approximation that the deviation

is a linear function of the temperature. Making this assumption we have,

$$\lambda = \lambda_0 - aT, \tag{4}$$

where $\lambda_0$ is the heat of vaporization at the absolute zero. Substituting for $\lambda$ its value from the well known equation

$$\lambda = RT^2 d\ (\log\ p)/dT \tag{5}$$

and integrating, we get the equation,

$$\log p = -\frac{\lambda_0}{RT} - \frac{a}{R}\log T + i \tag{6}$$

where $i$ is the constant of integration. This is of the form

$$\log p = A - \frac{B}{T} + c \log T \tag{7}$$

which is the well known empirical vapor pressure equation. Now

$$\lambda = \frac{RT^2 d(\log p)}{dT} = -R\frac{d(\log p)}{d(1/T)}.$$

In Table II, $\lambda$ is given in calories per gram molecule as calculated from the slope of a large scale log $p$ vs $1/T$ curve similar to that of Fig. 3. If these values of $\lambda$ are plotted as a function of $T$, two things are noticeable: (a) The graph is linear above the melting point; (b) there is a distinct* discontinuity at the melting point. While it appears that the

TABLE II

*Heat of vaporization of mercury, computed from vapor pressure curve*

| Temperature | | $\lambda$ |
|---|---|---|
| 289.21°K | 16.11°C | 15600 |
| 281.69 | 8.59 | 15800 |
| 273.97 | 0.87 | 15800 |
| 266.67 | − 6.43 | 16000 |
| 259.74 | −13.36 | 16100 |
| 253.16 | −19.94 | 16200 |
| 246.91 | −26.19 | 16300 |
| 240.96 | −32.14 | 16200 |
| 235.30 | −37.80 | 16400 |
| 229.17 | −43.93 | 17100 |
| 224.72 | −48.38 | 17200 |
| 219.78 | −53.32 | 17100 |
| 215.05 | −57.05 | 17150 |
| 210.52 | −62.58 | 17100 |
| 206.18 | −66.92 | 17100 |
| 0 | −273.1 | (19900) |

graph below the melting point is fairly straight, the points are too scattered to draw anything but very approximate conclusions both as

* It should be borne in mind that the four lower points are of little value in determining the slope as the probable error is large.

to the heat of fusion and the slope. This scattering of points is due to the fact that the ion current at these low temperatures is near the limit of the galvanometer used. We may, however, as an approximation draw the best possible straight line through these points parallel to the graph of the points above the freezing point. This extrapolates to $\lambda_0$ (solid) = 19,900 cal. The liquid curve gives $\lambda_0$(liquid) = 19,300 calories. Thus we have, $\lambda_0$(solid) $-$ $\lambda_0$(liquid) = 600 calories as the heat of fusion, which is in fair agreement with the experimental value of 570 calories.[12]

So far as is known to the writer, no experimental values of the heat of vaporization of mercury have been determined within the range of this experiment. Folger and Rodebush,[13] however, found the heat of vaporization at 142°C to be 14,490 calories per gram molecule. The writer found the value from the mean heat curve to be 15,700 calories at 20°C and 16,300 at $-39.5$°C or an average decrease of 10 calories per degree rise in temperature (i.e. in Eq. (4) $\alpha = 10$ cal./degree). Assuming their value is correct at 142°C, the mean temperature coefficient from 20° to 142° is 9.9 cal./degree, in practically perfect agreement. The value they calculated for 20°C (14,670 cal.) is, however, evidently too low.

The writer wishes to thank Professor A. Ll. Hughes for his untiring interest and helpful suggestions throughout this research.

WASHINGTON UNIVERSITY,
ST. LOUIS, MISSOURI,
February 13, 1925.[14]

[12] Phys. Chem. Tabellen (Landolt-Börstein-Roth), 4th ed., p. 829 (1912).
[13] Folger and Rodebush, Jour. Am. Chem. Soc. **45**, 2080 (1923).
[14] Received June 1, 1925—Ed.

# BOOK REVIEWS

**A System of Physical Chemistry. Vol. II. Thermodynamics,** W. C. M. Lewis. Issued as one of the textbooks of the Ramsay and Donnan series in Physical Chemistry. —This is the 4th edition revised and enlarged of a work that has already attained a very considerable circulation among physicists and chemists. While the greater part of the work is devoted to the application of thermodynamics to chemical equilibria, a discussion of the principles of thermodynamics is given in the first chapters.

Thermodynamics has always been a difficult subject for the student, probably because of the way in which it has usually been presented. The author follows the customary treatment but does very well with it, e.g. his presentation of the concept of entropy as a complete differential will probably be grasped by the average student as readily as any that can be given. He makes frequent use of the cycle in his derivations and many will approve this. It may be remarked, however, that the cycle is used to obtain a differential coefficient and when a mathematician wishes to differentiate he does not always go through the process of obtaining the increment of a function and passing to the limit, even in beginning calculus. The book appears to contain no discussion of absolute entropy or partial molal quantities. The chapters on activity and the Debye-Hückel theory of electrolytes should prove valuable. Many will feel that the concept of osmotic pressure has been given more space than it deserves.

The work is encyclopaedic in character, some of the chapters being little more than abstracts of original papers. A great many references to recent literature are given and the book should prove valuable to the advanced student of thermodynamics.— Pp. 489, Longmans Green and Co., New York, $4.75. W. H. RODEBUSH

**Ostwald-Luther, Physiko-Chemische Messungen, 4th Edition.** Edited by Carl Drucker.—The third edition appeared in 1909 and included 573 pages. The present edition has been enlarged through an extension of several sections and the addition of two chapters dealing, respectively, with x-ray analysis of solid substances and measurements relating to radio activity, making the total number of pages 814.

The earlier editions, after the first, were more or less outgrown at the time they came from the press. With the present edition an attempt has been made to bring the subject matter up to date. In this, the Editor has been only partially successful. An examination of the text shows that, with the exception of the newly added chapters, many of the methods described in detail are antiquated. In most instances literature references are given to more recent methods but a detailed description of these has usually been omitted and it is not, as a rule, possible for the reader to determine what method would prove the best suited to his purpose. A few examples may be given in illustration: The fifth chapter, comprising 36 pages is devoted to thermostats and thermostatic devices. Here we find illustrated the old thermostatic arrangement of Ostwald which at the present time is of historical interest only. Many of the devices and methods illustrated or described have long since been replaced by more refined ones. Chapter 6 is devoted chiefly to glass blowing. This section is inadequate in the present edition, as it was also in the earlier ones. It has little practical value either to the beginner or to the expert. Little is said regarding the properties of glass as a function of its composition, a matter which is of the greatest importance in both scientific and technical practice. A paragraph of four lines relates to the blowing of fused quartz and the one suggestion there made is misleading. Fused quartz is one of the most important laboratory materials of the present day and a knowledge of its properties is indispensable, while the technique of its manipulation is readily acquired. Four pages are devoted to methods for the purification

of water. The discussion indicates a lack of first hand knowledge of the modern technique of water purification. A very detailed description is given of the older forms of vacuum pumps while a description of mercury vapor pumps is omitted. Such pumps (of glass) may be constructed with ease and at a very low cost by the amateur as well as by the professional glass blower.

Too much space is devoted to older methods and far too little to newer and more refined ones which have superseded them. By elimination of the older material the necessary space could be obtained for an adequate discussion of contemporary practice. Those who have had considerable experience in the technique of physico-chemical measurements will find many valuable suggestions in this book, but it is not to be recommended to those who are not in a position to form their own judgment with regard to merits of different methods or appliances.—Pp. 814, 564 fig., 3 plates. Akademische Verlagsgesellshaft, Leipzig, 1925. CHARLES A. KRAUS

**Stellar Atmospheres:** A Contribution to the Observational Study of High Temperature in the Reversing Layers of Stars. CECILIA H. PAYNE. (Volume I of Harvard Observatory Monographs: Harlow Shapley, Editor).—It is seldom that a "thesis fulfilling the requirements for the degree of Doctor of Philosophy" requires such extended notice. This book, of about two hundred pages, is a valuable accession to the permanent literature of astrophysics; it discusses in a very readable fashion the interpretation, in the light of recent physical theory, of the stellar spectra obtained at Harvard.

The student of stellar atmospheres seeks to deduce from the spectrum of a star the physical conditions at its surface—in particular the temperature and density. The problem is complicated by the fact that the outer regions of a star are neither completely transparent nor completely opaque; some light reaches the spectroscope from depths of hundreds of kilometers, and both temperature and density increase downward. The laws of black-body radiation, the theory of gas-opacity, the Saha-Fowler theory of temperature-ionization, with the Fowler-Milne extension to the occurrence of maximum abundance of atoms of a given sort (as temperature and density vary)—these constitute the theoretical tools employed in this phase of astrophysics.

*Stellar Atmospheres* touches on each of these, and adds a valuable bibliography of the whole subject; consequently the book is worthy of a place in every physical, as in every astronomical, library. Chief place is given to observational material, including a detailed discussion, element by element, of lines in stellar spectra, and intensity-measurements, through the Harvard sequence, of lines of known series relations. The latter comprise a great amount of hitherto unpublished material. (These measurements are on an arbitrary scale; the problem of absolute measurements of line-intensity in stellar spectra remains to be solved.) The following are among the conclusions worked out: The surface temperature of the hottest stars is as high as 35,000°K; previous estimates of very low densities for stellar atmospheres ($10^{-4}$ atmospheric, or less) are well confirmed; the relative abundance of elements in stellar atmospheres is indicated as roughly the same as in the earth's crust—a fact of much importance for the student of atomic nuclei.

This book is the more deserving of attention because it is the first of a new type of publication from the Harvard Observatory.—Pp. x+216, 10 fig., 1 plate, Harvard Observatory, 1925. $2.50. JOHN Q. STEWART

**An Introduction to Fluid Motion.** W. N. BOND.—Professedly "a guide to one embarking on the study of fluid motion," this little book of 80 text pages presents manifold facts and formulas usually found in books on hydraulics and the motion of gases. It is a short cut to results rather than a systematic exposition. Euler's equations,

the stream function and velocity function are ignored, though vastly important in hydrodynamics.

Chapter I treats of steady flow in stream tubes and free jets, presenting the usual hydraulic equations and describing simple devices for determining velocity and pressure. Flow through an orifice is treated dimensionally, furnishing a first glimpse of the dimensional theory of fluid motion developed later.

Chapter II expands this theory and applies it to motion through tubes as well as orifices. Half this chapter is devoted to manometers and devices for determining the speed or form of flow through tubes.

Chapter III gives 10 pages to the motion of surface waves of a liquid; 4 to motion in channels and over weirs. The first is an elementary and interesting treatment of a large subject.

Chapter IV, in 12 pages, presents the important subject "motion of a body through a fluid." The treatment is unnecessarily qualitative, since we have useful quantitative expressions for the velocity and pressure about many geometrical forms, and for the resistance of spheres, cylinders, discs, etc. It furnishes interesting speculation on the generation and effect of eddies behind such bodies.

Chapter V, in 10 pages, discusses the effect of compressibility on fluid motion. It develops formulas for sound waves, the flow of gas through nozzles and orifices, the conservation of energy in gaseous flow.

The text has a pleasing number of footnotes citing important references, especially references to recent English writings on fluid motion. The citation of foreign sources, however, is too meager for a balanced educational work.—Pp. 94, 38 fig., Longmans, Green and Co., 1925. $1.65. A. F. ZAHM

**Mechanics and Heat.** WILLIAM BALLANTYNE ANDERSON.—This is a revised and enlarged second edition of a well written elementary text suitable for a high school or first year college course. The selection and arrangement of topics is along conventional lines. The presentation is clear, and many of the difficulties arising in the mind of the student which the ordinary text slides over without comment are discussed and explained. The author's denomination of kinetic reaction as a "resisting force" seems, however, rather unfortunate; for the average student has difficulty in thinking of a resisting force as anything other than a resistance proportional to some function of the velocity.—Pp. xiii+371, McGraw-Hill, 1925. $2.50. LEIGH PAGE

**A Treatise on Electricity, Second Edition.** F. B. PIDDUCK.—This is an excellent text of intermediate grade on the subject of electromagnetism. In addition to the usual treatment of the subjects of magnetostatics, electrostatics, and electric currents, the author has included fairly extensive chapters on Electricity in Gases, Röntgen Rays, Radioactivity, and the Electrical Theory of Matter, which are thoroughly up to date as regards the subject matter which they include. The last chapter, for instance, carries the Bohr theory through the theory of the Stark effect and the relativity theory of the fine structure of line spectra.

The book is prefaced by a mathematical introduction which has to do mainly with the important theorems of vector analysis which are needed in subsequent chapters To one who has been brought up on the suggestive notation of Gibbs the author's notation seems very artificial and awkward.

The printing is worthy of the high standard of excellence maintained by the Cambridge University Press. Table of contents and index are both provided.—Pp. xiv+664, Cambridge University Press, 1925. LEIGH PAGE

**Electricity and Magnetism.** R. G. SHACKEL.—This is an excellent text for a high school course in electricity and magnetism. The subject is introduced by a consideration

of the properties of magnets, static electricity coming next, and current electricity last The author is to be commended for developing the electron idea at the very start of the section on electrostatics, and explaining static charges and currents in terms of this conception. Only the most elementary mathematics is made use of—nothing more than the elements of algebra and geometry, and very little of these. The author discusses the concept of force and its measurement in an early chapter, so the book is suitable for a student who has had no previous acquaintance with the subject of physics.—Pp. vi +250, Longmans, Green and Co., London, 1925. $1.20. LEIGH PAGE

# AUTHOR INDEX TO VOLUME 26

References with (A) are merely to abstracts of papers presented at meetings of the Physical Society.


**Albers, V. M.** Photo-electric valve coated with potassium—**26,** 671

**Allison, Samuel K.,** and **Alice H. Armstrong.** Molybdenum K series lines—**26,** 701

———Relative intensities of some tungsten L series and Cu K series lines—**26,** 714

**Allison, Samuel K.,** and **William Duane.** Wavelengths of scattered x-rays—**26,** 300

**Armstrong, Alice H.** (see Allison, Samuel K.)

**Anderson, S. H.** An acoustic oscillograph—**26,** 287(A)

———An anomalous sound absorption coefficient —**26,** 288(A)

**Anderson, S. H.** and **G. G. Kretchmar.** Tungsten arc characteristics—**26,** 33

**Angell, M. F.** Thermal conductivity of some metals at high temperatures—**26,** 287(A)

**Banerji, Durgadas.** Scattering of light in mixtures of air and $CO_2$—**26,** 495

**Barker, E. F.** and **O. S. Duffendack.** Ionization of HCl by electrons—**26,** 339

**Bartlett, Russell S.** Photo-resistance effect for metals at low temperatures—**26,** 247

**Barton, Henry A.** Negative ion emission from oxide coated filaments—**26,** 360

**Birge, Raymond T.** Band spectra associated with carbon—**26,** 283(A)

———(see Hopfield, J. J.)—**26,** 283(A)

**Blake, F. C.** Precision x-ray measurements—**26,** 60

**Boucher, Paul E.** Mobility of negative ions in flames—**26,** 807

**Bowen, I. S.** and **R. A. Millikan.** Pp′ groups in atoms of the same electronic structure—**26,** 150

———Series spectra of $B_{II}$ and $C_{III}$—**26,** 282(A), 310

**Bozorth, Richard M.** Orientations of crystals in electrodeposited metals—**26,** 390

**Bramley, Arthur.** Striated discharge in hydrogen—**26,** 794

**Brewer, A. Keith.** Ionization in reacting gases—**26,** 633

**Buckley, O. E.** and **L. W. McKeehan.** Magnetic properties of permalloy—**26,** 261

**Caswell, A. E.** Thermo-electric properties of pure metals and alloys—**26,** 286(A)

**Chamberlain, Katherine.** Fine structure of x-ray absorption edges—**26,** 525

**Chenault, R. L.** (see Foote, Paul D.)—**26,** 165

**Collins, J. R.** Infrared absorption spectrum of water—**26,** 771

**Compton, Arthur H.** and **Alfred W. Simon.** Directed quanta of scattered x-rays—**26,** 289

**Compton, K. T.** and **C. C. Van Voorhis.** Ionization of gas molecules by electron impacts—**26,** 436

**Dahm, Thos. M.** Organic absorption media as color screens in the ultraviolet—**26,** 285(A)

**Davey, Wheeler P.** Lattice parameter and density of pure tungsten—**26,** 736

**Davis, Bergen.** Relation between critical potentials and indices of refraction—**26,** 232

**DeFoe, O. K.** (see Jauncey, G. E. M.)

**Derieux, J. B.** Reply to criticism by Sexl—**26,** 97

**De Vinney, S. S.** (see Ingersoll, L. R.)—**26,** 86

**Dixon, Alfred L.** (see Rodebush, Worth H.)—**26,** 851

**Duane, William** (see Allison, Samuel K.)—**26,** 300

**Duffendack, O. S.** (see Barker, E. F.)—**26,** 339

**Eckart, Carl.** Post-arc conductivity and metastable helium—**26,** 454

**Ellis, Joseph W.** Emission from the Bunsen Flame —**26,** 283(A)

———Infrared bands of $CO_2$—**26,** 469

**Erikson, Henry A.** Mobility of argon and hydrogen ions in air—**26,** 465

———Mobility of the ions of the active deposits of Th and Ra—**26,** 629

———Ions from hot platinum—**26,** 625

**Ewing, Scott.** Light scattering coefficient of some saturated vapors—**26,** 285(A)

**Foote, Paul D.** and **F. L. Mohler.** Photo-electric ionization of Cs vapor—**26,** 195

**Foote, Paul D., T. Takamine** and **R. L. Chenault.** Excitation of forbidden spectral lines—**26,** 165

**Fricke, Hugo.** Electric conductivity and capacity of disperse systems. II—**26,** 678

———Electric capacity of suspensions of red corpuscles of a dog—**26,** 682

**Graber, M. E.** Optical constants of magnesium and zinc crystals—**26,** 380
**Ghosh, R. N.** Duration of fluorescence of mercury vapor—**26,** 376

**Hall, Edwin H.** Measurement of the four magnetic transverse effects—**26,** 820
**Hamer, Richard.** Reflecting powers of elements in the ultraviolet—**26,** 285(A)
———"Raies ultimes" and photo-electric thresholds —**26,** 286(A)
**Harrison, George R.** and **J. C. Slater.** Line breadths and absorption probabilities in Na vapor—**26,** 176
**Hartig, Henry E.** Apparent transmission of low velocity electrons through Al foil—**26,** 221
**Hayner, Lucy J.** Persistence of the radiation excited in Hg vapor—**26,** 364
**Hildebrand, J. H.** Energy of combination of gaseous ions—**26,** 284(A)
**Hogness, T. R.** and **E. G. Lunn.** Ionization of hydrogen by electron impact—**26,** 44
———Ionization of nitrogen by electron impact— **26,** 284(A), 786
**Hopfield, J. J.** Series and multiplets in sulfur and chlorine—**26,** 282(A)
**Hopfield, J. J.** and **R. T. Birge.** Quantum analysis of new nitrogen bands in the ultraviolet—**26,** 283(A)
**Hoyt, Frank C.** Theory of relative intensities in series spectra—**26,** 749

**Ingersoll, L. R.** and **S. S. De Vinney.** Non-magnetic films of nickel—**26,** 86

**Jauncey, G. E. M.** and **O. K. DeFoe.** Number of beta-rays associated with scattered x-rays—**26,** 281(A), 433
**Jensen, Axel G.** Measuring microvoltages at radio frequencies—**26,** 118
**Jesse, William P.** Ionization in different gases by slow-moving electrons—**26,** 208
**Johnson, J. B.** Schottky effect in low frequency circuits—**26,** 71

**Kazda, C. B.** Photo-electric threshold for mercury— **26,** 643
**Kimball, A. L., Jr.** and **D. E. Lovell.** Variation of Young's modulus with temperature—**26,** 121
**Klein, A. L.** Secondary emission from a Ni surface due to slow positive ion bombardment—**26,** 800
**Knudsen, Vern O.** Speech reception; interfering effect of tones and noise—**26,** 133
———Effect of reverberation upon the quality of speech—**26,** 287(A)
**Kretchmar, G. G.** (see Anderson, S. H.)—**26,** 33
**Kwei, C. T.** Low-voltage arcs in hydrogen, nitrogen, and in certain mixtures—**26,** 537

**Langmuir, Irving.** Scattering of electrons in ionized gases—**26,** 585
**Lane, C. E.** Binaural beats—**26,** 401
**Linder, Ernest G.** Thermo-electric effect in single crystal zinc wires—**26,** 486
**Loria, S.** Indirectly excited fluorescence spectra— **26,** 573
**Loughridge, D. H.** Direction of ejection of photo-electrons produced by x-rays—**26,** 697
**Lovell, D. E.** (see Kimball, A. L., Jr.)—**26,** 121
**Lunn, E. G.** (see Hogness, T. R.)

**Magarian, M. C.** Tungsten K series rays scattered by graphite—**26,** 282(A)
**Martin, R. E.** Effect of light on thermal conductivity of Se—**26,** 475
**McAlister, E. D.** Parasitic thermo-electric forces in homogeneous metals—**26,** 286(A)
**McKeehan, L. W.** Theory of ferromagnetism—**26,** 274
———(see Buckley, O. E.)—**26,** 261
**Millikan, R. A.** Divisibility of the electron; nature of the evidence—**26,** 99
———(see Bowen, I. S.)
**Mohler, F. L.** Production of ions by electron collisions—**26,** 614
———(see Foote, Paul D.)—**26,** 195
**Monk, George S.** Secondary standards of wavelength in the spectra of Ne and Fe—**26,** 284(A)
**Mulliken, Robert S.** Isotope effect in band spectra III. Copper iodide—**26,** 1
———Spectrum of silicon nitride—**26,** 319
———One-valence-electron emitters of band spectra —**26,** 561

**Neuman, L. J.** Thermo-electric effects due to mechanical treatment—**26,** 286(A)

**O'Day, Marcus.** Extension of bar method of measuring specific heat—**26,** 287(A)

**Patterson, R. A.** Crystal structure of Ti and Cr— **26,** 56
**Petry, Robert L.** Secondary electron emission from Fe, Ni and Mo—**26,** 346
**Poindexter, Franklin E.** Mercury vapor pressure at low temperatures—**26,** 859
**Power, A. D.** Fluorescence of cadmium vapor—**26,** 761

**Rashevsky, N. P.** Kinetic theory of thermionic effect—**26,** 241

**Richtmyer, F. K.** Apparent shape of x-ray lines and absorption limits—**26,** 724

**Rodebush, Worth H.** and **Alfred L. Dixon.** Vapor pressure of metals: a new experimental method —**26,** 851

**Ross, P. A.** X-rays scattered by Mo—**26,** 281(A)

———Ratio of intensity of the Compton lines—**26** 282(A)

**Schumann, T. E. W.** Electrification of rain drops; Elster and Geitel's theory—**26,** 105

**Sexl, Th.** Electric charges on individual microscopic particles—**26,** 92

**Sharp, H. M.** Change of wave-length of scattered x-rays—**26,** 691

**Simon, Alfred W.** Electrostatic systems; quantitative theory—**26,** 111

———(see Compton, Arthur H.)—**26,** 289

**Slater, J. C.** Physically degenerate systems and quantum dynamics—**26,** 419

———(see Harrison, George R.)—**26,** 176

**Steinberg, J. C.** Relation between the loudness of a sound and its physical stimulus—**26,** 507

**Stewart, G. W.** Influence of a branch line upon acoustic transmission—**26,** 688

**Stewart, John Q.** Treatment of radiation-pressure and gas-pressure as due to inter-molecular forces —**26,** 491

**Stranathan, J. D.** Simultaneous high frequency and direct current resistances of fine wires—**26,** 500

**Takamine, T.** (see Foote, Paul D.)—**26,** 165

**Taylor, Geo. F.** Small resistance thermometer— **26,** 841

**Thomas, Charges H.** Soft x-rays from Fe, Co, Ni and Cu—**26,** 739

**Tolman, Richard C.** Maximum coefficients of absorption—**26,** 431

**Tschudi, E. W.** Impact of copper bars—**26,** 125

**Turner, Louis A.** Multiple x-ray ionization of light atoms—**26,** 143

**Van Voorhis, C. C.** (see Compton, K. T.)—**26,** 436

**Witmer, Enos E.** Critical potential of the negative band spectrum of nitrogen—**26,** 780

**Wolf, Alfred.** Theory of electrical conduction in metals—**26,** 256

**Woodruff, Albert E.** Photo-electric emission from Pt.—**26,** 655

**Zumstein, R. V.** Absorption spectrum of Pb vapor in the ultraviolet—**26,** 189

———The absorption spectrum of Mn vapor—**26,** 765

# ANALYTIC SUBJECT INDEX TO VOLUME 26

References with (A) are merely to abstracts of papers presented at meetings of the Physical Society.

**Absorption of light** (see also Spectrum)
screens for ultraviolet; organic media—**26,** 285 (A13)
theory, quantum—**26,** 431
**Acoustic oscillograph**
design—**26,** 287(A22)
**Acoustics**
absorption, anomalous, in auditorium—**26,** 288 (A24)
auditoriums; speech reception
effect of reverberation—**26,** 287(A23)
effect of tones and noise—**26,** 133
**Arc, electric** (see Spectra)
tungsten; characteristics—**26,** 33
**Arc, low-voltage**
electron velocity distribution—**26,** 585
helium in Hg; conductivity just after arc ceases—**26,** 454
hydrogen, $N_2$ and mixtures with Hg; characteristics—**26,** 537
**Atomic structure and dynamics** (see Quantum theory)
helium; life of metastable states $2S$ and $2s$—**26,** 454
**Audition**
binaural beats; objective and subjective—**26,** 401
loudness; relation to physical stimulus—**26,** 507
speech reception (see Acoustics)

**Book reviews**
Anderson, William Ballantyne; Physics for Technical Students—**26,** 416
———Mechanics and Heat—**26,** 871
Back, E. and A. Landé; Zeemaneffekt und Multiplettstruktur der Spektrallinien—**26,** 139
Berliner, Arnold, and K. Scheel; Physikalisches Handworterbuch—**26,** 415
Berthoud, Alfred; New Theories of Matter and the Atom—**26,** 413
Bond, W. N.; Introduction to Fluid Motion—**26,** 870
"Chemical Age" Chemical Dictionary—**26,** 142
Colebrook, F. M.; Alternating Currents and Transients—**26,** 524
Cranston, J. A.; Structure of Matter—**26,** 280
De Donder, Th.; Théorie Mathématique de l'Electricité—**26,** 140
Dingler, Hugo; Grundlage der Macschen Philosophie—**26,** 414
Drucker, C.; Ostwald-Luther, Messungen—**26,** 869
Duff, A. Wilmer; College Physics—**26,** 416
Gehloff, Georg (editor); Lehrbuch der Technischen Physik. Masse und Messen, Mechanik, Akustik, und Thermodynamik—**26,** 141
Georgii, Walter; Meteorologischen Messmethoden—**26,** 139
Ingersoll, L. R.; Laboratory manual of Experiments in Physics—**26,** 142
Johnson, K. S.; Transmission circuits for telephonic communication—**26,** 141
Lecher, E.; Kultur der Gegenwart; Physik—**26,** 280
Lertes, P.; Radio-amateur—**26,** 141
Lewis, W. C. M.; System of Physical Chemistry, Vol. II. Thermodynamics—**26,** 869
Luckiesh, M.; Foundations of the Universe—**26,** 413
Mariotte, Edme; Discours de la Nature de l'Air etc.—**26,** 142
Marx Handbuch der Radiologie, Vol. 6; Die Theorien der Radiologie—**26,** 414
Payne, Cecilia H.; Stellar Atmospheres—**26,** 870
Picard, Emile; Mélanges de Mathematiques et de Physiques—**26,** 417
Pidduck, F. B.; A Treatise on Electricity (second edition)—**26,** 871
Reese, H. M.; Light (second edition)—**26,** 524
Sachs, George; Grundbegriffe der Mechanischen Technologie der Metalle—**26,** 415
Schackel, R. G.; Modern School Electricity and Magnetism—**26,** 871

**Capacity** (see Electrical capacity)
**Compton effect** (see x-rays, scattering)
**Crystal structure and density**
films, sputtered; Ni—**26,** 86
metals
chromium and Ti—**26,** 56
electrodeposited; Cd, Co, Cu, Fe, Ni, Zn; orientations—**26,** 390
iron, pure—**26,** 60
sputtered Ni—**26,** 86
tungsten, pure—**26,** 736

**Density** (see Crystal structure)
**Discharge through gases** (see Arc)
hydrogen; striated; potential distribution, electron concentration and mean electron energy—**26,** 794

**Elastic properties**
Young's modulus; steel; variation with temperature—**26,** 121
**Electrical capacity**
suspensions of spheroids; theory—**26,** 678
red blood corpuscles of dog—**26,** 682
**Electrical conductivity and resistance**
films, sputtered
Ni; resistance—**26,** 86
photo-resistance effect—**26,** 247
temperature coefficient—**26,** 247
frequency effect; simultaneous high and low frequency measurements—**26,** 500
measurement; bar method; electrical and thermal conductivities, specific heat and Thomson effect for same specimen—**26,** 287(A21)
photo-resistance effect; sputtered films of Bi, Pd, Cu, Pt, Au, Ag, Te—**26,** 247
temperature coefficient for films—**26,** 247
theory, for metals—**26,** 256
**Electrical measurements**
voltages, micro-, at radio frequencies—**26,** 118
**Electrification**
drops; by collision with small drops—**26,** 105
rain; Elster and Geitel's theory—**26,** 105
**Electromagnetic transverse effects**
Ettingshausen effect
measurement—**26,** 820
for Au, Co, Ni, Pd—**26,** 820
films, sputtered Ni; Hall effect—**26,** 86
Hall effect
measurement—**26,** 820
for Au, Co, Ni, Pd—**26,** 820
for Ni films—**26,** 86
**Electrons**
charge
criticism of oil-drop experiments—**26,** 92
reply—**26,** 97
divisibility; discussion of evidence—**26,** 92, 99
mass; from x-ray Compton effect—**26,** 691
scattering, in ionized gases—**26,** 585
secondary
from Fe, Ni, Mo; 0-1500 v.—**26,** 346
from Ni; positive bombardment—**26,** 800
transmission through Al foil—**26,** 221
velocity distribution, in low-voltage arc—**26,** 585
**Electrostatic machine**
theory, general; cyclic—**26,** 111
**Ettingshausen effect** (see Electromagnetic transverse)

**Filament**
tungsten; effect of HCl on resistance—**26,** 339
**Films** (see Crystal structure, Electrical conductivity, Electromagnetic tranverse, Magnetic)
color of sputtered Ni—**25,** 86
**Flames** (see Ions, Spectra)
**Fluorescence and phosphorescence**
mercury vapor
discussion of experiments—**26,** 376
persistance—**26,** 264

**Gases**
pressure; theory based on repulsive inter-molecular forces—**26,** 491

**Hall effect** (see Electromagnetic transverse)

**Impact**
duration; copper and steel bars—**26,** 125
**Ionization** (see Potentials, critical)
by chemical reaction; oxidation of ethyl alcohol in contact with electrodes—**26,** 633
by electron impact
in A, CO, $CH_4$, He, $H_2$, $N_2$—**26,** 208
in A, He, $H_2$, Hg, HCl, $N_2$—**26,** 436
in helium with $H_2$; ions formed—**26,** 44
in hydrogen; ions formed—**26,** 44
in HCl—**26,** 339
in HCl, HgCl, Hg, I; ions formed—**26,** 614
in nitrogen; ions formed—**26,** 284(A11), 786
photo-electric, of gases—**26,** 195
**Ions** (see Electrons, Ionization, Positive rays)
combination of halide ions with alkali metals; energy calculated—**26,** 284(A12)
in flames; gasoline, hydrogen, HCl; mobility—**26,** 807
mobility
active deposits of Th and Ra—**26,** 629
argon and hydrogen ions in air—**26,** 465
ions in flames, negative—**26,** 807
ions from hot Pt—**26,** 625

**Leduc effect** (see Thermo-magnetic transverse)

**Magnetic properties**
films, sputtered Ni—**26,** 86
permalloy—**26,** 261
wire; demagnetising factor—**26,** 261
theory of ferromagnetism; relation to atomic magnetostriction—**26,** 274

**Magnetostriction effect**
permalloy—**26,** 261
relation to ferromagnetism; theory—**26,** 261
**Molecular aggregation**
in Na vapor at high temperatures—**26,** 176

**Nernst effect** (see Thermo-magnetic transverse)

**Optical constants** (see Absorption, Reflection, Refraction, Scattering)
magnesium and zinc crystals—**26,** 380

**Phosphorescence** (see Fluorescence)
**Photo-electric effect** (see also x-rays)
caesium vapor—**26,** 195
gases; measurement of ionization—**26,** 195
measurements; null method, eliminating fluctuations of arc—**26,** 655
mercury, flowing; threshold—**26,** 643
platinum; effect of heat treatment—**26,** 655
threshold and work function
mercury, flowing—**26,** 643
platinum—**26,** 655
relation to optical reflection—**26,** 285(A15)
relation to "raies ultimes"—**26,** 286(A16)
**Photo-electric valve**
dumb-bell, coated with K—**26,** 671
**Photo-resistance effect** (see Electrical conductivity)
**Photometer**
photo-ionization—**26,** 195
**Positive rays**
electron emission, from Ni surface—**26,** 800
reflection from Ni surface—**26,** 800
**Potentials, critical**
aluminum; from photo-electric effect, of electron impact—**26,** 221
calculated from dispersion formula—**26,** 232
cobalt, Cu, Fe, Ni; from photo-electric effect of electron impact—**26,** 739
determination from photo-electric effect of electron bombardment, Al—**26,** 221
Co, Cu, Fe, Ni—**26,** 739
hydrogen chloride; ionization—**26,** 339
multiplicity; suggestion—**26,** 150
nitrogen, negative bands—**26,** 780
spectral terms computed from—**26,** 232, 739
**Proceedings of American Physical Society**
Portland, Oregon, Meeting, June 19, 1925—**26,** 281

**Quantum theory** (see Absorption, Spectra, X-rays)
quantum dynamics; degenerate systems; weak quantization—**26,** 419

**Radiation pressure**
due to intermolecular forces; theory—**26,** 491
**Reflection of light**
theory; change in reflecting power in ultraviolet at photo-electric threshold—**26,** 285(A15)
**Refraction of light**
theory; application of dispersion formula to calculation of indexes from critical potentials—**26,** 232
**Resonance radiation** (see Fluorescence)

**Scattering of light**
in gases; mixtures of air and $CO_2$—**26,** 495
in vapors, saturated; ether, alcohol, etc.—**26,** 285 (A14)
**Schottky effect or Shot effect** (see Thermionic emission)
**Sound** (see Acoustics, Audition)
absorption, anomalous, in auditorium—**26,** 288 (A24)
resonators; theory—**26,** 688
transmission of a conduit; influence of branch line—**26,** 688
**Specific heat**
measurement; bar method—**26,** 287(A21)
**Spectra**
absorption
carbon dioxide, bands—**26,** 469
lead vapor, ultraviolet—**26,** 189
manganese vapor—**26,** 102
sodium; molecular broadening; values of probability coefficients—**26,** 176
theory; maximum absorption on basis of correspondence principle—**26,** 431
water; infrared; 0 to 95°C—**26,** 771
AlO bands—**26,** 561
ammonia bands—**26,** 537
bands
AlO; emitter—**26,** 561
ammonia, ultraviolet—**26,** 537
analysis, quantum
CO—**26,** 283(A8)
CuI—**26,** 1
$N_2$, ultraviolet—**26,** 283(A7)
SiN—**26,** 319
BeF; discussion—**26,** 561
BO; discussion—**26,** 561
CO; analysis—**26,** 283(A8)
$CO_2$, infrared; emission and absorption—**26,** 469
CN, discussion—**26,** 561
CuB, CuCl, CuF, CuI; excitation by active $N_2$—**26,** 1
CuI, 260 heads, analysis—**26,** 1

**Spectra**—bands (cont.)
electronic spectra; discussion—**26,** 1
emitters
aluminum—**26,** 561
ammonia, ultraviolet—**26,** 537
electronic spectra; theory—**26,** 1
nitrogen bands of Duffendack—**26,** 561
Schuster band—**26,** 537
flame, Bunsen, infrared—**26,** 283(A9)
grouping according to excess electrons of emitters—**26,** 561
one-excess-electron bands; BeF, BO, CO, CN, $N_2$, MgF, AlO, SiN—**26,** 561
isotope effect
CuI—**26,** 1
SiN—**26,** 319
MgF—discussion—**26,** 561
multiplicity; discussion—**26,** 561
nitrogen
analysis of ultraviolet—**26,** 283(A7)
critical potential—**26,** 780
emitter of Duffendack bands—**26,** 561
SiN; analysis; new bands—**26,** 319
theory; application (see analysis)
emission of electronic spectra—**26,** 1
water, infrared, 0-95°C—**26,** 771
BeF bands—**26,** 561
boron, $B_{II}$; classification; term values—**26,** 282 (A5), 310
BO bands—**26,** 561
cadmium; $pp'$ multiplet—**26,** 165
fluorescence excited by sparks—**26,** 761
carbon, $C_{III}$; classification; term values—**26,** 282(A5), 310
CO bands—**26,** 283(A8)
$CO_2$ bands—**26,** 469
chlorine, series and multiplets—**26,** 282(A6)
CN bands—**26,** 561
CuB, CuCl, CuF, CuI bands—**26,** 1
fluorescence, excited by sparks
cadmium vapor—**26,** 761
indium and Tl mixed with Cd—**26,** 761
thallium mixed with Hg—**26,** 573
helium, metastable; life in states $2S$ and $2s$—**26,** 454
indium; fluorescence of vapor—**26,** 761
intensities, relative; Na series; theoretical calculation of transition probabilities—**26,** 749
iron; secondary standards—**26,** 284(A10)
lead; absorption of vapor—**26,** 189
arc spectrum—**26,** 189
MgF bands—**26,** 561
manganese; absorption of vapor—**26,** 102

**Spectra** (cont.)
mercury; series; spectrogram—**26,** 165
neon; secondary standards—**26,** 284(A10)
nitrogen (see bands)
$pp'$ groups, for 2 and 3 valence electron atoms—**26,** 150
cadmium—**26,** 165
SiN bands—**26,** 319
sodium; absorption lines; broadening; transition probability coefficients—**26,** 176
standards, secondary; lines of Ne and Fe—**26,** 284 (A10)
thallium; fluorescence of vapor
with Cd—**26,** 761
with Hg—**26,** 573
theory (see bands)
absorption; transition probabilities for Na—**26,** 176, 749
calculation of coefficients on basis of correspondence principle—**26,** 431
fluorescence of mixed vapors; rôle of excited Hg atoms—**26,** 573
screening constants for regular doublets, Li to O—**26,** 310
selection principles; forbidden lines—**26,** 165
water, absorption bands, 0-95°C—**26,** 771

**Thermal conductivity**
measurement, bar method—**26,** 287(A21)
metals at high temperatures; Al, Cu, Ni, Zn—**26,** 287(A20)
selenium strip; effect of light—**26,** 475
**Thermal expansion**
typemetal—**26,** 841
**Thermionic emission of electrons**
Schottky effect, low frequency circuits—**26,** 71
theory, kinetic—**26,** 241
**Thermionic emission of ions**
from oxide coated filaments; oxygen negatives—**26,** 360
from Pt—**26,** 625
**Thermo-electric effects.**
aluminum; effect of pressure—**26,** 286(A17)
effect of compression—**26,** 286(A17)
effect of rolling—**26,** 286(A19)
effect of changing temperature gradient—**26,** 286 (A18)
theory, electron—**26,** 286(A17)
zinc, single crystal wire—**26,** 486
**Thermo-magnetic transverse effects**
Leduc and Nernst effects; measurement—**26,** 820
for Au, Co, Ni, Pd—**26,** 820

**Thermometer, resistance**
small; construction—**26,** 841

**Vapor pressure**
lead, 1118 to 1235°C—**26,** 851
measurement for metals—**26,** 851
mercury, 20 to −80°C—**26,** 859
170 to 203°C—**26,** 851
**Vaporization**
latent heat; lead—**26,** 851
mercury, 20 to −80°C—**26,** 859

**X-rays** (see X-ray spectra)
chemical effect—**26,** 525
photo-electric effect of soft rays; Al—**26,** 221
Co, Cu, Fe, Ni—**26,** 739
scattered; Compton effect
from Ag, Al, Cu, graphite, Pb, S; intensity ratio—**26,** 282(A3)
from Al and Li; intensity distribution—**26,** 300
from graphite; wave-length shift—**26,** 282(A4)
from paraffin; wave-length shift—**26,** 691
from molybdenum—**26,** 281(A2)
recoil electrons produced (see secondary rays)

**X-rays** (cont.)
secondary beta rays
direction of ejection—**26,** 289, 697
theory of number—**26,** 281(A1), 433

**X-ray spectra**
absorption edges
compounds—**26,** 525
K-edges; Ti, V, Cr, Mn—**26,** 525
Ag; sharpness—**26,** 724
phosphorus—**26,** 143
L-edges; Sn, Sb, Fe, I—**26,** 525
characteristic lines
K-series; Cu; relative intensities—**26,** 714
Mo; wave-lengths and intensities—**26,** 701
Mo; intensity distribution—**26,** 724
L-series; W, relative intensities—**26,** 714
terms connected with critical potentials—**26,** 232, 739
measurements; wave-length; corrections—**26,** 60
intensity distribution; instrumental factors—**26,** 724
theory; multiple K and L levels; screening constant—**26,** 143

L250

**L.250. QUARTZ SPECTROGRAPH.** This instrument will photograph emission and absorption spectra in the visible and ultra-violet regions from 185 to 800 Mu Mu.

Collimator and telescope lenses are of quartz, 25mm in aperture. The prism is of the cornu type (built up of two thirty degree prisms of left and right handed quartz, with faces in optical contact), and its faces are 20 mm high and 30 mm long. In this new model the plate holder and slide as well as the camera box are of metal throughout. The plate which is of the standard 3¼ x 4¼ inches size is shifted by rack and pinion motion, a millimeter scale on the slide serving to indicate the position of the plate. A shutter on the slit permits the taking of comparison spectra in juxtaposition. The necessary adjustments for focusing the lenses and tilting the plate are provided. The bellows on the camera is of black velvet, which is light tight and will not deteriorate with use.....$285.00

**L.250a. WAVELENGTH SCALE.** Accurately divided and figured on glass and calibrated individually for each instrument. By laying it on the spectrogram the wavelength may be read off directly.....$40.00


The
# GAERTNER SCIENTIFIC CORPORATION

SUCCESSOR TO WM. GAERTNER & CO.

ESTABLISHED 1896 INCORPORATED 1923

1201 Wrightwood Avenue CHICAGO, U. S. A.

**The New High Transmission Color Filters**

**Now Furnished with the**

# CENCO COLOR MIXER

**Greatly Improve its Performance**

No. 71165—$60.00

With this apparatus which embodies in actual form the Maxwell Triangle of Color, a complete lecture study of color can be made including:

1.—The Young-Helmholtz theory.
2.—Addition of colors.
3.—Subtraction of colors.
4.—Complementary colors.
5.—Subjective color illusions.
6.—Production of tints by mixing primary colors.

The color filters have been selected to transmit within narrow spectral limits the three primary colors postulated in the Young-Helmholtz theory.

*For Complete Description Ask for Bulletin No. AD31P*

**CENTRAL SCIENTIFIC COMPANY**

LABORATORY APPARATUS AND CHEMICALS

460 E. Ohio St. Chicago, U.S.A.

Barnes Books Publishing Service, Evanston, Illinois